

# A GELLAN-BASED FLUID GEL CARRIER FOR SPRAY DELIVERY

by

BRITT TER HORST

A thesis submitted to  
The University of Birmingham  
for the degree of  
DOCTOR OF PHILOSOPHY

School of Chemical Engineering  
College of Engineering and Physical Sciences  
The University of Birmingham  
May 2019

UNIVERSITY OF  
BIRMINGHAM

**University of Birmingham Research Archive**

**e-theses repository**

This unpublished thesis/dissertation is copyright of the author and/or third parties. The intellectual property rights of the author or third parties in respect of this work are as defined by The Copyright Designs and Patents Act 1988 or as modified by any successor legislation.

Any use made of information contained in this thesis/dissertation must be in accordance with that legislation and must be properly acknowledged. Further distribution or reproduction in any format is prohibited without the permission of the copyright holder.

## **Abstract**

Autologous cell transplantation is a promising approach to enhance burn wound re-epithelialisation. It was introduced to clinical practice decades ago with current delivery techniques involving spraying autologous cultured or uncultured cells in low-viscosity suspensions. This delivery method is limited since it results in an uneven distribution on the wound bed and cell loss as the liquid is not retained on the skin surface.

In this thesis, a sprayable gel that solidifies on the surface of the skin has been developed to circumvent this problem. A gellan-based fluid gel system was developed with flexible viscoelastic properties that can be tuned by a biocompatible polymer concentration and ionic strength to facilitate spray delivery. The material liquefies at high shear during spraying with self-healing properties of the gel causing it to solidify on the receiving surface. Results present the development and characterisation of a gellan fluid gel for the encapsulation and spray-delivery of cells onto surfaces, aiming for reduced cell spillage, improved spray uniformity and maintenance of cell viability and function.

Additionally, the same polymer was used to formulate a gellan film that can be rehydrated in acetic acid for the treatment of wound infections. Gellan is a versatile polymer as shown by the formulations explored in this study and a promising candidate for cell and drug delivery applications.

To my parents,  
who are **always** proud of me

# ACKNOWLEDGEMENTS

First and foremost, I would like to express a big thank you to my supervisor, Professor Liam Grover, whose continuous support, valuable scientific advice and patience throughout my PhD has been invaluable.

I extend my thanks to the NIHR SRMRC (Trauma Research) team of the University Hospitals Birmingham NHS Foundation Trust that supported me in my role as Clinical Research fellow and for giving me the chance to be involved in clinical research studies, which taught me valuable lessons on the direct and indirect influence of research on patients and their care while giving me the chance to keep connected with patients.

I would like to acknowledge the Scar Free Foundation for funding this work and the University of Birmingham for providing me with the opportunity to undertake my PhD project.

I want to thank all the past and current members of the HTI-lab for the fun times during and after work hours. I would especially like to thank Dr Gurpreet Birdi who started me off in cell culture and Mr Richard Moakes for his thorough rheology input. Many thanks to Fenella Halstead for the help with microbiology. As well as the many researchers I have been lucky enough to collaborate with from the University of Glasgow under the supervision of Professor Matthew Dalby.

Massive thanks goes to my amazing family for their encouragement through this process and for keeping me sane. And thanks to my dear friends that had to miss me on many fun occasions and still supported me, I would love to name you all but if you read this you know you are on the list (I'll make an exception for Pkempen2 as promised)! Finally, Radu, you have been there during the hard times making endless trips to Birmingham, you made me proud of my work and myself. I couldn't have done this without you.

# CONTENTS

<b>1</b>	<b>Introduction</b>	<b>1</b>
1.1	Burn injury . . . . .	2
1.2	Skin . . . . .	3
1.2.1	Epidermis . . . . .	3
1.2.2	Dermis and basement membrane . . . . .	7
1.3	Wound healing and keratinocytes . . . . .	8
1.3.1	The role of keratinocytes in wound healing . . . . .	8
1.3.2	Pathophysiology of burn injury . . . . .	11
1.3.3	Rationale for keratinocyte transplantation . . . . .	11
1.4	Cell transplantation technology . . . . .	12
1.4.1	Cell source . . . . .	12
1.4.2	Historical development of keratinocyte culture . . . . .	12
1.4.3	Progress towards xenobiotic free culture techniques . . . . .	13
1.4.4	Additions to keratinocyte culture . . . . .	14
1.5	Keratinocyte viability after transplantation . . . . .	16
1.6	Methods of keratinocytes transplantation . . . . .	16
1.6.1	Introduction: grafting of burn wounds . . . . .	16
1.6.2	Cultured keratinocyte sheets . . . . .	17
1.6.3	Autologous keratinocyte transplantation in suspension . . . . .	20
1.7	Hydrogels . . . . .	26
1.8	Methods of spray deposition . . . . .	42
1.8.1	Spray parameters and cell viability . . . . .	42
1.8.2	Spray systems . . . . .	43
1.9	Potential therapeutic applications . . . . .	45
1.9.1	Future approaches keratinocyte transplantation . . . . .	45
1.9.2	Future spray cell delivery systems for burns wound care . . . . .	45
1.10	Thesis overview . . . . .	46

<b>2</b>	<b>Gellan-based fluid gel carrier</b>	<b>48</b>
2.1	Introduction . . . . .	49
2.2	Material and methods . . . . .	51
2.2.1	Fluid gel preparation and characterisation . . . . .	51
2.2.2	Rheological measurements . . . . .	51
2.2.3	Microscopy of fluid gels . . . . .	53
2.3	Contact angle measurements . . . . .	53
2.4	Spray methods . . . . .	53
2.5	Spray analysis using water sensitive paper . . . . .	54
2.5.1	HDF cell culture . . . . .	55
2.5.2	Fluid gel encapsulation . . . . .	56
2.5.3	Live/Dead assay . . . . .	56
2.5.4	Alamar Blue Metabolic Activity . . . . .	57
2.5.5	Statistical Methods . . . . .	58
2.6	Results . . . . .	58
2.6.1	Fluid gel material and characterisation . . . . .	58
2.6.2	Biological response to fluid gel spray delivery . . . . .	69
2.7	Discussion . . . . .	72
2.8	Conclusion . . . . .	79
<b>3</b>	<b>Keratinocyte spray delivery</b>	<b>81</b>
3.1	Introduction . . . . .	82
3.2	Methods . . . . .	83
3.2.1	Fluid gel preparation and characterisation . . . . .	83
3.2.2	Keratinocyte culture and encapsulation . . . . .	84
3.2.3	Cell sedimentation in fluid gel . . . . .	84
3.2.4	Cell viability . . . . .	85
3.2.5	Morphology . . . . .	86
3.2.6	Alamar Blue Metabolic Activity . . . . .	87
3.2.7	In-Cell Western . . . . .	88
3.2.8	Scratch assay . . . . .	89
3.3	Results . . . . .	91
3.3.1	Material characteristics . . . . .	91
3.3.2	Cell viability . . . . .	96
3.3.3	Morphological changes in sprayed cells . . . . .	98
3.3.4	Cell function . . . . .	100
3.4	Discussion . . . . .	105
3.5	Conclusion . . . . .	111

<b>4</b>	<b>Formulation of acetic acid - gellan hydrogel dressing</b>	<b>112</b>
4.1	Introduction . . . . .	113
4.1.1	Burn wound infection . . . . .	113
4.1.2	Acetic Acid in burn wound treatment . . . . .	113
4.1.3	Acetic acid delivery systems . . . . .	115
4.1.4	Study rationale . . . . .	115
4.2	Methods . . . . .	116
4.2.1	Preparation gellan gel films . . . . .	116
4.2.2	Material characterisation gellan patches . . . . .	116
4.2.3	Release . . . . .	118
4.2.4	Agar disk diffusion assay . . . . .	121
4.3	Results . . . . .	121
4.3.1	Visual appearance of dressings . . . . .	121
4.3.2	Thickness . . . . .	121
4.3.3	Swelling capacity . . . . .	122
4.3.4	Dehydration . . . . .	123
4.3.5	Tensile strength . . . . .	124
4.3.6	Release . . . . .	125
4.3.7	Agarose diffusion . . . . .	126
4.3.8	Porcine wound model . . . . .	126
4.3.9	Antimicrobial effect . . . . .	127
4.4	Discussion . . . . .	128
4.5	Conclusion . . . . .	131
<b>5</b>	<b>Conclusions and future work</b>	<b>133</b>
5.1	Conclusions . . . . .	133
5.1.1	Chapter 1: Introduction . . . . .	133
5.1.2	Chapter 2: Gellan-based fluid gel carrier . . . . .	134
5.1.3	Chapter 3: Keratinocyte spray delivery . . . . .	134
5.1.4	Chapter 4: Formulation of acetic acid - gellan hydrogel dressing . . . . .	134
5.2	Limitations and future investigations . . . . .	135
	<b>Appendix A: Supplementary material Chapter 3</b>	<b>176</b>
	<b>Appendix B: Spray delivery of PRP</b>	<b>180</b>
B.1	Introduction . . . . .	181
B.2	Methods . . . . .	182
B.2.1	Platelet rich plasma preparation . . . . .	182

B.2.2	PRP fluid gel encapsulation . . . . .	182
B.2.3	PRP viability . . . . .	183
B.2.4	Platelet activation . . . . .	184
B.2.5	Platelet aggregation . . . . .	184
B.3	Results . . . . .	185
B.3.1	PRP preparation . . . . .	185
B.3.2	Spray delivery of PRP . . . . .	185
B.3.3	Fluid gel encapsulation of PRP . . . . .	186
B.4	Conclusion and future work . . . . .	188

**Appendix C: Publications**

## LIST OF FIGURES

1.1	Layers and function of the skin. . . . .	4
1.2	Keratinocyte differentiation and markers. . . . .	6
1.3	Role of keratinocytes in re-epithelialisation. . . . .	10
1.4	Methods of autologous keratinocyte transplantation to burn wounds. . . . .	18
1.5	Burn wound coverage with cultured epithelial autografts applied in sheets. . . . .	20
1.6	Spray delivery of cultured keratinocytes to enhance burn wound healing. . . . .	22
1.7	Bacterial cellulose cellular scaffold. . . . .	30
1.8	Cell compatibility of chitosan scaffolds. . . . .	32
1.9	The chemical structure of low-acyl gellan gum. . . . .	33
1.10	The development process of a cell laden hydrogel carrier for topical spray delivery. . . . .	47
2.1	Airbrush spray device and standardised set up . . . . .	54
2.2	Water-sensitive paper (WSP) sprayed with gellan and water . . . . .	55
2.3	Manufacture process and characteristics of gellan fluid gel. . . . .	59
2.4	Modulation of fluid gel properties. . . . .	62
2.5	Determination of fluid gel retention. . . . .	66
2.6	Structural stability on the receiving surface. . . . .	67
2.7	Spray features of gellan gum fluid gel . . . . .	68
2.8	Human dermal fibroblast response to fluid gel spray delivery. . . . .	70
2.9	Live/dead assay of HDFs encapsulated in gellan fluid gel . . . . .	71
3.1	Transwell assay . . . . .	85
3.2	Live/dead assay cell count . . . . .	86
3.3	Diagram of cell shape descriptors . . . . .	87
3.4	<i>In vitro</i> scratch assay wound density analysis method . . . . .	91
3.5	Viscoelastic properties of gellan fluid gel used for keratinocyte encapsulation . . . . .	92
3.6	Keratinocyte migration assay . . . . .	95
3.7	Growth curve of adult human epidermal keratinocytes . . . . .	96
3.8	Cytoskeleton and nucleus staining of sprayed and non-sprayed keratinocytes . . . . .	99

3.9	Metabolic activity of HEKa as determined by alamar blue . . . . .	100
3.10	<i>In vitro</i> wound scratch assay . . . . .	101
3.11	Scratch assay of control and encapsulated sprayed keratinocytes. Wound width and wound healing rate . . . . .	102
3.12	Cell viability of sprayed and non-sprayed human epidermal keratinocytes .	103
3.13	Cell viability of encapsulated sprayed and non-sprayed human epidermal keratinocytes . . . . .	104
3.14	In-Cell Western assay for laminin 5 and involucrin. . . . .	106
4.1	Chemical structure of acetic acid. . . . .	113
4.2	Tensile strength testing of dogbone shaped gellan films . . . . .	118
4.3	Acetic acid detection calibration curve . . . . .	120
4.4	Porcine wound model method . . . . .	120
4.5	Mean thickness (mm) of gellan films following rehydration. . . . .	122
4.6	Mean swelling (%) of gellan films compared to gauze following rehydration.	123
4.7	Mean dehydration (%) of gellan films compared to gauze following rehydration. . . . .	124
4.8	Tensile strength and Young's modulus of gellan films . . . . .	125
4.9	Acetic acid diffusion into agarose gel. . . . .	126
4.10	Acetic acid release form porcine wound model . . . . .	127
4.11	Gellan films microbiology . . . . .	128
A.1	Frequency dependence of a panel of gellan fluid gels. . . . .	177
A.2	Amplitude dependence of a panel of gellan fluid gels fitted for Herschel-Bulkley model. . . . .	178
A.3	Amplitude dependence of a panel of gellan fluid gels fitted for Herschel-Bulkley model. . . . .	179
B.1	Preparation of PRP . . . . .	183
B.2	Platelet activation following spray delivery. . . . .	186
B.3	Platelet viability following spray delivery. . . . .	187
B.4	Platelet aggregation in fluid gel. . . . .	188
B.5	Platelet viability following encapsulation in gellan fluid gel. . . . .	189

# LIST OF TABLES

1.1	Natural polymers and their properties commonly used for skin repair and regeneration. . . . .	27
2.1	Rheological properties of gellan fluid gels. . . . .	60
2.2	Fitting parameters from the Herschel-Bulkley model for gellan fluid gels. . . . .	65
4.1	Gellan film thickness . . . . .	122
4.2	Anti-microbial activity (zone of inhibition) of gellan dressings . . . . .	128
B.1	Mean blood values of P-PRP and L-PRP preparations . . . . .	185

<b>Abbreviation</b>	<b>Name</b>
CDC	Centers for Disease Control and Prevention
WISQARS	Web-based Injury Statistics Query and Reporting System
DNA	Deoxyribonucleic acid
GM-CSF	Granulocyte-macrophage colony-stimulating factor
IL-6	Interleukin 6
GAGs	Glycosaminoglycans
ECM	Extracellular matrix
TGF- $\beta$ 1	Transforming growth factor beta 1
TGF- $\beta$ 2	Transforming growth factor beta 2
TBSA	Total burned surface area
MSC	Mesenchymal stem cell
HFSC	Hair follicle stem cell
FBS	Fetal bovine serum
KGF	Keratinocyte growth factor
ASCs	Adipose derived stem cells
EGF	Epidermal growth factor
VEGF	Vascular endothelial growth factor
MTT assay	Methylthiazol Tetrazolium assay
DED	De-epidermalised dermis
AD	Anno Domini
CEA	Cultured epithelial autografts
FDA	Food and Drug Administration
NICE	National Institute for Health and Clinical Excellence
UoB	University of Birmingham
HA	Hyaluronic acid
LMW	low molecular weight
HMW	high molecular weight
CD44	cluster of differentiation 44
RHAMM	receptor for hyaluronic acid mediated motility
ESS	Engineered Skin Substitute

<b>Abbreviation</b>	<b>Name</b>
NA	Nasal atomizer
NaCl	Sodium chloride
PEG	Polyethylene glycol
WSP	Water-sensitive paper
TSA	Total sprayed area
RSF	Relative span factor
HDF	Human dermal fibroblasts
PI	Propidium Iodide
LVR	Linear viscoelastic region
ANOVA	Analysis of variance
DSC	Differential scanning calorimetry
HEKa	Adult human epidermal keratinocytes
HKGS	Keratinocyte Growth Supplement
BPE	Bovine pituitary extract
DAPI	4', 6-diamidino-2-phenylindole
EH	Ethidium Homodimer-1
PBS	Phosphate-buffered saline
DMSO	Dimethyl sulfoxide
CMFDA	5-chloromethylfluorescein diacetate
F-actin	Filamentous actin
LM-5	Laminin 5
BWI	Burn wound infections
MSSA	Methicillin-susceptible strain of Staphylococcus Aureus
MIC	Minimal inhibitory concentration
HCL	Hydrochloric acid
PAIT	Percutaneous acetic acid injection therapy
GG	Gellan gum
AA	Acetic acid

## PUBLICATIONS

- Chapter 6 - Natural Polymers: biomaterials for skin scaffolds. In *Biomaterials for Skin Repair and Regeneration*, Elsevier, 2019. **Britt ter Horst**, Naiem S. Moiemmen, Liam M. Grover. ISBN 9780081025468.
- Investigating the intra- and inter-rater reliability of a panel of subjective and objective burn scar measurement tools. Kwang Chear Lee, Amy Bamford, Fay Gardiner, Annarita Agovino, **Britt ter Horst**, Jon Bishop, Alice Sitch, Liam Grover, Ann Logan, Naiem Moiemmen. *Burns*, 2019. Doi: 10.1016/j.burns.2019.02.002
- A gellan-based fluid gel carrier to enhance topical spray delivery. **B. ter Horst**, R. J. A. Moakes, G. Chouhan, R. L. Williams, N. S. Moiemmen, L. M. Grover. *Acta Biomaterialia*, 2019. Doi: 10.1016/j.actbio.2019.03.036
- Structuring of soft materials across multiple length scales for biomedical applications. Megan E. Cooke, Dr. Simon W. Jones, **Dr. Britt ter Horst**, Prof. Naiem Moiemmen, Prof. Martyn Snow, Dr. Gurpreet Chouhan, Dr. Lisa Hill, Maryam Esmaeli, Richard A.J. Moakes, Dr. James Holton, Dr. Rajpal Nandra, Dr. Richard L. Williams, Prof. Liam M. Grover. *Advanced Materials*, 2017. Doi: 10.1002/adma.201705013

- Isolated dorsoradial capsular tear of the thumb metacarpophalangeal joint: Does congenital thumb hypoplasia and joint hypermobility predispose to this injury? Yvette Godwin, FRCS (plast); **Britt ter Horst**, MD; Godwin Scerri, FRCS(plast). *Annals of Plastic Surgery*, 2017. Doi: 10.1097/SAP.0000000000001202.
- Advances in keratinocyte delivery in burn wound care. **B. ter Horst**, G. Chouhan, N.M. Moiemmen, L.M. Grover. *Advanced Drug Delivery Reviews*, 2017. Doi: 10.1016/j.addr.2017.06.012.

In each chapter the author of this thesis (Britt ter Horst) has designed, undertaken, analysed and written the research. Likewise, in each publication listed, where the author of this thesis (Britt ter Horst) is the first author of the paper, the research has been designed, undertaken, analysed and written by the author. The subsequent authors have provided academic supervision by proof reading/approving the manuscripts, providing the research facility and/or teaching the handling of specific research equipment.

## CONFERENCE PAPERS: ORAL PRESENTATIONS

- UK Society for Biomaterials, University of Bath, UK. Cell-loaded gellan hydrogel carrier for topical spray delivery to enhance burn wound healing. *June 2018.*
- Scarcon, Amsterdam, the Netherlands. Cell-loaded gellan hydrogel carrier for topical spray delivery to enhance burn wound healing. *May/June 2018.*
- Sankey (senior) Research Prize University Hospitals Birmingham, UK. Cell-loaded gellan hydrogel carrier for topical spray delivery to enhance burn wound healing. *May 2018.*  
**Awarded runners up Sankey Prize**
- British Burn Association - Annual Meeting, Swansea, UK. Cell-loaded gellan hydrogel carrier for topical spray delivery to enhance burn wound healing. *April 2018.*
- The Society of Academic and Research Surgery - Annual Meeting, Nottingham, UK. Cell-loaded gellan hydrogel carrier for topical spray delivery to enhance burn wound healing and A histological and clinical study of Matriderm<sup>®</sup> burn scar reconstruction. *January 2018.*
- Annual Meeting of the German Society for Biomaterials, Würzburg, Germany. Cell-loaded gellan hydrogel carrier for topical spray delivery to enhance burn wound healing. *November 2017.*
- 17th European Burns Association Congress EBA, Barcelona, Spain. Prediction of mortality in burn patients: "The revised Baux Score is Alive and Well". *September 2017.*
- Advancing Tissue and Regenerative Engineering in UK Medicine Conference, Crewe Hall, UK. Novel assessment method to characterise spray delivery *April 2017.* **Travel award**

# CONTRIBUTIONS TO CLINICAL TRIALS

- A Multi-centre, Prospective Study to Examine the Relationship between Neutrophil Function and Sepsis in Adults and Children with Severe Thermal Injuries (SIFTI-1): *data collection*
- A Multi-centre, Prospective Study to Examine the Relationship between Neutrophil Function and Sepsis in Adults and Children with Severe Thermal Injuries (SIFTI-2): *patient recruitment, clinical study procedures, data collection*
- A Prospective, Longitudinal Study to Investigate the Effect of Thermal Injury on Intestinal Permeability and Systemic Inflammation (HESTIA): *clinical assessor, sub-Principal Investigator*
- A pilot randomised controlled trial to examine the efficacy and optimal dose of Acetic Acid to treat colonised burns wounds (AceticA): *protocol development, data analysis*
- A RandomizEd Trial of ENtERal Glutamine to MinimIZE Thermal Injury (Re-Energize): *patient recruitment, study drug prescription*
- Burns Objective Scar Scale (BOSS): *clinical study procedures*
- Gellan Contact Study (GCS): *clinical assessor*

All studies are/were carried out at University Hospitals Birmingham.

# CHAPTER 1

## INTRODUCTION

The original autologous keratinocyte culture and transplantation technique was introduced over 3 decades ago in burn patients to achieve faster re-epithelialisation. Various keratinocyte application methods have improved from cell sheets to single-cell solutions delivered with a spray system. However, further enhancement of cell culture, cell viability and function *in vivo*, cell carrier and cell delivery systems remain themes of interest. Hydrogels such as chitosan, alginate, fibrin and collagen are frequently used in burn wound care and have advantageous characteristics as cell carriers. It is likely that keratinocyte transplantation will in future be mediated by spray devices, but optimisation of application technique and carrier type is necessary. An overview of keratinocyte transplantation in burn wounds concentrating on application methods and future therapeutic cell delivery options with a special interest in hydrogels and spray devices for cell delivery is given.

The aim of this thesis is to determine what properties of the hydrogel are important to enable delivery of drugs or cells to promote wound healing, this is reflected by the following objectives:

- Design a hydrogel with optimal features for spray delivery
- The rheological properties of the hydrogel in comparison to current standards
- Investigate viability and function of encapsulated cells in the hydrogel environment and following spray delivery

- Explore other delivery techniques

The following chapter includes work that is published in the review paper *Advances in keratinocyte delivery in burn wound care*<sup>1</sup> and as a bookchapter entitled: *Natural polymers: biomaterials for skin scaffolds*<sup>2</sup>

## 1.1 Burn injury

Burn injuries are complicated wounds to manage with a relative high mortality rate in especially large area burns and elderly patients [1]. Substantial tissue damage and extensive fluid loss can cause impaired vital functions of the skin. Rapid epithelialisation is mandatory to restore the barrier function of the skin and enhance healing. Pathological scar formation (hypertrophic scarring) can occur as a long term sequelae of delayed wound healing. When healing is delayed, the potential short term common complications include wound infection affecting the local healing process or systemic inflammatory and immunological responses which subsequently can cause life threatening sepsis and multi-organ failure. In the United States, approximately 400,000 fire/burn injuries were recorded in 2017 in a population of about 326 million, including a total of 3398 (0.85 %) reported fatal injuries [2]. Fortunately, survival rates have improved drastically over the last century due to advancements in burn care such as early surgical intervention, critical care support and wound care [3, 4]. However, despite further technological advancements in the last 30 years, survival rates have not improved significantly over the last three decades and now seem to be plateauing in countries with high-standard burn care [5–7]. Furthermore, since modern standard burn care allows the majority of patients to survive thermal injury, other outcome measurements aiming to improve quality of life become more relevant. For example, shortening length of hospital stay, decreasing the number of trips to the operating theatre and optimizing the quality of restored tissue. Functional and aesthetic outcome of the restored tissue are reflected by scar quality in

---

<sup>1</sup>DOI: 10.1016/j.addr.2017.06.012

<sup>2</sup>Paperback ISBN: 9780081025468, expected publication date: 1<sup>st</sup> of July 2019.

terms of pigmentation, pliability, sensation, hair growth and function (prevention of scar contraction). All of these factors require a specialized approach aiming on regeneration of tissue instead of tissue repair. Progress in short term results (life saving wound coverage) remains essential. Subsequently, advances of long term results are desired to facilitate the need for quality of life improvement of the increasing population of burn survivors. Answers to these challenges are sought in the field of tissue engineering. Although, advances in engineered skin equivalents and cell-delivery to the wound bed are emerging in burn care, they currently do not meet the expected results and translation to clinical practice is challenging. Keratinocyte delivery was the first skin cell transplantation successfully translated to clinical burn care. In the last four decades this method has been investigated widely and numerous researchers have contributed to a variety of improvements.

## **1.2 Skin**

### **1.2.1 Epidermis**

The skin is the largest organ of the body and has a barrier function, preventing the passage of water, electrolytes and pathogens (Figure 1.1). The epidermis is predominantly formed from highly specialized epithelial cells called keratinocytes. Other cells which can be found in the epidermis include Langerhans' cells, melanocytes and Merkel cells, which are responsible for immune regulation, pigmentation and sensory function. Keratinocytes play a key role in epidermal restoration following injury through proliferation and re-epithelialisation (Figure 1.2). Solely epidermal injuries will achieve re-epithelialisation from proliferated keratinocytes and heal by regeneration without scarring [8, 9]. Differentiated keratinocytes perform their barrier function through the provision of a mechanical barrier in the formation of a keratinised layer and by reacting to invasion of pathogens via release of pro-inflammatory mediators which subsequently attract leukocytes to the site of invasion.

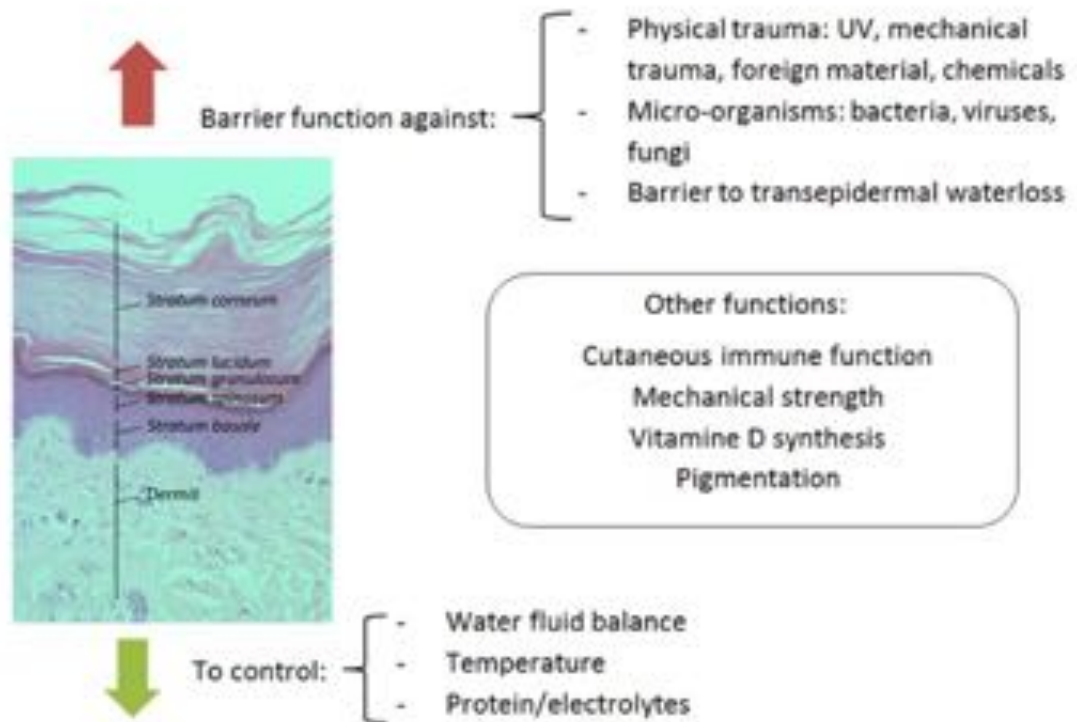


Figure 1.1: Layers and function of the skin. The uppermost layer of the skin is the epidermis. The epidermis consists of 5 main layers described from deep to superficial: stratum basale, stratum spinosum, stratum granulosum, stratum lucidum and stratum corneum. The epidermis has two distinct functions: a protective barrier function against trauma and fighting off pathogens as well as a controlling function regulating body temperature, fluid and electrolyte balance. Other functions of the epidermis include production of vitamin D, pigmentation, providing mechanical strength and it has a role in cutaneous immune function. [Source: histology image provided by Dr. GM Reynolds PhD CSci FIBMS, Liver Unit of Queen Elizabeth Hospital Birmingham, UK. Image adapted by Britt ter Horst, with permission from G M Reynolds.]

### **Keratinocyte differentiation and proliferation markers**

Keratinocytes proliferate from the basal cells of the innermost layer of the skin (stratum basale). The epidermal stem cells are attached by hemi-desmosomes to the stratum basale and can divide into either more stem cells, which persist indefinitely and to maintain the layer's regenerative capacity, or into transit amplifying cells which have limited division potential. As the transit amplifying cells continue to divide and proliferate, differentiation occurs. Throughout this differentiation process, the keratinocytes migrate upwards towards the stratum spinosum and stratum granulosum to eventually become

corneocytes which form a relatively impermeable outer layer, the stratum corneum. Once fully differentiated, these corneocytes lose their nucleus and cytoplasmic organelles and will eventually be shed off via desquamation. The estimated time for turnover from epidermal stem cell to desquamation in healthy human skin is around 39 days [10]. During this process, keratinocytes express several differentiation proteins including keratins which are intermediate filament proteins in epithelial cells. Keratins play a host of important function including the provision of structural support, protection of epithelial cells from mechanical and non-mechanical stress and the regulation of apoptosis and protein synthesis [11]. There are 37 known functional human epithelial keratin genes, divided in type 1 and 2 genes. Mutations in these genes are associated with skin diseases such as epidermolysis bullosa simplex (keratin 5, 14) with structural weak epidermal basal cells or epidermolytic hyperkeratosis (keratin 1 and 10) [12]. Keratin expression is frequently used as a marker for epidermal proliferation and differentiation in cell culture, with keratin 14 (K14) being used for the basal layer and keratin 10 for the spinous layer. Other differentiation markers starting at the basal layer are K5, and K15, spinous layers K1 and K10, transglutaminase and involucrin, at the granular layer. Filaggrin, loricrin and caspase-14 activation are hypothesised to play a role in terminal keratinocyte differentiation [13–15] (Figure 1.2).

### **Factors promoting keratinocyte differentiation**

A major regulator of keratinocyte differentiation is the calcium gradient. Extracellular calcium concentration is lowest in the stratum basale and gradually increases until the stratum granulosum. Elevated levels of extracellular calcium concentrations stimulate formation of intercellular contacts and the increase of intracellular free calcium concentrations via transmembrane calcium influx, which subsequently initiates differentiation via stimulation of the calcium receptor (CaR) [14]. This has consequences for the culture technique of keratinocytes *in vivo*, high calcium concentration induces differentiation, whereas in low calcium concentration keratinocytes remain proliferative [14–16]. E-cadherin provides ad-

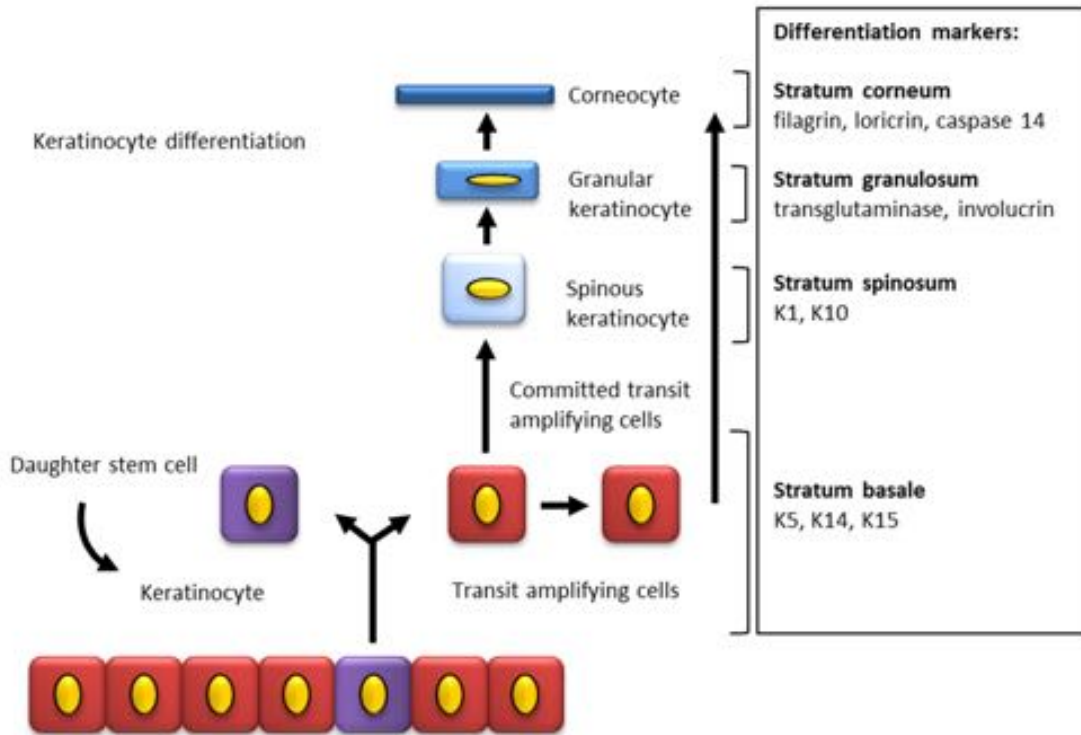


Figure 1.2: Keratinocyte differentiation and markers. Diagram is showing differentiation of keratinocytes in the epidermis with expression of stratification markers. Basal keratinocytes express Keratin 5, keratin 14 and keratin 15. When keratinocytes differentiate they move upwards into the suprabasal layers: stratum spinosum, stratum granulosum and finally stratum corneum. Differentiating keratinocytes express specific markers in each epidermal layer. [Source: Britt ter Horst]

herens junctions for adhesion between cells which is crucial for keratinocyte differentiation. In addition, following a signalling pathway e-cadherin can increase the intracellular calcium concentration [14, 17]. Furthermore, 1,25-Dihydroxyvitamin D3 (Vitamin D3) is known to influence keratinocyte differentiation by regulating gene expression and modulating calcium concentrations [18, 19]. Logically, factors that promote proliferation will inhibit differentiation of keratinocytes. Factors known to promote proliferation are TGF- $\alpha$ , vitamin A, transcription factor p63 and epidermal growth factor (EGF).

## **Keratinocyte interaction with other epidermal cells**

Within the epidermis, keratinocytes interact with other surrounding cell types for example, melanocytes. Melanin production (melanogenesis), occurs in the melanocytes and protects the DNA of melanocytes and keratinocytes from ultraviolet radiation and contributes to the colouration of the skin. Keratinocytes take up melanin via the melanin containing melanosomes produced by melanocytes [20]. The interactions between keratinocytes and fibroblasts in wound healing have been well described in literature, where a double paracrine signalling concept is proposed. Keratinocytes instruct fibroblasts to produce growth factors and cytokines such as keratinocyte growth factor, fibroblast growth factor-7, GM-CSF and IL-6 [21]. Consequently, expression of these growth factors initiates keratinocyte proliferation. The transcription factor activator protein-1 seems to play an important role in this process [22]. Furthermore, under the control of keratinocytes, fibroblasts can obtain a myofibroblast phenotype, which is important for wound contraction [21].

### **1.2.2 Dermis and basement membrane**

Underneath the epidermis, the dermal layer acts as a support network, providing strength and elasticity to the skin. Fibroblasts are the key cells of the dermis. Fibroblasts are responsible for the production and maintenance of the extracellular matrix which is formed by fibrous components (collagen and elastin) embedded in non-fibrous elements such as proteoglycans and glycosaminoglycans (GAGs). Collagens are the main structural element of the extracellular matrix (ECM) and provide tensile strength, regulate cell adhesion and support migration. Other cellular components include endothelial cells, smooth muscle cells and mast cells [23]. The vascular deep and superficial plexus lie within the upper and lower part of the reticular dermis respectively and supply the dermis and epidermis. The epidermis and dermis are firmly connected by the basement membrane, and the epidermal-dermal junction is bordered and stabilized by the anchoring of keratinocyte-derived collagen (type VII) fibrils into the dermis. Additionally, collagen XVII, a struc-

tural component of hemidesmosomes, mediates the anchoring of basal epithelial cells to the basement membrane [24]. If this junction is disrupted, serious morbidity such as seen in epidermolysis bullosa can occur [12]. Several structures originate in the dermis and extend into the epidermis such as sensory nerves, sweat glands and hair follicles. Hair follicles are lined with epidermal keratinocytes and contain multipotent stem cells [25]. Therefore, if the dermis is only partially injured these adnexal structures can deliver cells that can proliferate, migrate and regenerate the epidermis. However, the dermis lacks the intrinsic capability of regeneration and heals by fibrosis and scar formation. Sensory nerves are responsible for mediating pain and itch, control inflammation and there is evidence that shows that they may also influence the remodeling phase [9].

## **1.3 Wound healing and keratinocytes**

### **1.3.1 The role of keratinocytes in wound healing**

The skin barrier function can be disrupted by trauma such as a thermal injury. Wound healing usually occurs via four overlapping phases; haemostasis, inflammation, proliferation and remodeling. Normally this process is sufficient to allow the skin to repair itself after injury. However, extensive skin loss, as seen in burn victims, requires intervention to allow for tissue restoration. Burn injuries are often caused by heat, however, electricity, radiation, chemicals or friction can also result in similar injuries clinically [26]. Following thermal injury, a complex healing process will start with the involvement of numerous specialised and interacting cells, molecules and pathways. The cellular response involves macrophages, platelets, fibroblasts, epithelial and endothelial cells. In addition to the various cellular interactions, proteins and glycoproteins such as growth factors, cytokines, chemokines, inhibitors and their receptors can also influence healing. Although, burns heal differently from normal wound healing, the phases of healing remain the same [27]. Keratinocytes and fibroblasts play an important role in the proliferative phase which is focused on the replacement of the damaged ECM and restoration of tissue structure

and function. Activation of keratinocytes and fibroblasts by macrophages via cytokine and growth factor release causes angiogenesis, collagen production, ECM production and epithelialisation [28].

### **Angiogenesis**

The restoration of the vascular network is essential as angiogenesis supports cell activity by providing oxygen and nutrients to the wound bed. Once endothelial cells are activated by macrophages, they loosen their cell to cell junctions in order to migrate. This process as well as endothelial proliferation is encouraged by a hypoxic and acidotic environment which is typically found in wounds. Finally, revascularisation occurs when sprouted vessels organise into capillary networks. Vascularisation consequently neutralizes the hypoxic and acidotic wound environment and leads to decreased production of angiogenic factors. This eventually results in reduction of endothelial cell migration and proliferation [8, 29].

### **Epithelialisation**

Within hours of injury re-epithelialisation starts with a vital role being played by keratinocytes. The quantity of epidermal stem cells residing in stem cell niches such as in the hair follicles, sebaceous glands and basal layers of the interfollicular epidermis determines the regenerative capability of the skin [8, 25]. Activated by growth factors released by macrophages, keratinocytes migrate to the wound bed and fill the defect (Figure 1.3). In order for keratinocytes to start their migration they undergo phenotypical alterations by loosening of intercellular adhesions, although some desmosome contacts are sustained [8]. Furthermore, cells can separate from the basal layer once hemidesmosomes are disrupted which allows them to migrate laterally [8, 30]. When integrin receptors are expressed, the keratinocytes flatten and the altered basal keratinocytes migrate over the granulation tissue to form a monolayer of epithelial cells, but remain under the non-viable eschar of the burn wound. While moving they secrete proteolytic enzymes that enable the degradation of provisional matrix and promotes further cell migration [31]. After a confluent

sheet of cells covers the wound bed, the cells then divide to form a multi-layered stratified epithelium and mature under the influence of TGF- $\beta$ 1 and TGF- $\beta$ 2 [32]. Keratinocytes play a vital role in especially the proliferative phase of burn wound healing leading to epithelialisation and restoration of the vascular network. For this reason and the possibility of *in vitro* keratinocyte culture, keratinocytes are considered an excellent candidate for cell transplantation.

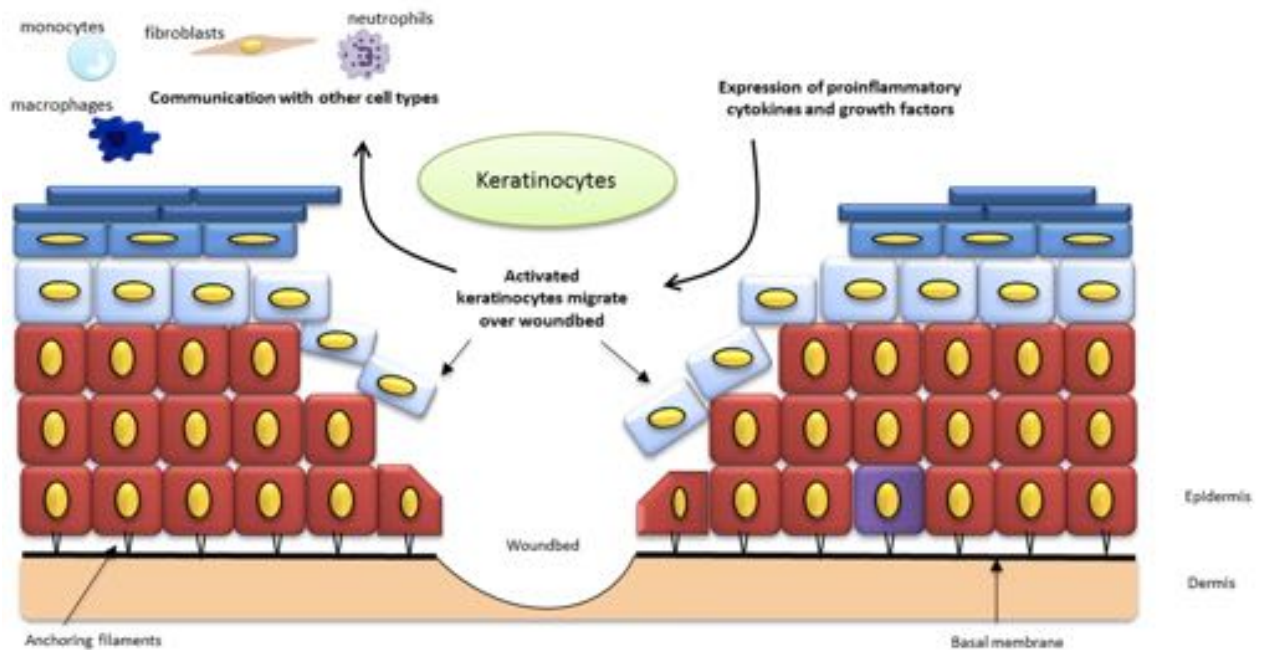


Figure 1.3: Role of keratinocytes in re-epithelialisation. Schematic illustration of a skin injury with keratinocytes as key cells. Keratinocytes are activated via pro-inflammatory cytokines and growth factors released in the wound bed. Once activated, keratinocytes from the wound edges and dermal appendages migrate over the provisional matrix and finally close the defect in a process called epithelization. When the basal layer is spared from injury, basal keratinocytes can support this process by upward migration as occurs in non-injured skin. Activated keratinocytes communicate with other cell types present in the epidermis. Epithelial cells proliferate and differentiate to achieve a stratified epithelium with restoration of the barrier function of the skin. Maturation of the wound continues over a period of several months with fibroblasts remodeling the underlying dermis.

### **1.3.2 Pathophysiology of burn injury**

Major burn injury, defined as approximately 20% of the total body surface area (TBSA) burned, causes burn shock due to severe haemodynamic and haematopoietic dysfunction [27] secondary to immediate evaporative and direct fluid losses [33], extensive loss of proteins, reduced colloid oncotic pressure and wound oedema development. Without intervention the fluid loss will result in desiccation of deeper tissues and further cell death leading to an increase in wound depth. A moist wound bed is necessary for epithelial cell movement and therefore for successful re-epithelialisation [9]. Furthermore, with disruption of the barrier function of the skin, microorganisms have easy access and when entering the microcirculation can cause systemic infection. Presence of these acute systemic responses are related with increased morbidity and mortality numbers [34, 35], especially in the elderly [1].

### **1.3.3 Rationale for keratinocyte transplantation**

Traditional therapy for severe burns is surgical debridement and autologous skin graft. However, with extensive burn injury healthy donor site is scarce and alternatives to restore skin function are necessary. When rapid epithelialisation can be achieved the skin barrier function is restored and this can determine a patient's likelihood of survival. Clearly, it is important in the treatment of a burn injury to focus on quick re-epithelialisation. Therefore, development of successful and efficient autologous skin replacement techniques is highly desirable. Wound closure will not occur without epithelialisation and epithelialisation will not occur without the presence of keratinocytes in the wound bed [8]. Therefore, keratinocyte transplantation was introduced as part of the burn wound care arsenal over 30 years ago. However, the original autologous keratinocyte transplantation technique has several disadvantages which has spurred researchers to seek for improvements in cell culture technique, delivery systems and also the optimisation of the timing of keratinocyte transplantation [36].

## 1.4 Cell transplantation technology

### 1.4.1 Cell source

Keratinocytes and their progenitor cells can be sourced locally from stem cell niches in hair follicles. Several stem cell niches are known: mesenchymal stem cells (MSC) resident in the dermal papilla and multipotent hair follicle stem cells (HFSC) and melanocyte stem cells in the superior bulge [37]. HFSCs are essential for normal morphogenesis of hair follicles, sebaceous glands and contribute to formation of the three epithelial cell lines [38]. Progenitor cells also reside in the bone marrow and could arise from embryonic cell lines [39].

### 1.4.2 Historical development of keratinocyte culture

The first successful *in vitro* human keratinocyte expansion, achieved by Rheinwald and Green in 1975, paved the way towards autologous cell transplantation in burn care [40]. Keratinocytes were successfully cultured in the presence of fibroblast feeder cells. However, to prevent these fibroblasts from outgrowing the keratinocyte population, irradiated murine 3T3 fibroblast feeder cells, which have lost their mitotic ability but remain metabolically active, were used [40]. Besides the use of feeder cells, culture media often contains fetal bovine serum with growth factors, hormones and antibiotics [40–42]. Keratinocytes are able to be grown into colonies and subsequently form a stratified epithelium and human keratinocyte stem cells were proven to have an enormous proliferation potential. Subsequently, small cell sheets of two or three layers of confluent keratinocytes were produced and not long after, the first human transplantation became a reality [43, 44]. Keratinocytes cultured for clinical use must have the regenerative capability to form an effective epidermis after transplantation. It is thought that *in vitro* differentiating keratinocytes do not contribute significantly to regeneration *in vivo* [45]. Instead, keratinocyte stem cells and their transient amplifying cells seem to have excellent regenerative capacities [46]. Thus, culturing keratinocytes that keep the ability to pro-

duce progeny once transplanted, seems key for successful epidermis formation following transplantation. The degree of differentiation *in vitro* can be controlled by the method of culture. Fully differentiated keratinocytes (confluent) multilayers as well as pre-confluent single cells can be produced and delivered to the wound bed [16, 47]. In a histological comparison of cultured pre-confluent and uncultured keratinocytes seeded on a collagen-GAG matrix in a pig model, both provided a fully differentiated epidermis in 14 days. A thicker and confluent cell layer, however, was obtained more rapidly with the cultured cells [48]. The original culture method has been the subject of much debate, because the murine fibroblast feeder layers can potentially result in transplantation of animal components with the keratinocyte product. Due to the serious risk of animal-derived disease transmission to human epithelium in the transplantation process, it is not advised to use undefined xenogeneic materials in the treatment of patients. Additionally, radioactive irradiation of murine fibroblasts in this technique is accompanied with higher costs and potential uptake of irradiated DNA via the murine fibroblasts into the transplanted keratinocytes might cause cell destruction [49].

### **1.4.3 Progress towards xenobiotic free culture techniques**

To limit or exclude the transmission risk, other keratinocyte culture protocols without feeder cells and limited or no use of xenogeneic media products have been developed [16, 47]. Jubin et al. showed that human keratinocytes can be successfully expanded in co-culture with non-irradiated autologous human fibroblasts in Rheinwald and Green medium, but still supplemented with fetal bovine serum (FBS) to maintain their proliferative phenotype *in vitro* [50]. A further approach to minimise xenogeneic products in culture media was introduced when serum free medium was used for the expansion of keratinocytes with non-irradiated human fibroblasts on several substrates [51]. However, FBS still had to be used to expand the human fibroblasts initially. Although the culture media are free of serum, often other products used in the culture media still contain animal-derived proteins. This could be solved by the use of only human material, how-

ever the risk of infection remains and high costs in an already expensive process makes this option less favourable. Successful culture of human keratinocytes in a serum-free and feeder-free culture was demonstrated *in vitro* in a skin equivalent model by Coolen et al. With the addition of collagen type IV, serum substitute and keratinocyte growth factor (KGF) a differentiated epidermis could be formed [52]. Lamb et al. demonstrated that although keratinocytes grown in serum-free and feeder-free conditions did show sufficient propagation, these cells were not able to support mature epidermis formation in an *in vitro* skin model. However, when re-introduced to serum-containing media they then did form a stratified epidermis. Moreover, when heat-inactivated serum was used an improved stratified epidermis was formed, indicating that serum products also contains (heat-sensitive) factors that can inhibit *in vitro* epidermis formation [53]. Lenihan et al. compared three commercially available feeder-free media systems; CnT-07 medium (CellnTech, Bern, Switzerland), EDGS (Gibco), S7 (Gibco) with the original Rheinwald and Green method [40] for expansion of human keratinocytes for clinical usage. A maximum of 3 weeks culture time (passaged twice) was allowed, as the ideal transplantation window was considered between 4 and 20 days. They found that all three feeder free culture media supported keratinocyte growth. However, the only fully xenobiotic free media (S7) had a low cumulative population doubling time and therefore did not reach sufficient cell numbers to be considered for clinical usage at day 21 and was therefore excluded from further analyses [54]. Using feeder-free and serum-free media is less labour intensive and beneficial for use in the clinical setting, further research will have to show whether keratinocytes maintain their proliferative potential *in vivo*. Besides elimination of xenobiotic materials from culture media, the elimination of antibiotics is a further goal to improve keratinocyte cell expansion for usage in the clinical setting [55].

#### **1.4.4 Additions to keratinocyte culture**

To further encourage and optimise skin regeneration following burn injury, improvements have been made to the keratinocyte transplantation process. These have included the

addition of multiple other cell types and growth factors during keratinocyte culture or transplantation. The addition of melanocytes in the keratinocyte culturing process has been proposed to solve the problem of potential irregular pigmentation of the post burn scar. Co-culturing of keratinocytes with melanocytes has been investigated in patients with vitiligo and in full thickness wound healing in animal models [56–59]. In humans, more evidence is available for uncultured cell suspensions containing keratinocytes and melanocytes for the treatment of hypopigmented lesions [60–63]. However, these pilot studies are limited by small sample sizes and lack of controls. Controlled clinical studies are needed to support the findings before this technique can be accepted as standard clinical practice. Cultured epithelial autografts lack a vascular plexus and burn wounds often have insufficient vascularisation due to the disruption of the dermal layer. Therefore, approaches to promote angiogenesis via the addition of autologous or allogenic endothelial cells into skin grafts have been proposed [64–66]. Also, adipose derived stem cells (ASCs) have received attention with respect to their potential to enhance wound healing. Huang et al. seeded human ASCs onto a dermal acellular skin substitute *in vitro* to enhance vascularisation. When transplanted to full thickness wounds in nude mice, an increase in blood vessel density was found two weeks post transplantation compared to controls [67]. Another approach is to add growth factors like epidermal growth factor (EGF) [68]. Additionally, co-delivery of cultured keratinocytes with EGF in a fibrin matrix demonstrated improvement of epidermal regeneration in full thickness wounds in a murine model [69]. Furthermore, Supp et al. genetically modified keratinocytes with an overexpression of vascular endothelial growth factor (VEGF) to stimulate angiogenesis in skin substitutes in animal studies [70–72]. Besides adding factors, modifications of the 3D structure of skin substitutes to stimulate faster ingrowth of vascular structures have also been proposed [73]. Of interest from a tissue engineering perspective, is whether transplanted cells actually survive and function *in vivo*.

## 1.5 Keratinocyte viability after transplantation

Cell survival of transplanted keratinocytes *in vivo* is of great interest for tissue engineering purposes. Vernez et al. evaluated the cell viability and apoptosis balance in clinical samples taken from cultured epidermal autografts prior to transplantation [74]. Although, all samples showed high levels of cell viability and low levels of apoptosis, variable biological activity of certain parameters between samples of different patients was observed. It was suggested that this could impact on therapeutic efficacy [74]. In a pig model Navarro et al. found no altered cell viability before and after spraying a suspension of cultured keratinocytes to full thickness wounds [75]. Duncan et al. examined cultured human keratinocyte proliferation measured with the MTT assay after spray delivery to a de-epidermalised dermis (DED) *in vitro* and found no significant cell death or reduced cell proliferation [41]. These studies seem to support that cells remain viable and maintain proliferative capability after spray cell delivery to a wound bed.

## 1.6 Methods of keratinocytes transplantation

### 1.6.1 Introduction: grafting of burn wounds

Ambroise Paré (1510–1590 CE) was probably the first to describe the surgical intervention for early excision of burn wounds [76]. Surgical burn care has progressed tremendously since then and methods which have now become well established in burn care include early excision of burn wounds, the development of autologous and allogenic skin grafts and the use of skin substitutes [77, 78]. Techniques involving transplantation of healthy human skin to damaged areas are still the gold standard in deep or full thickness burn wounds. However, challenges arise when large areas are affected and donor sites are scarce. Subsequently, many skin graft expansion techniques have been developed to reduce donor site size, these techniques include meshing of the graft (maximum expansion ratio of 1:9), modified meek technique (expansion ratio of 1:9), epidermal blister grafting (expansion

ratio of 1:1) and several techniques of micro grafting such as epidermal CelluTome™ micro-grafting (expansion ratio of 1:6), or XpansionKit® micro-grafting (maximum expansion ratio: 1:100). Developers of cellular based techniques claim to deliver even higher expansion rates, such as cultured epithelial sheets (expansion rate 1:1000) and uncultured cell suspensions (maximum expansion rate 1:100) [79–81]. However, to the knowledge of the authors no other studies have been able to support these findings. Furthermore, procedures to harvest skin are time consuming, can lead to longer healing times with prolonged hospital stay and can be accompanied by donor site complications. Additionally, skin grafts do not always meet the desired cosmetic outcomes. Therefore, methods to enhance the results of skin grafting and alternatives to it have been subject of much research in the last few decades. Specifically, progress towards a permanent epidermal replacement or its improved regeneration is the main goal of cellular based therapy. In Figure 1.4 different methods of autologous keratinocyte transplantation are schematically summarized.

## **1.6.2 Cultured keratinocyte sheets**

### **Cultured autologous keratinocyte sheets**

In 1981, O’Connor et al. reported the first transplant of cultured autologous keratinocytes to treat a burn injury [44]. Cultured epithelial autografts (CEA) were developed to replace the epidermis and restore the barrier function of the skin [82–84]. In the last three decades CEAs have been adapted and introduced to the clinical setting (Figure 1.5). Nowadays, several commercialised bioengineered skin products derived from autologous cells are available. In general, clinicians harvest autologous skin and the company produces a graftable substrate seeded with the autologous cells for clinical use in approximately 2 weeks (Epicel, Genzyme, Cambridge, MA and Laserskin, Fidia, Italy). The timeframe wherein viability of the grafts can be ascertained (shelf-life) is 24–48 hours. These services will often involve high costs and a certain waiting time and narrow application timeframe. In 2007, the FDA approved the use of CEAs for use in patients with deep dermal or full thickness burns greater than, or equal to 30% TBSA (Epicel,

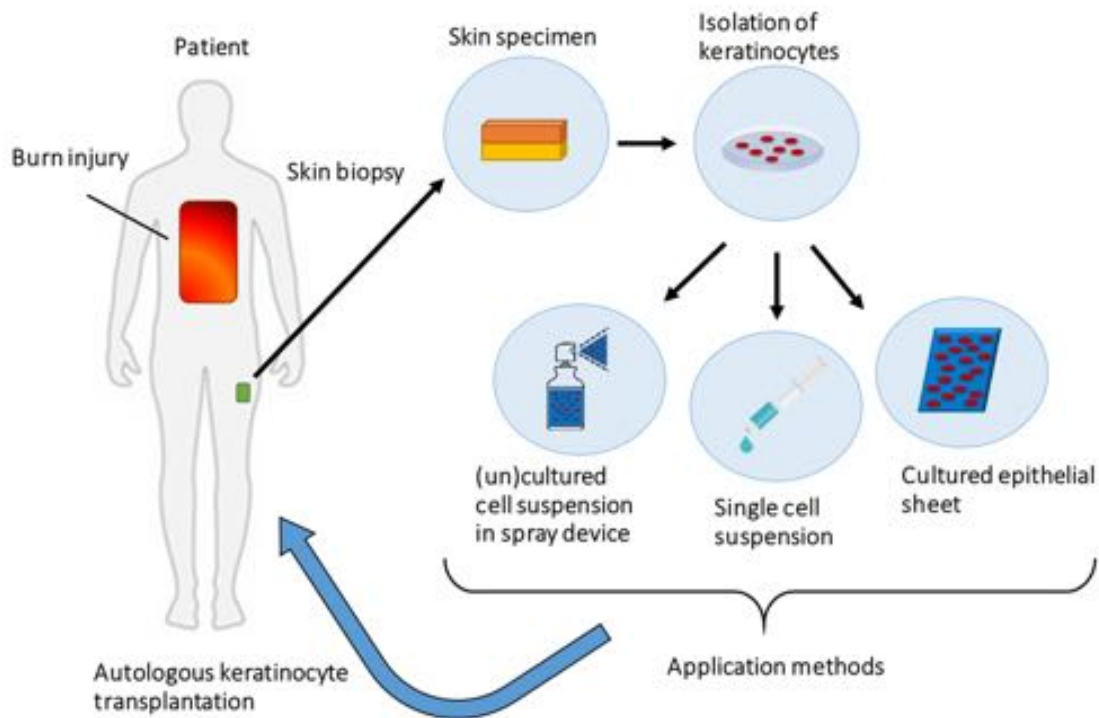


Figure 1.4: Methods of autologous keratinocyte transplantation to burn wounds. In patients with burn injury keratinocytes can be isolated from a small skin biopsy as illustrated above. The autologous keratinocytes can be cultured and delivered to the wound bed of the patient by several methods. First to be developed was a sheet of cultured epithelial cells, thereafter a single cell suspension applied to the wound by dripping from a syringe and latest development is application of cultured or uncultured cells in single-suspension with a spray device.

Genzyme, Cambridge, MA) [44, 82]. The main advantage of cultured epithelial autografts is that large areas of the body can be covered with autologous cells derived from a small biopsy and improvement in the speed of re-epithelialisation has been reported. In terms of cosmetic results, CEA seems to have better results when compared to wide mesh autograft in extensive burns [85]. However, several authors who have reviewed the use of cultured epithelial autografts in burn care have found variability in terms of graft take and cosmetic outcomes [47, 86, 87]. A major disadvantage of this technique is the long time interval between biopsy and grafting. Although the average culture time has improved from 5 weeks [44] to about 3 weeks [88, 89], variability among patients has

been described, especially among different age groups [90]. Following burn excision, the wound can be temporary covered with allograft and/or xenograft dressings for several weeks until CEA is ready. However, this is related to a higher risk of wound colonization and infection [47]. The ideal timing for keratinocyte transplantation is difficult to determine as it is dependent on several factors including hospital facilities and patient conditions [89, 91]. Furthermore, both short and long term clinical limitations such as the formation of bullae, poor take rates, fragility of the sheets and wound contractures have been reported [91–93]. These may be due to the lack of a dermal component that is necessary to support the new epidermal layer. The restoration of the dermis is important for the skin to regain mechanical strength and to facilitate adherence of the new or transplanted epidermis [37]. Although in one study, an advanced application technique with allograft wound bed preparation and combination of CEA with wide meshed autograft seems to improve take rates up to 84% [94]. Cell culture is an expensive process and the cost/benefit relationship of this method is heavily debated [95]. Finally, the potential of graft site malignancy after keratinocyte transplantation has been highlighted [96, 97]. However, the type of malignancy reported, squamous cell carcinoma, is also known to occur in burn wounds and scars in the absence of keratinocyte transplantation [98].

### **Dermal substitutes including cultured keratinocytes**

With a complete absence of a dermal component, the cultured keratinocytes are thought to be of limited value in treating full-thickness burns due to the poor quality of the resulting epidermis. Consequently, this has led researchers to optimise the wound bed via the use of allogenic or artificial substitutes prior to keratinocyte transplantation. A further approach is to grow or seed the cultured keratinocytes on a (dermal) substitute to facilitate secure transplantation and improve healing potential [83]. This concept was introduced by Hansbrough and Boyce in 1989 [99]. Many types of delivery systems have since followed, and have been extensively discussed in the literature throughout the years [84, 100, 101]. Limitations in keratinocyte cell culture methods and transplantation have

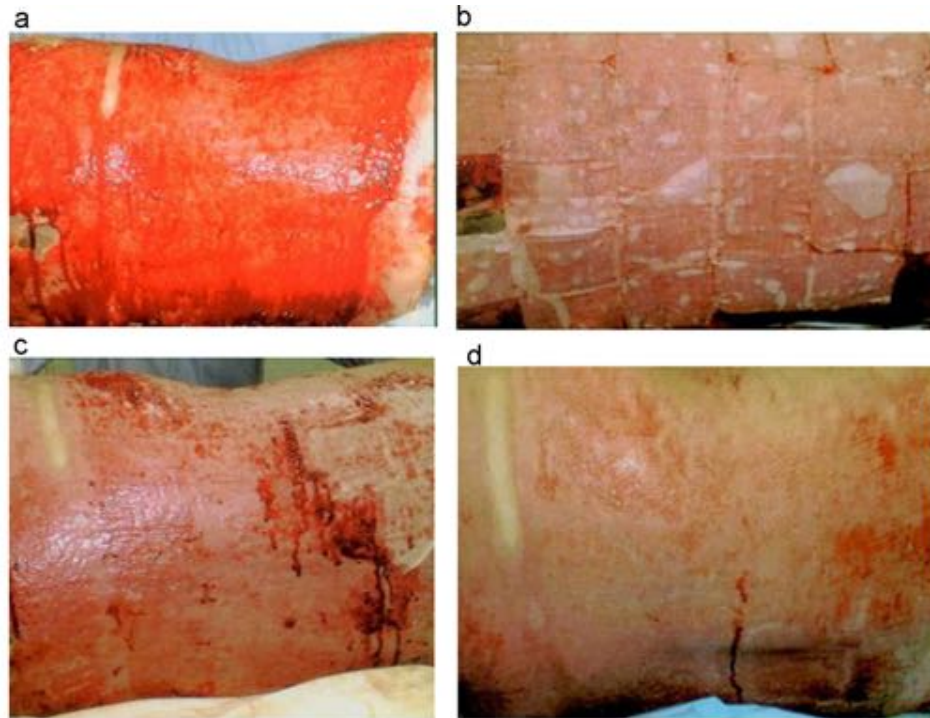


Figure 1.5: Burn wound coverage with cultured epithelial autografts applied in sheets. In this example, successful burn wound healing in about 2 weeks was achieved when the sheets were removed a week after application. a) Deep second degree burn in the back of a 29-year old patient after excision of the burn b) application of cultured keratinocyte sheets c) removal of sheets 8 days after surgery and d) complete healing 16 days after surgery. [Reprinted from Burns Volume 41, Issue 1, Pages 71–79, Cultured autologous keratinocytes in the treatment of large and deep burns: A retrospective study over 15 years, Celine Auxenfans, Veronique Menet, Zulma Catherine, Hristo Shipkov, Pierre Lacroix, Marc Bertin-Maghit, Odile Damour, Fabienne Braye, Copyright (2017), with permission from Elsevier.]

impeded the widespread use of this technique in the clinical setting. The use of single-cell suspension was introduced predominantly to shorten the culture time.

### 1.6.3 Autologous keratinocyte transplantation in suspension

To overcome the main negative features of epidermal sheets which are the long culture times and poor cell adhesion to the wound bed, delivery of cells in suspension has been investigated. While epidermal sheets contain cultured confluent cells that passed the phase of exponential growth, cell suspension delivery systems can be designed to contain pre-confluent cells. Ideally, these cells are harvested or passaged when reaching a 70–80%

coverage of culture dishes to ensure their proliferative capability and avoid confluence, hence the term pre- or sub confluent cells. When a sufficient cell number is reached (after approximately 2 weeks of culture), the cells are detached and suspended in a saline solution for clinical use. As differentiation *in vitro* is not desirable, keratinocytes in a pre-confluent suspension form are often preferred for transplantation (Figure 1.6). Nowadays, several commercially available spray cell delivery products are used clinically to enhance burn wound healing. These techniques can be categorised by the type and level of confluence of the transplanted cells.

### **Pre-confluent keratinocytes suspension**

The use of pre-confluent cells can shorten culturing time and facilitate more rapidly available cellular grafts, which in theory is likely to reduce the risk of wound infections and consequently the length of hospital stay [102, 103]. A commercial suspension consisting of autologous pre-confluent keratinocytes has been available since 2007 for aerosol delivery. Hartman et al. treated 19 patients with deep dermal face and neck burns with a spray apparatus with an estimated spray pressure of 8.2 mmHg, which seems to be a surprisingly low delivery pressure using autologous cultured epithelial cells of 80–90% confluence at the end of passage 0 [104]. An alternative commercially available cell spray system is Keraheal<sup>TM</sup>, which was developed by MCTT, Korea. This system utilises an autologous non-differentiated pre-confluent keratinocyte suspension, which is sprayed to the burn wound followed by fibrin spray application. The Keraheal<sup>TM</sup> methodology is similar to conventional CEA and requires 2–3 weeks of culture time, but the cells are provided in a suspension instead of sheet. To date, two single centre retrospective studies have evaluated the clinical outcomes of the sprayed cell suspension in combination with wide meshed skin grafts in a total of 39 (6 patients who died or were lost to follow up were excluded from follow up analyses) patients with severe burns. Graft take rate two weeks after application is surprisingly different between the studies, but after 8 weeks the take rates are both above 90%. A follow up of 1–2 years was achieved in both studies with



Figure 1.6: Spray delivery of cultured keratinocytes to enhance burn wound healing. In this example, a mixed depth burn to the abdomen was treated with solely sprayed cultured keratinocytes (no additional mesh grafting) 27 days after injury. The wound was considered to have healed completely 10 days after treatment. Unfortunately, long term outcomes in terms of scar quality were not available for this patient. [Reprinted from Burns Volume 36, Issue 3, Pages e10–e20, Sprayed cultured autologous keratinocytes used alone or in combination with meshed autografts to accelerate wound closure in difficult-to-heal burns patients, S. Elizabeth James, Simon Booth, Baljit Dheansa, Dawn J. Mann, Michael J. Reid, Rostislav V. Shevchenko, Philip M. Gilbert, Copyright (2017), with permission from Elsevier.

a Vancouver scar scale (VSS) assessment. Scar evaluation 12 months after surgery was lower in Lee et al. [103] with an average VSS of 3 compared to an average VSS of 5 in Yim et al. [102]. Various developers have introduced adjustments to the technique in terms of the application device, cell detachment process, confluency of transplanted cell and application setting in order to meet clinical needs.

## Uncultured keratinocytes suspension

A further approach is the use of uncultured autologous cells for direct application onto burn wounds without pre-processing in a tissue culture lab. In a single procedure, a small piece ( $2 \times 2$  cm) of skin is harvested by the surgeon and then placed in an enzymatic solution followed by manual scraping of the epidermal layer, the skin specimen is placed in a buffer solution and subsequently filtered before use. The company provides a kit which allows the clinical team to process the cells in a single treatment session without the need for a lab technician or transport of the cells elsewhere [86, 105]. The use of an uncultured mixture of autologous epidermal cells (keratinocytes, melanocytes, dermal fibroblasts) was introduced to clinical practice in 2005 as a standardized spray device under the name ReCell<sup>®</sup> (Avita Medical Europe Ltd., Melbourne, UK). The purported benefits of this system are the elimination of lengthy culture times and the delivery of a mixture of autologous epidermal cells [106]. Since its introduction, several studies have demonstrated promising outcomes with the use of ReCell<sup>®</sup> for acute burn wounds or in the treatment of hypopigmentation. These studies ranged from case reports to larger comparative studies [61, 107–111]. Although most papers have shown promising results, the potential value of spray cell transplantation in burns is difficult to evaluate due to the heterogeneity of the studies in terms of clinical outcomes explored, patient population, wound characteristics, type of treatment and study design [101]. Gerlach et al. used a similar approach with direct application of an uncultured autologous epidermal suspension on the wound bed using a fine needle spray in a single treatment session. Although, a small number of patients was treated and results were not compared to controls [105, 112]. The question arises whether a large wound area can be covered by the harvest of cells without expansion from a small skin specimen. In an *in vitro* study an expansion ratio of over 1:100 was calculated for uncultured cells sprayed with a density of 104 cells/cm<sup>2</sup> for an estimated surface coverage [81]. However, there is no other literature to support the claimed expansion rate. To allow the comparison of clinical data, it has been recommended by the National Institute for Health and Clinical Excellence (NICE)

that studies evaluating spray delivery of uncultured cells need to include at least: the time to 95% healing of the burn wound, length of hospital stay, scar assessment, physical function and cosmetic appearance of the burned area and compare these results with the current standard of care [113]. To date, randomized controlled clinical trials and non-commercial studies investigating effectiveness compared to conventional treatment are lacking. Challenges arise in consistent assessment for burn wound healing as objective non-invasive assessment tools have not yet been incorporated widely in routine burn care and might not be superior to visual expert assessment [27]. Therefore, researchers rely on subjective clinical assessments for acute burn wound healing and late outcomes in terms of scarring [114].

### **Allogeneic neonatal keratinocytes suspension**

Several research groups have explored the possibility of the transplantation of fetal allogenic cells with the purpose of stimulating regeneration of residual cells in the wound. Neonatal foreskin derived allogenic cells have low immunogenic properties which is preferred in tissue transplantation. This work has resulted in the creation of skin substitutes that have been seeded with allogenic cells such as Apligraf (Organogenesis, Canton, MA) and Orcel (Ortec International, Inc., New York, New York). Similar to the developments in autologous cell delivery, allogenic cell suspensions have also been investigated as an alternative method of cell delivery. A cell suspension, code named HP802-47, which contains allogenic neonatal non-proliferating human keratinocytes and fibroblasts in thrombin was developed for the use in chronic wounds. Multi-centre randomized controlled phase IIa and IIb studies were conducted and have demonstrated promising outcomes in wound closure of venous leg ulcers [115–119]. Subsequently, a double blinded Phase III study followed in North America and Europe comparing wound closure after HP802-247 treatment or placebo in venous leg ulcers. However, the study was unexpectedly halted in the preliminary stages due to disappointing results [120]. No clinical studies have been conducted for the treatment of burn wounds with HP802-247.

## **Other clinical studies using cell sprays**

Delivery of mesenchymal stem cell (MSC) to (burn) wounds is considered very promising due their capacity to differentiate into multiple lineages and potential beneficial effects on the immune response [55, 66, 121]. However, only few clinical studies investigated the use of mesenchymal stem cells to treat burn wounds have been performed so far [122–124]. Ueda conducted a pilot study of 10 patients treated with cultured mucosal epithelial autograft (CMEA) delivered to deep dermal burn wounds without adverse events and a healing time of approximately 12 days (range 7–14 days) [125]. Iman et al. compared spray delivery versus intradermal injection of autologous cultured keratinocyte-melanocyte suspension to treat hypopigmented burn scars in a total of 28 patients. Although patients might show a beneficial result with pigmentation, no statistical difference in type of application was found [60]. Cell transplantation techniques have changed significantly after the introduction of different cell-carriers and various forms of cell spray techniques. Nevertheless, some shortcomings of the suspension application technique have yet to be addressed. For example, spraying on an uneven wound bed that often also occurs on a curved body contour, can result in uneven spreading of the cell suspension or dripping off the wound bed [47, 126]. A potentially useful development of keratinocyte transplantation is to improve the method of delivery in order to optimise cell delivery to the designated area and stimulate cell adherence to the wound bed. More recently, cell transplantation exploiting hydrogel carriers have gained interest among researchers. In the past decade biomaterials to mediate cell delivery and accommodate cells in a 3D microenvironment have been investigated. A plethora of synthetic and natural polymers which may form hydrogels have been studied as potential cell delivery vehicles due to their ability to integrate with healthy tissue.

## 1.7 Hydrogels

Hydrogels are defined as polymer networks with the ability to swell and absorb water within their structure. Due to their hydrophilic nature and flexibility they are very similar mechanically to human soft-tissue. Both natural and synthetic hydrogels could be considered for tissue engineering. Natural hydrogels benefit from high biological affinity and are often easily degradable, but the risk of infection transmission and difficulties with purification has increased the popularity of synthetic hydrogels [127, 128]. Biopolymer gels can be formed out of polysaccharides or proteins. For example, polysaccharides obtained from plants (gum acacia, guar gum, starch, psyllium [129]), seaweeds (alginate, agarose, carrageenans), micro-organisms (dextran, gellan gum) or animal derived (chitosan, chitin, hyaluronic acid) and proteins gained from animal or human tissue (collagen, fibrin, gelatin, elastin) or animal products (silk sericin, silk fibroin) [130].

### Polysaccharides

Polysaccharides are often used in wound dressings as shown in Table 1.1, examples are calcium alginate, cellulose and chitosan-based dressings. The use of polysaccharides has also found its way in tissue engineering for wound healing. Polysaccharides consist of linked monosaccharides and are sourced from renewable resources such as plants and animals. As these resources are widely available in nature, polysaccharides are an attractive candidate for researchers. The most commonly used polysaccharides and proteins for skin repair applications are listed in Table 1.1.

#### *Alginate*

Alginate is a linear anionic polymer that consists of mannuronic acid referred to as M blocks and guluronic acid (G block) units. Alginates with a high proportion of G blocks are easier to process and seem to have lower immunogenicity and therefore, are more suitable for biomaterials [131]. Alginate is usually sourced from the cell wall of brown algae but can also be synthesized by certain bacteria. Its widespread use in biomedical

Table 1.1: Natural polymers and their properties commonly used for skin repair and regeneration. ECM = extracellular matrix. <sup>a</sup> polymer can be modified to be biodegradable, <sup>b</sup> starch derivatives have cell binding capacities, <sup>c</sup> derivatives are biodegradable.

Type	Polymer	Source	Degradation	Biodegradable	Cell binding
Polysaccharides	Agarose	Red algae	Non-degradable	No	Low
	Alginate	Brown algae	Ion exchange	No <sup>a</sup>	Low
	Carrageenan	Red algae	Ion exchange, enzymatic cleavage	No	Low
	Starch	Plants	Enzymatic cleavage	Yes	High <sup>b</sup>
	Cellulose	Plants, wood	Enzymatic cleavage	No	Low
	Chitosan	Crustaceans, fungi	Ion exchange	Yes	High
	Hyaluronic acid	ECM (animal derived), bacterial fermentation	Enzymatic cleavage	Yes	High
	Gellan gum	Bacteria	Thermal, enzymatic cleavage, ion exchange (hydrolytic degradation)	Yes	Low
	Dextran	Bacteria	Phagocytosis	Yes <sup>c</sup>	Low
	Bacterial cellulose	Bacteria	Enzymatic cleavage	No	Low
Proteins	Collagen	ECM (animal derived)	Enzymatic cleavage	Yes	High
	Fibrin	Blood (heterologous, autologous)	Enzymatic cleavage	Yes	High
	Gelatin	ECM, collagen	Enzymatic cleavage	Yes	High
	Elastin	ECM	Enzymatic cleavage	Yes	High
	Silk sericin	<i>Bombyx mori</i>	Thermal, pH responsive	Yes	High
Silk fibroin	<i>Bombyx mori</i>	Proteolytic	Yes	High	

applications is due to beneficial properties like biocompatibility, non-immunogenicity, simple gelation process, ability to control its degradation and relatively low cost. Alginate is a versatile polymer, its mechanical properties can be tuned by the type and concentration

of crosslinker [132]. Alginate can form hydrogels by ionic crosslinking with cations such as  $\text{Ca}^{2+}$ . The divalent cations will bind exclusively to the G blocks. Covalent cross-linking is another approach, but as the reagent can be cytotoxic a secondary cleaning step is often required. While covalent crosslinking is permanent, ionic crosslinking can be reversed. Also, photo-crosslinking under mild conditions has been introduced for *in vivo* gelation of alginate onto the eye [133]. Lack of cell adhesion ligands and its poorly controlled natural degradation have limited its suitability for some applications. However, alginate can be modified to gain higher cell adhesivity by peptide coupling such as arginyl-glycyl-aspartic acid (RGD) to the polymer [134, 135]. Degradation can be influenced by the amount of G blocks present, with higher content resulting in slower degradation. Oxidation of photo-crosslinked alginate prior to methacrylation has shown to speed up biodegradation due to a higher susceptibility to hydrolysis [136]. Commercially available alginate based wound dressings such as Kaltostat<sup>®</sup> and AlgiSite<sup>®</sup> are widely used in acute burn care, donor wound site coverage [137, 138], venous leg ulcers [139] and pressure ulcers [140]. Although (calcium) alginate dressings have been used for many years in wound care, clinical data is still poor as not many well-designed clinical trials have been conducted [141]. Numerous researchers have demonstrated that cells can be successfully encapsulated in alginate hydrogels [142, 143]. Alginate as a culture matrix can improve proliferation of microencapsulated human pluripotent stem cells [144] and supports viability and function of other cell types [132, 135, 145]. Alginate based macroporous systems for cell culture are now commercially available with different pore sizes to suit specific cell types. These sterile scaffolds are ionically gelled and then dried. After rehydration and cell seeding they turn into hydrogels [135]. The first transplantation of alginate beads with encapsulated pancreatic cells into the human body happened in the 1980's [146]. Despite attempts to encapsulate skin cells into alginate scaffolds [145], a similar development for alginate based cellular regenerative scaffolds to treat wounds has not been established.

## *Cellulose*

Cellulose is the most abundant biopolymer in nature and can be derived from a variety of organisms such as plants (vascular plants or algae) and bacteria (*Acetobacter Xylinum*). Biosynthesis of bacterial cellulose fibrils eventually results in the development of a large nanofibrous-network on the outer side of the bacterium with a macroscopically gelatinous appearance [147]. These fibers are around 20–100 nm thick and oriented in an uni-directional fashion [148]. Cellulose derived from plants or specifically wood generally have a smaller diameter (3–5 nm) forming bundles of 20–50 nm thick [149, 150]. Other differences are the higher water holding capacity and lower crystallinity of bacterial cellulose [147]. Cellulose hydrogels can be formed by crosslinking solutions of cellulose derivatives such as methylcellulose and sodium carboxymethyl cellulose [151].

Hydrogels can also be formed by ion-crosslinking of negatively charged nanofibrillated cellulose (wood-derived) with divalent or trivalent cations [149, 152]. Bacterial cellulose has gained interest for the development of skin replacement therapy because of its 3D architecture with high mechanical strength, high water holding capacity and biocompatibility. Interestingly, its natural negatively charged surface can be altered with or without [153] the use of matrix ligands to improve cell attachment.

Clinically available acellular products such as Biofill<sup>®</sup> (Fibrocel) or Nanocell<sup>®</sup> (Thai Nano Cellulose Co Ltd), are available for the treatment of a variety of wounds (burns, chronic ulcers, following excision of skin cancers and as donor site dressing) [154, 155]. Recently, a bacterial cellulose hydrogel was proposed as cell carrier and wound dressing to stimulate wound healing in a full thickness mice model. Bacterial cellulose hydrogel was mixed with an acrylic acid solution and cells (human keratinocytes and dermal fibroblasts) were seeded into the hydrogel. The results, as shown in Figure 1.7, indicate that this scaffold seems to be suitable as cell carrier and full thickness wound healing in a mice model was achieved, however the scaffold was not compared to a control treatment [156].

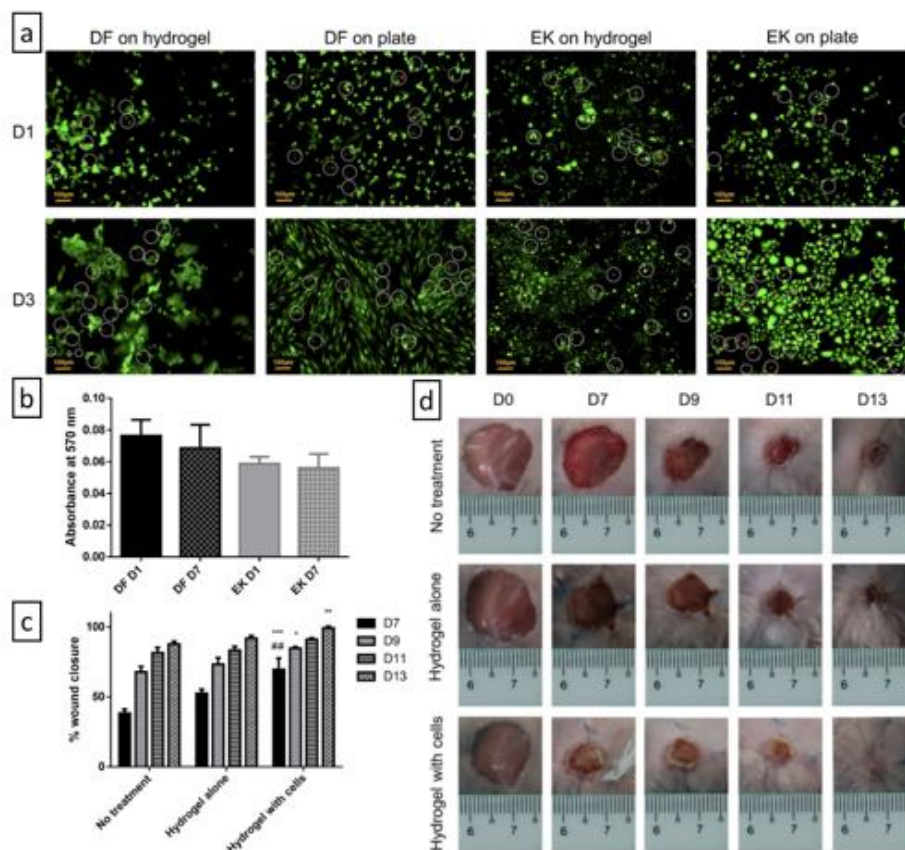


Figure 1.7: Bacterial cellulose cellular scaffold. Live and dead stain of dermal fibroblasts (DF) and epidermal keratinocytes (EK) on the bacterial cellulose hydrogel and on culture plastic at day 1 and day 3 (a). MTT assay results for proliferation of cells on the hydrogel at day 1 and day 7 showed no significant differences between any of the groups (b). Percentage of wound healing of full thickness punch biopsy wounds in rats treated with bacterial cellulose hydrogel with and without cells and no treatment control. Significant differences with the no treatment group are marked with (\*), (\*\*), (\*\*\*) for ( $p < 0.05$ ), ( $p < 0.01$ ) and ( $p < 0.001$ ) respectively (c). Clinical photos taken at day 0, 7, 9, 11, 13 (d). Figures were adapted from Yun et al. [156], open access article, published under Creative Commons Attribution 4.0 International License (<http://creativecommons.org/licenses/by/4.0/>).

### *Chitosan*

Chitosan is a polysaccharide obtained from de-acetylated chitin which is the structural component in the exoskeleton of crustaceans or fungi [157]. The polymer is named chitosan when over 50% of chitin is de-acetylated. It is a weak base that can be dissolved in acidic solutions, this could be a limitation for applications where solubility in a pH neutral environment is desired. Chitosan has unique characteristics as it is one of few cationic natural polymers and can form polyelectrolyte complexes with polymers of the opposite

charge [158]. Chitosan has gained interest for tissue engineering purposes due to its many advantageous properties: it is non-toxic, promotes haemostasis, high cell adhesivity and is biodegradable [131, 159]. A relatively rapid biodegradation *in vitro* has been described with the use of lysozyme [160]. Degradability of chitosan can be influenced by a higher degree of deacetylation [160] and molecular weight [161], resulting in slower degradation in the body. However, its degradation in the body is not yet fully understood [162]. Crosslinking techniques that successfully formed hydrogels include ionic [163], chemical [164], physical crosslinker [165] and photo-polymerization [166]. But chitosan on its own has weak mechanical properties and modifications or blending with other polymers is often required.

The positive charge of chitosan is of particular interest for researchers as adherence to negatively charged surfaces or cells is increased [167]. As a wound dressing chitosan has shown to be haemostatic, anti-microbial and improve wound healing [168], especially in burn wounds [169]. Its antimicrobial properties are thought to be caused by the ionic bonding of chitosan onto negatively charged bacteria surfaces leading to altered permeability with intracellular content being released and ultimately cell death [170]. The influence of chitosan on platelets is not well understood, but platelets seem to adhere to chitosan derivatives and aggregate causing a thrombogenic effect [171]. The haemostatic effect of chitosan has led to commercially available dressings such as HemCon<sup>®</sup> bandage (HemConMedical Technologies, Inc.) and Celox<sup>®</sup> gauze (MedTrade) marketed for the local treatment of bleeding wounds [172]. Chitosan is a bioactive polymer that has a promise as scaffold for tissue regeneration as it is cytocompatible towards many cell types [173]. Hilmi et al described the use of a chitosan 3D culture scaffold with incorporation of human dermal fibroblasts and reported cell survival up to 14 days. The interconnected pores that were formed were considered to support fibroblast attachment to the scaffold (Figure 1.8b-d) [174]. Keratinocytes and especially fibroblasts seem to adhere better onto chitosan with a lower degree of deacetylation as shown in Figure 1.8a [175].

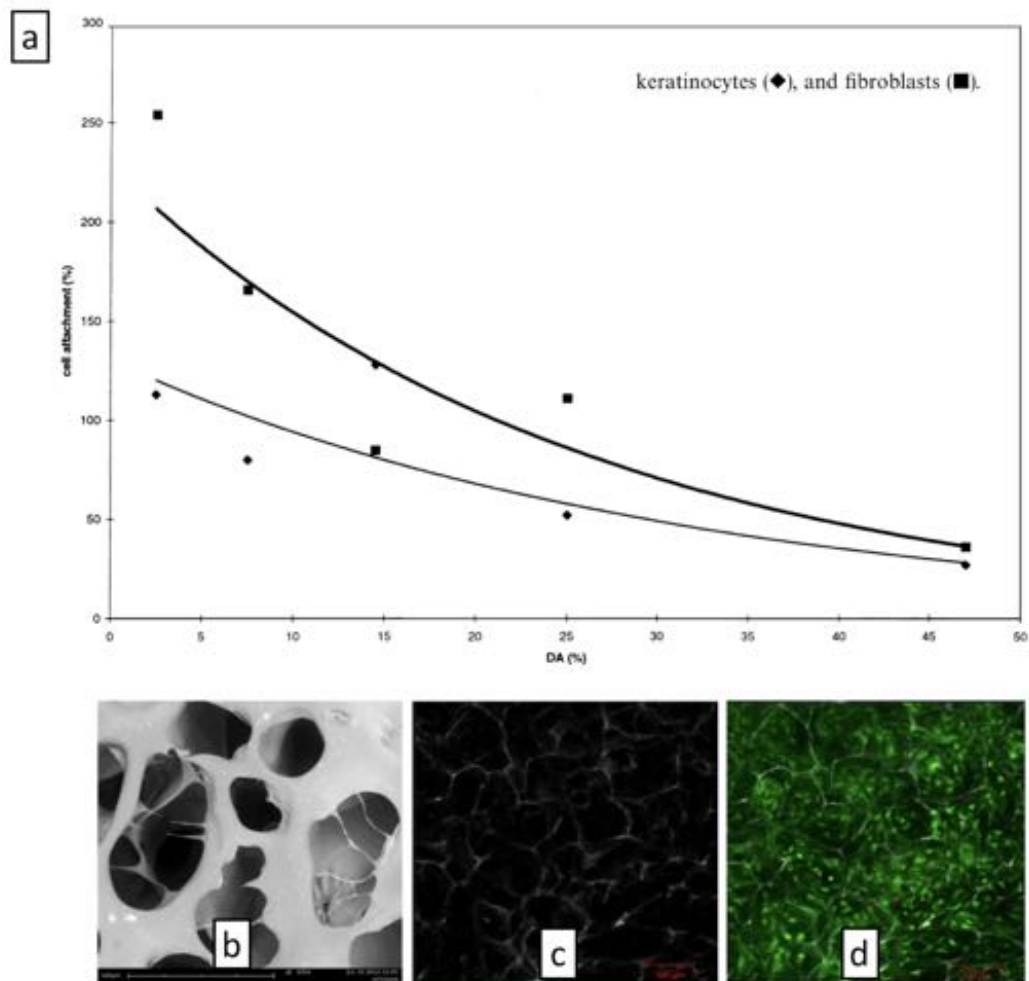


Figure 1.8: Cell compatibility of chitosan scaffolds. Cell adhesion of keratinocytes and fibroblasts to chitosan decreases when degree of acetylation (DA%) increases (a). Scanning electron microscope of a porous chitosan scaffold with interconnected pores, scale bars  $140\ \mu\text{m}$  (b). Confocal microscopy images of the scaffold used as 3D templates for human dermal fibroblasts culture showed homogeneously spread and viable cells, scale bars  $100\ \mu\text{m}$  (c, d). Permission to publish figure (a) was obtained from Elsevier [175]. Figures (b, c, d) were adapted from Hilmi et al [174], open access article published under Creative Commons Attribution License (<http://creativecommons.org/licenses/by/2.0>).

### *Gellan*

Gellan gum is a FDA approved product that is regularly used in the food industry as a thickener. It is a hydrophilic anionic polysaccharide produced by the bacterium *Pseudomonas elodea* that consists of D-glucuronic acid, L-rhamnose and D-glucose subunits [176]. The favourable physicochemical features of gellan has generated much interest for its use in pharmaceutical and biomedical applications [130]. The enzyme galactoman-

nanase can degrade gellan [177], but also common human enzymes such as lysozyme or trypsin [178]. Native gellan gum is acylated and is often referred to as high-acyl group, the deacylated form (or low-acyl gellan) is more commonly used in tissue engineering (chemical structure illustrated in Figure 1.9), the rate of degradation is slower in low acyl group gellan as shown by Lee et al [179]. However, it remains unclear whether gellan completely degrades in the body as Ferris et al noted degradation in terms of mass loss up to 28 days, but no further degradation in the following 140 days [180].

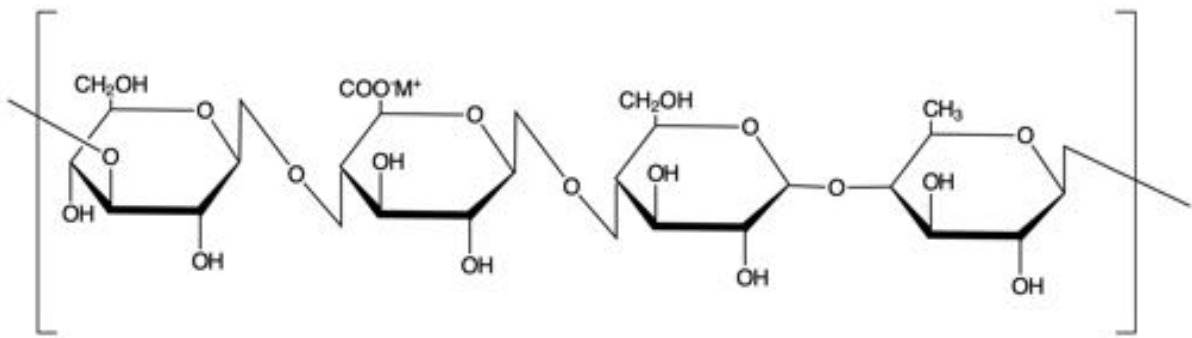


Figure 1.9: The chemical structure of low-acyl gellan gum.

In terms of tissue engineering, gellan-based injectable materials have previously been used for cartilage reconstruction [181]. Various autologous cell types such as preosteoblasts, fibroblasts and chondrocytes were successfully encapsulated within a hydrogel [181, 182]. Furthermore, a topical application of gellan in the form of an anti-adhesive and non-toxic dressing was found to stimulate healing and improved the scarring outcome in a rodent study [183]. However, no gellan based skin scaffolds are available for clinical use at the moment.

### *Dextran*

Dextran is a hydrophilic natural polysaccharide produced by bacteria and its degradation occurs via phagocytosis [184]. Dextran derived hydrogels can be formed by chemical or physical cross-linking or via radical polymerisation. Since dextran based hydrogels have a limited cell adherence and do not seem to affect cell viability, they have been used in drug

delivery. These features in combination with slow degradation have limited its use for tissue engineering in wound healing. Therefore, research groups have attempted to tailor the properties of dextran hydrogels to improve its cell adhesion [185], biocompatibility [186] and have modified its degradation profile [187] to ultimately enhance functionality in tissue engineered scaffolds for burn wound healing [188]. The application of an acellular dextran hydrogel has been investigated in full thickness burns in mice and was found to stimulate angiogenesis and skin regeneration [188]. Similar results were seen in a full thickness porcine model, and additionally an improved dermal reconstruction and re-innervation was observed [189]. More recently, a hypoxia-inducible dextran hydrogel promoting neovascularization has been proposed by the same research group [190]. In terms of cell delivery to wounds, keratinocytes have been seeded into collagen-coated dextran microspheres transplanted as micrografts to full thickness wounds in athymic nude mouse model, but intradermal epithelial cysts were formed possibly due to high carrier adherence and slow degradation of the microspheres [191].

#### *Hyaluronic acid*

Hyaluronic acid (HA) is an anionic, linear polymer that is present in all living organisms and can be found in connective tissue especially in the dermis of the skin, but it is also abundant in vitreous humor of the eye and synovial fluid. It can be derived from many tissues via extraction and enzyme digestion methods or by bacterial synthesis. HA is an important glycosaminoglycan consisting of d-glucuronic acid and N-acetyl-d-glucosamine. Degradation in natural tissue occurs by enzymatic cleavage with different types of enzymes among tissues [192]. Rapid biodegradation is found to be problematic in certain biomedical applications, for example, in a rodent study a half-life of only 24 hours following joint and skin injection was found [193]. Hence, for biomedical applications HA requires modification to be able to form a hydrogel and also to reduce biodegradation *in vivo* [194] which then can be administered by injection or incorporated in dressings [195]. Examples of HA hydrogels formed by chemical crosslinking are dermal fillers with

prolonged durability, histological studies have reported HA presence in the skin for up to 9-23 months [196]. As a highly hydrophilic polymer its use as lubricant and biological absorber injected to deteriorating joints has been widely explored [197]. A variety biological functions of HA have been recognized such as its role in cell motility, adhesion and regulation [198]. The chain length and molecular weight of hyaluronic acid plays an important role in its biological function. In an *in vitro* cell study, rat cardiomyocytes underwent ischemic-reperfusion injury and were incubated with low molecular weight HA (LMW-HA, 100 kDa) or high molecular weight HA (HMW-HA 1000kDa) and it was found that cell viability and wound healing (scratch wound assay) of HMW-HA pre-treated cells were significantly improved. Proteomic expression assays demonstrated a significant recovery of cytoskeleton regulation proteins in samples following injury when pre-treated with HMW-HA and not with LMW-HA, suggesting cytoskeletal rearrangement by HMW-HA [199]. Likewise, Wu et al investigated the effect of HA in chemically burned (alkali) human corneal cells and suggested superior cell viability and more rapid wound healing in cells treated with HMW-HA (1525 kDa) when compared to LMW-HA (127kDa) [200]. However, in other studies focussing on wound healing, small HA fragments seem to have a beneficial effect on wound healing [201], potentially due to its role in stimulating pro-inflammatory mediators [202]. Advantages of LMW-HA is its solubility in serum making it suitable for systemic distribution. Furthermore, HA can bind to CD44 and receptor for HA-mediated motility (RHAMM) cell surface receptors. Binding of HA to CD44 triggers internalization, because CD44 is overexpressed in cancer cells it can be used in anticancer drug delivery [202]. HA interaction with RHAMM is linked to cell motility and cell focal adhesion and interplays with CD44. HA can be functionalized with cell adhesion peptides to enhance cell attachment to other cell types [195]. The diversity in chemical modification techniques offers opportunities for copolymeric biomaterials and makes HA a versatile polymer for the use in tissue engineering. Cells that are naturally surrounded by HA rich connective tissue in the body have commonly been encapsulated into HA scaffolds such as chondrocytes and dermal fibroblasts. A plethora of biomedical

materials based on hyaluronic acid derivatives have been commercialised for deteriorating joints, (commercial) skincare and wound healing purposes. For wound healing specifically, rodent full thickness skin wound models have suggested a beneficial effect of HA to wound healing [203] using scaffolds containing HA [204–208]. A scaffold available for human use is hyalomatrix<sup>®</sup> (Anika therapeutics, former Fidia Advanced Biopolymers, Padua, Italy), a sterilized matrix based on hyaluronic acid derivate (benzyl ester of hyaluronic acid) with an outerlayer of semi-permeable silicone. The scaffold can be directly delivered to the wound bed and aims to attract cellular ingrowth of fibroblasts and ECM components and promote vascular ingrowth. It has been used as dermal replacement in serious surgical wounds [209] and following scar release in adult patients with final autologous skin graft applied to most patients in 2-4 weeks after scaffold placement [210]. Gravante et al used Hyalomatrix<sup>®</sup> in paediatric burn patients as dermal replacement therapy following dermabrasion debridement and considered it safe to use and reported no adverse events [211]. However, no large good quality control studies in humans are available that focus on wound healing. Hyalograft<sup>®</sup> is a HA scaffold seeded with autologous human dermal fibroblasts. Han et al compared the use of an acellular HA scaffold (Hyalomatrix) to the same scaffold seeded with human dermal fibroblasts (Hyalograft) in terms of wound healing in 35 patients with a soft tissue defect to the face following basal cell carcinoma removal. Although the study lacks statistical power, the outcomes were in favour of the cellular scaffold with less scar contracture and a flatter scar compared to the acellular scaffold [212].

### *Starch*

Starches can be derived from widespread available plant sources such as potato, corn, rice, oat [213], or wheat [214]. Thermosensitive starch hydrogels can be formed by  $\beta$ -glycerol phosphate cross-linking [215]. Chemically modified starches have been used for drug delivery and tissue engineering. For example, an injectable starch-chitosan hydrogel was developed for the delivery of chondrocytes by Vioych et al. Due to the non-ionic nature

of starch it can easily blend with other polymers and in this study, starch was found to increase the pore size and water absorption ability of the resulting polymer blend [215]. Although, starch-based hydrogels are easily available and degraded by enzymatic degradation it has not been widely explored for wound healing purposes [214].

## **Proteins**

A protein is a linear polymer made up from amino acids. The DNA code in cells is converted to synthesize proteins, a process undertaken by a range of other cellular components, the type and composition of the amino acids determines the proteins' final structure and function [216]. Proteins can be derived from blood products (fibrin), mammalian tissue (collagen, gelatin and elastin) or other animal products (silk fibroin and silk sericin). Advantages in using proteins are that they are biodegradable and usually enhance cell adhesion to the scaffold. Some disadvantages are a low mechanical strength of protein skin scaffolds and the availability and costs of human/animal products. The properties of proteins for the use in skin scaffolds are listed in Table 1.1. The most abundant protein in the human body and the main structural component of the dermal layer of the skin, is collagen. Therefore, many bio-engineered skin scaffolds consist out of collagen. However, researchers have been exploring other proteins for the development of skin scaffolds. Here, we describe those proteins that have most commonly been incorporated in cellular and acellular skin scaffolds.

### *Silk proteins*

Silk produced by the silk worm *Bombyx mori* contains two major proteins named silk sericin and silk fibroin. Due to its mechanical strength and biocompatibility, fibroin has been widely used in textiles, drug delivery and as a biomaterial [217]. For example, a fibroin/hyaluron scaffold supporting mesenchymal stem cell adhesion has been developed [218]. Alterations to fibroin degradability and surface modification have been successfully performed to meet biomedical needs [219]. Fibroin fiber ropes have been used as suture

material for closure of surgical wounds for many years, and this clinical success has paved the way for its use in other different biomedical applications such as solubilized fibers to produce sponges, films and hydrogels used in wound healing and tissue engineering [220]. For example, in the development of a tympanic membrane replacement, a fibroin substrate that stimulates human keratinocyte growth was engineered [221].

In contrast, silk sericin has not yet been explored that extensively, and for many years silk sericin was discarded as a waste product in the derivation of fibroin. Sericin is the glue that is found between the fibroin fibers. Its positive features such as non-immunogenicity, serum-dependent cell-adherence and its specific anti-oxidant, anti-bacterial and anti-coagulative features make sericin a promising candidate for biomedical applications such as in skin regeneration [222–224]. Teramoto et al described a low cell-adherence where other studies have shown a high cell adherence in different cell types [223–225]. These contrasting results might be explained by a serum-dependent cell adherence of sericin.

### *Fibrin*

Fibrin is an insoluble protein, a product from fibrinogen found in blood plasma. Upon tissue injury the proteolytic thrombin is activated which cleaves the soluble fibrinogen into the insoluble protein fibrin. Because it naturally forms a fibrous mesh that acts as blood clotting agent, it has been widely investigated for wound healing applications. Especially, as a haemostatic tissue sealant [226] in surgical wound closure where a hydrogel can be dripped or sprayed onto a wound surface to enhance healing or as glue when subsequently a skin graft is applied on top. Fibrin has been translated to clinical practice successfully in the form of a spray, powder or sheet consisting of fibrin, thrombin, calcium ions, factor VIII and a protease [227]. This tissue sealant has shown to enforce engraftment of autologous skin grafts in burn wound care [228] and skin substitutes [229]. Because activation by thrombin is required these products are usually provided in a dual syringe system that can mix upon application to the body. Some products such as Cryoseal<sup>®</sup> (Thermogenesis, US) [230] and Vivostat<sup>®</sup> (Vivolution A/S, Denmark) utilize autologous

blood plasma for on-site preparation of the sealant, however, this can be a disadvantage in patients that are potentially haemodynamic unstable. An alternative is the use of FDA approved human pooled plasma (Artiss). However, the high costs of the system limits its widespread use globally [228, 231]. Other proteins that have been used as tissue sealants are gelatin and albumin, however gelatin has not been used for skin wounds. Although albumin based tissue adhesives are FDA approved for cardiac and vascular surgery [232], no reports in skin wounds have been found. Also polysaccharides like chitosan, chitin, dextran, chondroitin sulfate, hyaluronic acid can be used to form tissue adhesives [227]. Chitosan as a positively charged polymer is thought to attract red blood cells which accelerates the blood clotting. A sponge form of chitosan is on the market as haemostatic, adhesive material in acute wound care [172]. Although dextran, chondroitin sulfate and hyaluronic acid show promise as tissue adhesive in corneal defects [233–235], their use in skin wounds has not been explored yet. Fibrin is easily degraded by proteolytic enzymes in the body and therefore fibrin-hydrogels or scaffolds usually have weak mechanical properties. Improving these mechanical properties can be achieved by optimizing crosslinker concentration, pH [236], or utilizing degradation regulators and fibrin stabilisers such as aprotinin and tranexamic acid [237]. Additionally, to reinforce fibrin scaffolds they can be combined with other polymers to form interpenetrating polymer networks (IPN) [238]. Encouraging results have been established by a fibrin-hyaluronic network with increasing structural stability of the gel, but decreased proliferation of encapsulated fibroblasts occurred in stiffer materials [239]. Besides its role in blood clotting, the fibrin network is also a nest for cells to attach, proliferate and migrate through. Fibrin as a sealant has also been used to coat scaffolds for improved cell adhesion [240] and in bilayered substitutes as a natural barrier to separate the epidermal and dermal layer. Due to its high biocompatibility and high affinity to cells, a variety of cell types have been encapsulated in fibrin carriers such as fibroblasts [241], keratinocytes [242, 243], mesenchymal stem cells [123] and combinations of cells seeded into or onto fibrin scaffold [244] or gels [195, 245]. Although, degradation of autologous fibrin is rapid, no toxic by-products are released in

the natural degradation process and no rejection occurs upon transplantation. Fibrin gel in its natural form seems most suitable for applications that do not require a high mechanical strength or long duration in situ. Recently, the addition of angiogenesis stimulating factors to fibrin scaffolds has been shown to improve the regeneration of ischemic tissue [246]. Interestingly, higher thrombin concentration in fibrin matrices appears to diminish neovascularisation and epithelisation time [247]. This is potentially due to slow scaffold degradation as thrombin activates factor XIII which induces the cross-linking of fibrin monomers and consequently reduces the natural degradation process.

### *Collagen*

Collagen is the most abundant protein in the human body and the main component of the extracellular matrix [248]. It is the main structural protein in the dermal layer of the skin with an essential role in wound healing. Therefore, many skin scaffolds have been developed based on collagen as primary component [249]. A total of 29 collagen types have been described. Collagen type 1 is most frequently used in skin scaffolds as it is the abundant protein in native dermal tissue. In the early 80's Burke and Yannas published their first clinical study of a permanent artificial dermal template based on bovine collagen and shark chondroitin 6-sulfate which led to the development of the commercialised dermal substitute Integra [250, 251]. At the same time, the first burn patient was treated by grafting of their wounds with cultured autologous keratinocytes [44] following the method that Rheinwald and Green had developed just a few years before [40, 43]. Based on the recent developments in that decade Hansbrough and Boyce were able to develop a collagen-glycosaminoglycan scaffold seeded with viable cultured autologous keratinocytes and fibroblasts and published successful engraftment into burns patient [99].

Ever since, collagen-based materials in different forms have been developed for wound healing and translated to clinical practice. Such as hydrogels for hydration of dry wounds (Woun'Dres<sup>®</sup> Collagen Hydrogel), as injectable scaffold [65], collagen sponges [143] (Skin-

Temp™II Dressings for superficial wound and blisters), powder [252] and an extensive list of collagen films/dressings [253]. The natural mechanical strength of collagen is weakened by its extraction process. To reinforce the collagen and control its *in vivo* degradation, new bonds can be formed by *in vitro* crosslinking. Collagen hydrogels are typically formed by chemical, physical or enzymatic crosslinking [249]. Such as in Pelnac<sup>®</sup>, a lyophilized porcine atelocollagen porous sponge that is crosslinked by 0.05 M acetic acid containing 0.2 wt% glutaraldehyde [254]. For biomaterials, chemical crosslinking is usually less suitable as cytotoxicity can occur upon degradation *in vivo* [255]. Other forms include composite acellular skin substitutes such as Biobrane, Integra [256] and Matriderm<sup>®</sup> [64]. In Matriderm<sup>®</sup> collagen type III and V is incorporated in combination with type 1 collagen and coated with elastin hydroxylate [257].

The majority of cellular skin scaffolds available on the market are based on animal derived collagen. Collagen based cellular skin substitutes include Orcel<sup>®</sup>, StrataGraft<sup>®</sup>, Apligraf<sup>®</sup> [84, 258], DenovoSkin<sup>®</sup>, Transcyte<sup>®</sup> [259] and Engineered Skin Substitute (ESS) [260]. These substitutes are incorporated with autologous cells from a healthy part of the patient's skin or allogenic cells. More recently, the incorporation of adipose derived stem cells in a collagen hydrogel was investigated and seem to improve wound healing in a rodent burn model [261].

Collagen gels as bio-ink [262] and in cell-laden bioprinted scaffolds have also been studied. For example, in an attempt to stimulate vascularisation in neural tissue, Lee et al conducted an experimental study where cells, collagen and VEGF-releasing fibrin gel were bioprinted to form a scaffold [263].

### **Hydrogels in burn care**

Hydrogels currently available for patient care have been reviewed by many researchers, but a skin substitute that is able to achieve complete skin regeneration has not yet been reported [84, 264–267]. However, hydrogels play a promising role in the development of next generation skin substitutes in burn care and are often used as wound dressings

[141, 268], regenerative scaffolds or delivery devices for cells and therapeutic e.g. drugs, growth factors etc. Hydrogels have several characteristics to promote skin healing such as the ability to absorb and release water, which is useful in regulating burn wound exudate. Furthermore, the architecture of hydrogels can be modified to mimic the body's own extracellular matrix and their tunable mechanical properties can provide customised elasticity and flexibility [127, 269] and make them suitable candidates for skin regeneration [68, 261, 270–274].

## 1.8 Methods of spray deposition

### 1.8.1 Spray parameters and cell viability

Cell transplantation can be achieved by several techniques. In this section the focus lies on cell transplantation to the tissue via aerosol or spray delivery. Sprayed cells are expected to be damaged at time of impact to the receiving surface. Following impact, the cell membrane can elongate and deform. Cell rupture and subsequently cell death can occur in largely overstretched cell membranes [275]. More precisely, cells can tolerate a cell membrane area stretch of up to 5% before it becomes detrimental to cell survival. Cell elongation, deformation and subsequent cell survival depends on many variables such as target surface characteristics, viscosity of the transporting fluid/media and velocity of the delivered cell containing droplet, nozzle distance and diameter. Veazey et al. investigated the cell viability of xenogeneic 70% confluence fibroblasts immediately after aerosol delivery with an airbrush system and their growth behaviour in a culture model [276]. The airbrush system used could be adjusted for different nozzle diameters (312, 494, 746  $\mu\text{m}$ ) and air pressure at delivery (ranging from 41 kPa to 124 kPa). It was found that cell viability directly measured post aerosol delivery significantly decreased with higher pressure and smaller nozzle diameter. For cell proliferation studies, only the highest pressure with smallest nozzle diameter combination showed a delayed population doubling time and the time to reach confluence was doubled [276]. In another *in vitro* study

with 80% confluence neonatal dermal rat fibroblasts an analytical model was proposed to describe the impact of several spray parameters in a droplet-based spray application to the cell viability. Stiffness of the tissue surface, high cell-viscosity and cell velocity had a negative influence on cell viability post spray impact, whereas a larger cell-containing droplet diameter had a positive effect on cell viability. The latter was explained as a cushioning effect of the droplet to the surface protecting the cell within the droplet [277]. In other words, cell viability is expected to be highest in large and low-viscosity single cell-containing droplets sprayed with low-velocity onto a soft tissue surface. Wounds would serve as a soft receiving surface for cell transplantation and can be expected to be highly viscous when hydrogels are used. Hence, tailored spray devices, with pressures and nozzle diameters optimized for cell survival can play an important role in improving cell delivery.

## 1.8.2 Spray systems

Spray systems are being widely used in many industries. Surprisingly little research has focused on the influence of the type of aerosol device on mammalian cell survival after transplantation.

### Low and high pressure spray nozzle

Fredriksson et al. evaluated 7 different application techniques for cell transplantation on cell viability and proliferation in an *in vitro* study. Based on current clinical practice they included commercially available spray systems: spray nozzle systems such as the Harvest SK/S Spray Applicator Kit<sup>®</sup>, high and low pressure Tissomat applicator in combination with a Duploject<sup>™</sup> spray nozzle, a Duploject<sup>™</sup> spray nozzle without additional pressure control and two non-spray systems: pipetting and paintbrushing. This study showed an approximate 50% drop in viable cell count immediately after transplantation when using a high pressure device (200 kPa) and a further decline to nearly 40% viable cell count after 2 weeks of culturing, which was comparable to the paintbrush [278]. In contrast, Harkin et al. measured a 20% higher post aerosol delivery cell survival with similar pressures

[279]. The immediate cell survival is comparable with other studies utilising low pressure delivery methods/systems [276]. Although no statistically significant differences were displayed, the poorest cell viability after 2 weeks was seen in the high pressure device and paintbrush [278]. Fredriksson et al. hypothesised that an additional application of fibrin sealant might improve cell survival. Furthermore, the authors emphasized the importance of measuring the proliferation capacity of cells post aerosolisation, since a large difference was seen in their data among the different devices. Interestingly, the delivery pressure and nozzle diameter of clinically used manual cell spray devices is unclear and might impact on cell viability and proliferation capacity. Aerosol delivery with handheld airbrush systems with adjustable airpressure supply have also been previously investigated and studies have demonstrated consistent acceptable cell viability of above 80% with low delivery pressure (below 69 kPa) [276]. According to Veazey et al, this system should also be compatible with alginate, gellan, hyaluronic and hyaluronate-based hydrogel cell carriers [280]. However, to date, there is no published data to support this statement.

### **Liquid atomizer**

Liquid atomizers or nebulizers originally designed for aerosol drug delivery to the trachea have also been explored for cell delivery. In burns, inhalation injury can occur with damage to the trachea and drug- or cell delivery could be used to improve the healing of these injured areas. Sosnowski et al. investigated the use of 5 different atomizers for cell delivery to the trachea in terms of cell viability. However, a droplet size below 20  $\mu\text{m}$  was found to be incompatible for fibroblast encapsulation and 3 nebulizer devices had to be excluded. The nasal atomizer (NA) and Microsprayer Aerosolizer (MSA) had above 90% viable cells post spraying, but the viable cell count in the NA group declined to 65% 48h after spraying, indicating that it was a more destructive aerosol technique [281].

All spray cell delivery techniques have been investigated *in vitro* or rodent studies, which has led to the development of commercial spray devices that are now available in clinical practice for burn wound treatment.

## 1.9 Potential therapeutic applications

### 1.9.1 Future approaches keratinocyte transplantation

Several reviews in the last decade have discussed the future implications of skin tissue engineering and/or specifically keratinocyte cell transplantation in the treatment of burns [36, 37, 55, 266, 267, 282]. Larger burn wounds often require mesh grafting. Autologous epidermal cell transplantation can complement mesh grafting by stimulating rapid epithelialization, which is highly desirable to improve patient's chance of survival and eventually improve scarring. Burns specific clinical studies investigating keratinocyte transplantation are available, but due to heterogeneity of the studies and different outcome parameters the evidence remains low. Comparative trials with standardized outcomes and ideally randomized treatment for available cell transplantation techniques are required. Due to the disadvantages of CEA sheets, future research is focused on optimizing keratinocyte proliferation by transplantation of pre- or sub confluence cells. Further improvement of keratinocyte culture method in terms of culture time, reducing infection risk and elimination of xenobiotic products and also antibiotics needs to be further investigated. Graft attachment in keratinocyte transplantation remains an important focus for research. Boyce and Supp developed a cultured skin substitute containing cultured human keratinocytes and fibroblasts attached to a collagen-glycosaminoglycan matrix which seems to form a basement membrane at the dermal-epidermal junction *in vitro* [283]. Importance of basement membrane formation and rapid epithelialisation has to be taken into account in next generation cell spray or carrier delivery methods [283, 284].

### 1.9.2 Future spray cell delivery systems for burns wound care

Spray cell delivery to burn wounds can overcome the major issues of conventional grafting techniques by reducing donor site and enhance fast re-epithelialisation. The available delivery systems can be improved by optimizing spray features to aim for high cell viability and proliferation. This should be tailored according to cell type and receiver surface.

Spray features to optimise might be: air delivery pressure, nozzle designs, carrier type and depending on technique of delivery, cell containing droplet size [276, 277, 281, 285]. Further research should take into account the importance of preventing cell damage, since this could reflect poor proliferation [276, 278]. Hydrogels could potentially serve as a mechanical protection for the cells during transplantation and provide structural support once transplanted. Although *in vitro* studies have shown good short term cell survival post aerosol delivery, clinical studies have not been able to show similar results as yet. The challenge for researchers is to develop a feasible spray delivery system with acceptable cell viability and proliferation which can be translated to clinical studies. Also, current clinical cell spray devices could potentially benefit from these optimized features.

## **1.10 Thesis overview**

Spray cell delivery to enhance wound healing is limited by its carrier causing cell spillage. In this thesis a biocompatible hydrogel as cell carrier has been developed aiming to improve uniformity of the spray distribution and adherence to the receiving surface while maintaining cell viability as graphically illustrated in Figure 1.10. The development and material characteristics of a suitable cell carrier for spray delivery are presented in Chapter 2. Effects of encapsulation and spraying on cell viability and function have been investigated in Chapter 2 and Chapter 3. Chapter 4 presents the formulation of a gellan hydrogel wound dressing containing acetic acid to treat burn wound infection. Finally, Chapter 5 provides a summary of the findings, limitations and directions of future work based on the presented results in this thesis.

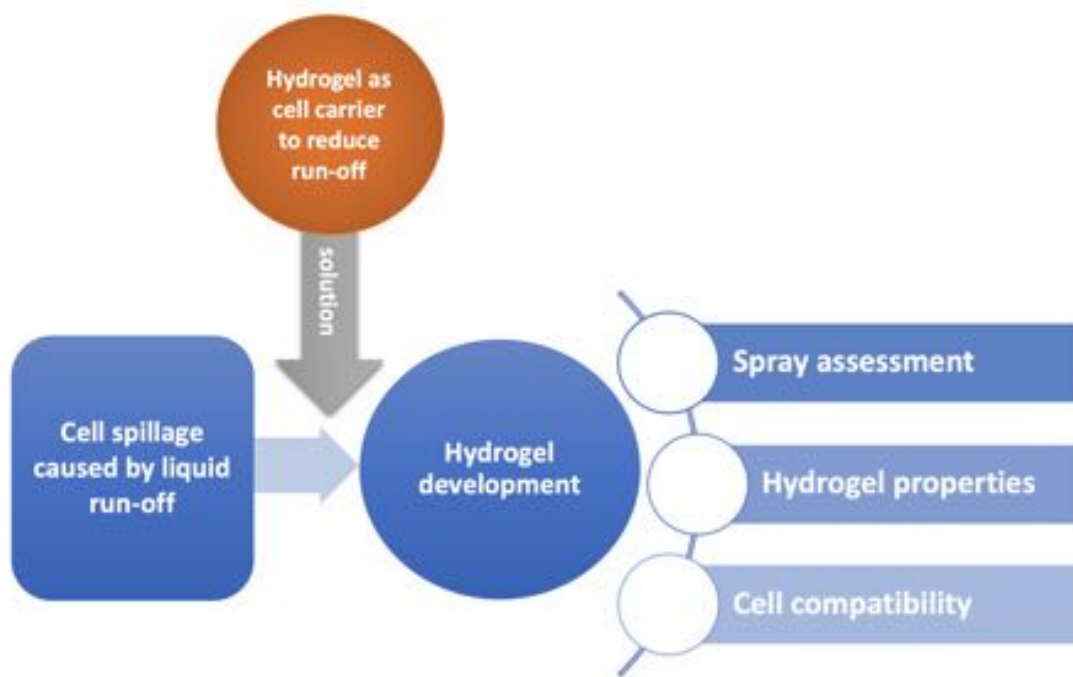


Figure 1.10: The development process of a cell laden hydrogel carrier for topical spray delivery.

## CHAPTER 2

# GELLAN-BASED FLUID GEL CARRIER

The following chapter includes work that was also presented in the published paper *A gellan-based fluid gel carrier to enhance topical cell spray delivery*<sup>2</sup>.

Autologous cell transplantation was introduced to clinical practice nearly four decades ago to enhance burn wound re-epithelialisation. Autologous cultured or uncultured cells are often delivered to the surface in saline-like suspensions. This delivery method is limited because the sprayed suspension forms droplets upon deposition that run across the wound bed, leading to uneven coverage and cell loss. A way to circumvent this problem would be to use a gel-based material to enhance surface retention. Fibrin systems have been explored as co-delivery system with keratinocytes or as adjunct to ‘seal’ the cells following spray delivery, but the high costs and need for autologous blood has impeded widespread use. Aside from fibrin gel, which can exhibit variable properties, it has not been possible to develop a gel-based carrier that solidifies on the skin surface. This is because it is challenging to develop a material that is sprayable but gels on contact with the skin surface. This study reports the use of an engineered carrier device to deliver cells via spraying, to enhance retention upon a wound. The device involves shear-structuring of a gelling biopolymer, gellan, during the gelation process; known as a fluid gel. The formulation of gellan gum fluid gels are reported, formed with 0.75 or 0.9% (w/v) polymer and varying salt concentrations. The rheological properties and the propensity of the material to wet a surface were determined for polymer modified and non-polymer modified cell suspensions. The gellan fluid gels had a significantly higher viscosity and contact angle when compared to the non-polymer carrier. The shear thinning property of the material enabled it to be applied using an airbrush and spray angle, distance and air pressure were optimised for coverage and cell viability. Viability of human fibroblasts was not impeded by encapsulation in the gellan fluid gel or spraying, platelets were activated by spraying and did not survive long term encapsulation in fluid gel.

---

<sup>2</sup>DOI: 10.1016/j.actbio.2019.03.036

## 2.1 Introduction

Large surface area wounds, such as those seen in burns patients, compromise the barrier function of skin and when coupled with extensive fluid loss causes an impairment of vital bodily functions which can result in death. Rapid epithelialisation is essential to restoring the function of the skin and in the longer-term, to reduce the likelihood of scarring [286]. Current clinical practice includes transplantation of autologous skin from a healthy site of the body, however, challenges arise when a limited number of donor sites are available. One approach to overcome this issue is to deliver autologous skin cells (usually keratinocytes) in suspension following a period of culture, or directly after harvest from the patient, to the wound [287]. Cell transplantation techniques have evolved from syringe-dripping to spraying systems [47]. The major advantage of the spray technique is rapid delivery to large and geometrically complex areas of the body. For medical applications, a minimum distance of 10 cm from the body is necessary to allow safe application without the risk of an air embolus, this is easily achieved in topical application (in comparison with endoscopic surgery). Even though spraying presents great potential for topically applying cells in suspension, there are still many drawbacks, including: spillage of cells from the wound bed and uneven spreading [47, 288]. This results in the application of dressing materials around the wound as a means to retain as many cells on the wound bed as possible [289]. Although poor retention is considered a critical disadvantage of the cell spraying methodology amongst clinicians, it has not as of yet received much attention within the published literature. Autologous fibrin sprays similar to fibrin glue have been proposed to retain sprayed epithelial cells at the wound [229, 288]. High costs and the need for patient's own blood-derived fibrin, however, have impeded widespread use of this technique to date. While hydrogels have gained huge and sustained interest for therapeutic delivery systems, development of a practical system for topical spray delivery is technically challenging; requiring either in-situ gelation on the surface of the wound or a sufficiently high viscosity to be retained on the wound but not clog the spray nozzle. Fluid gels have shown continued promise to address these issues, whereby at rest act

in a pseudo-solid fashion but can be made to flow under shear [269]. This is derived through the processing of a hydrogel during its sol to gel transition. The application of shear during the sol-gel transition has been previously shown to support the formation of discrete gel particles, which in close proximity interact with one another in suspension to give reversible shear thinning and solid-like behaviours. Furthermore, fluid gels have been previously shown to demonstrate yield stresses once at rest [290]. The presence of yield stresses and yielding behaviours has generated much debate within the rheological literature, due to a long understanding that “everything flows” [291]. However, it is generally accepted that in practise, within timescales relevant to the material in question, a material has a yield stress if it does not flow below a defined threshold [292]. The importance of engineering yield-stresses into fluids has been recently highlighted by Nelson and Ewoldt [292] demonstrating a clear set of design principles for such materials. Here they have highlighted the synergistic link between customer need/material specification and the materials microstructure, allowing for its application, an example of this would be paint where the presence of a dynamic yield stress allows it to “stick” to the wall without running [293, 294]. Such principles were used to design a biopolymer hydrogel with viscoelastic properties that allow the material to liquefy when passing through the nozzle, but restructure to a weak gel on the receiving surface. Thus, facilitating retention of cells on the receiving surface and not impair the spraying process itself (Figure 2.5).

Biopolymer hydrogels are widely used in burn wound care as dressings, and tissue-engineered scaffolds with or without bioactive compounds [127]. These gel systems can mimic the 3D architecture of native extracellular matrix (ECM)[127]. The ability of these gels to entrap relatively large volumes of water per %wt of polymer is beneficial for maintaining a moist wound environment and allows for rapid diffusion of nutrients and metabolites [295]. Gellan gum was used as the biopolymer of choice in this study because it can be processed into a hydrogel with highly tunable mechanical properties [269]. Gellan gum hydrogels can be designed for many biomedical applications [296] and in many forms

including shear-thinning gels named ‘fluid gels’ [297, 298]. To date, surprisingly little research has focused on quantifying the uniformity of sprayed solutions for wound coverage and the influence of spraying on mammalian cell survival after transplantation [276, 278]. This study addresses some of the problems of current spray delivery systems and proposes gellan fluid gel as a material that could be utilised to enhance cell retention on a surface following spraying.

## **2.2 Material and methods**

### **2.2.1 Fluid gel preparation and characterisation**

Low acyl gellan gum stock solutions 1% (w/v) and 0.83% (w/v) were prepared by the addition of gellan powder [Kelcogel<sup>®</sup> obtained from Azelis, Hertford, UK] to sterile water at 65 °C under constant agitation. Following, stocks of NaCl cross-linker solutions were prepared to concentrations of 0.1, 0.2, 0.3, 0.4 and 0.5 M in sterile water. Final polymer sols were subsequently formed by mixing aliquots of both gellan with cross-linker stock solutions (9:1) at 65 °C, resulting in final concentrations of either 0.9% (w/v) or 0.75% (w/v) polymer - 10 mM, 20 mM, 30 mM, 40 mM and 50 mM NaCl. Gellan sols were then added to the cup of a couette (Cup diameter 28 mm, vane diameter, 26 mm) rheometry set-up (Kinexus Ultra, Malvern Pananalytical, UK) at 60 °C. After allowing thermal equilibrium to be reached, the system was cooled at a rate of 1 °C min<sup>-1</sup> to 20 °C under constant shearing, 450 s<sup>-1</sup>; unless stated otherwise. Post-production shear was removed, and fluid gels stored at 4 °C until further testing/use.

### **2.2.2 Rheological measurements**

All rheological measurements were performed at 25 °C using a Kinexus Ultra rheometer (Malvern Pananalytical, UK) equipped with 40 mm parallel plates (1 mm gap height), 48 hours post-processing.

Small deformation rheometry was undertaken varying both amplitude and frequency.

Amplitude data was obtained in strain-controlled mode, ranging from 0.1 to 500% logarithmically at a constant frequency of 1 Hz. Linear viscoelastic regions (LVRs) were determined and a common strain of 0.5% was found to be common across all systems. This strain was then used for all frequency sweeps ranging between 0.1 and 10 Hz. Single frequency data was collected as a function of temperature at 0.5% strain and 1 Hz. Temperature ramps were applied at 1 °C min<sup>-1</sup> and moduli (G' and G'') obtained.

Non-linear rheology was determined using shear ramps in shear rate mode. Ramps were undertaken from 0.1 to 600 s<sup>-1</sup> logarithmically over a 3-minute timescale. Hysteresis of the systems was probed by undertaking a second sweep immediately after the first, from 600 s<sup>-1</sup> back to 0.1 s<sup>-1</sup>. Data from the second ramp was fitted to the Herschel-Bulkley model (Equation 2.1) to determine the dynamic yield stress ( $\sigma_y$ ).

$$\sigma = \sigma_y + K\dot{\gamma}^n \quad (2.1)$$

Where  $\sigma_y$  is the yield stress, K is the consistency factor,  $\dot{\gamma}$  is the shear rate and n is the flow index.

The yield stress was compared to the maximum stress on the material at an inclining substrate to investigate whether flow is induced. Maximum stress was determined by Equation 2.2

$$\sigma_{max} = \rho \times g \times h \times (\sin\beta) \quad (2.2)$$

Where  $\sigma_{max}$  is the maximum stress on the material,  $\rho$  the material density (kg m<sup>-3</sup>), g the gravitational acceleration of 9.807 m s<sup>-2</sup>, h is the height (m) and  $\beta$  the angle of inclined substrate.

### 2.2.3 Microscopy of fluid gels

Micrographs of the fluid gel systems were undertaken using a Leica DM6000 microscope (Leica Microsystems, UK). Firstly, fluid gels were diluted at a ratio of 4:1 in PEG400, via slow addition of the PEG under constant agitation. Post-dilution, one drop of the system was dispensed onto a microscope slide and coverslip placed over the top. Images were obtained at x20 magnification using phase contrast to distinguish between the continuous and particulate phases. ImageJ was used to add scale bars. Images presented are typical representations of the systems, compared against a minimum of 5 other micrographs.

## 2.3 Contact angle measurements

The static contact angle of sodium chloride and gellan fluid gel droplets on a variety of surfaces at room temperature were determined by imaging and subsequent measurement with ImageJ software using the DropSnake Plugin [299]. A 60  $\mu\text{l}$  droplet was dropped onto the test surfaces and imaged. Three repetitions were performed, each sample was measured three times and the mean contact angle was calculated. Substrates used included: gelatin 5% w/v (prepared with deionized water and bovine gelatin, stirred and allowed to set at 4 °C for a minimum of 60 minutes), alumina ceramic (referred to as ceramic), porcine epidermis and porcine subcutis. Porcine skin (Arun Meats & Livestock LTD, UK) was kept frozen and thawed before use.

## 2.4 Spray methods

Materials were delivered through an airbrush with external mixture and a standard medium size nozzle of 750  $\mu\text{m}$  in diameter (Badger, Universal 360 model, US) as illustrated in Figure 2.1A. An oil-free air compressor (Badger BA1100, US) was used as the air source with air pressure regulator. Air pressure at delivery (10-15 psi), nozzle diameter (750  $\mu\text{m}$ ), application distance (10-15 cm) and spray angle from spray tip to

receiving surface (45°) were standardized (Figure 2.1B). The airbrush system was cleaned and the nozzle rinsed thoroughly with ethanol 70% and allowed to air dry in the laminar flow hood before each spray cell experiment. Between experiments the nozzle was purged with 1 ml ethanol 70% and 1 ml culture media to ensure no cells from a previous application remained.

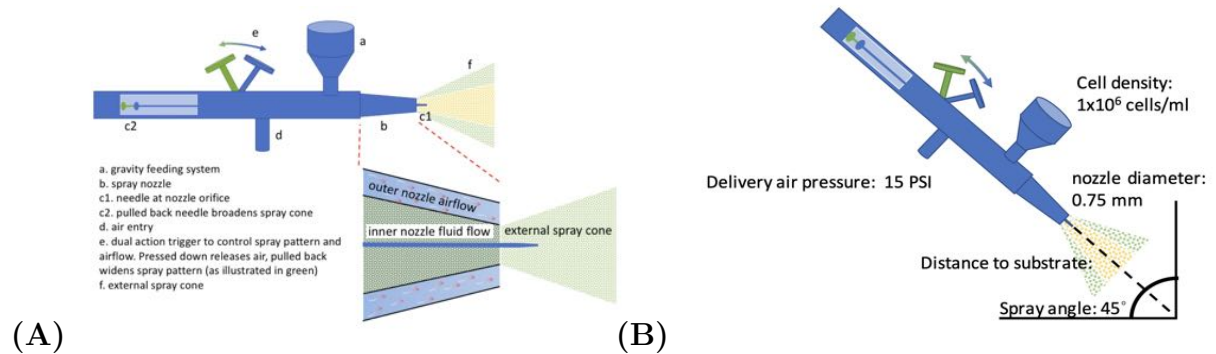


Figure 2.1: Airbrush spray device and standardised set up

## 2.5 Spray analysis using water sensitive paper

For investigation of uniform distribution following spraying the individual droplet size, droplet size distribution and area covered by the gel was compared to control liquid (water or sodium chloride). Water-sensitive paper (WSP) of 26 mm x 76 mm (John Rhodes AS Ltd, Evesham, UK) was utilized to compare gellan fluid gel to the control liquid in a standardized fashion (Figure 2.2). Yellow coloured spray cards coated with bromoethyl blue dye turn blue when in contact with water. Measurements included: the percentage area covered by sprayed volume (%coverage), droplet size and droplet size distribution. Volumes of 50  $\mu$ l or 25  $\mu$ l were sprayed with an airbrush onto the WSP and allowed to dry for up to 60 min. A minimum of 3 repetitions was performed. Images were obtained directly following spray application, dried spray cards were scanned at 600x600 dpi (Konica Minolta scanner, bizhub c3350). Images were analysed with ImageJ Software, a colour threshold was set and the image was converted to a binary image. Then, percentage of coverage was calculated by the ratio of original (white pixels) to

covered area (black pixels) with Equation 2.3.

$$\%coverage = \frac{Area_{covered}}{Area_{original}} \times 100 \quad (2.3)$$

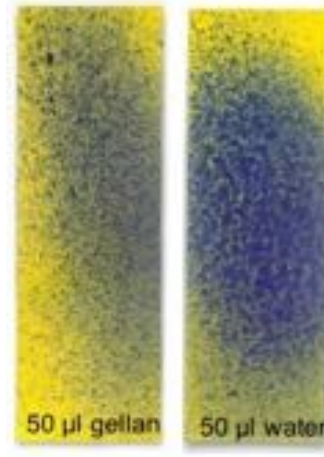


Figure 2.2: Water-sensitive paper (WSP) sprayed with gellan and water

For droplet size the ‘Particle Analysis plugin’ was used. Obtained parameters include droplet diameter (D) in mm, droplet area (A) in mm<sup>2</sup> and total sprayed area (TSA) in mm<sup>2</sup>. A value where 50% of the total sprayed volume consists of drops with diameter larger than the median value and 50% smaller than the median value (DA50) could be obtained from the data. Next, DA10 and DA90 were obtained, similar to DA50, but for 10% and 90%. Relative Span factor (RSF), a single number reflecting the uniformity of the droplet size distribution was calculated in accordance with Equation 2.4:

$$RSF = \frac{DA90 - DA10}{DA50} \quad (2.4)$$

### 2.5.1 HDF cell culture

Human dermal fibroblasts (HDF) were grown in Dulbecco’s Modified Eagle’s medium – high glucose (DMEM) (Sigma, UK), supplemented with 10% fetal bovine serum (FBS), 1.5% penicillin-streptomycin and 2.5% L-glutamine. Culture media was changed every 2-3 days. Culture media was changed every 2-3 days and cells were harvested when they

reached 80% confluence. Cells until passage 10 were used. All cultures were maintained in the incubator under stable conditions of 5% humidity, temperature of 37 °C and 100 % humidity.

### 2.5.2 Fluid gel encapsulation

HDFs were detached from cell culture flask using TrypLE solution (Sigma, UK), buffered with fibroblast culture media and centrifuged at 1000 rpm for 3 min. Cells were suspended in gellan fluid gels (0.9% or 0.75% (w/v)) at a concentration of  $1-2 \times 10^6$  cells/ml. Cell solutions were pipetted on culture petri dishes or sprayed with the airbrush device into cell culture treated 24-well plates and fresh culture media was added before samples were incubated (at 5% CO<sub>2</sub>, temperature 37 °C, 100% humidity) for later experiments or directly stained for imaging.

### 2.5.3 Live/Dead assay

Calcein acetocymethylester (Calcein AM) (Invitrogen, UK) was used to stain live cells and Propidium Iodide (PI) (Invitrogen, UK) was used to stain dead cells. Calcein AM/PI stain was added to 1 ml of DMEM, samples were immersed in 100 µl/ml of this solution for 20 min in the incubator. Samples were visualized using confocal microscopy (Olympus, Fluoview FV100), showing viable cells green (Calcein AM) and non-viable cells red (PI). Laser setting 488 nm and 543 nm for Calcein AM and PI respectively. Cell viability was measured with ImageJ software, images were split in the colour channels red (dead cells) and green (live cells). For each sample, cells were automatically counted by using the particle size plugin of ImageJ. Percentage of viable cells were calculated by Equation 2.5.

$$viable\ cells(\%) = \frac{number\ of\ viable\ cells}{total\ number\ of\ cells\ (live + dead\ cells)} \times 100 \quad (2.5)$$

## 2.5.4 Alamar Blue Metabolic Activity

Encapsulated and control HDFs were seeded or sprayed into 24-well tissue cultured plates at a density of  $5 \times 10^4$  per well for cells in gel and  $1 \times 10^4$  for cells in medium. Fresh growth medium at a volume of 1 ml was added, cells were then incubated for a minimum of 24 hr (at 5% CO<sub>2</sub>, temperature 37 °C, 100% humidity) together with negative control wells including medium and gellan fluid gel. Metabolic activity was assessed at day 1, 3 and 7 for all 4 conditions by incorporating 10% Alamar Blue reagent (Life Technologies, UK) into the culture medium. After an incubation time of 4 hours, absorbance was read at 570nm and 600nm using a microplate reader (Multiskan FC, Thermo Scientific, UK). Percentage reduction was calculated by comparing absorbance to negative control wells with Equation 2.6.

$$\text{Percentage reduced}(\%) = \frac{(\epsilon_{ox2} \times A1) - (\epsilon_{ox1} \times A2)}{(\epsilon_{red1} \times B2) - (\epsilon_{red2} \times B1)} \times 100 \quad (2.6)$$

A1 = absorbance at 570 nm test well

A2 = absorbance at 600 nm test well

B1 = absorbance at 570 nm control well

B2 = absorbance at 600 nm control well

Standard molar extinction coefficients for oxidized ( $\epsilon_{ox}$ ) and reduced ( $\epsilon_{red}$ ) form of AlamarBlue<sup>®</sup> were used:

$\epsilon_{ox1} = 80,586$  at 570 nm

$\epsilon_{ox2} = 117,216$  at 600 nm

$\epsilon_{red1} = 155,677$  at 570 nm

$\epsilon_{red2} = 14,652$  at 600 nm

## 2.5.5 Statistical Methods

Mean values and standard deviations are plotted unless stated otherwise. Unpaired t-tests and two-way ANOVA were performed using Prism 7 (GraphPad software, CA, USA) with a significance of  $p < 0.05$ .

## 2.6 Results

### 2.6.1 Fluid gel material and characterisation

#### Fluid gel production

The preparation of fluid gels has been depicted in Figure 2.3a using a schematic of the cup and vane set-up. Here a constant shearing force is applied to a gellan sol as it is forced, thermally as the system is cooled, through a sol-gel transition: as such the gelation becomes confined by degree of shear applied, resulting in the formation of a particulate suspension of microgel particles Figure 2.3b and Figure 2.3 [297]. The formation of such systems was monitored via changes in viscosity as a function of temperature (Figure 2.3d). Figure 2.3d highlights that at a critical temperature an increase in the system viscosity was observed, dependent on the concentration of crosslinker in agreement with data published for quiescent gels [300]. The increase in viscosity results from the formation of particles which trap the continuous aqueous phase resulting in an effective change in the particle volume until a plateau is reached [301, 302]. Such particles were studied using optical microscopy, showing anisotropic particles with varying length to width ratios (visually observed) dependent on the salt concentration (Figure 2.3b and 2.3c, 50 and 10 mM NaCl respectively).

Mechanical responses have been shown in Figures 2.3e and 2.3f, demonstrating the typical viscoelastic properties of the fluid gel. Figure 2.3e compares the flow profile of the fluid gel against that of the current standard used for cell spraying (0.9% saline solution). The saline solution demonstrated a linear relationship between the shear stress and rate,

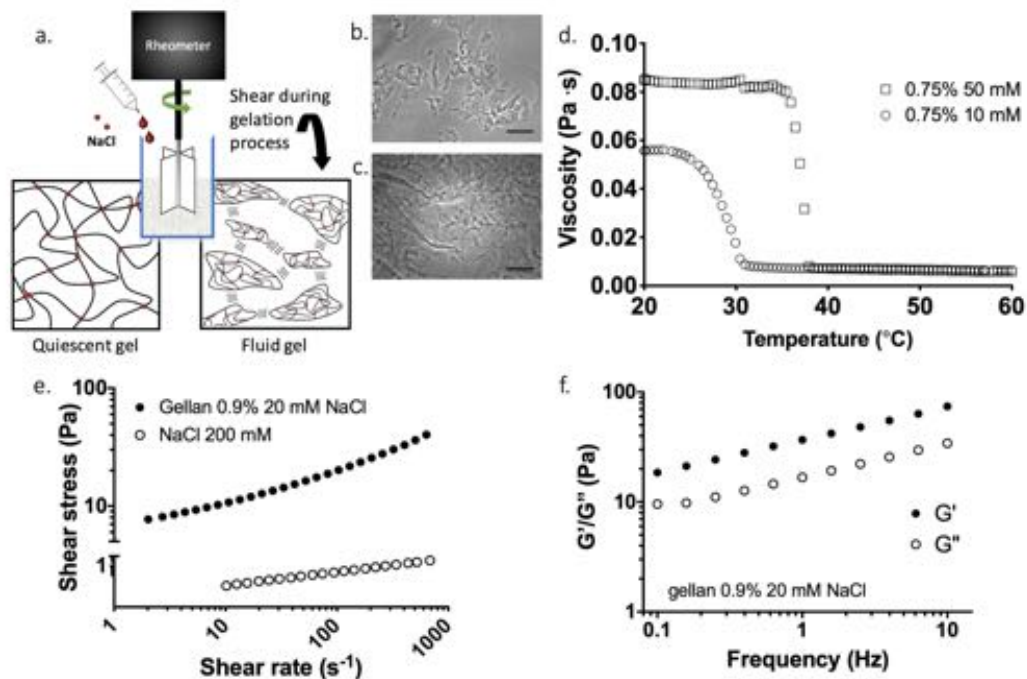


Figure 2.3: Manufacture process and characteristics of gellan fluid gel. a) Fluid gel manufacture process as adapted from Cooke et al, 2018 with permission [269]. Micrographs of diluted 0.75% fluid gels in 4:1 PEG:gellan ratio, manufactured with 50 mM NaCl (b) and 10 mM NaCl (c), scale bar = 100  $\mu\text{m}$ . d) Flow profiles for the formation of gellan fluid gel (0.75% (w/v), 10 mM and 50 mM NaCl) gelation of fluid gel occurs as temperature is decreasing under a constant shear rate of  $450 \text{ s}^{-1}$ . Values presented are of one representative measurement. e) Flow profiles of post-production of gellan 0.9%, 20 mM NaCl demonstrated a non-Newtonian shear thinning behaviour with higher viscosity at low shear compared to 200mM sodium chloride showing a linear relationship typical of a Newtonian fluid.  $N=3$  for gellan and  $N=2$  for NaCl. Mean values presented, error bars are SD (smaller than icon and therefore not visible). f) Frequency dependence of 0.9% (w/v) gellan fluid gel (20 mM NaCl) with gradually increasing  $G'$  and  $G''$  modulus under increasing frequency typical of a weak gel system. Mean values of 3 individual measurements presented, error bars are SD (smaller than icon and therefore not visible)

typical of a Newtonian system where the viscosity is independent of the shear rate. In contrast, the fluid gel exhibited a shear thinning profile, typical of such systems [297], with a much greater viscosity in comparison to the saline. Linear rheology was further probed using frequency dependent measurements to better understand the materials behaviour at rest (Figure 2.3f). Data suggests the formation of a weakly gelled network, both dependent on frequency and displaying large values of  $\text{Tan } \delta$  (ratio of loss to storage modulus;  $G''/G'$ ) [303, 304], again previously reported as typical characteristics of such

systems [269, 297, 304]. The calculated loss tangent was  $>0.1$  for all gels, as shown in Table 2.1.

Table 2.1: Rheological properties of gellan fluid gels. All gels were fabricated with low acyl gellan gum powder and cross-linked with sodium chloride (NaCl) until a final concentration of 0.75% (w/v) or 0.9% (w/v) with a constant shear rate ( $450 \text{ s}^{-1}$ ) during the gelation process. Flow profiles for 3 individual samples per gel composition was measured at  $25 \text{ }^\circ\text{C}$  and viscosity at a shear rate of  $205 \text{ s}^{-1}$  shown, mean with standard deviation (SD) is presented. Viscosity of all gels is higher than control liquid (NaCl) and dependent on cross-linker and polymer concentration.  $G'$  at frequency of 1 Hz is presented, %strain at which loss of storage modulus occurs indicating the end of the LVR, loss tangent ( $G''/G'$ ), a loss tangent of  $>0.1$  indicates a weak gel [304], as shown here all fluid gels compositions can be considered weak gels. \*1 sample of 200 mM NaCl was tested, viscosity measured at shear rate of  $205 \text{ s}^{-1}$ .

Material	Solution concentration	Cross-linker concentration (mM)	Mean viscosity (Pa.s) (SD)	$G'$ (Pa) (SD)	Strain	
					end LVR (%)	Loss tangent ( $G''/G'$ )
Gellan	0.75% (w/v)	10 mM	0.085 (0.001)	5.99 (0.17)	15.87	1.03
		20 mM	0.076 (0.000)	10.45 (0.42)	12.00	0.70
		30 mM	0.086 (0.002)	36.46 (3.42)	6.39	0.35
		40 mM	0.110 (0.002)	105.74 (5.48)	4.02	0.21
		50 mM	0.118 (0.005)	215.03 (35.89)	2.52	0.16
	0.90% (w/v)	10 mM	0.117 (0.001)	12.54 (0.29)	12.00	0.84
		20 mM	0.125 (0.003)	36.81 (1.28)	22.26	0.45
		30 mM	0.135 (0.006)	94.45 (7.97)	6.39	0.27
		40 mM	0.143 (0.002)	171.23 (10.36)	4.02	0.21
		50 mM	0.177 (0.011)	388.47 (100.14)	2.52	0.17
Sodium chloride	200 mM	-	0.004*	-	-	-

## Modulation of fluid gel properties

Manipulation over the material properties of the fluid gels was probed systematically as a function of both polymer and cross-linker concentrations; with a view to improve the characteristics required for enhanced “spray-ability”. Flow behaviour and viscosity for the fluid gel systems have been shown in Figure 2.4a Figure 2.4b. All systems showed a high degree of shear thinning as the shear rate was increased from  $0.1$  to  $600 \text{ s}^{-1}$  (Figure

2.4a). Shear profiles were used to estimate the behaviour of the fluid during spraying. This was achieved by comparing data. As previously described by Hendriks et al.[277] the expected shear rate  $\dot{\gamma}$  encountered during spraying can be estimated by calculating the nozzle-induced shear rate  $\dot{\gamma}$  in  $\text{s}^{-1}$  during spraying with Equation 2.7.

$$\dot{\gamma} = \frac{V}{D_N} \quad (2.7)$$

- $\dot{\gamma}$  = shear rate in  $\text{s}^{-1}$
- $V$  = velocity of liquid ( $\text{m s}^{-1}$ )
- $D_N$  = diameter of nozzle (m)

Standard nozzle diameter of the airbrush is  $750 \mu\text{m}$  ( $7.5 \times 10^{-4} \text{ m}$ ). Flow velocity ( $v$ ) was calculated by Equation 2.8

$$Q = v \times A \quad (2.8)$$

- $Q$  = volumetric flow rate ( $\text{m}^3 \text{ s}^{-1}$ )
- $v$  = flow velocity ( $\text{m s}^{-1}$ )
- $A$  = column cross-sectional area ( $\text{m}^2$ )

For the standard nozzle size of  $750 \mu\text{m}$ , the nozzle induced shear rate of gellan 0.9% hydrogel was estimated at  $223 \text{ s}^{-1}$ . Viscosities were obtained and compared at the calculated shear rate were derived from rheology testing (Figure 2.4b). For airbrush application, the estimated viscosity of the material was shown to be a function of both polymer and NaCl concentration. At comparative cross-linking concentrations, the higher polymer systems resulted in increased fluid gel viscosities. Additionally, a linear correlation between cross-linker concentration and viscosity was observed, again where higher concentrations of the cross-linker formed more viscous suspensions. However, ultimately all systems were characterised by a low spraying viscosity,  $8.4 \times 10^{-2} \text{ Pa.s}$  ( $\pm 6.7 \times 10^{-4}$ ) to  $1.8 \times 10^{-1} \text{ Pa.s}$  ( $\pm$

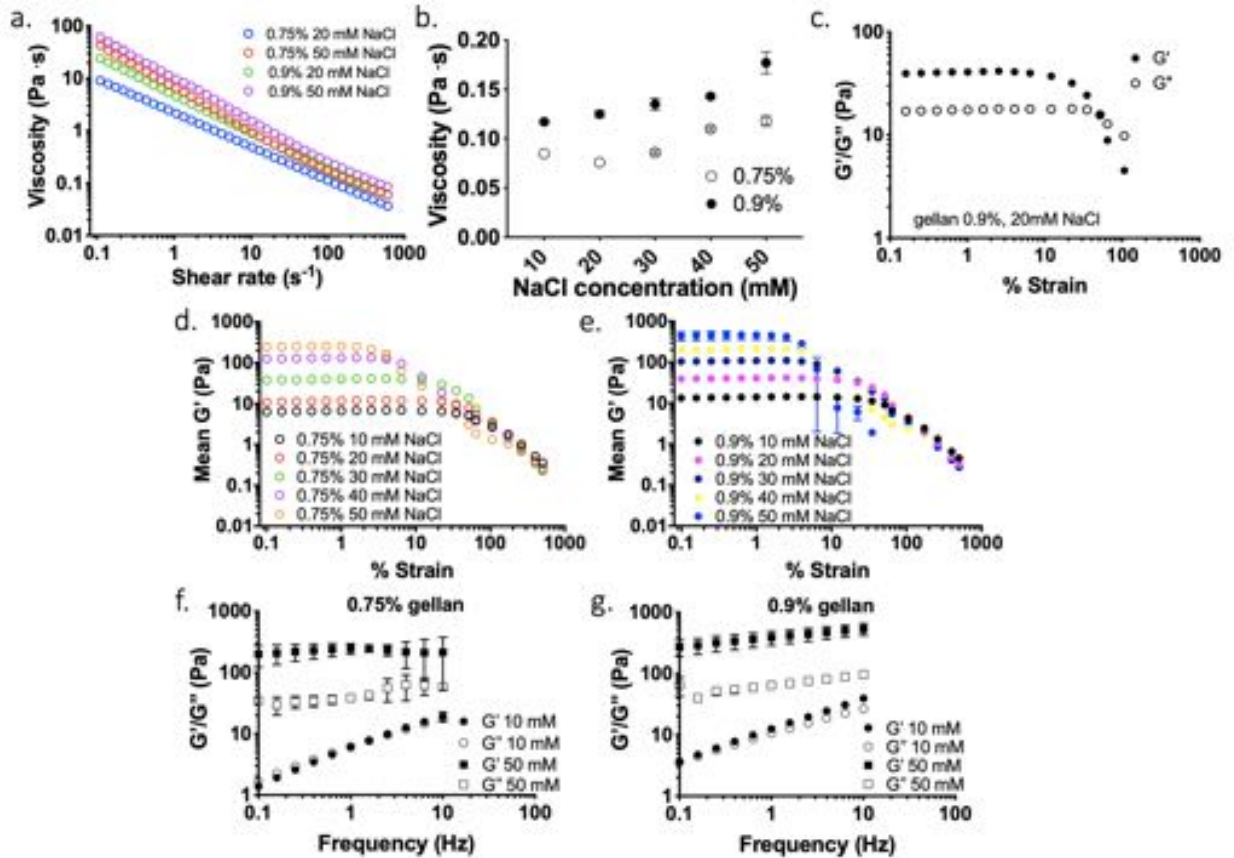


Figure 2.4: Modulation of fluid gel properties. a) Demonstrates that gellan fluid gels behave as shear-thinning materials (non-Newtonian), since viscosity decreased as shear rate increased. Four compositions of gellan fluid gel (0.9% (w/v), 20 mM and 50 mM NaCl and 0.75% (w/v), 20 mM and 50 mM NaCl) presented. b) Increasing crosslinker or polymer concentration results in higher viscosity as demonstrated here. Data is mean viscosity at shear rate 205 s<sup>-1</sup> c) Amplitude dependence of storage and loss moduli in gellan 0.9%, 20 mM as representative gel shows that under increasing strain eventually G' and G'' will cross-over resulting in a G'' dominated system indicating more liquid like behaviour under high strain. Storage modulus as a function of the polymer and salt concentration of 0.75% fluid gels (d) and 0.9% fluid gels (e) shows an earlier loss of storage modulus (shorter LVR's) in higher salt-concentrations. f) Frequency dependence of four systems is shown here to illustrate influence of salt-concentration on viscoelastic-properties, from viscoelastic-solids at 10 mM NaCl concentrations to gel-like behaviours at 50 mM NaCl concentrations. G'' (open signs) and G' (closed signs) values are presented. Unless stated otherwise, mean values of three independent measurements are presented, error bars represent the standard deviation. Mean values of 3 individual measurements presented, error bars are SD (smaller than icon and therefore not visible).

1.2 x 10<sup>-2</sup>). Although such viscosities are considered in this case low, they are still over an order of magnitude greater than the viscosity of the current standard delivery medium used for cell spraying.

The amplitude dependence (reflected in percentage strain) of the storage and viscous moduli are presented in Figure 2.4c. Under increasing strain all tested compositions of gellan fluid gels eventually underwent a cross over showing a transition in  $G'$  dominance to systems governed by  $G''$  (full data range shown in supplementary Figure A.3 panel of gels). The data highlights one of the important properties of the fluid gels, where at large deformations the suspensions act as liquid-like materials, enabling flow. Changes in the degree of bulk suspension elasticity ( $G'$ ) as a function of the polymer and salt concentration has been demonstrated in Figure 2.4d and Figure 2.4e. Here both the magnitude of  $G'$  and length of the LVR were observed to be a function of the polymer and cross-linker concentrations, with the LVR shortening and modulus increasing with elevated salt concentrations.

Frequency data obtained for the fluid gel formulations highlighted a change in mechanical behaviour with frequency sweeps of 10 mM NaCl systems demonstrating initial  $G'$  dominated systems with clear cross-overs to  $G''$  domination Figure 2.4f and Figure 2.4g. However, at higher salt concentrations (>20 mM to 50 mM) plots showed  $G'$  dominance over the whole frequency range studied, with both  $G'$  and  $G''$  demonstrating some frequency dependence, typical of viscoelastic gel-like fluids. Gel strength was observed to increase, described by a reduction in  $\tan \delta$  (Table 2.1 and supplementary Figure A.1) as a function of both salt and polymer concentration.

A simple experiment to demonstrate the clinical challenge of spray run-off has been shown in Figure 2.5a, in which the control (sodium chloride) instantly flows on vertical tilted porcine skin surface in comparison to the retained fluid gel. Fluid gel hysteresis was probed to study the time dependent behaviours of the systems post spraying, using consecutive shear ramps: increasing and decreasing in shear rate ( $0.1- 600 \text{ s}^{-1}$  and  $600$  to  $0.1 \text{ s}^{-1}$ ). Direct comparison of the flow profiles suggests little change, with a large degree of the initial viscosity of the system is recovered almost instantaneously, Figure 2.5b. The rheological phenomenon known as the dynamic yield stress was examined to describe the ability of the fluid gel to be maintained upon the skin without flowing. The

Herschel-Bulkley model can be used to determine the yield stress of a fluid [305]. Data fitted to the model presented for the second sweep (example shown in Figure 2.5c and supplementary Figure A.2). Yield stress plotted as a function of the fluid gel formulations have been presented in figure 2.5d (full data presented in Table 2.2). Fitting to the 10 mM NaCl systems for both polymer concentrations resulted in negative values, indicating an inadequate means of describing the yield-stress fluid. However, a linear correlation between NaCl concentration and yield stress was observed for the higher concentrations. A simple gravitational model described for “sagging” was used to assess fluid gel resistance to flow on an inclined plane. The gravitational forces, described as ‘maximum stress on the material at an inclined surface’ were calculated with Equation 2.2 using the following values: material density of  $1020 \text{ kg m}^{-3}$  for fluid gel (0.9%, 20 mM NaCl), assuming a fluid gel thickness of  $1.0 \times 10^{-4} \text{ m}$  and a substrate angle of  $45^\circ$ . The calculated maximum stress was observed to be lower than the yield stress of the gel, with values of 0.85 Pa and 1.777 Pa respectively.

### **Spray-ability of the fluid gel carrier**

Spreading properties of the fluid gels in comparison to saline solution were investigated to gain further information of both coverage and run-off. The contact angles for the fluid gel and control (NaCl) were measured on a variety of substrates, comparing their wetting ability. Gellan fluid gels exhibited a significantly higher mean contact angle than NaCl on gelatin ( $63.3^\circ$  vs  $44.4^\circ$ ,  $p < 0.001$ ), porcine epidermis ( $54.8^\circ$  vs  $25.37^\circ$ ,  $p < 0.001$ ) and porcine dermis ( $59.7^\circ$  vs  $36.6^\circ$ ,  $p < 0.001$ ) describing lower wettability, resulting in reduced spreading. There was no significant difference found for contact angles on ceramic, with a mean contact angle of  $37.5^\circ$  for gellan fluid gel and  $35.8^\circ$  for NaCl (Figure 2.6a).

Flow and spreading due to the thermo-responsive properties of the gellan was also investigated. The effect of increasing temperature on the degree of structure within the fluid gels system was investigated as a function of  $G'$  and  $G''$  (Figure 2.6b). Increasing temperature resulted in a reduction in the storage modulus, as the junction zones that

Table 2.2: Fitting parameters from the Herschel-Bulkley model for gellan fluid gels. Values presented are mean of 3 individual measurements, yield stress (+ SD), K is the consistency index, n is the flow index. E is standard error, presented for each fitting value and R square as value for goodness of fit.

Gellan concentration (% w/v)	Final NaCl concentration (mM)	Mean Yield Stress (SD)	$E_Y$	K	$E_K$	n	$E_n$	$R^2$
0.75%	10	-0.655 (0.005)	0.072	2.508	0.049	0.360	0.004	0.9995
	20	0.250 (0.018)	0.156	1.945	0.108	0.377	0.010	0.9965
	30	2.130 (1.306)	0.208	1.657	0.125	0.409	0.016	0.9928
	40	3.854 (0.084)	0.436	1.405	0.302	0.466	0.021	0.9848
	50	5.231 (0.227)	0.436	1.247	0.461	0.496	0.023	0.9804
0.90%	10	-0.848 (0.016)	0.291	3.844	0.060	0.340	0.070	0.9387
	20	1.777 (0.091)	0.226	2.860	0.156	0.383	0.010	0.9969
	30	4.446 (0.098)	0.305	2.508	0.184	0.413	0.015	0.9934
	40	5.357 (0.072)	0.806	2.166	0.653	0.441	0.023	0.9775
	50	7.036 (0.572)	1.600	2.921	1.454	0.423	0.030	0.9624

create the 3D matrix began to break down, resulting in fluid-like behaviour of the gels. In general, a reduction in storage modulus appeared to occur between 30 – 40 °C for all gels, as shown in (Figure 2.6c), this range includes peripheral skin temperature. Based on the rheological data, gellan fluid gel with 0.9% polymer concentration and 20 mM NaCl cross-

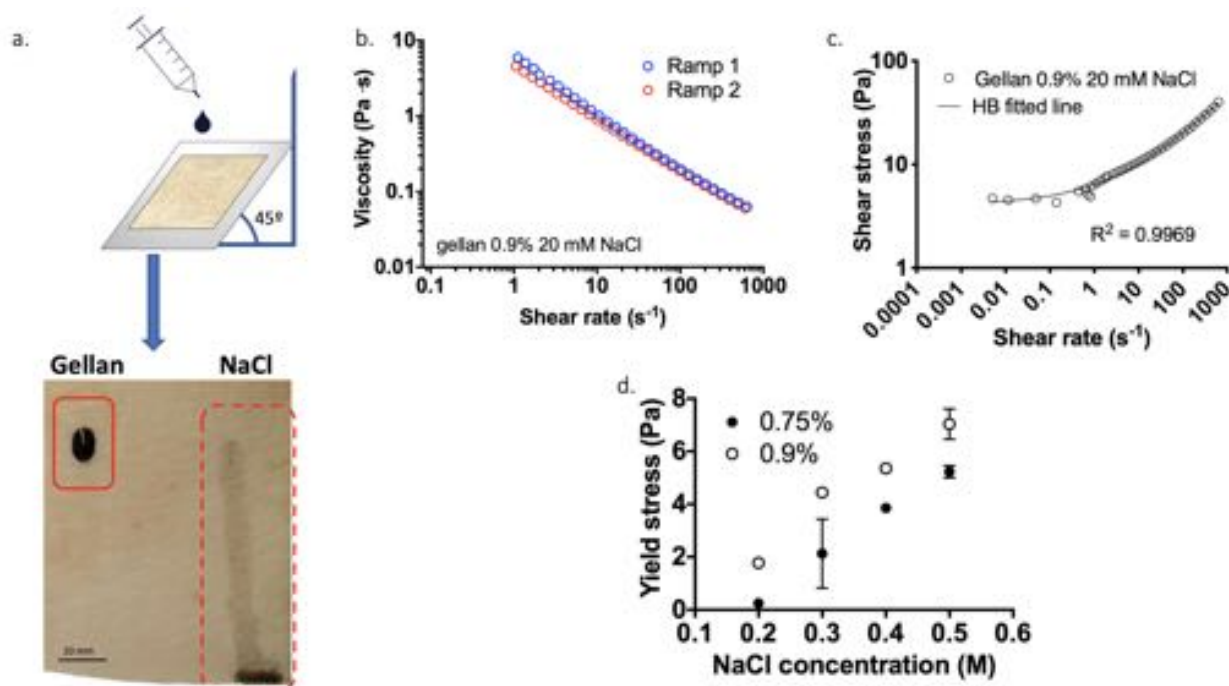


Figure 2.5: Determination of fluid gel retention. a) gellan fluid gel (0.9% (w/v), 20 mM NaCl) and sodium chloride (200mM) were dyed with acrylic black ink (Daler Rowney Bracknell, UK). Gellan fluid gel (left) and sodium chloride (right) droplets applied to tilted porcine skin at the same time. A low rate of spreading of the gellan fluid gel compared to sodium chloride was macroscopically observed. b) Viscosity of gellan fluid gel under increasing (ramp 1) and decreasing (ramp 2) shear rates over a known time frame. Plotted data includes mean viscosity of 0.9% (w/v), 20 mM NaCl prepared under same conditions, error bars represent SD. Increase in shear rate leads to shear thinning (decrease in viscosity) and decreasing the shear rate allows the gellan fluid gel to recover, demonstrated as increased viscosity resulting in a small thixotropy. Mean values of 3 individual measurements presented, error bars are SD (smaller than icon and therefore not visible) c) Herschel-Bulkley model fitted for 0.9%, 20 mM NaCl gel showing an excellent fit to the model represented in a  $R^2$  of 0.9969. d) Yield stresses determined using the Herschel-Bulkley model for 0.75% and 0.9% fluid gels with 20, 30, 40 and 50 mM NaCl. Yield stress was found to increase in higher polymer concentration gels and in higher salt-concentrations. Mean values of 3 individual measurements presented, error bars are SD.

linker concentration was considered most suitable for the cell spray application (further discussed later), and thus used for further studies.

Spray coverage (% coverage) is the proportional area of receiving surface covered by sprayed material (gellan hydrogel or control liquid). A higher percentage of area was covered with water compared to gellan hydrogel, although these differences were not statistically significant 2.7c and Figure 2.7d. As expected, a higher percentage coverage was

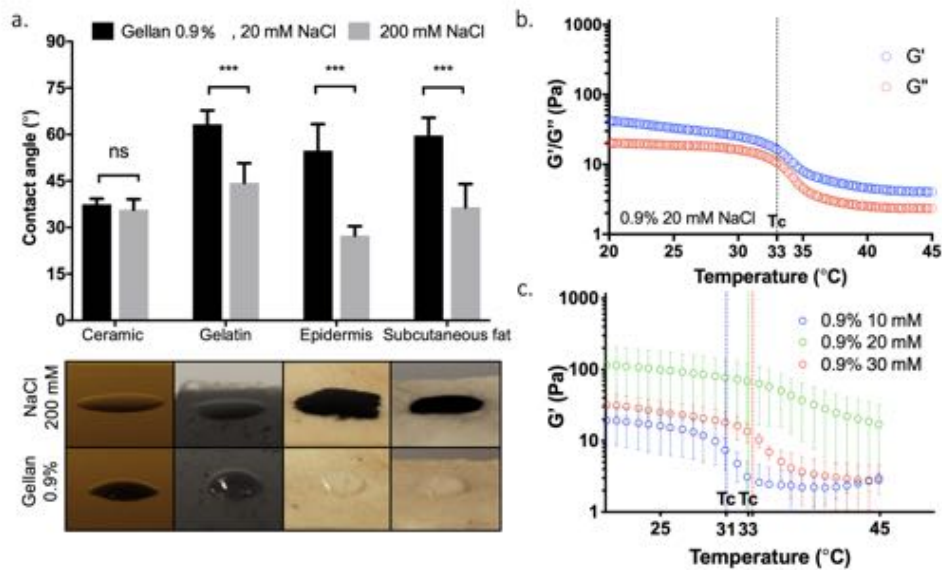


Figure 2.6: Structural stability on the receiving surface. a) Mean contact angles of gellan fluid gel (0.9% (w/v), 20 mM) compared with control liquid (sodium chloride, 200 mM) on a variety of surfaces. Three repetitions for each surface and three measurements per repetition were performed. Error bars represent SD. Gellan fluid gel demonstrates larger contact angles on all tested surfaces compared to control liquid. b) Thermo-responsive properties of gellan (0.9%, 20 mM NaCl) was probed by investigating viscoelastic properties under increasing temperature. Increasing temperature resulted in a reduction in the storage modulus, resulting in fluid-like behaviour of the gel. Tc denotes the critical temperature at which the elastic structure starts to rapidly break down. Values presented are of one representative measurement. c) The storage modulus against rising temperatures in a panel of gellan fluid gels is presented. Gels with higher cross-linker concentrations de-structure (show fluid like behaviour) at higher temperature levels. Mean values of 2 individual measurements presented, error bars are SD.

achieved when sprayed volume was increased, however, this was not proportional, i.e. doubling the volume did not double the area covered 2.7d. There was a non-statistically significant positive correlation between sprayed volume and percentage coverage for gellan hydrogel ( $p=0.301$ , 95%CI: 33.09, 11.86; Pearson correlation 0.820) and water ( $p=0.065$ , CI95%: -34.066, 1.308; Pearson correlation 0.723). This could be explained by the observed accumulation of droplets (especially in the centre of the sprayed area) with increasing volumes.

Individual droplet size was determined for all sprayed cards with ImageJ Software. The minimum cut off droplet size was set at  $0.01 \text{ mm}^2$ . Mean droplet size of water ( $5.5 \times 10^{-2} \text{ mm}^2$ ) and gellan fluid gel ( $5.2 \times 10^{-2} \text{ mm}^2$ ) was not found to be significantly different

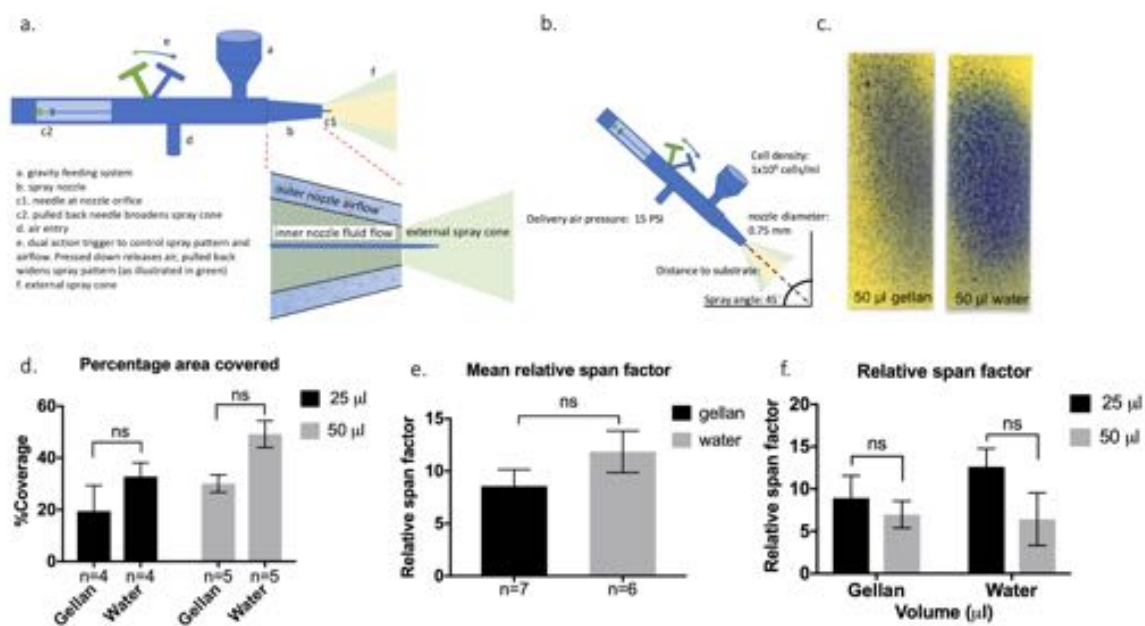


Figure 2.7: Spray features of gellan gum fluid gel. 0.9% (w/v) gellan fluid gel with 20 mM NaCl cross-linker was used for all spray experiments presented in this figure. Mean values are presented, error bars represent SD. a) Schematic illustration of airbrush and its nozzle. b) Schematic of standardized airbrush spray experiment set up. c) Illustration of water-sensitive paper with area coverage demonstrated for sprayed gellan fluid gel and control (volume of 50  $\mu\text{l}$ ). d) percentage of area covered seems higher with sprayed water compared to gellan fluid gel, but no statistically significant difference was found. e-f) A lower mean relative span factor was calculated for gellan fluid gels (gellan) in comparison to control liquid (water) for both sprayed volumes together (e) and separated (f), this difference was more profound when looking at low sprayed volumes of 25  $\mu\text{l}$ , indicating a more uniform spray distribution for the gel, but no statistical difference was found.

( $p=0.326$ , 95%CI: -0.011, 0.004). On the other hand, the gellan fluid gel has a lower mean relative span factor (RSF) of 8.57 indicating a more uniform drop size distribution compared to the water (11.84). However, this difference was not found statistically different ( $p=0.457$ , 95% CI: -8.77, 2.23). Droplet size distribution dependence on sprayed volume was investigated by comparing the RSF of two sprayed volumes per material. Gellan fluid gel showed a smaller decline in RSF when a smaller volume is sprayed compared to water, but this difference was not found significant ( $p=0.854$ , 95% CI: -12.00, 4.62 for 25  $\mu\text{l}$  and  $p=0.654$ , 95%CI: -33.24889, -4.89256 for 50  $\mu\text{l}$ ). (Figure 2.7e and Figure 2.7f).

## 2.6.2 Biological response to fluid gel spray delivery

### HDF cell viability

Limited evidence of airbrush cell spray systems has been published, with most data presenting moderate cell viability (69%-70% survival) following spraying in Hank's Balanced Salt Solution [280] or cell culture media [75]. As investigated by Hendriks et al. [277] certain spray conditions impact on cell viability such as receiving tissue/substrate stiffness, viscosity of cell carrier, nozzle-surface distance and delivery pressure. Therefore, all these conditions were standardised to reduce bias as described in the methods section. The study aimed to develop a cell carrier with maintaining a cell viability comparable to current spray systems. Cell viability of sprayed encapsulated human dermal fibroblasts was evaluated at days 1, 3, and 7 using live/dead assay as demonstrated in Figure 2.8. Cells remained viable in the gellan fluid gel up to at least day 7, with a mean cell viability of 88.0% (range 80.6% - 96.9%). Encapsulated HDFs attached to the bottom of the culture disks at day 7 (Figure 2.9c) and spreading of the cells was observed at day 14 (Figure 2.9d). Therefore, it can be assumed that cells are able to leave the gel, whether this is by active migration or passive sedimentation needs to be confirmed. Sprayed HDFs encapsulated in gellan fluid gel maintained similar high viability throughout the studied period, there was no statistically significant difference between the application methods (Figure 2.8b).

The effects of spraying and encapsulation were also investigated for platelets derived from whole blood. The results are less promising in terms of viability post-spraying or encapsulation, however, a potentially interesting finding of platelet activation upon spraying could be further explored for topical platelet applications. The preliminary results of this work are presented in Appendix B.

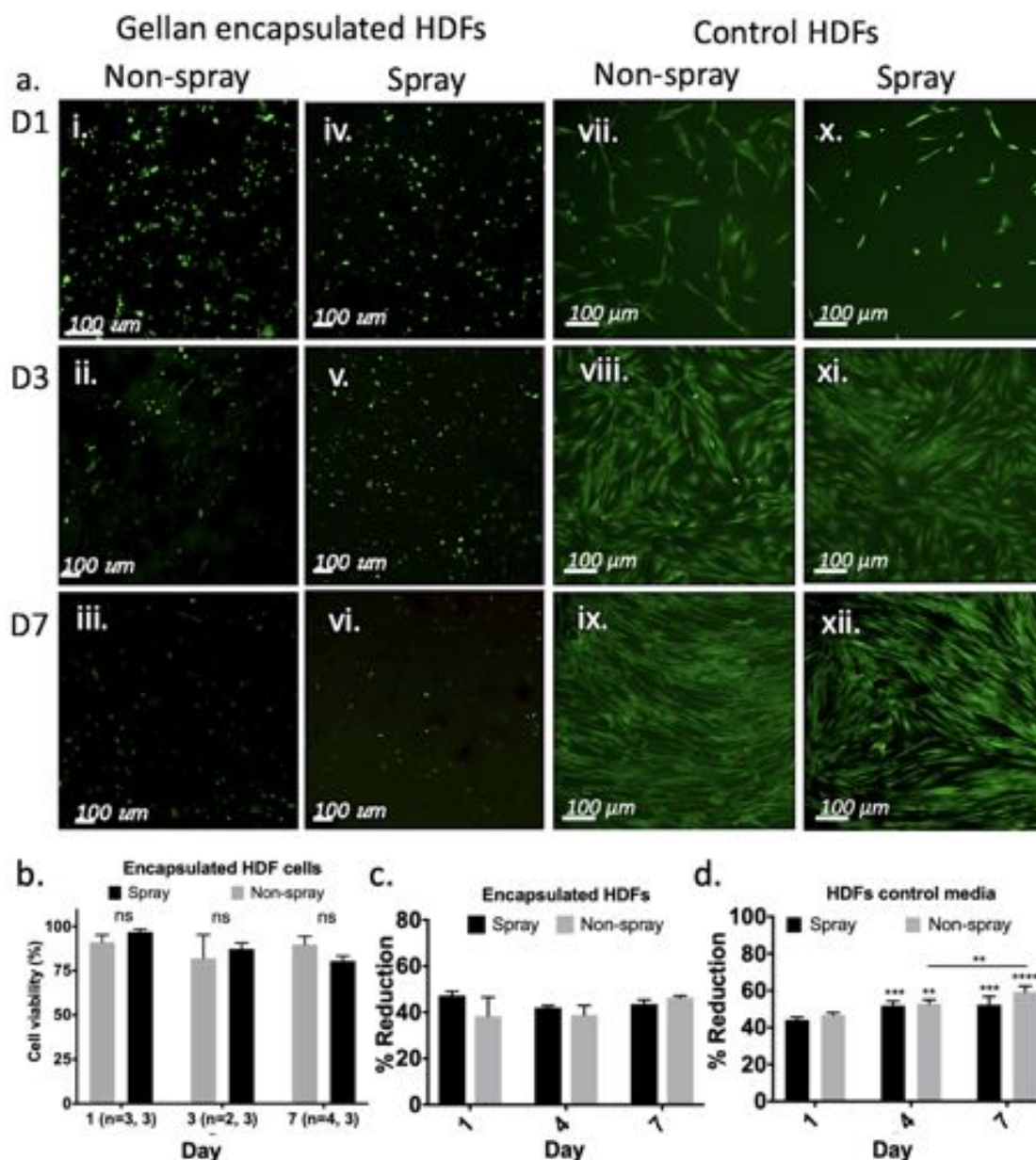


Figure 2.8: Human dermal fibroblast response to fluid gel spray delivery. ai-axii) Fluorescence cell viability assay of encapsulated human dermal fibroblasts (HDF) before (i-iii) and after (iv-vi) spraying shows similar high cell viability. Similar for good viability is seen in sprayed cells (x-xii) in control medium compared to non-sprayed cells (vii-ix). b) No significant differences between the two groups on each timepoint was found. Presenting data is mean cell viability and SD. c,d) Alamar blue assay of encapsulated and control HDFs. %Reduction of encapsulated sprayed and control cells did not change significantly over the studied period. Statistically significant differences were found for cells sprayed in medium, comparing day 1 to day 4 and day 7 and in non-sprayed cells also between day 4 and day 7. Significant differences found by two-way ANOVA and post-hoc statistical testing is indicated by \*( $p < 0.05$ ), \*\*( $p < 0.01$ ), and \*\*\*( $p < 0.001$ ), which correspond to p values in brackets. Data are presented as the means (+SD) from one experiment, performed in triplicate.

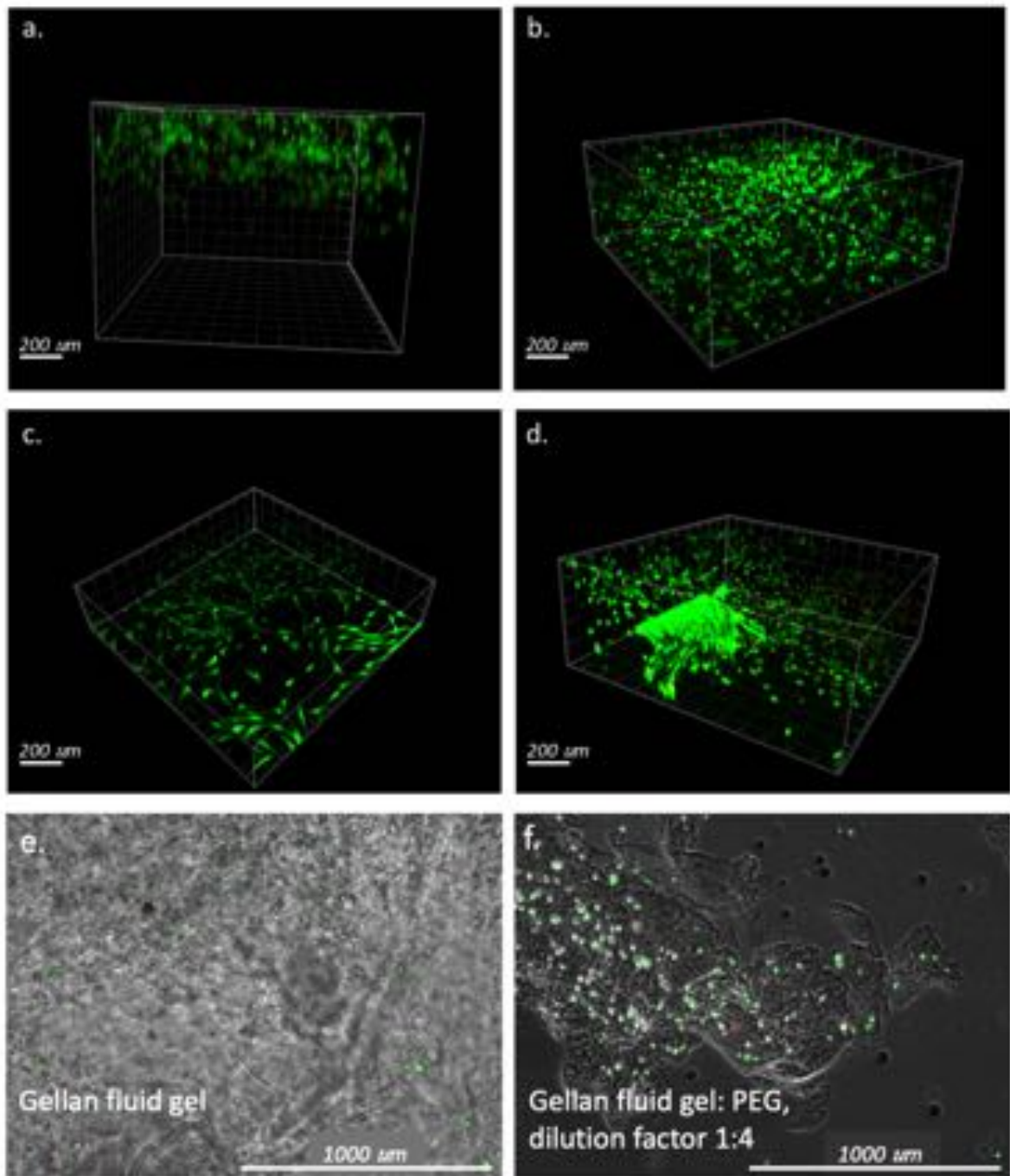


Figure 2.9: Live/dead assay of HDFs encapsulated in gellan fluid gel. Z-stack image of fluorescence cell viability assay of human dermal fibroblasts (HDF) after 1 day (a), 3 days (b), 7 days (c) and 14 days (d) of encapsulation in gellan fluid gel (live cells stained green, dead cells stained red). Cells are viable and attach to the bottom of the well and seem to migrate out of the gel. Position of cells within the gel is shown in micrographs of encapsulated cells in gellan fluid gel (e) stained with fluorescence live/dead dye and in PEG diluted fluid gel (f). Images were obtained at day of encapsulation.

## Metabolic activity

Alamar blue, a non-toxic reagent used to quantify the cellular metabolic activity, was used to investigate metabolic activity of encapsulated and sprayed cells. Data shown in Figure 2.8c-d shows metabolic activity directly measured via absorbance, expressed by percentage of reduction. Percentage reduction of encapsulated cells remained stable over the tested period of 7 days. Whereas cells in culture medium showed a significant increase in percentage reduction indicating a proliferation of the cells following delivery Figure 2.8d. No statistically significant differences of sprayed cells compared to non-sprayed cells were found. Data implies that proliferation capacity of encapsulated cells is limited, while cell viability remains high.

## 2.7 Discussion

Cell spraying techniques have been translated to clinical practice, but limited success finds them not routinely used within burns care [101]. Several features of the cell solution could be compromising the full potential of the technology: e.g. cell-spillage, non-uniform distribution [47] and decrease in cell viability following transplantation [278].

This study aimed to remedy this clinical problem by engineering a sprayable gellan-based fluid gel, to enable cells to be transplanted to the receiving surface without spillage and/or loss of cell viability. The polymer used to prepare the hydrogel was gellan gum, a polysaccharide derived from the bacterium *Pseudomonas elodea*, comprised of D-glucuronic acid, L-rhamnose and D-glucose subunits. This natural polymer is FDA approved as a food additive, however, has also found its way to the pharmaceutical and biomedical industry due to its biocompatibility in a range of tissues - demonstrating non-cytotoxic behaviour. A plethora of biomedical applications for gellan gum have been reported, such as regeneration of cartilage [181, 306], neural tissue [307] or intervertebral discs [308] and topical applications to enhance wound healing [309], have arisen from its diverse nature lending it to applications such as injectables, films/dressings, eye drops

and cell culture matrices [182].

Cross-linking of gellan gum can be achieved using ionic cross-linkers with monovalent cations ( $\text{Na}^+$  or  $\text{K}^+$ ) resulting in the formation of weaker gels than comparative divalent cations [298, 300, 310]. Strong gels, although they do not disintegrate easily upon the wound bed like weak gels, do not easily conform to the body resulting in poor bioavailability. Even though on a bulk scale weaker gels are prone to breaking-up, the ability to get them to conform and disintegrate on a microscale presents an advantage for sprayed cell applications; as a gradual form of degradation is desired to release the cells and eventually remove the foreign material. The lack of cell binding capacity of gellan also means that cells do not necessarily attach to the material readily [311], which is again beneficial for rapid cell release from the gel to tissue. Furthermore, adhesive cells such as fibroblasts and keratinocytes are dependent on adhesion to exhibit differentiation, therefore adhesive cells can be encapsulated in gellan hydrogel while potentially preserving their differentiation potential.

Fluid gels formulated with gellan therefore propose an ideal matrix for cell delivery, via spraying; demonstrating key rheological properties needed for both spraying and contouring to the wound surface for the release of cells in situ (Figure 2.3). Fluid gels are formed via the application of constant confinement (mechanical shear) to a biopolymer undergoing a sol-gel transition [297, 312]. Applying this technique to gellan results in the restriction of ordering during the random coil to helix transition, preventing the formation of a continuous gelled network, and forming a particulate suspension; where particle growth is governed ultimately by the interplay between gelation kinetics and degree of confinement acting within the system [313] (Figure 2.3a). This was demonstrated by the change in gelling profiles for the 0.75% (w/v) fluid gels prepared using either 10 or 50 mM NaCl. Here, for the same degree of confinement applied (a shear rate of  $450 \text{ s}^{-1}$ ), systems resulted in very different gelling temperatures and final viscosities (although it is key to note that these viscosities are found well within the systems shear thinning region). In this case the heightened concentration of crosslinker has prompted gelation at

higher temperatures, as expected from literature, as the salt ions promote the formation of helices with tighter binding and stronger junction zones [314]. Changes in the viscosity of the two systems is described in a similar way, where tighter binding and stronger junction zones between polymer chains results in more rigid particles [314] and a subsequent increase in suspension viscosity as demonstrated by Adams et al. [315] in accordance with Snabre and Mills [316]. Micrographs of the systems suggested changes in particle morphology (Figure 2.3b and Figure 2.3c). Differences in particles formed under the same degree of shear are likely to reflect a change in the mechanism of formation, as detailed by Fernández Farrés et al. [290]: who demonstrated that at faster gelation kinetics large gelled entities were initially formed that became broken down in flow, whereas as when gelation is much slower, particles were formed within the elongation flow itself - within the rheometer geometry [290, 297, 317] (although further characterisation of the systems here is needed to qualitatively address key parameters including particle size and degree of anisotropy to draw stronger conclusions on this area).

Systematic modulation of the fluid gel properties, in order to optimise the system for spray applications was achieved through careful control over the formulation; varying both the biopolymer and cross-linker concentrations. Changes in the microstructure were probed using small deformation rheology. Frequency dependence sweeps of low salt concentration systems demonstrated an initial  $G'$  domination with a clear cross-over to  $G''$  domination. Whereas at higher salt concentrations, these cross-overs did not occur and  $G'$  dominated over the whole frequency range studied, but both  $G'$  and  $G''$  are demonstrating some frequency dependence, with decreasing values for the loss tangent ( $\tan \delta$ ) as a function of increasing salt concentrations. Gel-like mechanical spectra arise from the restriction of polymer movement preventing the polymers from relaxing. However, within the gel systems, polymer re-arrangement results in viscous dissipation of energy ( $G''$ ) [318, 319]. The reduction in  $\tan \delta$  suggested increased hinderance within the gelled matrix, as polymer re-arrangement becomes increasingly prohibited, due to a higher crosslink density at higher salt concentrations. This has also been seen in the frequency depen-

dence data which indicates that the fluid gels became stiffer at a high frequency due to the rapid relaxation time of short chain segments. On a bulk scale, this results in the formation of stiffer particles, with suspensions exhibiting increased storage moduli [315]. Meanwhile  $G''$  also increased with increasing frequency, contributing to recoverable deformation and energy dissipation, especially in fluid gels with a low crosslinking degree (10 mM NaCl). However, it is key to note that although the suspension rheology is governed primarily through the stiffness of the particles, weak interactions between particles [269, 290, 297, 313] effectively resulted in the suspensions demonstrating mechanical spectra which fall somewhat between those typical of entangled polymers and strong-gels [297].

Strain sweeps were used to explore the nature of the weak forces between suspended particles. It has previously been proposed that during the conformational change of the biopolymer during cooling (coil to helix formation) complete polymerisation at the particle interface becomes prevented [297, 313]. This results in points of weak association between particles. On deformation the fluid gel suspensions reached a critical strain at which they no longer act linearly. This critical strain is principally related to the proximity of gellan chains to each other and the number of weak interactions (hydrogen bonds etc.) at both the particle interfaces, and interstitial gellan remaining within the aqueous phase [320]. At larger deformations physical debonding between particle-particle and particle-interstitial gellan can occur resulting in a reduction in storage modulus. Reduced deformation of the fluid gel particles as a function of the increased stiffness (at higher salt concentrations) results in a shortening of the contact zones between particles, effectively reducing the degree of interactions between polymer chains [315]. This explains the reduction in LVR with increasing salt concentrations. Furthermore, it is hypothesised that changes in particle morphology (smaller discrete through to long ribbon-like particles) may also play a role within the particle contact time; as the longer “ribbon-like” particles remain in contact across much larger strains (deformations) before the systems begin to breakdown [317, 321]. Again, such inferences require further quantification of the

micrographs obtained.

The effects of formulation on suspension viscosity were studied in respect to sprayability. The effect of salt concentration has been previously described within the manuscript, however, viscosity modulation was also achieved by changing the concentration of polymer. Once gelled under shear, the formation of particulates resulted in entrapment of the continuous aqueous phase, effectively increasing the volume occupied by the particles. In correspondence with work published by Adams et al. [315], a direct correlation between the initial polymer weight fraction and particle phase volume can be assumed, as such the increase in viscosity thus becomes a function of the particle packing fraction; with rheologies typical of highly concentrated systems [322]. However, at shear rates comparable to those expected during spraying, all systems resulted in a degree of shear thinning that allowed application.

Fluid gel systems exhibited very little thixotropy, recovering much of their original viscosity once shear had been removed. Flow profiles were compared to the Herschel-Bulkley equation, which highlighted the presence of a yield stress for all systems formulated with  $> 20$  mM NaCl. Again, similar trends to the small deformation rheology were observed, where increases in both salt and polymer concentrations, tended towards larger yield stresses. Such overlap implies a common mechanism, whereby increased crosslink density and subsequent interactions (increased  $G'$ ), results in connected particles that require a critical stress in order to induce flow. Yielding values were compared to gravitational stresses, as a simple force balance. In all cases where yielding behaviour was observed, the fluid gel yield stress surpassed that of the gravitational stress, suggesting long residence times on the skin, where many of the surfaces are contoured. Clinically this means the finite gelled layer would remain in situ until mechanically removed, likely during dressing changes or other cleaning processes.

Following the ability to spray, spreading of the material post-application is also important: as large degrees of spreading lead to vast amounts of run-off and too little prevents the formation of a continuous layer. Complete wetting of a material to the surface occurs

when the contact angle is near to  $0^\circ$  as high wetting requires small contact angles  $<90^\circ$ , while large contact angles refer to low wettability  $>90^\circ$  [323]. Contact angles obtained for the fluid gel systems across a variety of materials including biological substrates encountered within a burn environment: epidermis and subcutaneous fat (Figure 2.5a). The gellan-based systems showed a significant increase in contact angle ( $p < 0.001$ ) across the gelatin, epidermis and subcutaneous fat substrates. This is a result of enhanced viscosity which strongly influences the liquid-surface. Fluid gels are enriched with the presence of polar groups, long polymer chains and possibly additional side chains causing a slower spreading, and less spillage. Whereas the low-viscosity saline solutions (such as sodium lactate and sodium chloride solutions), currently used as the delivery vehicle of choice in sprayed cell systems, exhibit low cohesive forces suggesting stronger adhesive forces to the substrate resulting in high wettability.

Spreading as a result of the thermo-reversible nature of the gellan gels was also probed, in respect to temperatures associated with burns wounds. Average peripheral skin temperatures lie around  $34^\circ\text{C}$  [324], but can vary greatly in critically ill patients, especially following burn injuries  $p < 0.001$  when room and body temperatures are deliberately increased [324, 325]. Upon heating, the gels showed weakening of the interactions between the particles as demonstrated by a reduction in  $G'$  at a critical temperature,  $T_c$  (Figure 2.5b). This loss of storage modulus is caused by the gel melting (initially by melting of residual unaggregated helices and secondly by melting of the aggregated double helices [298]), with  $T_c$  correlating closely with literature obtained using as differential scanning calorimetry (DSC) [? ]. Structural weakening was shown to be influenced by salt concentration as expected from literature. As such, delayed onset of gel breakdown could be achieved by increasing the cross-linker concentration (Figure 2.5c), corresponding to data by Morris et al [298]. Ultimately the balance between the mechanical behaviour of the gels and weakening is important as a certain degree of gel breakdown is desired, so cells are easily able to be released from the gel. Also, to improve patient experience the remaining polymer can be taken off the skin with cleaning solution warmed to skin temperature.

The fluid gel composition can be tuned to these specific needs and highlighted the 0.9% (w/v), 20 mM NaCl formulation as the optimal system to trial as the cell delivery vehicle.

Current cell spray delivery systems have been used clinically by manufacturers guidance only. Quantifying the total area covered by the cell sprays has been investigated sparsely [81]. Furthermore, uniformity of the sprayed solutions could provide information on even cell distribution indirectly informing on required cell density. In this study, spray coverage and uniformity of distribution was quantified using water-sensitive paper (WSP) (Figure 2.7c). The technique was used to quantify sprayed gellan fluid gel in terms of percentage coverage and droplet size by a similar method utilizing ImageJ software described by Ferguson et al. [326, 327]. A trend towards lower coverage of the gellan hydrogel was seen (Figure 2.7d), likely explained by preserved droplet stability (shape) as a result of larger contact angles, however, such differences were not statistically significant.

The high cell viability following encapsulation in this study is supported by the current literature, with successful encapsulation of numerous cell types reported in quiescent gellan hydrogels [181, 296, 307, 328]. After 7 days of culturing within the fluid gel, cell attachment to the bottom of the well was noted, suggesting movement of the fibroblasts (Figure 2.9). Adherence, elongation and spreading of the fibroblasts over the plastic was also observed. Data suggested that the fluid gel support migration of the cells whilst preserving their cell function. Such observation correspond to the findings by Ferris et al. reporting cell settling of mouse myoblasts in gellan fluid gel [180]. It is proposed that such movement is facilitated either by passive sedimentation through the gelled particles or active migration of the cells out of the gel as seen in alginate-based fluid gels [329]; however, further study on environmental conditions that might influence this migration is needed.

Cell viability post-spraying is an important factor to consider, as numerous mechanical stresses during the spraying process can be detrimental to the cell's integrity [278]; causing structural cell damage such as membrane elongation, adverse cell responses (e.g. some cell differentiation processes are mechanically activated) or diminished cell viabil-

ity after deposition. Several parameters influence the shear stresses exerted on the cell systems during spraying such as nozzle diameter, viscosity of the material and velocity at delivery [277]. Previous studies based on saline carrier systems demonstrate a survival rate of >90% when a low air pressure and large nozzle sizes were used [276]. This study demonstrates a comparable level of viability when spray nozzles with similar diameters and air pressure were used, compared to current commercially available spray systems. Modification of viscosity provided by the fluid gel system can be crucial to protecting the cells, providing a cushioning effect during delivery [277]. Data has shown that metabolic activity of encapsulated sprayed cells is similar to non-encapsulated cells at day 1 and remains stable for 7 days (tested period). Because the metabolic activity of non-encapsulated cells increases over time following spraying whereas encapsulated cells expressed a steady level metabolic activity, it is possible that the proliferation capacity of encapsulated cells is restricted in the fluid gel. But the introduction of a structured fluid gel has not compromised cell viability following spraying in an *in vitro* setting. Although demonstrated *in vitro*, within a clinical setting, cells are sprayed into a hostile wound environment, potentially exposed to further mechanical trauma by wound dressings. It is suggested that the fluid gel carrier may provide extended shielding, enhancing the potential of the cells by allowing time for migration and adhesion within the local tissues. The findings of this study support that gellan fluid gel is a promising cell carrier for fibroblast spray delivery, but further research is needed to investigate this technique in an *in vivo* model.

## 2.8 Conclusion

The work presented here demonstrates the development of a gellan-based fluid gel system, with flexible viscoelastic properties that can be tuned to facilitate spray delivery requirements such as: liquefying at high shear during spraying, self-structuring post-spraying and resistance to flow once in situ. Spray assessment of the gellan fluid gel demonstrated

higher contact angles and limited runoff of the receiving surfaces when compared to a current clinically available cell carrier. Furthermore, cell compatibility to the gellan fluid gel was high, with good cell viability over a 7-day timescale. Additionally, viability of the encapsulated cells was not compromised following the spraying process. Therefore, gellan fluid gels provide a promising candidate for cell encapsulation, bridging the clinical need for sprayed systems and allowing retention to the wound site. However, future work will need include other cell types and focus on functional and proliferation behaviour of transplanted cells with a view to translation of the technique within *in vivo* models.

## CHAPTER 3

# KERATINOCYTE SPRAY DELIVERY

Spray delivery of epidermal cells has successfully translated to clinical practice to treat burn wounds. However, the technique has not yet been widely accepted due to limited retention and disputable cell viability and function in the wound. This study has evaluated a method for delivering cells with an aerosol device using a gellan-based 'fluid gel' (a shear-thinning gel system). The viscoelastic properties allow the material to liquefy upon spraying and restructure rapidly on the surface. Our results demonstrate that both spraying and encapsulation of human epidermal keratinocytes have some adverse effects on cell viability and function, but cells are recoverable to a certain extent. A cumulative effect occurs when combining both spraying and encapsulation in gellan fluid gel, with detrimental effects to cell viability and function. These findings indicate that encouraging results from earlier work with encapsulated fibroblasts could not be readily adopted for keratinocytes, suggesting a cell-type dependent response to this delivery technique.

### 3.1 Introduction

Skin damage can occur as a result of burns, skin blistering diseases, ulcers, trauma and other skin diseases. Any breach of the skin barrier can introduce microbial infection and delayed healing can cause scarring. Early wound closure of large defects is critical and can be achieved by traditional skin grafting, however, to cover extensive injuries large areas of autologous donor skin are required. Donor skin sparing techniques that achieve rapid wound healing have received much attention and improvements are ongoing. Examples include: cultured epithelial autografts (CEA) [44], artificial skin with cells incorporated [283] and skin cell spray techniques [105, 211]. Single cell delivery of (sub)confluent cells in solution via an aerosol system was introduced to overcome the issues of conventional grafting techniques by reducing donor site area, enhance fast re-epithelialisation and to reduce/eliminate culture time. Positive clinical outcomes of keratinocyte spray delivery have been published in the literature [105, 211, 330]. However, surprisingly little research has focused on *in vitro* cell viability and function after spray-delivery. Available research has shown moderate to high viability of sprayed keratinocytes with no statistical differences when compared to non-sprayed cells after 3 days [106], 7 days [41] and up to 14 days [278]. Results of these studies should be compared with caution as different spray applicators, cell types and/or spray methods were used. In this study the spraying method was standardized.

In this study, a previously engineered biopolymer based cell carrier is used to enhance retention upon a wound [269]. A sprayable hydrogel must have a certain low viscosity to facilitate homogeneous cell distribution and yet, solidify rapidly to retain cells on the wound. This is achieved by applying shear during the gelation process, forming a fluid gel with shear-structuring properties that allowed for delivery of cells via spraying. Previous work showed that the viability of encapsulated human dermal fibroblasts in gellan gum fluid gel was not compromised, in agreement with data published for other cell types encapsulated in gellan hydrogels [181, 182, 307, 308]. These promising results have not yet been established in keratinocytes, but with a successful cell-spray application already

in place, this could open the possibility for improving current keratinocyte spray systems rapidly. Furthermore, expanding controlled cell deposition with gellan fluid gel-based carrier system to other clinical application systems including endoscopic, arthroscopic and laparoscopic procedures, is an opportunity to enhance minimally invasive cell therapy for tissue regeneration. Therefore, the aim of this study was to examine the effect of encapsulation and spray delivery of human epidermal keratinocytes in gellan fluid gel in terms of cell viability, proliferation, cell migration and differentiation in comparison to non-encapsulated cells.

## **3.2 Methods**

### **3.2.1 Fluid gel preparation and characterisation**

Low acyl gellan gum stock 1% (w/v) solution was prepared by the addition of gellan powder [Kelcogel<sup>®</sup> obtained from Azelis, Hertford, UK] to sterile water at 65 °C under constant agitation. Following, a NaCl cross-linker solution (0.2 M concentration) was prepared with sterile water. Then, polymer sols were formed by mixing gellan with cross-linker (9:1 ratio) in a cell stirrer and autoclaving at (at 121 °C,) resulting in a final concentration of 0.9% (w/v) polymer - 20 mM NaCl. Gels were then cooled to 20 °C under continuous stirring and stored at 4 °C until further use. Gel temperatures were raised to 37 °C for cell encapsulation.

Rheological measurements were performed with a Kinexus Ultra rheometer (Malvern Pananalytical, UK) equipped with 40 mm parallel plates and a gap height of 1 mm. To determine the viscoelastic behaviour, small deformation rheometry was undertaken: an amplitude sweep from 0.1 to 700% was applied at an angular frequency of 1 Hz and the linear viscoelastic region (LVR) was determined. Frequency sweeps ( $\omega=0.1-10$  Hz) were carried out to investigate the ‘strength’ of the gel [318]. All measurements were taken at 25 °C and 0.5% strain within the linear viscoelastic region (LVR), informed by amplitude sweep measurements. Further, flow behaviour was studied by increasing the

shear rate from 0.1 to 600 s<sup>-1</sup> over a 3 minute timescale. To probe hysteresis, shear rate was immediately reduced back from 600 s<sup>-1</sup> to 0.1 s<sup>-1</sup>.

### **3.2.2 Keratinocyte culture and encapsulation**

Adult human epidermal keratinocytes (HEKa) were obtained from Gibco (lot nr 1781895 and 1989906). Keratinocyte culture media was prepared from EpiLifeKit<sup>®</sup> medium with 60  $\mu$ M calcium chloride (Gibco, UK) and supplemented with Human Keratinocyte Growth Supplement (HKGS) containing 0.2% v/v bovine pituitary extract (BPE), 5  $\mu$ g/ml bovine insulin, 0.18  $\mu$ g/ml hydrocortisone, 5  $\mu$ g/ml bovine transferrin; and 0.2 ng/ml human epidermal growth factor (all from Gibco, UK). Culture media was changed according to suppliers' guidelines and only cells of passage 2 to 4 were used. All cultures were maintained in the incubator under stable conditions of 5% humidity, temperature of 37 °C and 100 % humidity. Cells were harvested when they reached approximately 80% confluence.

Then, cells were resuspended in gellan fluid gel and delivered at a seeding density of 4.0 x 10<sup>4</sup> viable cells/cm<sup>2</sup> or in culture media, with a seeding density of 2.0 x 10<sup>4</sup> (sprayed) and 1.0 x 10<sup>4</sup> (non-sprayed) viable cells/cm<sup>2</sup>. Directly following mixing, cell solutions were pipetted or sprayed with the airbrush device (Badger, US) into tissue culture 24-well plates as described in Chapter 2 - Spray methods, fresh culture media was added and samples were incubated (at 5% CO<sub>2</sub>, temperature 37 °C, 100% humidity) until further testing.

### **3.2.3 Cell sedimentation in fluid gel**

Chemotactic migration of keratinocytes towards a layer of dermal fibroblasts was investigated with a modified Boyden well chamber technique using a ThinCert<sup>TM</sup> 12-well transwell system with 8  $\mu$ m pore size (Greiner bio-one,UK). Human dermal fibroblasts were seeded in 12-well tissue culture plates in HDF media (prepared as described in Chapter 2-Cell culture). After 3 hours, HDF culture media was changed to keratinocytes media.

Then, control and encapsulated keratinocytes were either sprayed or pipetted into  $0.8 \mu\text{m}$  pore size transwells and placed into wells with or without HDF seeded on the bottom. A total of 4 conditions were tested as illustrated in Figure 3.1. After 2 days, the inserts were gently removed and placed in 3 subsequent baths of sterile PBS to wash and then fixed with 4% paraformaldehyde for 20 min and permeabilised with 0.5% Triton-X dissolved in PBS for 30 min, both at room temperature. Finally, 3 washes with PBS before inserts were cut out and mounted on coverslips with DAPI-mounting media. The number of cells present on the underside of the coverslip were imaged with a Zeiss Axiovert fluorescence microscope.

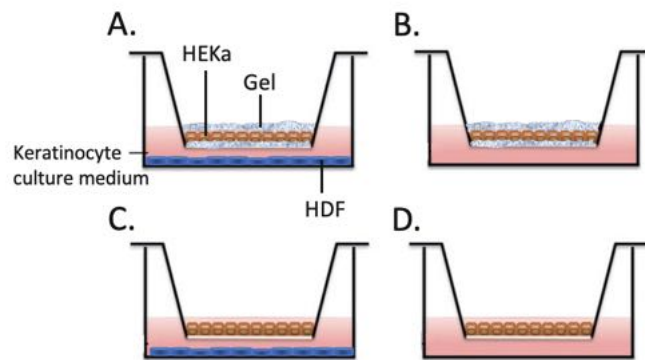


Figure 3.1: Transwell assay. Human epidermal keratinocytes were seeded in a  $8 \mu\text{m}$  pore size transwell insert in either gel (A) and (B) or keratinocyte culture media (C) and (D). Chemotaxis in the presence (A and C) or absence (B and D) of human dermal fibroblasts was assessed. Migration of keratinocytes through the pore membrane was imaged at day 2.

### 3.2.4 Cell viability

Green-fluorescent Calcein Acetocymethylester (Calcein AM) (Invitrogen, UK) was used to stain live cells and red-fluorescent Ethidium Homodimer-1 (EH) (Thermofisher, UK) was used to stain dead cells. Live/dead stain was added to 1 ml of cell specific culture medium, samples were immersed in  $100 \mu\text{l/ml}$  of this solution and incubated for 20 min. Samples were then visualized using confocal microscopy (Olympus, Fluoview FV100) and images produced with Imaris software (Bitplane, UK) or fluorescent microscope (Cytation

5, Biotek, UK), showing viable cells green (Calcein AM) and non-viable cells red (PI or EH). Laser setting 488 nm and 543 nm for green and red fluorescent respectively.

### Cellular analysis

Automated cellular analysis was performed using Cytation 5 fluorescent microscope with Genzyme5 3.04 software (Biotek, UK). Figure 3.2 gives an example of automated live/dead cell counting by masking the individual green or red channels. Identical settings based on cell size ( $5\mu\text{m}$  to max  $160\mu\text{m}$ ) were used for all samples to select cells. Cell count and average cells size was automatically obtained.

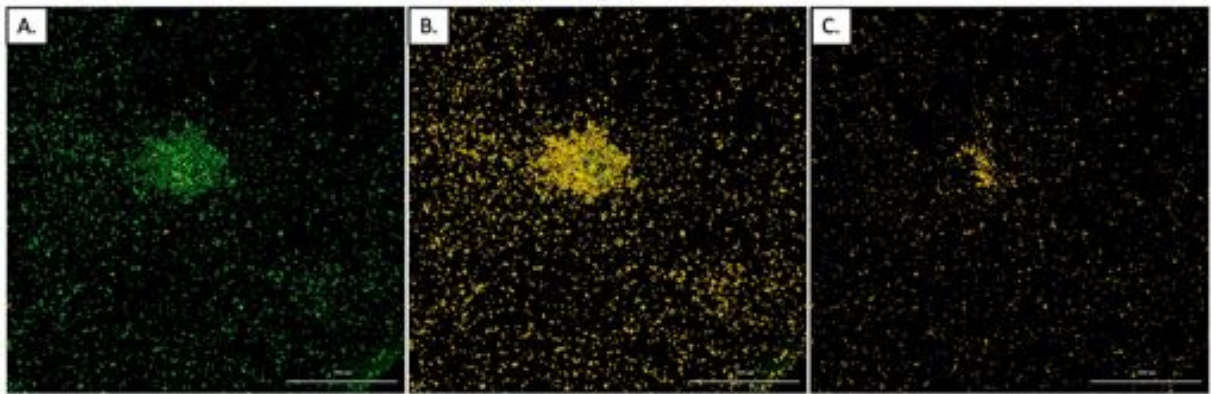


Figure 3.2: Example of live/dead assay cell count of human epidermal keratinocytes. The generated image of entire 24-well stained with green (live) and red (dead) fluorescent stains (A), both the green (B) and red (C) fluorescent cells are masked for counting. Scale bars are  $3000\mu\text{m}$ .

Based on live and dead cell counts, the percentage of viable cells could be calculated with Equation 3.1.

$$viable\ cells(\%) = \frac{\text{number of viable cells}}{\text{total number of cells (live + dead cells)}} \times 100 \quad (3.1)$$

### 3.2.5 Morphology

Cells were washed using sterile PBS and subsequently fixed with 4% paraformaldehyde for 20 min at room temperature. Next, cell were permeabilised with 0.5% Triton-X dissolved

in PBS for 30 min at room temperature. Samples were washed several times with PBS in between all steps. Cells were stained with Alexa Fluor 488 phalloidin (Thermo Fisher, UK) and DAPI at 0.5-1  $\mu\text{g}/\text{ml}$  for F-actin and cell nucleus respectively. Fixed and stained cells were visualised directly with confocal microscopy or fluorescent microscopy, laser settings for excitation: 495 nm and emission: 518 nm and stored at 7  $^{\circ}\text{C}$  protected from light until testing. Images were then analysed with either ImageJ software, using the particle size plugin [299] or with Genzyme 5 3.04 software. Individual cell shape was analysed with shape descriptors as graphically illustrated in Figure 3.3. The circularity is derived from area and perimeter measurements with a value of 1 indicating a perfect circle, Equation 3.2.

$$\text{Circularity } (0 - 1) = 4\pi \frac{\text{Area}}{\text{Perimeter}^2} \quad (3.2)$$

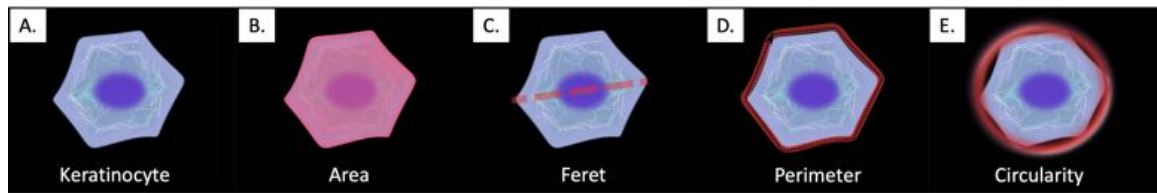


Figure 3.3: Diagram of cell shape descriptors illustrates the normal shape of a human epidermal keratinocytes (A), measurements of cell size (Area in  $\mu\text{m}^2$ ) (B), the maximum cell length (Feret in  $\mu\text{m}$ ) (C), cell circumference (Perimeter in  $\mu\text{m}$ ) (D) and circularity on a scale of 0-1 (E).

### 3.2.6 Alamar Blue Metabolic Activity

Encapsulated and control HEKa were seeded or sprayed into 24-well tissue cultured plates at a density of  $4.0 \times 10^4$  viable cells/ $\text{cm}^2$  in gellan fluid gel or  $2.0 \times 10^4$  (sprayed) and  $1.0 \times 10^4$  (non-sprayed) viable cells/ $\text{cm}^2$  in culture media. Metabolic activity of keratinocytes was investigated by incorporation of 10% Alamar Blue. Experiments were performed in 24-well culture tissue plates over a study period of 14 days as described in detail in Chapter 2 - Alamar Blue Metabolic Assay. Absorbance was measured at 570nm and 600nm.

Results are presented as the percentage reduction (Equation 2.6) and as percentage difference in reduction between treated and untreated cells (Equation 3.3).

$$Percentage\ difference(\%) = \frac{(\epsilon_{ox2} \times A1) - (\epsilon_{ox1} \times A2)}{(\epsilon_{ox2} \times B1) - (\epsilon_{ox1} \times B2)} \times 100 \quad (3.3)$$

A1 = absorbance at 570 nm test well

A2 = absorbance at 600 nm test well

B1 = absorbance at 570 nm control well

B2 = absorbance at 600 nm control well

Standard molar extinction coefficients for the oxidized ( $\epsilon_{ox}$ ) form of AlamarBlue<sup>®</sup> were used:

$\epsilon_{ox1} = 80,586$  at 570 nm

$\epsilon_{ox2} = 117,216$  at 600 nm

### 3.2.7 In-Cell Western

In-Cell Western assay is a technique that allows cellular protein quantification without the need for cell lysis (as in original Western blot assays). This technique was preferred here as retrieving cells from the 3D gel matrix might be accompanied with (further) cell damage and cell loss. Sprayed and non-sprayed cells in 24 well plates were washed carefully with PBS and fixed with 10% v/v formaldehyde/PBS with 2% sucrose for 15 min at 37 °C. Cells were permeabilized (10.3g sucrose, 0.292 g NaCl, 0.006 g MgCl<sub>2</sub>, 0.476 g Hepes in 100 ml PBS, adjusted to pH 7.2 with 0.5 ml Triton X) at 4 °C for 4 minutes. Then, cells were blocked in blocking buffer, 1% milk protein in 0.1% Tween 20/PBS (PBST) at room temperature for 1,5 hours on a shaker. Cells were incubated for at least 2.5 hours with primary antibodies diluted in PBST. Primary antibodies: anti-involucrin

antibody (abcam, ab68) at 1 mg/ml and anti-laminin 5 antibody (abcam, ab14509) at 10  $\mu$ g/ml in blocking buffer at room temperature. Followed by 5x 5 min washes with wash buffer (0.1% PBST). Then, cells were incubated with 1:800 diluted infra-red labeled secondary antibodies; IRDye<sup>®</sup> 800 CW Goat anti-Mouse (LI-COR 926-32210) , IRDye<sup>®</sup> 800CW Goat anti-Rabbit (LI-COR 926-32211) and 1:500 diluted CellTag 700 stain (LI-COR 926-41090) for 1 hour at room temperature, followed by 5x 5 min washes with wash buffer (0.1% PBST). Plates with 2D samples were then dried for at least 2 hours and PBS was added to 3D sample plates to avoid drying out of the gel. Samples were stored at 4 °C until subjected to LI-COR Odyssey Sa scanner equipped with ImageStudioLite software to read the protein of interest with infrared signal at 800 nm and CellTag at 700 nm. Data presented is fluorescent intensity of the protein of interest (Laminin 5 or Involucrin), normalized against cell number as detected with CellTag 700 stain.

### **3.2.8 Scratch assay**

Monolayers of HEK293 cells passage 2 were grown in 24 well tissue culture plates until confluent. Monolayers were fluorescently labeled red with CellMask<sup>TM</sup> Deep Red Plasma membrane stain (ThermoFisher, UK). Briefly, stock solution of the stain was prepared in DMSO (1000x). Monolayers grown to confluence were incubated with 100  $\mu$ l stain per well for 10 min at 37 °C and 5% CO<sub>2</sub>. Then, stain was removed and samples washed 3 times with PBS. Fresh media was added and samples were imaged immediately or placed in incubator. A total of 5 conditions were tested on top of the monolayers and compared to control wells with only HEK293 monolayers. Conditions included: cell-free gel seeded on top, HEK293 encapsulated in gel sprayed, HEK293 encapsulated non-spray, HEK293 sprayed in media and HEK293 in media non-spray. Cells added on top of monolayers were pre-labeled with 5-chloromethylfluorescein diacetate (CMFDA), CellTracker<sup>TM</sup> Green (ThermoFisher, UK), in order to track whether delivered cells would contribute to wound healing. Conditions were added and cultures were incubated for 2 hours. Then, wells were scored using a 200  $\mu$ m sterile pipette tip in a linear fashion to leave a 0.5-0.7 mm wide wound area. Four

repetitions of each condition were performed. Culture medium was removed immediately and replaced with fresh medium and cultures were maintained at 37 °C and 5% CO<sub>2</sub>. Wells were imaged up to 4 days post-scratch.

## Imaging

Wound closure was monitored by collecting images at set time points (2 hrs, 24 hrs, 48 hrs, 96 hrs and 120 hours) after the scratch was performed using Cytation 5 equipped with Genzyme5 3.04 software (Biotek, UK). Images of the entire scratch were made at timepoint zero (2 hours after scratch) and the area of scratch was selected (region of interest) and an automated cell count with total object area ( $\mu\text{m}^2$ ) within this region was obtained. In following timepoints the object area was compared to the previously determined scratch area to analyse cell infiltration into the wound. Automated cell count and object area measurement for red and green fluorescently stained cells was performed with the cellular analysis plug in as shown in Figure 3.4. Data presented as the extent of wound closure of the scratch by measuring wound width and rate of closure (Equation 3.4) over the studied period.

$$\text{Rate of cell migration (nm/hour)} = \frac{(W_i - W_f)}{t} \quad (3.4)$$

- $W_i$  = initial wound width (nm)
- $W_f$  = final wound width (nm)
- $t$  = time (duration of migration in hours)

To account for changes in cell density due to proliferation the data has also been presented as percentage wound confluence, calculated with the following Equation 3.5:

$$\text{wound confluence (\%)} = \frac{(\text{Object Area}_t - \text{Object Area}_0)}{(\text{Area}_{total}) - \text{Object Area}_0} \times 100 \quad (3.5)$$

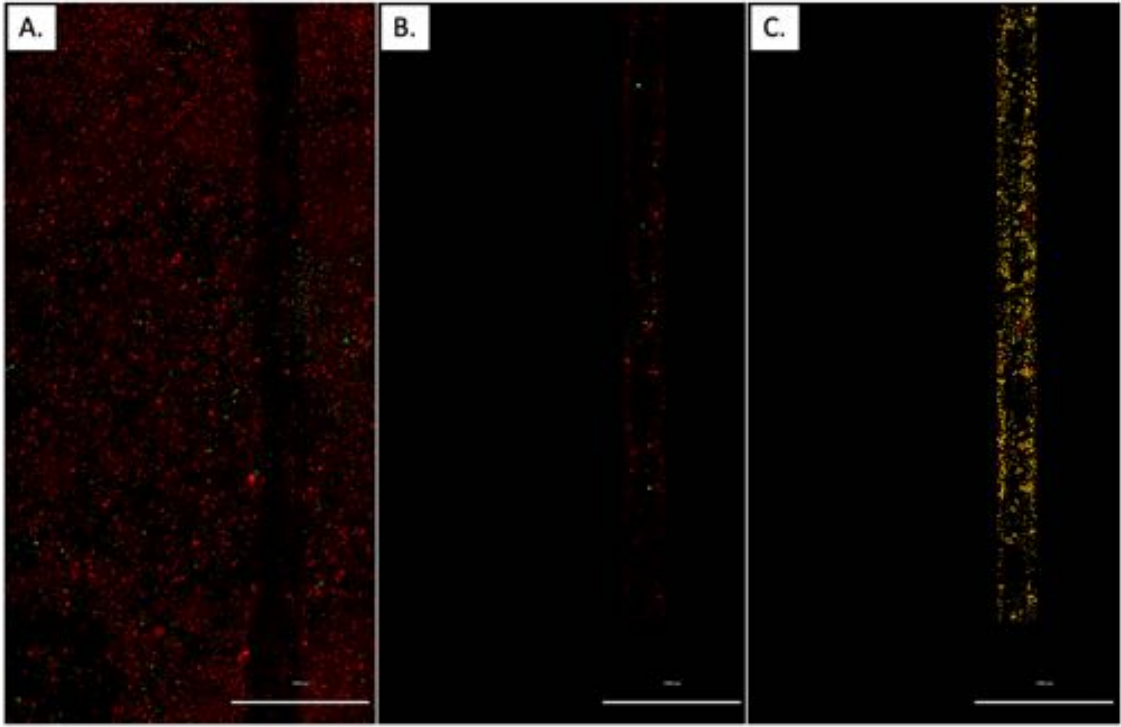


Figure 3.4: *In vitro* scratch assay wound density analysis method. The scratch was identified in the total image (A) and a rectangle closely surrounding the wound edges was selected (B), within this region the total object area of fluorescently stained red (RFP) and green (GFP) cells was measured. Scale bars are 2000  $\mu\text{m}$ .

- Object area<sub>t</sub> = Density of the wound area at time (t) in  $\mu\text{m}$
- Object area<sub>0</sub> = Density of the wound area at time point zero in  $\mu\text{m}$
- Area<sub>total</sub> = Total area of region of interest ( $\mu\text{m}^2$ )

## 3.3 Results

### 3.3.1 Material characteristics

#### Fluid gel production and characterisation

Gellan fluid gels were prepared by applying a constant shear during the sol-gel transition phase as previously described [269, 297, 301, 312]. Viscoelastic properties of gellan fluid gel were examined by rheology.

The frequency sweep measurements (obtained within LVR) allowed for investigation

of the elastic and viscous moduli at variable frequencies, an example is demonstrated in Figure 3.5A. Frequency dependence of gellan fluid gel demonstrates a weak gel system with gradually increasing  $G'$  and  $G''$  modulus under increasing frequency, typical of fluid gels [297]. Weakly associated single helices are not destroyed hence  $G'$  remains greater than  $G''$  at higher frequencies. Additionally, the calculated loss tangent ( $\tan \delta = G''/G'$ ) is  $> 0.1$ , as seen in weak gels (data not shown)[304].

The amplitude dependence of the elastic and viscous moduli are presented in Figure 3.5B. Under increasing strain, a cross-over from an elastic ( $G'$ ) to viscous ( $G''$ ) dominated system was observed. Thus, at large deformations the suspension acts as a liquid-like material, which enables flow, a typical property of a fluid gel.

In order to estimate the behaviour during spraying, the system was subjected to increasing shear ramps starting from  $0.1$  to  $700 \text{ s}^{-1}$  and a second sweep immediately after to test hysteresis. Results demonstrated a high degree of shear thinning at increasing shear rates and once shear was removed the system recovered to its original viscosity.

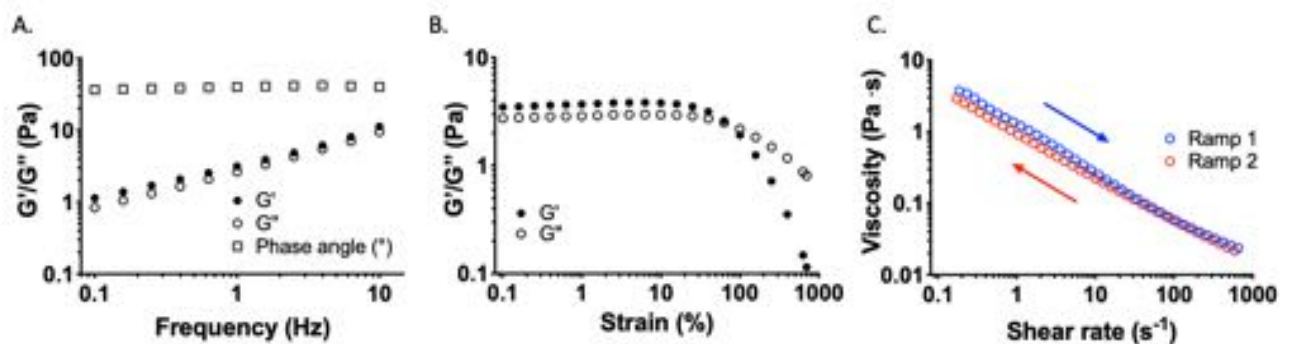


Figure 3.5: Viscoelastic properties of gellan fluid gel used for keratinocyte encapsulation.

## Sedimentation

Sedimentation velocity of cells through the gel was estimated using Stokes' law as calculated by Equation 3.6, where the sedimentation velocity is given by the force acting upon the particle influenced by gravity and particle density in comparison to liquid density. The force acting in resistance is based on the particle's size and viscosity of the liquid.

$$v = \frac{2}{9} \frac{\rho_p - \rho_f}{\eta} \cdot (g \cdot r^2) \quad (3.6)$$

- $v$  = sedimentation velocity (m/s)
- $\rho_p$  = particle density (kg/m<sup>3</sup>)
- $\rho_f$  = fluid density (kg/m<sup>3</sup>)
- $\eta$  = viscosity fluid (Pa·s)
- $g$  = gravitational acceleration (m/s<sup>2</sup>)
- $r$  = particle radius (m)

Cell density of 1.05 kg/m<sup>3</sup> [331] was used for fibroblasts, keratinocytes and platelets.

The fluid gel density was calculated by Equation 3.7:

$$\rho = \frac{M}{V} \quad (3.7)$$

- $\rho$  = density of gel [0.9%, 20 mM NaCl] (kg/m<sup>3</sup>)
- $M$  = mass of the gel (kg)
- $V$  = volume of the gel (m<sup>3</sup>)

Viscosity (within the range of gellan fluid gels as presented in Chapter 2) was plotted against the expected time for particles (eg cells) to settle in 1 mm thick layer of the fluid gel. The gravitational acceleration is a given value of 9.81 m/s<sup>2</sup>. Lastly, the particle radius was derived from the average cell size: for fibroblasts 15  $\mu\text{m}$ , keratinocytes 10  $\mu\text{m}$  and platelets 0.2  $\mu\text{m}$ .

As shown in Figure 3.6E, the estimated time of cells to sediment in the gel is dependent on the size of the particle, with longer sedimentation time for smaller particles (eg platelets) compared to larger cell types (keratinocytes and fibroblasts). It is important to note that cell size can differ according to differentiation status[332].

Low sedimentation rate implies that the particle (eg cell) has a tendency to float and high sedimentation rate indicates that the particle sinks quicker in the fluid. The Stokes' law assumes a laminar flow, spherical particles, a homogeneous material with smooth surfaces and that particles do not interfere with each other. Furthermore, a potential active migration of cells towards chemoattractants present in either medium or towards the air-liquid interface (as seen in keratinocytes) can not be taken into account.

### **Transwell assay**

Since mobilization of cells out of the gel is required to contribute to wound healing, we next determined whether keratinocytes seeded in the gel could migrate in a chemotactic transwell assay toward dermal fibroblasts. As expected, keratinocyte migration through the gel is restricted in comparison to cells in culture media. Keratinocyte migration was highest in wells without gel (Figure 3.6), however, no statistical significant differences were found between presence or absence of dermal fibroblasts in the well. Therefore, soluble factors excreted by the fibroblasts do not seem to have a chemoattractive effect in this experiment. Likewise, in the presence of fibroblasts, encapsulated keratinocytes do not migrate quicker. However, the potential effect of robust chemoattractants present in *in vivo* wound environments might facilitate active migration of the cells out of the gel.

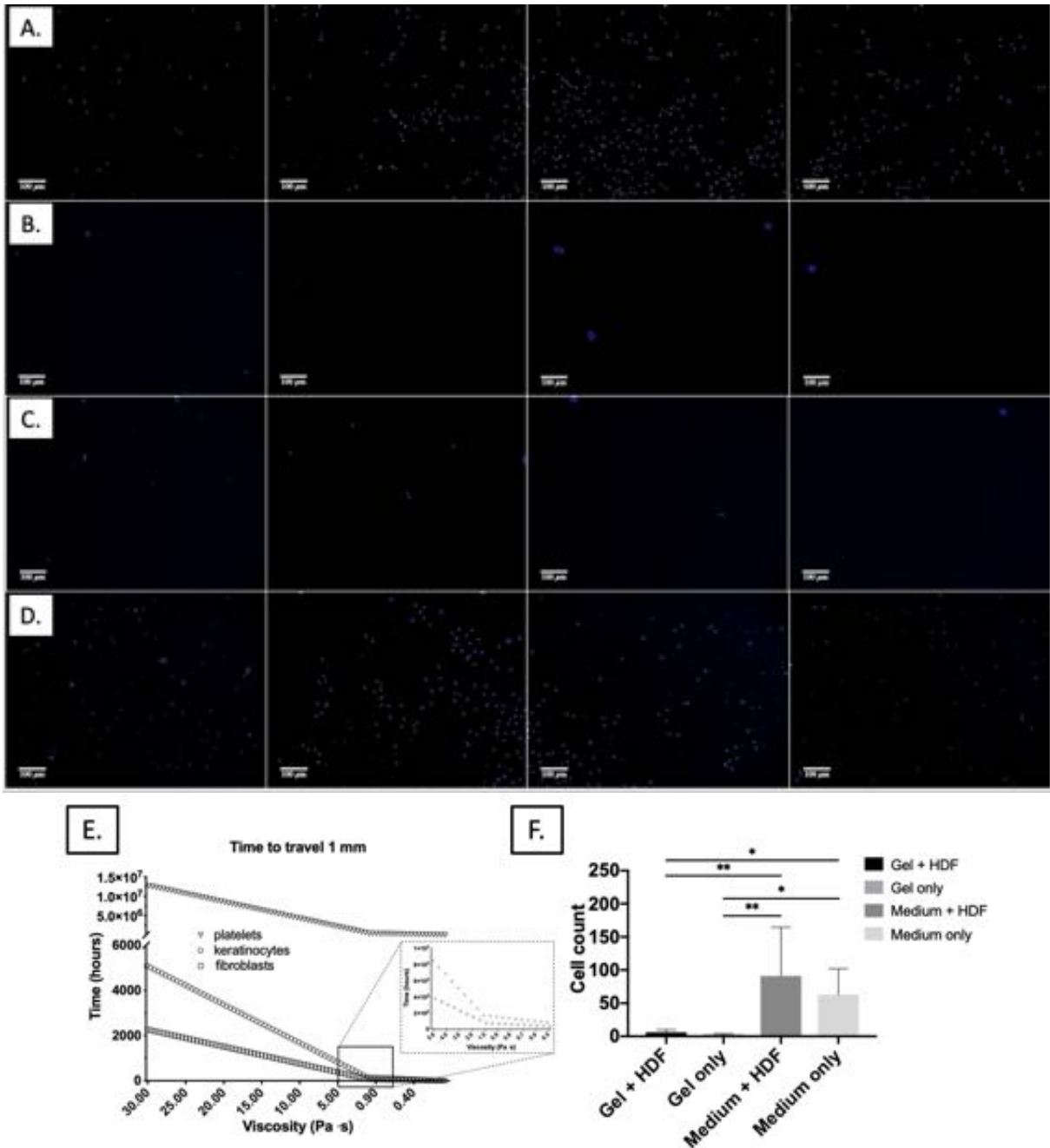


Figure 3.6: Keratinocyte migration assay with presence or absence of human dermal fibroblasts as chemoattractant. Keratinocytes in medium (A, D) have a higher number of cells migrating through the insert compared to keratinocytes seeded in gel (B, C). In A and C, HDFs were seeded at the bottom as chemoattractant. Four representative images of each condition are presented, scale bars are  $100\mu\text{m}$ . (E) Estimated time to sediment in 1 mm layer of fluid gel in 3 cell types, derived from sedimentation velocity calculated based on Stokes' Law. (F) Cell count of keratinocytes migrated through the inserts. Values represent mean, errorbars are SD. Significant differences found by one-way ANOVA with post-hoc statistical significance analysis indicated by p values of  $* < 0.05$ ,  $** < 0.01$  and  $*** p < 0.001$ .

### 3.3.2 Cell viability

#### Growth curve

Growth of HEK<sub>a</sub> was systematically investigated at set time points by trypan blue exclusion. Figure 3.7 shows the 3 phases of cell growth over a period of 7 days. Cells were subcultured when still in exponential phase, usually around day 4 or 5.

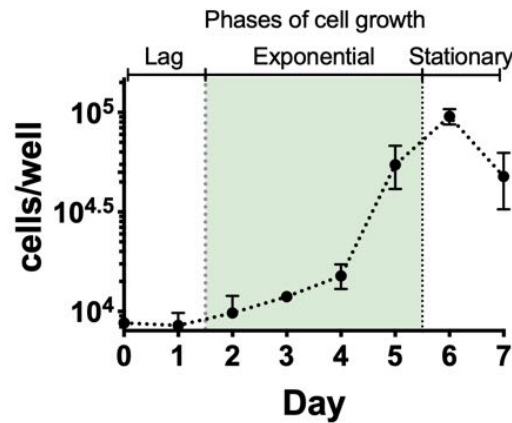


Figure 3.7: Growth curve of adult human epidermal keratinocytes. Green area indicates exponential phase. Experiments were performed in triplicates per timepoint. Values presented are mean + SEM.

The population doubling time was approximately 13 hours (SD 0.30) for cells in exponential phase as calculated with Equation 3.8.

$$\text{Population doubling time} = \frac{T \ln 2}{\ln\left(\frac{X_e}{X_b}\right)} \quad (3.8)$$

- $X_b$  = cell number at beginning of incubation time
- $X_e$  = cell number at end of incubation time
- $T$  = incubation time (hours)

#### Live/dead assay

Cell viability of sprayed and non-sprayed human epidermal keratinocytes was evaluated at days 1, 4, 7, 10 and 14 using live/dead assay as demonstrated in Figure 3.12. Percentage

viability of sprayed cells was lower than non-sprayed cells up to day 7, however these differences were not found to be statistically significant. At day 10 and day 14 sprayed cells showed a higher percentage viability (probably due to overconfluence of control wells causing cell death). Average viability of sprayed cells dropped from 77.4% at day 1 to 40.7% at day 4, but then increased again to 88.9% on day 10. Probably due to proliferation of viable cells at the bottom of the well.

It was found that cells encapsulated in gellan fluid gel had a lower mean cell viability at day 1 than non-sprayed cells in medium (77.3% and 93.9% respectively) (Figure 3.13). The viability of encapsulated cells remained high up to day 4 with a mean of 68.6% viable cells. But, a significant decline of mean cell viability to 28.6% was seen at day 7, by then the cells that have diffused out of the gel adhered to the bottom of the culture plastic and show normal morphology. However, it seems that those cells that remain in the gel environment die (Figure 3.13B). A sharp incline in mean percentage of viable cells is again seen at day 10 with approximately 78% viable cells, this percentage is constant until the end of the studied period (day 14). Likewise, probably explained by the proliferation of viable adherent cells.

The effect of spraying fluid gel encapsulated keratinocytes on cell viability follows a similar trend with significantly lower percentage of viability in sprayed cells compared to non-sprayed cells at all timepoints. Interestingly, the negative effect of spraying is more profound when cells are encapsulated in the gellan fluid gel when compared to cells sprayed in normal culture medium. This result is in contrast with our previous reported outcomes of spray delivery of encapsulated fibroblasts in Chapter 2.

From these results it is clear that encapsulation of cells in the fluid gel system is less successful in terms of cell viability than in normal cell culture medium, however, a majority of cells still remain viable and are able to multiply when diffused out of the gel. Spray delivery of encapsulated cells was detrimental for cells, with a very limited amount of cells surviving in the gel. Interestingly, previous reports suggested an increased survival of cells delivered in higher viscosity environments as the gel was expected to work as

cushioning effect [277]. Perhaps what happens is that sprayed cells respond differently to the stress response than non-encapsulated cells. With cells being entrapped in the gel experiencing solely autonomic feedback and no feedback from surrounded cells. Lack of cell to cell interactions as well as attachment to ECM components might have forced keratinocytes into committing to differentiation or apoptosis. Furthermore, keratinocyte size is related to the level of differentiation, with non-multiplying cells being larger and more likely to stay trapped in the 3D gel system. Non-sprayed cells that are unable to diffuse out of the gel stay rounded and also become unviable by day 7. Despite addition of cell specific culture medium on top, the gel system does not seem to provide the ideal culture environment for these kind of cells. Incorporation of cell media or growth factors into the gel might be beneficial and worth exploring in future studies. However, when used as rapid delivery method with applying a thin layer of gel, this system could still be of benefit for cell delivery.

### **3.3.3 Morphological changes in sprayed cells**

Morphological features of the cell can give clues on its physiological state and 2D measurements are commonly used as quantitative measures of cell shape. To examine the morphological changes occurring following spray delivery, cells were fixed, permeabilised and stained for F-actin and DAPI to visualise the cytoskeleton and cell nucleus respectively. As shown in Figure 3.8, at 24 hours following delivery, the sprayed cells are smaller and have a more rounded phenotype with actin fibre accumulation at the cell borders. Although, average cell size, circumference and circularity of sprayed cells seemed different from non-sprayed cells at day 1, no statistically significant differences were found which might be related to low numbers of non-sprayed cells that could be examined due to overlap of individual cells (Figure 3.8B). These results suggest a stress response of cells delivered with the airbrush system. To examine whether spraying has a long term effect on cell shape, cells were again examined following a culture period of 2 weeks as shown in Figure 3.8. Non-sprayed cells show a cobble stone morphology typical for keratinocytes,

but also elongated cells can be found. Cell shape of sprayed cells was not significantly different after 2 weeks of culturing, however, the sprayed cells were significantly smaller than non-sprayed as reflected by area, cell circumference and feret outcomes at week 2 (Figure 3.8B). Thus, spraying induces morphological changes in keratinocytes which can still be observed after two weeks of culturing.

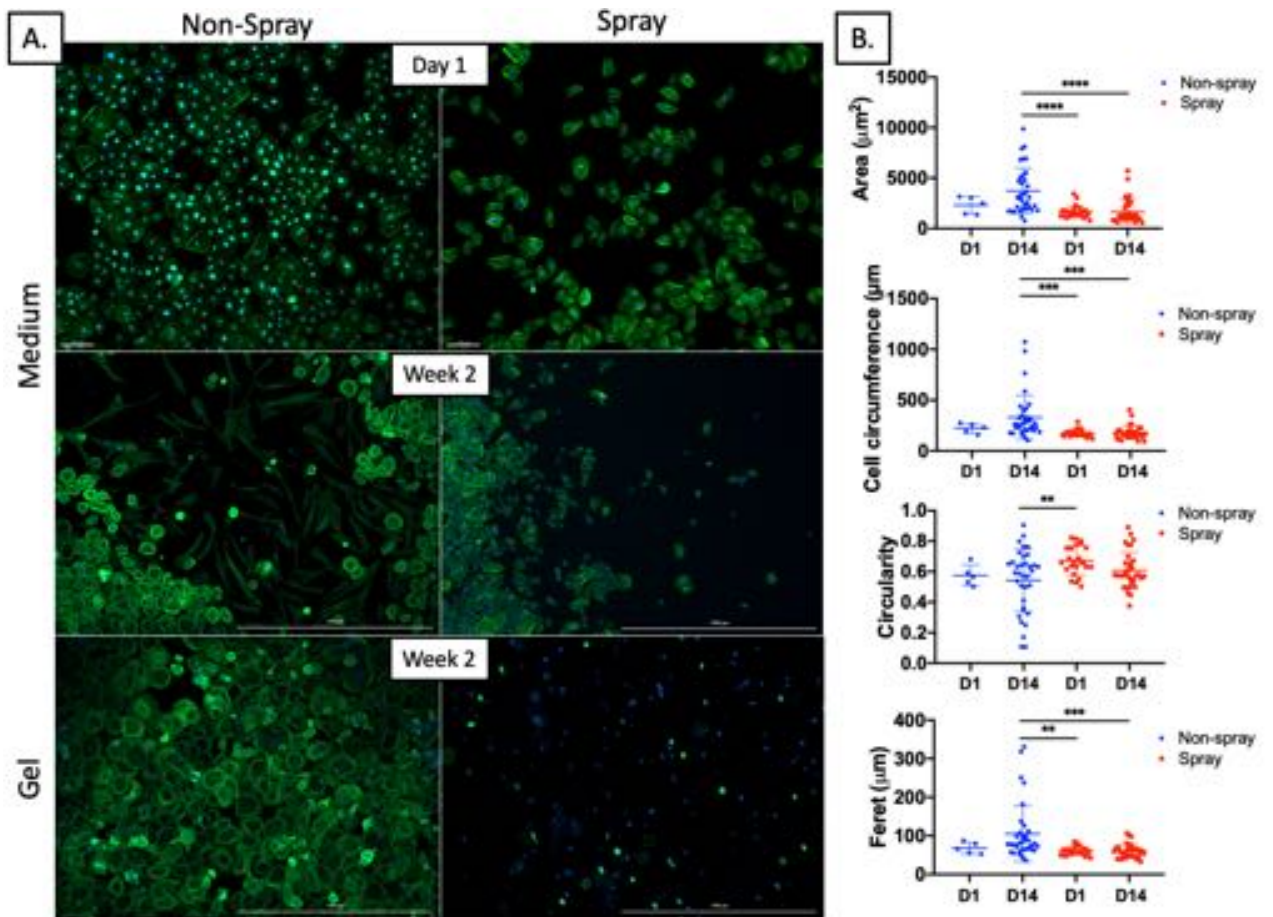


Figure 3.8: Cytoskeleton (f-actin) and nucleus (DAPI) staining of non-sprayed and sprayed keratinocytes (A). Scalebars are 100  $\mu\text{m}$  for day 1 images and 1000  $\mu\text{m}$  for week 2 images. (B) Cell shape measurements of sprayed and non-sprayed human epidermal keratinocytes in medium per parameter at day 1 and week 2. Data presented as individual values and mean with SD. Significant differences found by one-way ANOVA with post-hoc statistical significance analysis indicated by p values of \* $<0.05$ , \*\* $<0.01$  and \*\*\* $p <0.001$ .

### 3.3.4 Cell function

#### Proliferation

The Alamar blue assay was implemented to quantitatively investigate the metabolic activity of sprayed HEKa. This assay allowed for continuation of cell culture, giving the opportunity to assess viability (with live/dead staining) on the same cell population. As shown in Figure 3.9 A and B, metabolic activity of sprayed cells is reduced in comparison to non-sprayed cells. Interestingly, this effect is more profound in cells encapsulated in fluid gel as is in agreement with the viability assay. In all groups except sprayed encapsulated cells, the metabolic activity increases again over time, indicating that viable delivered cells are able to recover and proliferate. From this data, cell proliferation seems restricted by encapsulation and spraying with lower percentage reduction at all timepoints when compared to control keratinocytes, especially since a lower number of cells was delivered to the control wells.

When comparing sprayed and non-sprayed conditions directly, sprayed cells underperform in terms of metabolic activity as demonstrated in Figure 3.9C. The amount of reduction of encapsulated cells in the sprayed wells is less than 50% of that of the non-sprayed wells for all timepoints. In cells delivered in media the percentage difference is initially 71%, meaning that the metabolic activity in the sprayed wells is inhibited by 29% when compared to non-sprayed wells.

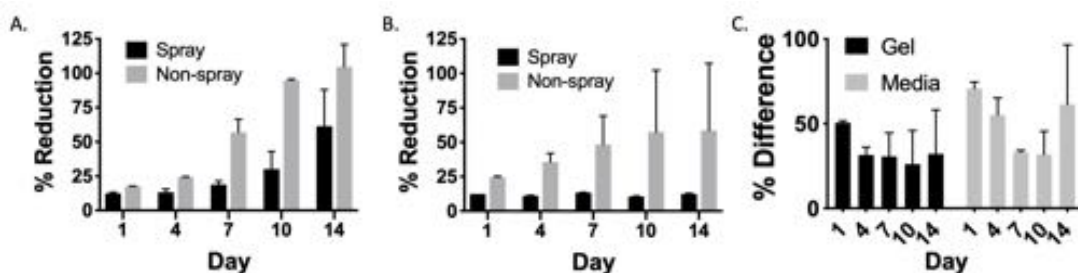


Figure 3.9: Metabolic activity of HEKa as determined by alamar blue. Percentage reduction for sprayed and non-sprayed HEKa in culture medium (A) and gel (B) was compared. Percentage difference between treated (i.e. sprayed) and non-treated (i.e. pipetted) cells delivered in gel or media (C). Values are mean percentage (2 individual experiments, minimal 4 repetitions), errorbars are SD.

## Wound healing

*In vitro* wound healing was assessed by a scratch assay of HEKCa monolayers combined with 5 conditions: cell-free fluid gel, sprayed and non-sprayed keratinocytes in medium and sprayed and non-sprayed keratinocytes in fluid gel. For distinction between wound healing from the existing wound edges and cells delivered on top; cells in the monolayer were stained red and cells applied on top of the monolayer stained green. In general, cells delivered on top of the monolayers did not seem to contribute significantly to wound healing as only few green stained cells were found in the wounded area in comparison to red stained cells infiltrating from the wound edges. Differences between cell densities of sprayed cells in gel or media are shown in Figure 3.10C.

Theoretically, soluble factors secreted by spray delivered cells could impact on wound healing of the monolayers underneath. When looking solely at the monolayers, Figure 3.10B demonstrates a higher mean object area (i.e. cell density) for monolayers with cells sprayed in media compared to cells sprayed in gel at all timepoints except at 2 hours. However, no statistical significant differences were found for the mean cell density between gel and media groups.

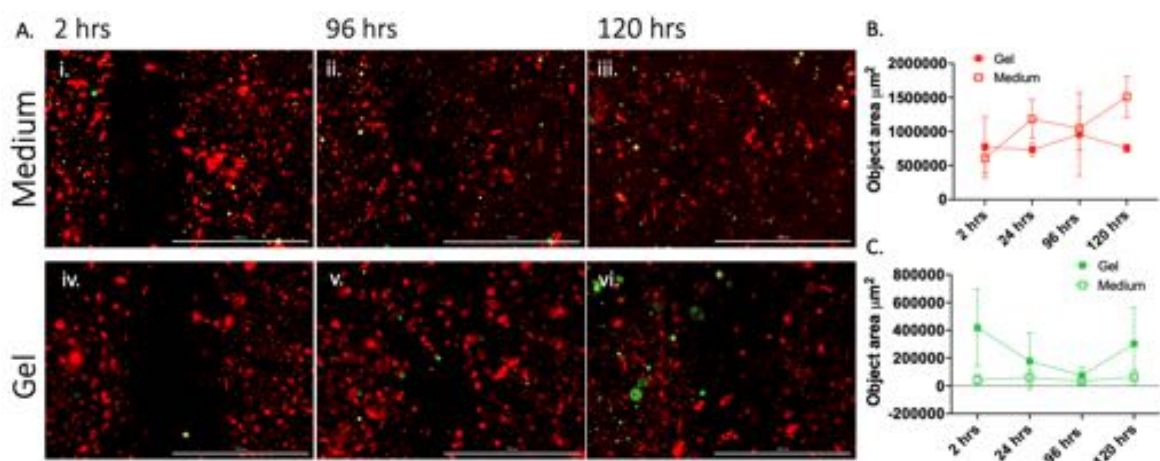


Figure 3.10: *In vitro* wound scratch assay of sprayed human epidermal keratinocytes. Representative micrographs of a monolayer of HEKCa (red) with sprayed keratinocytes in culture medium (green)(Ai-iii) or encapsulated in fluid gel (Aiv-vi) taken at 2 hours, 96 hours and 120 hours after scratch. Cell density measured as the mean object area ( $\mu\text{m}^2$ ) of monolayer cells fluorescently stained red (B) and sprayed cells, fluorescently stained green(C). Scalebars are 1000  $\mu\text{m}$ .

Furthermore, the presence of cell-loaded fluid gel did not seem to enhance healing rates of the monolayers as reflected in the rate of wound closure as calculated from repeated wound width measurements (Figure 3.11A). Sprayed cells delivered in medium had a smaller mean wound width at 120 hours after the scratch (Figure 3.11A), but despite near or complete closure of 3 out of 4 wounds, no significant differences of wound healing rate could be found when compared to cells sprayed in gel (Figure 3.11B).

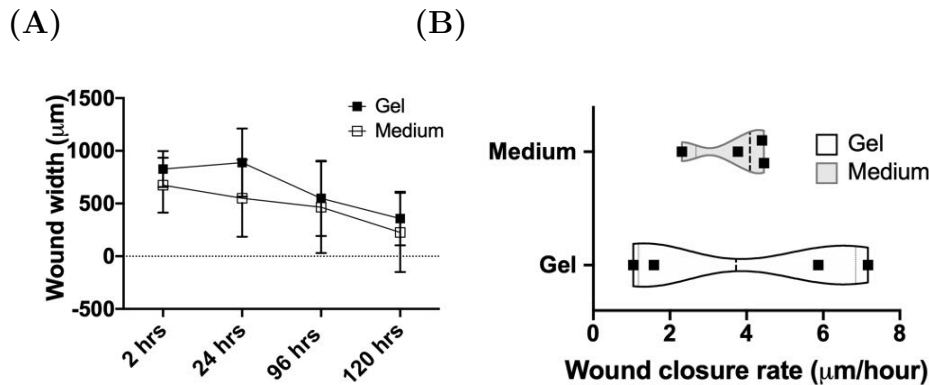


Figure 3.11: Scratch assay of control and encapsulated sprayed keratinocytes. Wound width (A) and wound healing rate (B). Values presented are mean and standard deviation.

## Differentiation

Keratinocytes express distinctive marker genes at each differentiation stage [287]. Here, we examined expression of two keratinocyte differentiation markers 3 days and 1 week following spray-application. A marker for basal keratinocytes is laminin 5 (LM-5). Laminin 5 is an important component of the basement membrane and plays a role in regulating cell adhesion as well as cell migration in wound healing [333].

A higher level of laminin-5 was expressed by keratinocytes delivered in medium when compared to encapsulated cells (Figure 3.14A). All cells came from the same population and cultured under identical conditions, thus, encapsulation in fluid gel has a restrictive effect on LM-5 expression at day 3. At a later timepoint, expression of LM-5 has increased in encapsulated cells, especially in sprayed keratinocytes. Likewise, sprayed keratinocytes

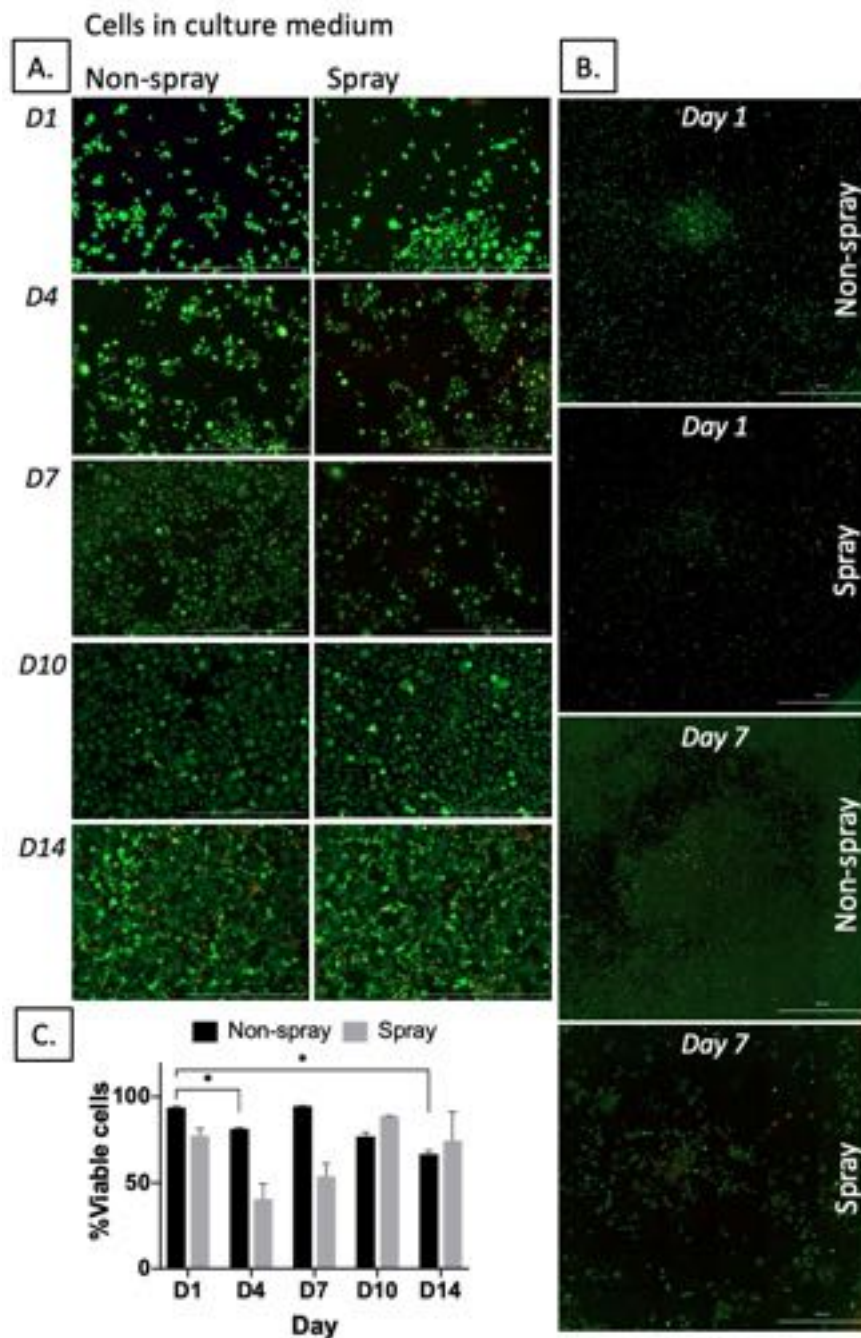


Figure 3.12: Cell viability of sprayed and non-sprayed human epidermal keratinocytes. Both conditions eventually reach confluence as shown in representative images taken for each condition and timepoint (A), but images of the entire well obtained by capturing of 8x6 individual images (montage) show that pipetted cells reach confluence earlier compared to sprayed cells (B). C) Automated cell count of live and dead cells presented as percentage viable cells in the entire well. Data presented as mean of duplicate measurement with SD.

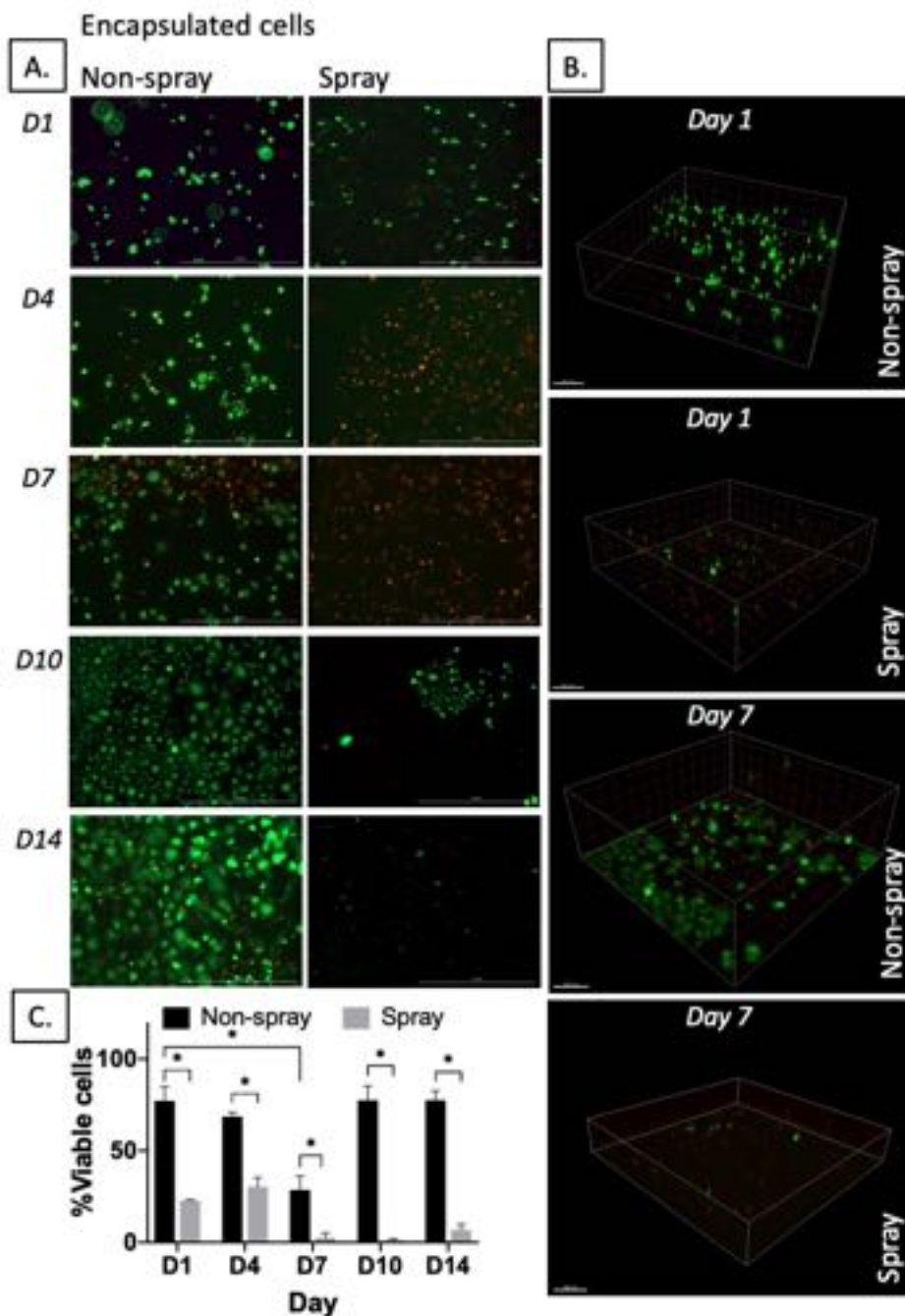


Figure 3.13: Cell viability of encapsulated sprayed and non-sprayed human epidermal keratinocytes. Representative images taken for each condition and timepoint (A) show a high viability of pipetted encapsulated cells, however poor survival of sprayed encapsulated cells was noted. Z-stack confocal images are demonstrating that pipetted cells maintain good viability during the studied period, while sprayed cells have poor viability from day 1 with little recovery (B). (C) Automated cell count of live and dead cells presented as percentage viable cells in the entire well. Data presented as mean duplicate measurement, errorbars represent SD.

in medium having higher LM-5 expression could indicate a cell response to trauma (Figure 3.14C).

Keratinocytes that have left the basal layer and are enlarging synthesise involucrin, a marker for terminal differentiation. Higher values of involucrin were found in encapsulated cells, especially those that were sprayed, at day 6 following application, indicating that encapsulated cells can commit to differentiation (Figure 3.14B and D). In contrast, involucrin levels in cells delivered in medium were very low at 1 week after delivery, with no difference between sprayed and non-sprayed cells. Migratory keratinocytes do not usually commit to differentiation, cells at the wound edge proliferate and migrate to close the wound before restoring the barrier function by stratification (eg differentiation). Since keratinocytes delivered in medium are not confined by a matrix like encapsulated cells, a more migratory behaviour is expected.

### 3.4 Discussion

The clinical outcomes of spray delivery of autologous human keratinocytes have been investigated widely, with variable results in terms of graft take and healing time. But *in vitro* cell studies on long term effect of spraying are lacking. Furthermore, current clinically adopted spray systems struggle to retain cells on the wound, cell spillage is an unaddressed clinical problem that could be circumvented by the introduction of a gellan - fluid gel based cell carrier, as investigated here.

Gellan gum is an anionic heteropolysaccharide derived from the bacterium *Pseudomonas elodea*, consisting of D-glucuronic acid, L-rhamnose and D-glucose subunits, it can form a thermo-reversible gel in the presence of ions upon temperature decrease. FDA and European Union (E418) approved as food additive and for medical use, making it also an attractive agent for a wide range of pharmaceutical and biomedical applications. For example, as encapsulating agent in controlled drug delivery systems [334] and more recently,

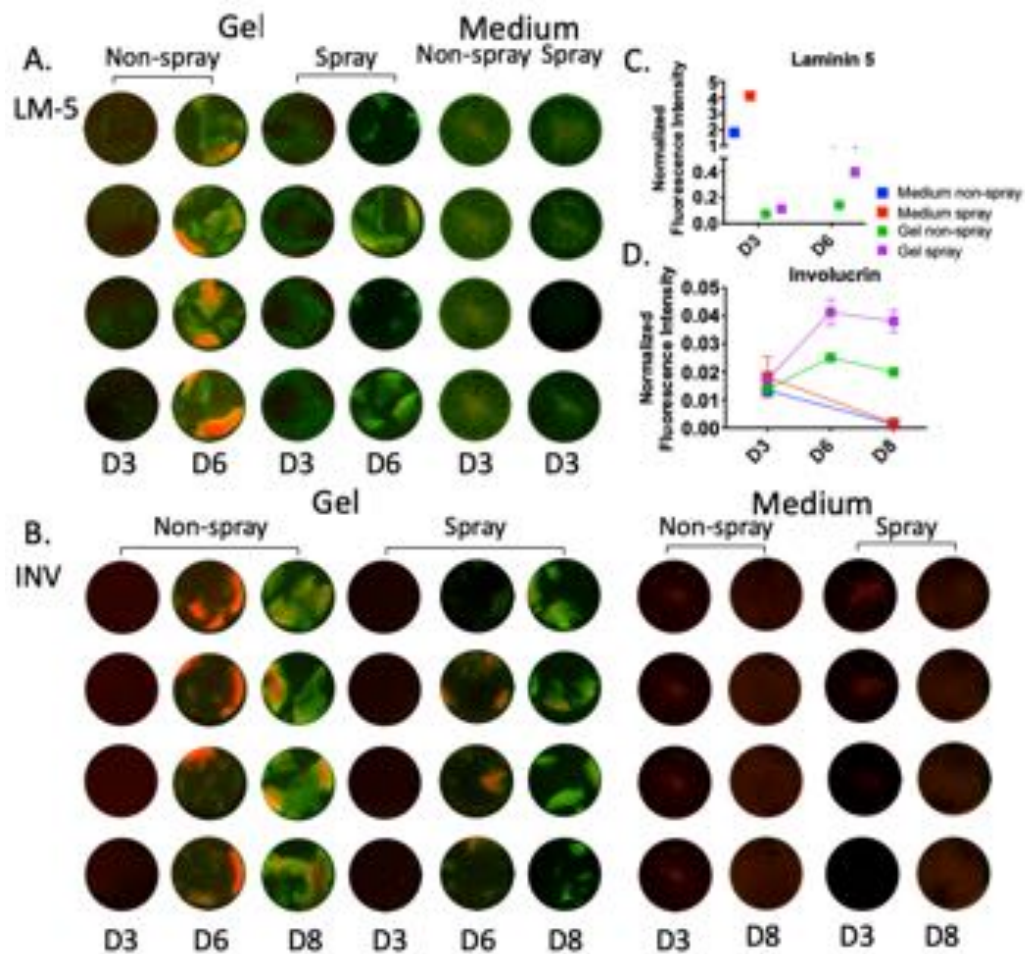


Figure 3.14: In-Cell Western assay for the keratinocyte differentiation markers laminin 5 (A) and involucrin (B) in sprayed and non-sprayed encapsulated and control keratinocytes. LM-5 = laminin 5, INV = involucrin. Normalized fluorescent intensity of laminin 5 (C) and involucrin (D). Data presented as mean (n=4), errorbars represent SD (not visible when smaller than icon).

as a material for tissue engineered scaffolds[179], injectables[181] and bio-inks[180, 335]. A gellan fluid gel system was prepared by applying shear during the gelation process, producing a shear-thinning system referred to as 'fluid gel'. In gellan, applying shear during the random coil to helix transition restricts the orderly formation of a continuous gelled network, instead, a particulate suspension is formed with weak associations between the particles (typical for fluid gels [269, 297]). Rheological characterization demonstrated that gellan fluid gel has specific viscoelastic properties that behaves as a liquid under high shear (when passing through the spray nozzle), but restructures to a weak gel on the

receiving surface facilitating retention of cells on the surface (Figure 3.5).

Following the investigation into the mechanical properties of the fluid gel, the cell viability of encapsulated cells was compared to that of non-encapsulated cells. As described in other cell depositing technologies such as 3d bioprinting, cell viability can be jeopardized by harsh extrusion methods such as large pressure drops in extrusion bioprinting disrupting cell membranes causing cell death [336] or laser-assisted printing with thermal damage to cells occurring[337]. Taken these challenges into account, researchers have now shown encouraging results with highly viable and differentiating cells, for example Fu et al. showed that bioprinted epithelial progenitors in a gelatin-based porous construct can form glandular morphology [338]. Cubo et al. bioprinted a two-layered skin equivalent including a fibrin-based layer with dermal fibroblasts embedded and a keratinocytes layer on top, *in vivo* formation of stratified skin was found in a murine model [339]. These exciting developments potentially pave the way for 3D printed skin[340]. Moreover, these advances are particularly interesting as similarities between nozzle based bioprinting and spray-assisted cell delivery exist. For example, knowledge on printer extrusion settings (such as pressure, shear and temperature at delivery), nozzle diameters and bio-ink fabrication could be translated to other cell-deposition applications such as cell-spraying.

In this study, it was found that keratinocytes encapsulated in fluid gel remained viable initially, but eventually seemed to die. Encapsulated cells kept a rounded phenotype as shown in Figure 3.13B-Day 1 and their metabolic activity was lower than non-encapsulated cells. However, an increasing proliferative capacity was observed at later timepoints indicating either proliferation of remaining viable cells in the gel or more likely, proliferation of cells that were able to diffuse out of the gel and attached to the bottom of the well as captured with confocal microscopy at day 7 (Figure 3.13B). As a result, viable cell numbers are again increasing after day 7 (3.13C) as the viable multiplying cells will soon outnumber the unviable cells entrapped in the gel. These results indicate the importance of cells to reach the wound bed and therefore migration of the cells towards a chemoattractant was tested in a transwell assay. As expected from the estimated

sedimentation rate, diffusion of cells through the porous membrane was restricted by the gel with significant differences between cells seeded in the gel and in culture medium (Figure 3.1F). Interestingly, the presence of a chemoattractant (HDFs in this case) did not influence the diffusion or migration of keratinocytes through the membrane.

Likewise, the effect of spray delivery on viability and function of keratinocytes was investigated. In contrast with previous work based on encapsulated fibroblast spray-delivery (Chapter 2), it was found that low pressure spray delivery was compromising viability and function of encapsulated keratinocytes as reflected in decreasing viable cell numbers (Figure 3.13C) and low metabolic activity (Figure 3.9B) throughout the studied period. This effect was less evident in non-encapsulated cells, with cell viability again increasing after day 4 and confluence was reached by day 10-14. Also, metabolic activity of sprayed cells recovered to >50% reduction by two weeks of cells culturing. A possible explanation for low cell viability following spraying of encapsulated cells is the use of a high cell density. With cells in close proximity of each other the local stress on a cell is increased during delivery as shown in a computational model by Nair et al. [341] and by a 3D alginate model from the same group [342].

The morphology of sprayed cells was examined by visualizing filamentous actin (f-actin), a major constituent of the cytoskeleton network [343]. The actin cytoskeleton interacts with focal complexes at the edge of the cell generating traction forces that facilitate cell migration and f-actin is part of the lamellipodia that enhance matrix adhesion[333]. Keratinocytes are robust cells that can endure higher compression forces than other cell types [344], however, it is possible that pressure at spray delivery can induce some cell membrane disruption. In this study, differences in organization of the f-actin cytoskeleton between sprayed and non-sprayed cells were found, confirming a level of stress with smaller cells and more f-actin deposition at the cell borders at day 1 (Figure 3.8A). Accumulation of contractile stress fibers as observed in sprayed cells on day 1 could lead to apoptosis, likely explaining the significant drop of viable cells on day 4 (Figure 3.12C). In addition, the potential lack of cell-to-cell contact and cell matrix adherence could drive keratinocytes

into a specific type of programmed cell death: anoikis [345]. The significantly smaller cell size found in sprayed cells after 2 weeks of culturing, indicate a potential slower or incomplete recovery following spraying (Figure 3.8). Indeed, proliferation (as measured by metabolic activity) of sprayed cells stayed behind that of non-sprayed cells (Figure 3.9). Next, we examined whether cells delivered to a wound contribute to wound healing and can be found in the wound bed. In the medium group one well showed limited healing, whereas the 3 other wells were nearly or completely healed within 120 hours. In contrast, the gel group, showed less evident healing for 3 out of 4 wells, but, 1 well did show complete confluence of the wounded area within 120 hours. Despite consistent experiment conditions, these results seems to reflect that wound healing is not always reproducible. Although some differences between the groups were observed, no statistically significant differences were found, most likely due to the large standard deviations given by wide varying outcomes within the groups. Therefore, differences between the groups cannot be guaranteed to cause the differences seen in this experiment.

The differentiation capacity of sprayed and encapsulated keratinocytes was investigated by measuring laminin-5 and involucrin expression. LM-5 deposition appears to be critical for the organisation of the basal membrane zone and for cell migration during re-epithelialization[346]. Cells delivered in medium expressed high levels of LM-5 after 3 days of culturing (Figure 3.14), this may indicate that cells start upregulating LM-5 as a response to cell delivery, whether this is caused by a response to inflammatory cytokines released following trauma or because cells are actively migrating, needs further investigation. As there are no other ECM products or cells available in the system, keratinocytes rely on autocrine signaling pathways for response to trauma and subsequently stimulation of repair via migration (re-epithelialization) and proliferation[347]. Interestingly, cells encapsulated in fluid gel do not express high levels of LM-5 at day 3, but a slight increase is observed in sprayed cells which might indicate some attempt to migratory behaviour of activated keratinocytes.

When cells leave the basal layer and commit to differentiation, markers such as keratin 1,

10 and involucrin are expressed [287]. Here, differentiation of keratinocytes was probed by measurement of involucrin, a marker for terminal differentiation synthesized in the spinous layer of the epidermis. Involucrin expression of all groups was similar at day 3, but a marked raise of expression was noted for cells encapsulated in fluidgel after one week of culturing.

Involucrin expression is linked to increased cell size and change in cell shape to a more flattened phenotype as part of the differentiation process, cells lose ECM connection and upward migration occurs[348]. As the gellan gel-network does not provide ECM-like binding sites, the encapsulated cells cannot bond to either the ECM or other cells and as a result, the onset of terminal differentiation and thus premature involucrin expression might occur [349]. Furthermore, cells in single-cell suspension are prone to early differentiation [350]. Interestingly, *in vitro* cultured keratinocytes on plastic can synthesize involucrin immediately above the basal layer [351]. However, at one week of culturing, involucrin levels of cells delivered in medium was very low, suggesting that cells did not commit to terminal differentiation at that point, but perhaps were still in a migratory state.

Gels formulated with gellan gum have previously shown to be a promising candidates for cell encapsulation [269, 311, 352]. Our earlier work has demonstrated beneficial material characteristics of gellan fluid gel with good spray-ability and limited run-off from the wound area, this material was compatible for HDF encapsulation. However, these encouraging results can not directly be translated to keratinocytes. As this study has shown that spray-delivery of keratinocytes changed the cell morphology and has an impact on cell function in terms of metabolic activity and protein expression. Furthermore, when encapsulated in gellan fluid gel, keratinocytes remain initially viable, but soon show altered behaviour in terms of decreased metabolic activity, remain a rounded phenotype when entrapped in the gel and eventually lose viability. As a result, migratory behaviour of encapsulated cells seem limited with premature differentiation as shown by involucrin expression.

### 3.5 Conclusion

By using a previously engineered biopolymer fluid gel to encapsulate human epidermal keratinocytes, we aimed to address the issue of poor retention of cells to the wound bed - a limitation in current cell-spray systems. The response of human epidermal keratinocytes to encapsulation in a biopolymer fluid gel and subsequently spray delivery was investigated. Spray delivery itself, has a negative effect on keratinocytes as shown by changes in the morphology and reduced metabolic activity in comparison to non-sprayed cells. However, recovery seems to occur with a confluent monolayer being formed after 10 days of culturing. Encapsulated cells also showed recovery following delivery, as measured by an increase in percentage viable cells and metabolic activity over a timescale of 2 weeks. However, spray delivery of encapsulated keratinocytes has a significant detrimental effect on cell viability and cell function in terms of metabolic activity, wound healing and differentiation.

Therefore, gellan fluid gel in the current formulation did not seem to be an ideal *in vitro* 3D culture system for keratinocytes, but the potentially positive effects of *in vivo* wound environment conditions on keratinocyte function were not taken into account here. Thus, when used as rapid delivery method by applying a thin layer of gel, this system could still be of benefit for cell delivery as it facilitates homogenous coverage of complex wound areas. Data presented suggests that cells used for cell-spraying applications must not only be robust enough to survive the process, but also be able to recover from mechanical and/or physiological stresses once transplanted, to ensure highly proliferative and functional cells that contribute to the wound healing process. Future work should focus on cell carrier systems that are individualized for the specific needs of certain cell types and their application methods.

## CHAPTER 4

# FORMULATION OF ACETIC ACID - GELLAN HYDROGEL DRESSING

Antimicrobial skin dressings to treat infected (burn) wounds without causing antibiotic resistance are in great demand. Acetic acid is a known antimicrobial agent to treat wound infections, acetic acid soaked in sterile gauze can be applied to infected wounds, however, rapid drug release and adherence to the woundbed leading to traumatic removal are considered disadvantageous.

In the present study, a gellan-based hydrogel film is used to deliver diluted acetic acid to the wound bed. The gellan films are rehydrated in acetic acid solutions prior to application and compared to medical gauze. The prepared gellan films are transparent, anti-adherent and could possibly improve patient comfort when compared to gauze. The results of this study show that by increasing the acetic acid content in rehydration fluids, the swelling capacity and thickness of the gellan films decrease, which is not observed in gauze. However, the mechanical properties in terms of tensile strength increase in higher concentrations of acetic acid rehydration fluids. When compared to gauze, the gellan films have similar release kinetics but seem to dehydrate slower. Microbial action was probed using a disk diffusion test on a blood agar plate seeded with *Pseudomonas Aeruginosa*, the gellan films provided anti-microbial action when rehydrated in 3-5 % acetic acid with zone of inhibitions up to 5 mm.

Taken together, the capacity of the gellan films to absorb and release diluted acetic acid was shown and the physical properties are superior to medical gauze. The gellan films have shown promising results to be used as wound dressing application, but further studies are needed optimize release kinetics.

## 4.1 Introduction

### 4.1.1 Burn wound infection

Burn wound infections (BWI) can cause delayed healing, poor scarring and invasive infection leading to sepsis which can result in death of the patient [353, 354]. Burn wound infection and secondary sepsis are considered the most serious complications in thermally injured patients [355]. The major cause of death in severely burned patients (>40% TBSA) is sepsis secondary to inhalation injury or any form of infection such as BWI [355]. Burn wound infections account for approximately 9% -17% of all burn injury related complications [356, 357]. Pruitt et al. reports that invasive burn wound infections account for 5% of all burn treatment complications in a healthy patient population (U.S. Army Burn Center between 1986-1995)[353]. Invasive BWI undoubtedly requires intravenous or oral antibiotics; however, nosocomial BWI can also be targeted with a wide variety of topical agents such as silver nitrate, povidone iodine, topical antibiotics or acetic acid. To date, no consensus regarding superiority of a certain topical agent for the prevention or treatment of BWI has been reached (European Burn Association guidelines) [358]. Because bacterial resistance is an increasing worldwide concern, antimicrobial effective topical agents that do not increase the risk of resistance and are non-toxic to cells involved in the wound healing process are required.

### 4.1.2 Acetic Acid in burn wound treatment

Acetic Acid is a simple carboxylic acid that consists of an acetyl group and a hydroxyl group. It is a product of ethanol oxidation and wood distillation (Figure 4.1) [359].

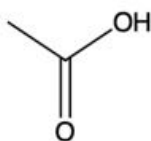


Figure 4.1: Chemical structure of acetic acid - C<sub>2</sub>H<sub>4</sub>O<sub>2</sub>.

Cells naturally contain acetic acid at a low level. Acetic acid is also found in human vaginal lubrication, probably playing a role in reducing microbicidal activity [360]. Acetic acid has been used as an antibacterial and antifungal agent for thousands of years, more recently acetic acid has been a widely used topical antiseptic agent for the treatment of burns wounds and has been shown to have activity against Gram-negative organisms including *Pseudomonas Aeruginosa* [361]. The common application method is to soak gauze in a 1-5% w/v acetic acid solution and place this directly on the cleaned burn wound or on top of a protective layer such as paraffin gauze. These dressings are then protected with more layers of (paraffin) gauze. Changing dressings is required to observe, clean and redress the wound; patients often require additional analgesia during these procedures [362]. It is documented that many patients complain of stinging and pain on application of acetic acid to wounds, in particular if a strength of 5% is used [363]. Higher concentrations can lead to severe complications and induce skin injury [364]. During the treatment of colonised burn wounds it is important to maintain a balance between microbicidal activity and tolerability. *In vitro* studies have been conducted examining the minimum inhibitory concentrations (MIC) of acetic acid before and after evaporation and exposure to gauze. These showed that the methicillin-susceptible strain of *S. Aureus* (MSSA) had an MIC of 0.312% and a methicillin-resistant strain was less susceptible, MIC = 0.625%. Strains of *A. baumannii* also had a MIC of 0.312% and all strains of *Pseudomonas Aeruginosa* were susceptible, MIC = 0.166% [365]. The mechanism of action in wounds is still unclear [366] but could be related to lowering the pH level of the wound milieu, which can inhibit growth of many pathogenic bacteria and their protease activity. Another effect of low pH at the infection site is the induced release of oxygen towards the cells resulting in higher concentration of reactive oxygen species that is known to promote wound healing [367]. However, Bjarnsholt et al treated *P. Aeruginosa* cultures with hydrochloric acid (HCL) and acetic acid with the same low pH (range 4.33-6.0) and found a beneficial effect of acetic acid in comparison to HCL, indicating that the mechanism of action of acetic acid is not merely due to an acidic effect. Interestingly, a pH dependency for acetic acid

was found with samples treated with low pH (<4.76) being significantly more effective than higher pH treatment (>4.76) [368]. Acetic acid can diffuse through the cell wall of bacteria and acidify the cytoplasm causing disruption of the cell function [369, 370].

### 4.1.3 Acetic acid delivery systems

Diluted acetic acid is routinely applied to infected wounds in clinical practice. The established method is to drench a compress in the solution and apply to the wound [366]. Other medical applications of diluted acetic acid include its use in ear drops to treat otitis externa [371], as urological irrigation solution [372], or as acidic vaginal gel for the treatment of bacterial vaginosis [373]. In more concentrated dilutions (up to 50%) it has been used in sclerotherapy for renal cysts [374, 375] and as ultra-sound guided percutaneous acetic acid injection therapy (PAIT) for hepatocellular carcinoma [376].

### 4.1.4 Study rationale

Acetic acid can be used as an antimicrobial agent to treat wound infections (especially known for *P. Aeruginosa* treatment). Effectiveness of acetic acid in concentrations of 0.3-5% has been proven *in vitro* against several bacteria [365] and fungi [377]. Numerous clinical studies investigating effectiveness of acetic acid against wound infection have supported these results [361, 363, 366, 378, 379]. Currently, a pilot trial comparing the antimicrobial effectiveness and tolerability of acetic acid 0.5% versus 2% in patients with burn wounds is performed (ongoing study).

Clinically adopted protocols advise to soak the diluted acetic acid in sterile gauze and apply this to the wound. The dressings are usually changed to ensure an active dose of diluted acetic acid in the wound. As dressing changes are related to discomfort and pain for patients [380], minimizing these dressing and improving the comfort of the dressings is key. These issues can be addressed by applying a hydrogel based dressing hydrated with diluted acetic acid to the wound. In this way, a slower release of the acetic acid

can be achieved resulting in fewer dressing changes. Furthermore, comfort of the dressing material is improved by using a soft hydrogel compared to gauze that is known to adhere to the woundbed.

The aim of this study is to optimise the composition of gellan gum hydrogel film for the uptake and release of acetic acid in wounds.

## **4.2 Methods**

### **4.2.1 Preparation gellan gel films**

Low-acyl gellan gum (kelcogel LOT #: 5C1623A ) was used for preparation of all gellan films. A 2 % (w/v) gellan solution was prepared by adding gellan powder to deionised water, the solution was heated until 70 °C. Solution was allowed to cool until 60 °C, if applicable, at this stage PBS was added. Next, gellan solutions were casted in 10x10 cm square culture plates on a low speed orbital shaker to enhance even distribution and were then dried in a pre-heated vacuum oven (Thermo Scientific; VT 6060 M) set on 40-42 °C for a total duration of 17 hours. In the last 2 hours a vacuum was applied to remove moisture. Films were harvested and stored individually in sealed bags in a dry environment at room temperature until further use.

### **4.2.2 Material characterisation gellan patches**

#### **Swellability**

Five different rehydration fluids were used including deionized water (H<sub>2</sub>O), 5% acetic acid solution (w/v) (Huddersfield Pharmacy Specials, UK), 1% acetic acid solution (w/v), sodium chloride 0.9% (w/v) and acetic acid diluted in sodium chloride until a final concentration of 1% acetic acid (w/v) and 0.72% NaCl (w/v). Dry weight of all gellan patches was measured. Next, gellan patches prepared with and without PBS were immersed for 5 minutes in rehydration fluids at room temperature. Excess fluid was lightly wiped by filter

paper and weighted (PM460 Delta Range balance, Mettler-Toledo Ltd, UK) immediately, at 30 min, 90 min and 20 hours after immersion. Percentage of swelling was calculation with Equation 4.1.

$$Swelling (\%) = \frac{(W_s - W_d)}{W_d} \times 100 \quad (4.1)$$

- $W_d$  = Weight of dry polymer (g)
- $W_s$  = weight of swollen polymer (g)

### **Thickness**

Thickness of gellan films was measured with a digital caliper following 5 min rehydration in the dedicated fluid, for each sample 3 measurements from different sections of the film were obtained.

### **Tensile strength**

The gellan films were rehydrated for 5 minutes and cut into dogbone shaped samples using a 3D-printed cutter with specified dimensions [381] as shown in (Figure 4.2A and Figure 4.2B). Samples were directly loaded onto the testing machine (Bose ElectroForce 5500, TA Instruments) equipped with WinTest<sup>®</sup> software package as shown in Figure 4.2C. All tests were run with a crosshead speed of 0.1 mm/s at room temperature until breakage of specimens occurred.

The tensile stress (Equation 4.2) and strain (Equation 4.3) were calculated from displacement (mm) and load (N). Youngs modulus was calculated from the linear region of the stress-strain curve (Equation 4.4). All tests were repeated at least 3 times per sample.

$$\sigma = \frac{Force}{Area} \quad (4.2)$$

With  $\sigma$  is stress (Pa), Force being the load in (N) and the Area ( $\text{mm}^2$ ) was determined by the width (4 mm) times the depth (thickness) of the tested sample.

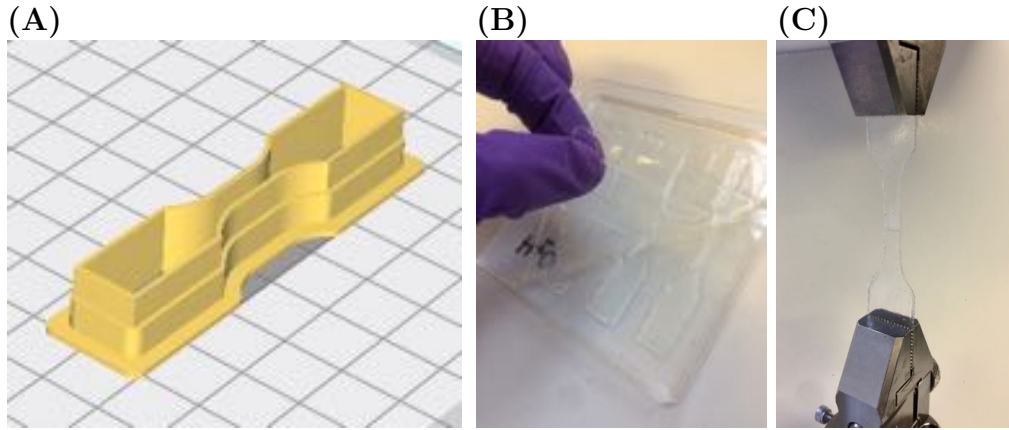


Figure 4.2: Tensile strength testing of dogbone shaped gellan films

$$\epsilon = \frac{\Delta L}{L} \quad (4.3)$$

- $\epsilon$  = strain
- $\Delta L$  = displacement (mm)
- $L$  = length of narrow section dogbone (14.9 mm)

$$E = \frac{\sigma}{\epsilon} \quad (4.4)$$

- $E$  = Young's modulus (N/mm<sup>2</sup>)
- $\epsilon$  = strain (%)
- $\sigma$  = stress (Pa)

### 4.2.3 Release

#### Diffusion through agarose gel

Gellan patches were rehydrated into H<sub>2</sub>O 1%, 3% and 5% acetic acid solutions (w/v) and cut into squares to fit cuvettes. An agarose 1% (w/v) gel was prepared by addition of agarose (Fisher Scientific, UK) to H<sub>2</sub>O heated to 80 – 90 °C under constant mechanical stirring, gel formation occurred upon cooling to room temperature and an pH indicator was

added to the cooling gel. Rehydrated gellan-only patches were placed on top of agarose gel filled cuvettes and photographs were taken at 5 min and 14 hours after application.

### Release into wound bed

Release of acetic acid was quantified with an enzymatic detection kit, K-ACETAK(Megazyme), based on the following reactions:

1. Acetate + ATP  $\xrightarrow{\text{acetate kinase}}$  acetyl-phosphate + ADP
2. ADP + PEP  $\xrightarrow{\text{pyruvate kinase}}$  ATP + pyruvate
3. Pyruvate + NADH + H<sup>+</sup>  $\xrightarrow{\text{D-lactate dehydrogenase}}$  D-lactic acid + NAD<sup>+</sup>

*ATP= Adenosine triphosphate, ADP= Adenosine diphosphate, PEP = Phosphoenolpyruvate, NADH= Nicotinamide adenine dinucleotide (reduced form), NAD<sup>+</sup> = Nicotinamide adenine dinucleotide (oxidized form)* Reagents were prepared following suppliers' guidelines. Briefly, reagent 1 contained NADH, ATP, PEP and PVP mixed with H<sub>2</sub>O and reagent 2 contained a buffer, preservative, acetate kinase, pyruvate kinase and D-lactate dehydrogenase suspension. The absorbance was measured at 340 nm with a Spark<sup>®</sup> microplate reader before (A<sub>0</sub>) and after the reaction (A<sub>1</sub>), the difference (ΔA) was calculated. First, a calibration curve was performed with acetic acid concentration ranging from 0 - 1.8 g/L as shown in Figure 4.3. Good linearity is shown for concentrations up to 0.9 g/L (R<sup>2</sup> = 0.9701) and less so when the full range of concentrations was included (R<sup>2</sup> = 0.9274), attempts to improve accuracy of the reading included: decreasing volumes to allow for better mixing, prolonging the reaction time and lowering the amount of NADH in the reaction, these attempts did not improve accuracy and the initial method was used for further experiments. However, lowering the amount of NADH in the reaction resulted in lower absorbance values, now clearly within the detection limits of the plater reader and therefore the adapted reagent 1 was used for further experiments.

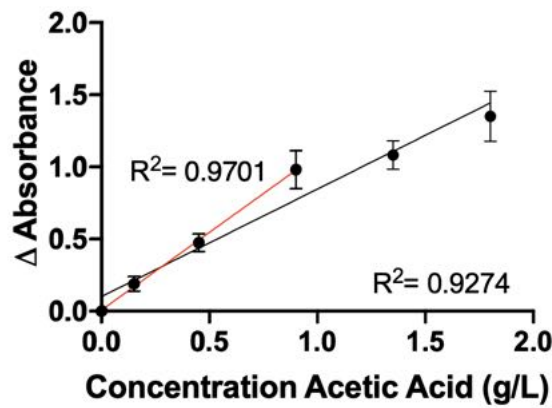


Figure 4.3: Acetic acid detection calibration curve. Values represent absorbance difference of A0 and A1 both measured at 340 nm.

Then, the release of acetic acid was measured in an *ex vivo* porcine skin wound model as illustrated in Figure 4.4. Porcine skin wounds were created by scoring patches of 1x1 cm<sup>2</sup> with a scalpel in 4 directions, each 10 times. Then the skin was hydrated in H<sub>2</sub>O for 2 hours, excess fluid was removed from the epidermis and the skin was incubated at 34 °C and 5% CO<sub>2</sub> while hydrated with H<sub>2</sub>O for another 2 hours. Samples of gellan-only dressing and gauze were cut in 1x1 cm<sup>2</sup> square patches, rehydrated in 0%, 1%, 3% and 5% w/v acetic acid solutions for 5 min and placed on top of porcine wounds. Weight of dry and wet (before application to pig skin) was measured. Samples were removed after 1, 6, 12 and 24 hrs and diluted in 50 ml H<sub>2</sub>O for 24 hours. Then, aliquots of diluted dressings were taken and acid acid was detected as described above.

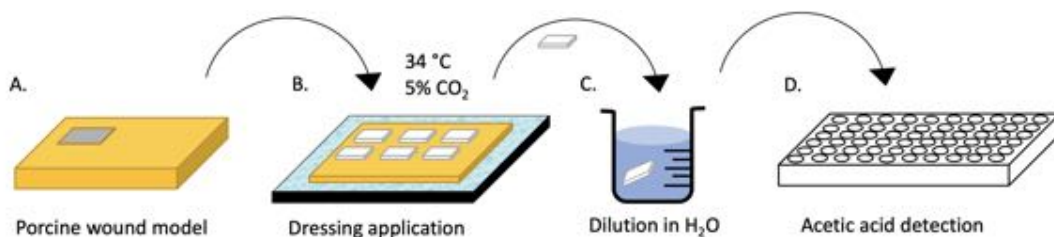


Figure 4.4: Porcine wound model method

#### 4.2.4 Agar disk diffusion assay

Antimicrobial effect of the gellan films and gauze were compared. The disk diffusion assay was performed with blood agar prepared by the clinical microbiology lab at UHB<sup>1</sup> and plated with *Pseudomonas Aeruginosa* for 24 hours. Then, 6 mm diameter round punch biopsies were taken from the gellan patches and multiple layers of medical gauze cut in similar shape samples. All samples were rehydrated for 5 minutes in the test agents (1%, 2%, 3%, 4%, 5% acetic acid solutions (w/v) and H<sub>2</sub>O). When the solution has an antimicrobial effect, a clear zone around the sample can be observed (=zone of inhibition), here, measured after 24 hours of incubation.

### 4.3 Results

#### 4.3.1 Visual appearance of dressings

All the investigated gellan films are transparent with a square shape and smooth surface, with dry gellan films being thin and delicate. After rehydration the gellan films remained transparent and exhibited a softer touch, especially those rehydrated in H<sub>2</sub>O and low-acetic acid concentration fluids. All films were non-adhesive to skin when rehydrated, but preparations rehydrated in H<sub>2</sub>O were more fragile to handle. Rehydration increased the thickness of the films and a higher concentration of acetic acid present in the rehydration fluid resulted in dressings with a firmer consistency.

#### 4.3.2 Thickness

Transparent gellan films were prepared with low-acyl gellan gum and the thickness of hydrated systems was measured. Table 4.1 shows the mean thickness (SD) of different compositions of gellan patches per rehydration fluid. In general, it was found that thickness of the systems is highly dependent on the type of rehydration fluid used with systems

---

<sup>1</sup>with help from Dr. Fenella Halstead, NIHR SRMRC Clinical Scientist - Microbiology

rehydrated in H<sub>2</sub>O being significantly thicker than other rehydration fluids. Gellan films prepared with PBS (GGPBS) (Figure 4.5B) have thicknesses ranging from 0.17 mm (5% AA w/v) to 0.59 mm (H<sub>2</sub>O rehydration). Overall mean thickness of gellan patches prepared without PBS (GG) was thinner and ranged from 0.14 mm until 0.46 mm when rehydrated in 5% AA w/v and H<sub>2</sub>O respectively (Figure 4.5A). In both types of films, the amount of acetic acid added to the rehydration fluid negatively influenced the thickness, with a statistically significant difference found in gellan only systems.

Table 4.1: Gellan film thickness. All measurements are performed in triplicates, values are mean thickness in mm (SD).

	Rehydration fluid				
	H <sub>2</sub> O	1% Acetic acid (w/v)	5% Acetic acid (w/v)	0.9% NaCl (w/v)	1% Acetic acid (w/v) in 0.72% NaCl (w/v)
Gellan - PBS	0.59 (0.05)	0.21 (0.01)	0.17 (0.00)	0.27 (0.03)	0.20 (0.01)
Gellan	0.46 (0.04)	0.23 (0.01)	0.14 (0.01)	0.20 (0.01)	0.16 (0.01)

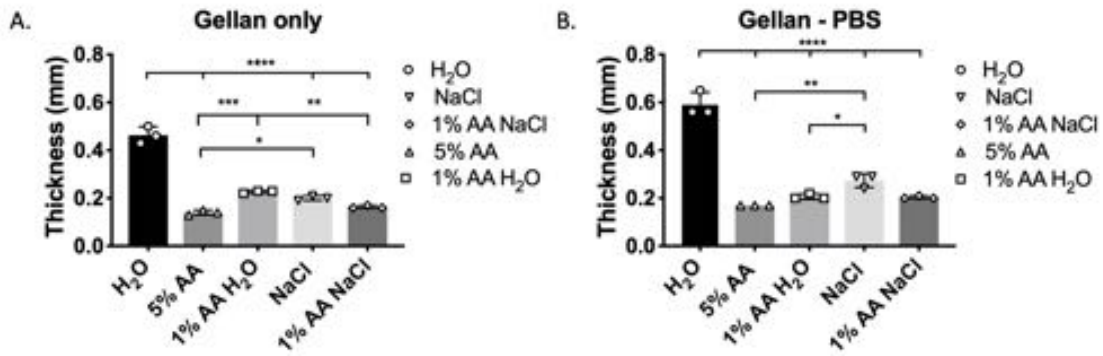


Figure 4.5: Mean thickness (mm) and standard deviations of gellan films prepared with PBS (B) or without (A) following rehydration. Significant differences found by one-way ANOVA with post-hoc statistical significance analysis indicated by p values of \* $<0.05$  , \*\*  $<0.01$  and \*\*\* $<0.001$ .

### 4.3.3 Swelling capacity

Dry weight of gellan patches and medical gauze (Synergy, UK) was measured. Subsequently, the weight was measured directly following rehydration of the samples and

swelling rate (in %) was calculated as shown in Figure 4.6. All preparations showed a positive swelling capacity that ranged from 582% to 2234% with the maximum value attained for gellan films rehydrated in H<sub>2</sub>O. Swelling capacity of the fabricated films follows a similar pattern as the thickness outcomes, with a lower percentage of swelling for films rehydrated in higher acetic acid concentration fluids, except for gellan patches without PBS that were rehydrated in 1% AA sodium chloride solution. Furthermore, only those preparations rehydrated in H<sub>2</sub>O reached a higher swelling capacity than medical gauze as shown in Figure 4.6. It was found that swelling of medical gauze was not influenced by the type of rehydration fluid. Whereas both the gellan patches have a large range of swelling with largest increase in weight found for systems rehydrated in H<sub>2</sub>O and a decrease in swelling capacity noticed with increasing concentrations of acetic acid present in the solvent fluid. Hence, solvent composition influences the swellability of the gellan patches strongly. Swelling is increased when lower concentrations of acetic acid are used in the rehydration fluid.

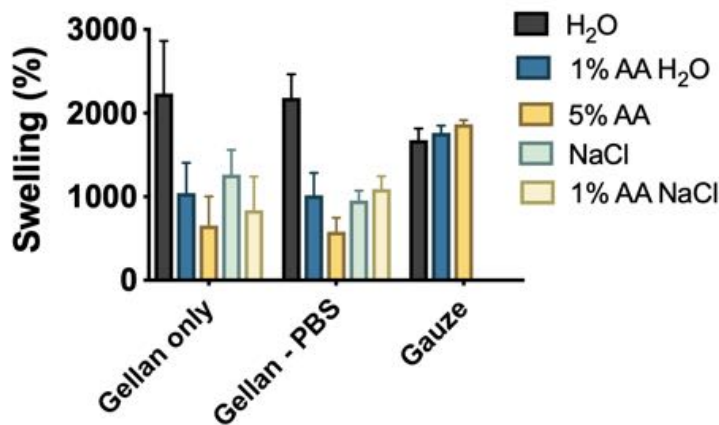


Figure 4.6: Mean swelling (%) of gellan films compared to gauze following rehydration.

#### 4.3.4 Dehydration

In order to evaluate the ability of gellan films to retain water following application, gellan films were allowed to dry and weight was measured 30 min, 90 min and 20 hours after

rehydration at ambient conditions as shown in Figure 4.7. Gellan films showed a larger water holding capacity than gauze with slower decrease of weight loss as calculated by percentage mass loss of swollen state. In a physiological environment the dressings would be exposed to a moist woundbed and covered with a secondary dressing, it can be expected that the preparations are able to absorb wound exudate. This is of great value because besides releasing the acetic acid in the wound, the gellan films are able to retain water for longer, resulting in a moist wound environment necessary for wound healing.

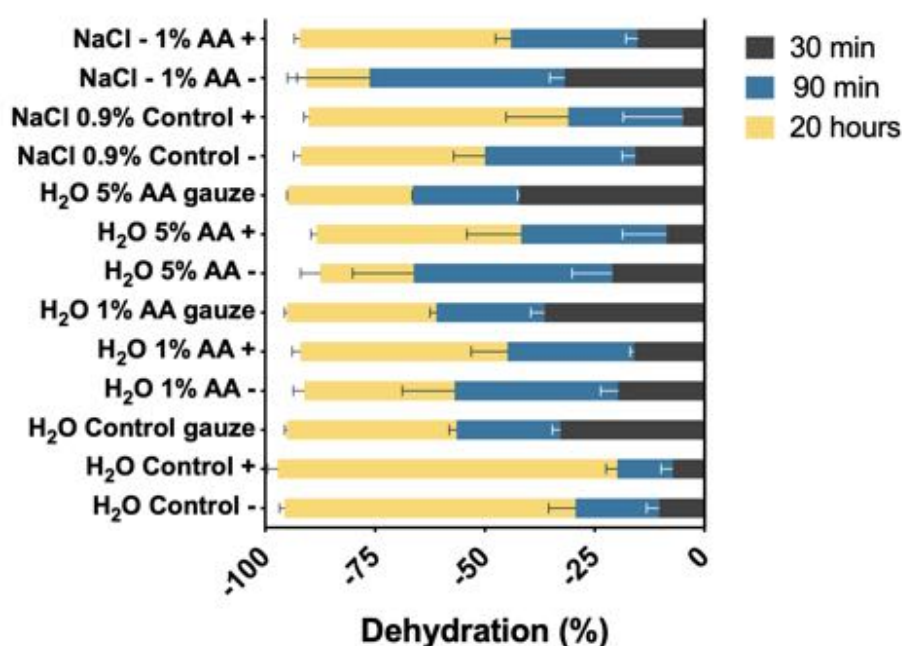


Figure 4.7: Mean dehydration (%) of gellan films compared to gauze at 30 min, 90 min and 20 hours after rehydration. Values presented are mean percentage dehydration of 3 individual measurements, errorbars are SD.

### 4.3.5 Tensile strength

The mechanical strength of the gellan films was determined by measuring the amount of tensile stress needed for the gellan films to rupture. A general correlation is evident between amount of acetic acid in the solvent fluid and Young's modulus; preparations rehydrated in 5% AA endured highest stress before failure (tensile strength) 4.8A,B and had the largest Young's modulus 4.8E. As expected, the lowest maximum stress upon

failure and lowest Young's modulus were measured for gellan films rehydrated in H<sub>2</sub>O, resulting in dressings that are less practical as they rupture easily upon handling. However, the greatest elongation properties were seen in dressing rehydrated in 0.9% NaCl, followed by gellan-PBS films rehydrated in 1% AA NaCl (Figure 4.8C,D).

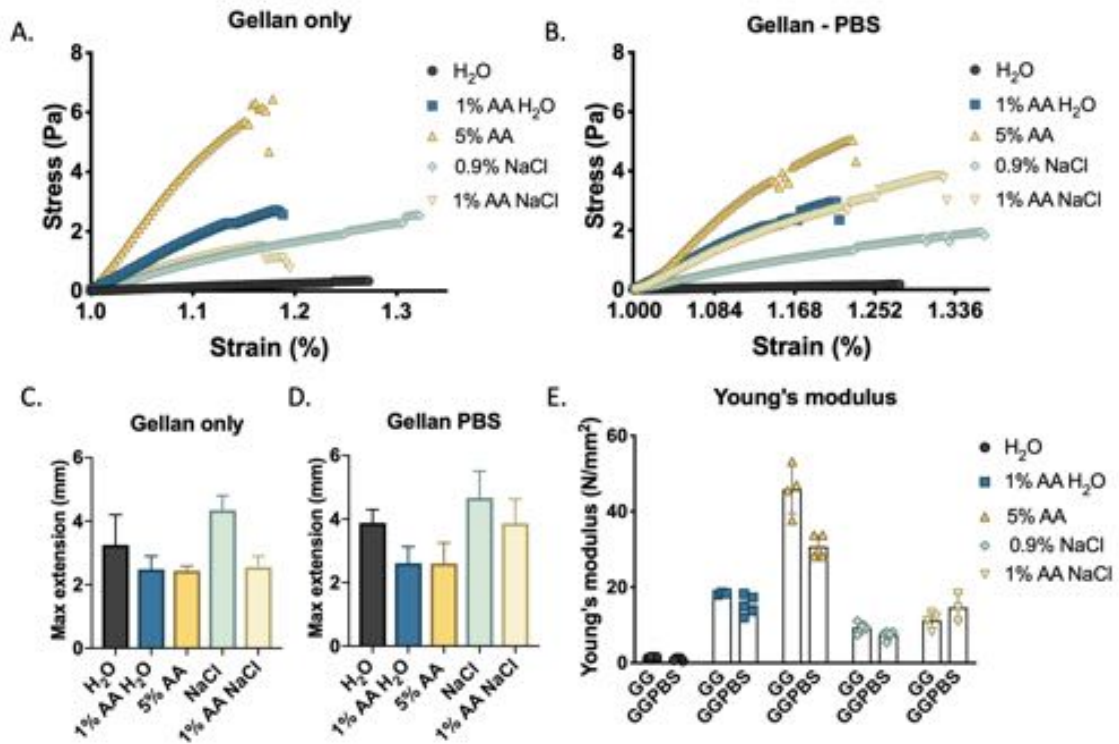


Figure 4.8: The tensile stress-strain curves for gellan only (A) and gellan-PBS films (B) show a relationship between solvent formulation and tensile strength. Mean values of 3 individual experiments are shown. Elongation as measured by maximum extension (mm) at point of failure of gellan-only (C) gellan-PBS dressings(D). Young's modulus of gellan films prepared with (GG) and without PBS (GGPBS) (E). Values presented are mean Young's modulus and individual measurements, errorbars are SD.

### 4.3.6 Release

Release of acetic acid into the wound should occur in a controlled manner instead of rapid release seen in gauze soaked in acetic acid. Mechanical properties of gellan films indicate that the solvent formulation influences swelling ratio and strength of the preparations. Release of acetic acid into the wound is assumed as mass loss occurs at ambient temperatures.

### 4.3.7 Agarose diffusion

Diffusion of acetic acid through a higher viscosity environment was tested by placing the rehydrated dressings on pH indicating agarose gel. As expected, when dressings are rehydrated in higher concentrations of acetic acid, a larger diffusion grade was observed (Figure 4.9). Whether this effect can similarly be observed as a concentration of acetic acid in the wound was examined by a wound model based on porcine skin.

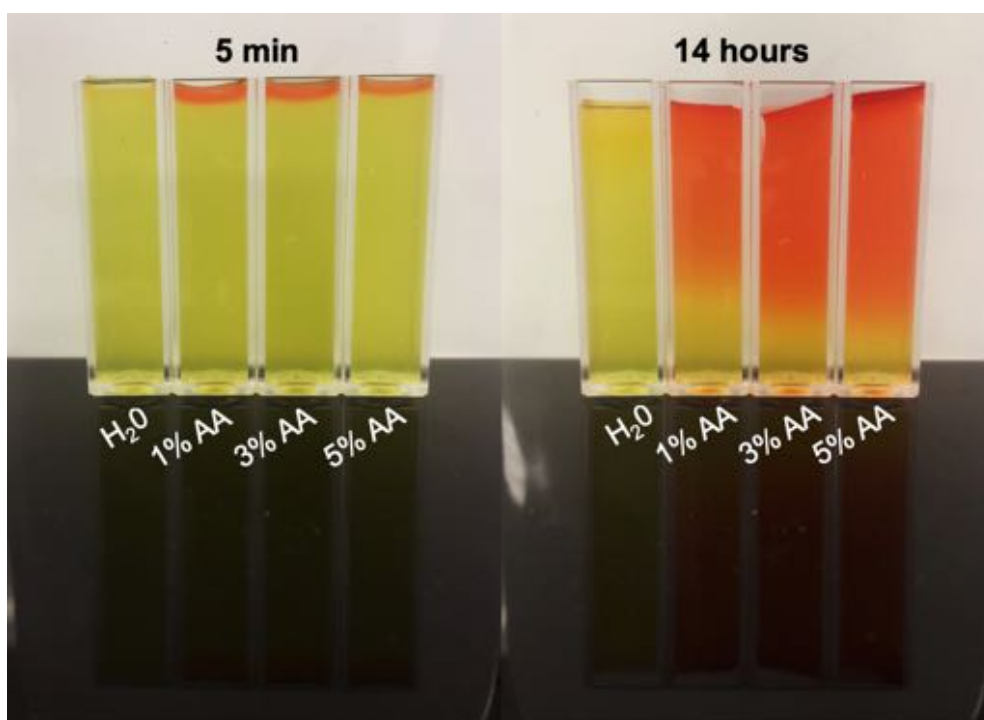


Figure 4.9: Acetic acid diffusion into agarose gel.

### 4.3.8 Porcine wound model

The effect of acetic acid loading on the release rates was investigated for gauze and gellan-only formulations. It was hypothesized that the concentration release for formulations containing lower concentration of acetic acid would be low, while the release should increase with increasing amount of acetic acid absorbed in the dressings. However, it was found that when normalized against H<sub>2</sub>O, the absorbance differences in all samples were

extremely low with many negative values in the gellan group (Figure 4.10). Absorbance differences from gauze samples were low at all timepoints and concentrations, but mainly positive values were found, indicating a trace of acetic acid left in the dressing.

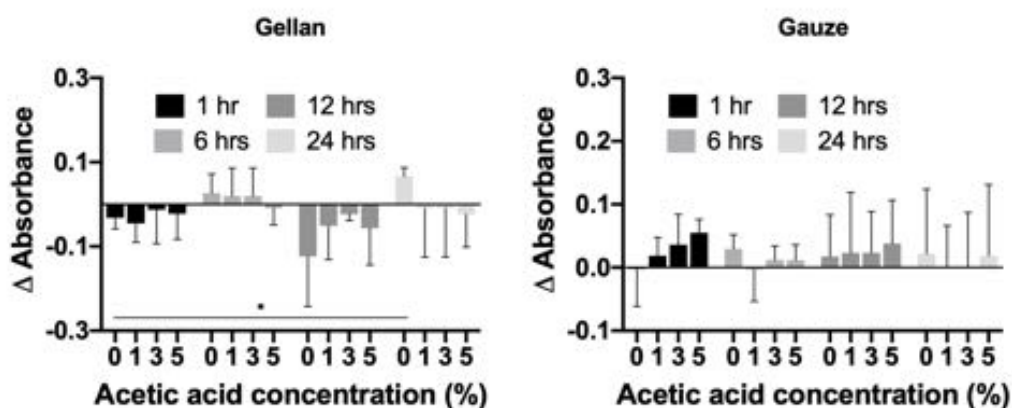


Figure 4.10: Acetic acid release from porcine wound model normalized against H<sub>2</sub>O sample. Data presented is mean of 3 individual measurements per timepoint with standard deviation. Significance tested with two-way ANOVA.

### 4.3.9 Antimicrobial effect

Anti-microbial activity of acetic acid rehydrated gellan patches was compared to medical gauze. Larger zones of inhibition were present for gauze samples rehydrated in acetic acid when compared to the gellan patches for the full range of acetic acid concentrations tested. However, the gellan patches could be accurately cut into 6 mm round (punch biopsy) samples, whereas, the gauze was cut in similar samples, but due to difficulty to handle and frail edges, larger samples were used (Figure 4.11). Acetic acid has an anti-microbial effect as growth was only observed under/on gellan patches rehydrated in H<sub>2</sub>O. Gellan patches provided anti-microbial action when rehydrated in 3-5 % acetic acid with zone of inhibitions up to 5 mm (Table 4.2). Although no growth was seen under the samples rehydrated in lower concentrations (1-2% acetic acid), no zone of inhibition was present either. These preliminary results indicate that acetic acid released from the dressings has an anti-microbial effect against *Pseudomonas Aeruginosa*, however, further studies with larger numbers are needed to validate these results.

Table 4.2: Anti-microbial activity (zone of inhibition) of gellan dressings

	H <sub>2</sub> O	5% AA	4% AA	3% AA	2% AA	1% AA
Gellan only	no zone*	5.0	3.2	no zone	no zone	no zone
Gellan - PBS	no zone*	3.6	2.4	1.2	no zone	no zone
Gauze	no zone	10.3	13.1	9.4	5.1	3.5

AA = acetic acid. \*growth under disk. All values presented are zone of inhibition in mm.

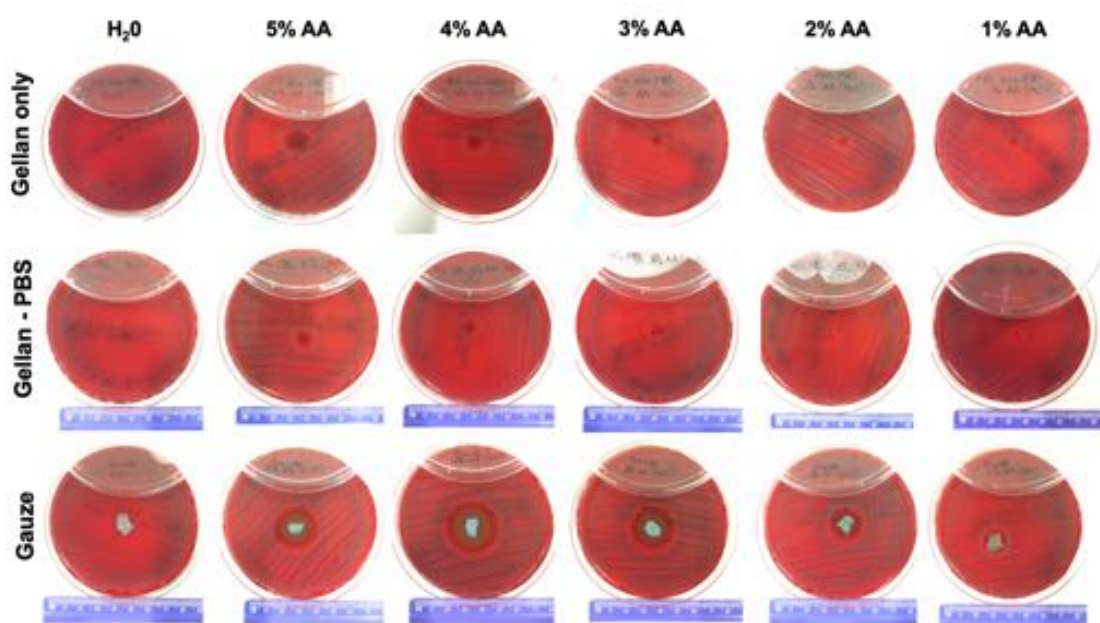


Figure 4.11: Gellan patches anti-microbial activity against *Pseudomonas Aeruginosa*

## 4.4 Discussion

With antibiotic resistance rising worldwide [382], the need to treat infections with antimicrobial effective topical agents that do not increase the risk of resistance and are non-toxic to cells involved in the wound healing process are required. Patients suffering from burn injuries have a disrupted skin barrier which substantially increases the risk of developing hospital-associated infections[383]. Acetic acid has been used in health care as an antimicrobial agent to treat chronic and burn wound infections. Beneficial results

have been shown with acetic acid solutions up to 5% [361, 366, 368]. However, nowadays lower concentrations seem to be preferred to avoid burning sensations and complications at the wound site [364]. It is known that wound dressing changes cause significant pain to patients resulting in administration of pain medication and in extensive wounds sedatives are often required to minimize discomfort [384]. Furthermore, the current application technique can result in painful removal due to incorporation of the dressing material into the wound, this can be avoided by applying a protective layer underneath the acetic acid gauze. However, this additional barrier will most likely decrease the amount of acetic acid released in the wound. Therefore, a non-adhesive soft dressing that can absorb acetic acid solution and subsequently release it into the woundbed is desired.

In this study, the composition of a transparent gellan gum hydrogel film for the uptake and release of acetic acid has been designed and its properties investigated. Gellan gum is an exopolysaccharide that is produced through aerobic fermentation by the bacterium *Pseudomonas elodea*, it consists of D-glucuronic acid, L-rhamnose and D-glucose subunits. Mostly known in the food industry as a thickener, this natural polymer has also gained interest for the use in biomedical applications because it can form a thermoreversible gel, is biocompatible and has highly tunable mechanical properties. In terms of tissue engineering purposes, gellan-based materials have been investigated for the use in ocular or oral drug delivery [385, 386], reconstruction of cartilage [181], neural tissue [307], intervertebral discs [308] and intra-abdominal anti-adhesion barrier [183]. As a wound dressing, gellan has been found to be non-toxic, stimulate healing and reduced scarring in a rodent study [387].

A particular advantageous property is the transparency of the prepared gellan films as transparent dressings give the clinician an opportunity to review the wound without having to remove or replace the dressing allowing for frequent wound examinations and early intervention if needed. The results of this study have shown that gellan films have a good swelling capacity resulting in soft and pliable films when rehydrated. Although lacking the transparency, anti-adhesiveness and soft surface of gellan films, gauze is also an effective

delivery vehicle for acetic acid solutions with a constant swelling rate for all rehydration fluids studied (Figure 4.6). In contrast, the swelling capacity and thickness of the films decreases upon increase of acetic acid concentration in the solvent. Similarly, mechanical strength as measured by the amount of tensile stress required for films to rupture, was increased when gellan films were soaked in increasing concentrations of acetic acid. The increased mechanical strength was expected since low-acetyl gellan is known to be acid-sensitive [388, 389]. Norton et al. showed gellan gel strengthening following acid (HCL) soaks resulting in a transition from fluid to solid gels. [390], it is suggested that the cross-linking between the polymer chains is strengthened by exposure to acid [391]. Furthermore, it was found that rehydrated gellan films demonstrated a slower decrease of weight loss at ambient temperatures when compared to gauze, especially at the early timepoint of 30 minutes (Figure 4.7). This is clinically relevant as dressing changes often take some time to complete depending on the size of the wound, dressings that dehydrate - due to evaporation of the solvent - are more likely to adhere to the woundbed as is seen in medical gauze.

Next, the release of acetic acid into the wound bed was probed using a porcine wound model. From the gellan films tested, only at one timepoint (6 hours) acetic acid detection was higher than the control (H<sub>2</sub>O). Gauze samples did produce slightly higher values, with the highest mean value measured of 0.06 for 5% acetic acid following 1 hour application. These results could indicate a couple of things; first, the majority of the acetic acid is released into the wound bed and therefore values are low; secondly, the samples have been overdiluted resulting in barely detectable values or thirdly, performance of the assay was not optimized. Other drug release studies focussing on gastrointestinal tract drug-delivery have used gellan beads as delivery vehicle, they have shown sustained drug release properties when carefully selecting cation-induced ionotropic gelation strategies [334, 392]. Agnihotri et al. prepared beads in high (pH 9) and low (pH 5) media, low pH media created more porous beads leading to a rapid release of the drug (cephalexin)[334]. Babu et al. formulated gellan macrobeads with Amoxicillin encapsulated, they found that

increase of drug concentration, decrease of polymer concentration and lower electrolyte concentration (calcium chloride) in the crosslinker solution affected the drug release rate positively [392]. Thus, by controlling the degree of hydrogel swelling through crosslinking either during or after hydrogel preparation, the release of drugs can be controlled [393]. However, with acetic acid being a very small molecule, it is likely that diffusion through pores happens rapidly despite adjusting the swelling kinetics.

A proof of concept study was conducted to examine antimicrobial efficacy of the gellan films compared to gauze. Although gauze showed larger zones of inhibition, this is likely contributed to the larger samples used in this study. Therefore, further studies should aim to eliminate differences between tested and control dressings for example by standardizing the dry weight of each sample. However, the preliminary results of this study have demonstrated that gellan films rehydrated in acetic acid solutions of 3-5%, have an antimicrobial effect against *Pseudomonas Aeruginosa*. Further studies are needed to validate these results and investigate the anti-microbial effects on other bacterial strains.

## 4.5 Conclusion

The work presented here demonstrates the formulation of a gellan film rehydrated in acetic acid for the treatment of wound infections. The physical properties of the gellan film; high water holding capacity, transparency and anti-adhesiveness to the woundbed facilitate clinical needs such as close wound monitoring and painless dressing removal. Tensile strength assessment of the gellan films demonstrated higher resistance to rupture and increased Young's modulus when higher concentrations of acetic acid solutions were used. Similarly, swelling capacity (%) of the gellan films was dependent on acid concentration, but less swelling was observed when compared to medical gauze. Furthermore, acetic acid release was measured by an enzymatic assay showing low values for both gellan films and gauze, indicating a potentially high early release of acetic acid in the woundbed. However, further studies are needed to investigate the release kinetics in more detail to

confirm current results.

Overall, gellan films are a promising candidate for topical wound applications to deliver acetic acid, but future work is needed to finetune the delivery vehicle in order to confirm sustained release of acetic acid in the woundbed and validate preliminaray results regarding antimicrobial effect. *In vivo* studies comparing the gellan film to current standards will eventually need to confirm effectiveness and practicality in the clinical setting.

## CHAPTER 5

# CONCLUSIONS AND FUTURE WORK

## 5.1 Conclusions

### 5.1.1 Chapter 1: Introduction

This chapter provided the reader with an updated overview on cell spray techniques for skin wounds and natural polymer based materials to enhance skin wound healing. Skin wounds and in particularly burn wounds can leave disabling and disfiguring scars on the outside and inside. Skin grafting has been the gold standard treatment to cover large body surface area wounds, however, with more people surviving devastating injuries, quality and appearance of the healed tissue becomes more important. There is currently no adequate engineered scaffold that results in complete regeneration of the full function of the skin that can replace autologous skin grafts entirely. Efforts have been made to minimize the grafted area by developing a method of isolating skin cells that can subsequently be cultured in the lab into a cell sheet (CEA) or delivered to the wound via spraying in a single cell solution. Cell spraying presents great potential for topically applying cells in suspension, but poor retention of the material on the wound results in cell spillage.

The aim of this thesis was to develop a carrier capable of spraying cells to the surface of a wound while maintaining cell viability and improving cell retention. This was achieved by identifying a suitable polymer and formulating a shear thinning gel that is spray-able and self-structuring.

### **5.1.2 Chapter 2: Gellan-based fluid gel carrier**

The formulation and characterisation of a gellan-based fluid gel carrier were presented in this chapter. All the systems were found to have a degree of shear thinning that allowed spray application and recovered much of their original viscosity once shear had been removed with reduced run-off. The viscoelastic properties of the systems were dependent on both polymer and cross-linker concentrations and the properties of the gel could be modulated based on these variables. Furthermore, cell compatibility was not compromised by encapsulation or spraying as shown by good viability, however, proliferation capacity of encapsulated fibroblasts might be limited.

### **5.1.3 Chapter 3: Keratinocyte spray delivery**

Following the encouraging results from encapsulating fibroblasts, this chapter investigated the effect of encapsulation and spraying of human epidermal keratinocytes on viability and function. Results indicate that a combination of spraying and gellan fluid gel encapsulation has a negative effect on keratinocyte viability and function. The current gel carrier was less effective for spray delivery of encapsulated keratinocytes, suggesting a cell-type dependent response to this delivery technique. However, keratinocytes can recover from spraying itself, forming a confluent monolayer with normal morphology. Similar, once retrieved from the gel, cells could form a viable confluent monolayer after one week of culturing. The carrier system could potentially be used as rapid delivery system in its current form, but optimizing the gel to improve outcomes is thought to be feasible.

### **5.1.4 Chapter 4: Formulation of acetic acid - gellan hydrogel dressing**

The final chapter focusses on a different topical application method using the same polymer. Chapter 4 describes the work involved formulating a gellan film that can be rehydrated in acetic acid for the treatment of wound infections. This work is in continuation

of earlier work by our department, when a gellan film was developed for the delivery of decorin to reduce scarring in burn wounds. Gellan films were superior to the conventional delivery vehicle (gauze) in terms of having a high water holding capacity, being transparent and anti-adhesive to the woundbed, but not for swelling capacity, release kinetics and anti-microbial outcomes. Furthermore, a general correlation is evident between concentration acid in the solvent fluid and the swelling index; gellan films rehydrated in high pH achieved higher water absorption capacity than low pH solvents. A similar relation was found for mechanical strength, this can be explained by the increased crosslinking of gellan under acidic conditions.

In conclusion, the gellan films have favourable properties for topical wound application, but further work is needed to confirm preliminary results found in this study and the dressing could potentially be further developed to enhance sustained release of acetic acid without compromising practicality in a clinical setting.

## **5.2 Limitations and future investigations**

The findings of Chapter 2 support that gellan fluid gel is a promising cell carrier for fibroblast spray delivery. It would be interesting to investigate whether this material is beneficial for the use of other delivery techniques such as spreading, injection, bio-printing or in the form of a wound dressing. Based on the desired application features, this could be achieved by altering the formulation of the gel as discussed in Chapter 2, for example by changing polymer and cross-linker concentrations and the shear rate during production. Further work could also focus on investigating fluid gel properties of other (natural) polymers and polymer blends, some promising candidates that have showed improved wound healing when used in topical applications are discussed in Chapter 1. Although the main focus of this study was the formulation of a hydrogel carrier, the biological response of fibroblasts to the system could have been further explored. Further studies could investigate fibroblast function in terms of migration capacity, growth factor release,

interaction with other cell types and this technique should eventually be tested in an *in vivo* wound healing model.

The results of Chapter 3 pave the way for future research directions exploring cell-matrix interactions for example by studying focal adhesion expression in sprayed and encapsulated keratinocytes. The ability of cells to create focal adhesions has possibly been compromised by the spraying, in combination with the lack of ECM components in the matrix; anoikis could have occurred as the cells have lost integrin-dependent anchorage. Viability and adhesion of cells could potentially be improved by optimizing the gel system by incorporating ECM-like components and addition of culture media into the system. Spraying onto culture plastic is not a good representation of the physiological wound environment, a next step would involve creating a substrate more similar to skin in terms of stiffness and providing cell-anchoring sites on protein-coated surfaces or more complex 3D cell- or tissue derived matrices.

Furthermore, it would be interesting to investigate the response of keratinocyte spray delivery in an *in vivo* wound model, the natural occurring growth factors, ECM components, other cell types and cytokines might stimulate keratinocyte to migrate out of the gel and contribute to wound healing.

Chapter 4 describes the formulation of a gellan hydrogel dressing for the release of acetic acid in the wound. Initial results encourage the use of gellan as a topical wound dressing, but future work is needed to validate the current outcomes in terms of antimicrobial effect against a variety of common microbes. Besides disk diffusion assays, other approaches such as determination of the minimum inhibitory concentration (MIC) and the ability to prevent biofilm formations is required for more robust evidence to justify *In vivo* studies. Eventually, *In vivo* clinical trials comparing the gellan film to current standards will need to confirm effectiveness and practicality in the clinical setting.

The effect of acetic acid concentration on the materials' properties could be investigated in further detail, for example by examining the average pore size and pore size distribution,

as this might give further clues to permeability and release kinetics of the drugs loaded into the hydrogel matrix. Regarding the release kinetics of acetic acid, it would be worthwhile to optimize the use of the commercial detection kit (K-ACETAK, Megazyme) to provide more reliable outcomes. Furthermore, the release of acetic acid in a wound bed is expected to be very different than in a buffer solution due to presence of electrolytes, protein-rich wound exudate and additional dressing material etc, yet, the use of more standardized drug release assays such as a dialysis method[394], could provide more insight in release dynamics of the dressing. An alternative approach to adjust release kinetics is to develop a more complex dressing design with multiple layers that release for example with multiple layers of different degradation/release rates or by creating drug-loaded reservoirs within the dressing.

## LIST OF REFERENCES

- [1] P C Jackson, J Hardwicke, A Bamford, P Nightingale, Y Wilson, R Papini, and N Moiemmen. Revised estimates of mortality from the Birmingham Burn Centre, 2001-2010: a continuing analysis over 65 years. *Ann Surg*, 259(5):979–984, 2014.
- [2] CDC National Center for Injury Prevention and Control. Unintentional Fire/Burn Nonfatal Injuries and Rates per 100,000. Technical report, 2017.
- [3] T Osler, L G Glance, and D W Hosmer. Simplified estimates of the probability of death after burn injuries: extending and updating the baux score. *J Trauma*, 68(3):690–697, 2010.
- [4] J Tobiasen, J M Hiebert, and R F Edlich. The abbreviated burn severity index. *Ann Emerg Med*, 11(5):260–262, 1982.
- [5] M J Muller and D N Herndon. The challenge of burns. *Lancet*, 343(8891):216–220, 1994.
- [6] G McGwin Jr., J M Cross, J W Ford, and L W Rue 3rd. Long-term trends in mortality according to age among adult burn patients. *J Burn Care Rehabil*, 24(1):21–25, 2003.
- [7] N A Forster, M Zingg, S R Haile, W Kunzi, P Giovanoli, and M Guggenheim. 30 years later—does the ABSI need revision? *Burns*, 37(6):958–963, 2011.
- [8] I Pastar, O Stojadinovic, N C Yin, H Ramirez, A G Nusbaum, A Sawaya, S B Patel, L Khalid, R R Isseroff, and M Tomic-Canic. Epithelialization in Wound Healing: A Comprehensive Review. *Adv Wound Care (New Rochelle)*, 3(7):445–464, 2014.
- [9] D N Herndon. *Total burn Care*. Saunders Elsevier, Edinburgh, 2017.
- [10] G D Weinstein, J L McCullough, and P Ross. Cell proliferation in normal epidermis. *J Invest Dermatol*, 82(6):623–628, 1984.
- [11] L H Gu and P A Coulombe. Keratin function in skin epithelia: a broadening palette with surprising shades. *Curr Opin Cell Biol*, 19(1):13–23, 2007.

- [12] M B Omary, P A Coulombe, and W H McLean. Intermediate filament proteins and their associated diseases. *N Engl J Med*, 351(20):2087–2100, 2004.
- [13] A C Steven, M E Bisher, D R Roop, and P M Steinert. Biosynthetic pathways of filaggrin and loricrin—two major proteins expressed by terminally differentiated epidermal keratinocytes. *J Struct Biol*, 104(1-3):150–162, 1990.
- [14] D D Bikle, Z Xie, and C L Tu. Calcium regulation of keratinocyte differentiation. *Expert Rev Endocrinol Metab*, 7(4):461–472, 2012.
- [15] G Denecker, P Ovaere, P Vandenabeele, and W Declercq. Caspase-14 reveals its secrets. *J Cell Biol*, 180(3):451–458, 2008.
- [16] S T Boyce and R G Ham. Calcium-regulated differentiation of normal human epidermal keratinocytes in chemically defined clonal culture and serum-free serial culture. *J Invest Dermatol*, 81(1 Suppl):33s–40s, 1983.
- [17] C L Tu and D D Bikle. Role of the calcium-sensing receptor in calcium regulation of epidermal differentiation and function. In *Best Practice and Research: Clinical Endocrinology and Metabolism*, volume 27, pages 415–427, 2013.
- [18] M J Su, D D Bikle, M L Mancianti, and S Pillai. 1,25-Dihydroxyvitamin D3 potentiates the keratinocyte response to calcium. *J Biol Chem*, 269(20):14723–14729, 1994.
- [19] Y Oda, C L Tu, A Menendez, T Nguyen, and D D Bikle. Vitamin D and calcium regulation of epidermal wound healing, 2016.
- [20] M Cichorek, M Wachulska, A Stasiewicz, and A Tyminska. Skin melanocytes: biology and development. *Postepy Dermatol Alergol*, 30(1):30–41, 2013.
- [21] S Werner, T Krieg, and H Smola. Keratinocyte-fibroblast interactions in wound healing. *J Invest Dermatol*, 127(5):998–1008, 2007.
- [22] A Szabowski, N Maas-Szabowski, S Andrecht, A Kolbus, M Schorpp-Kistner, N E Fusenig, and P Angel. c-Jun and JunB antagonistically control cytokine-regulated mesenchymal-epidermal interaction in skin. *Cell*, 103(5):745–755, 2000.
- [23] T Rozario and D W DeSimone. The extracellular matrix in development and morphogenesis: A dynamic view, 2010.
- [24] C Has and J S Kern. Collagen XVII. *Dermatol Clin*, 28(1):61–66, 2010.

- [25] V Levy, C Lindon, Y Zheng, B D Harfe, and B A Morgan. Epidermal stem cells arise from the hair follicle after wounding. *The FASEB Journal*, 21(7):1358–1366, may 2007.
- [26] World Health Organization (WHO). Burns fact sheet.
- [27] M P Rowan, L C Cancio, E A Elster, D M Burmeister, L F Rose, S Natesan, R K Chan, R J Christy, and K K Chung. Burn wound healing and treatment: review and advancements. *Crit Care*, 19:243, 2015.
- [28] G C Gurtner, S Werner, Y Barrandon, and M T Longaker. Wound repair and regeneration. *Nature*, 453(7193):314–321, 2008.
- [29] R Grose and S Werner. Wound-healing studies in transgenic and knockout mice. *Mol Biotechnol*, 28(2):147–166, 2004.
- [30] S H Litjens, J M de Pereda, and A Sonnenberg. Current insights into the formation and breakdown of hemidesmosomes. *Trends Cell Biol*, 16(7):376–383, 2006.
- [31] P Chen and W C Parks. Role of matrix metalloproteinases in epithelial migration. *J Cell Biochem*, 108(6):1233–1243, 2009.
- [32] C K Jiang, M Tomic-Canic, D J Lucas, M Simon, and M Blumenberg. TGF beta promotes the basal phenotype of epidermal keratinocytes: transcriptional induction of K#5 and K#14 keratin genes. *Growth Factors*, 12(2):87–97, 1995.
- [33] B E Zawacki, K W Spitzer, A D Mason Jr., and L A Johns. Does increased evaporative water loss cause hypermetabolism in burned patients? *Ann Surg*, 171(2):236–240, 1970.
- [34] T N Pham, L C Cancio, and N S Gibran. American Burn Association practice guidelines burn shock resuscitation. *J Burn Care Res*, 29(1):257–266, 2008.
- [35] E V Robins. Burn shock. *Crit Care Nurs Clin North Am*, 2(2):299–307, 1990.
- [36] L Lootens, N Brusselaers, H Beele, and S Monstrey. Keratinocytes in the treatment of severe burn injury: an update. *Int Wound J*, 10(1):6–12, 2013.
- [37] A D Metcalfe and M W Ferguson. Tissue engineering of replacement skin: the crossroads of biomaterials, wound healing, embryonic development, stem cells and regeneration. *J R Soc Interface*, 4(14):413–437, 2007.
- [38] J A Nowak, L Polak, H A Pasolli, and E Fuchs. Hair follicle stem cells are specified and function in early skin morphogenesis. *Cell Stem Cell*, 3(1):33–43, 2008.

- [39] A B M Hilmi and A S Halim. Vital roles of stem cells and biomaterials in skin tissue engineering. *World Journal of Stem Cells*, 7(2):428, 2015.
- [40] J G Rheinwald and H Green. Serial Cultivation of strains of human epidermal keratinocytes- formation of keratinizing colonies from single cells. *Cell*, 6:331–344, 1975.
- [41] C O Duncan, R M Shelton, H Navsaria, D S Balderson, R P Papini, and J E Barralet. In vitro transfer of keratinocytes: comparison of transfer from fibrin membrane and delivery by aerosol spray. *Journal of Biomedical Materials Research. Part B, Applied Biomaterials*, 73(2):221–228, 2005.
- [42] C Rasmussen, C Thomas-Virnig, and B L Allen-Hoffmann. Classical human epidermal keratinocyte cell culture. *Methods in Molecular Biology*, 945:161–175, 2013.
- [43] H Green, O Kehinde, and J Thomas. Growth of cultured human epidermal cells into multiple epithelia suitable for grafting. *Proceedings of the National Academy of Sciences*, 76(11):5665–5668, nov 1979.
- [44] N E O'Connor, J B Mulliken, S Banks-Schlegel, O Kehinde, and H Green. GRAFTING OF BURNS WITH CULTURED EPITHELIUM PREPARED FROM AUTOLOGOUS EPIDERMAL CELLS. *The Lancet*, 317(8211):75–78, 1981.
- [45] Y Poumay and M R Pittelkow. Cell density and culture factors regulate keratinocyte commitment to differentiation and expression of suprabasal K1/K10 keratins. *Journal of Investigative Dermatology*, 104(2):271–276, 1995.
- [46] Y Barrandon, N Grasset, A Zaffalon, F Gorostidi, S Claudinot, S L Droz-Georget, D Nanba, and A Rochat. Capturing epidermal stemness for regenerative medicine. *Semin Cell Dev Biol*, 23(8):937–944, 2012.
- [47] D L Chester, D S Balderson, and R P Papini. A review of keratinocyte delivery to the wound bed. *J Burn Care Rehabil*, 25(3):266–275, 2004.
- [48] C E Butler, I V Yannas, C C Compton, C A Correia, and D P Orgill. Comparison of cultured and uncultured keratinocytes seeded into a collagen-GAG matrix for skin replacements. *Br J Plast Surg*, 52(2):127–132, 1999.
- [49] A Heiskanen, T Satomaa, S Tiitinen, A Laitinen, S Mannelin, U Impola, M Mikkola, C Olsson, H Miller-Podraza, M Blomqvist, A Olonen, H Salo, P Lehenkari, T Tuuri, T Otonkoski, J Natunen, J Saarinen, and J Laine. N-Glycolylneuraminic Acid Xenoantigen Contamination of Human Embryonic and Mesenchymal Stem Cells Is Substantially Reversible. *Stem Cells*, 25(1):197–202, 2007.

- [50] K Jubin, Y Martin, D J Lawrence-Watt, and J R Sharpe. A fully autologous co-culture system utilising non-irradiated autologous fibroblasts to support the expansion of human keratinocytes for clinical use. *Cytotechnology*, 63(6):655–662, 2011.
- [51] T Sun, M Higham, C Layton, J Haycock, R Short, and S MacNeil. Developments in xenobiotic-free culture of human keratinocytes for clinical use. *Wound Repair Regen*, 12(6):626–634, 2004.
- [52] N A Coolen, M Verkerk, L Reijnen, M Vlig, A J van den Bogaerdt, M Breetveld, S Gibbs, E Middelkoop, and M M Ulrich. Culture of keratinocytes for transplantation without the need of feeder layer cells. *Cell Transplant*, 16(6):649–661, 2007.
- [53] R Lamb and C A Ambler. Keratinocytes propagated in serum-free, feeder-free culture conditions fail to form stratified epidermis in a reconstituted skin model. *PLoS ONE*, 8(1):e52494, 2013.
- [54] C Lenihan, C Rogers, A D Metcalfe, and Y H Martin. The effect of isolation and culture methods on epithelial stem cell populations and their progeny-toward an improved cell expansion protocol for clinical application. *Cytotherapy*, 16(12):1750–1759, 2014.
- [55] K L Gardien, E Middelkoop, and M M Ulrich. Progress towards cell-based burn wound treatments. *Regen Med*, 9(2):201–218, 2014.
- [56] L Guerra, S Capurro, F Melchi, G Primavera, S Bondanza, R Cancedda, A Luci, M De Luca, and G Pellegrini. Treatment of "stable" vitiligo by Timedsurgery and transplantation of cultured epidermal autografts. *Arch Dermatol*, 136(11):1380–1389, 2000.
- [57] S Bottcher-Haberzeth, A S Klar, T Biedermann, C Schiestl, C Meuli-Simmen, E Reichmann, and M Meuli. "Trooping the color": restoring the original donor skin color by addition of melanocytes to bioengineered skin analogs. *Pediatr Surg Int*, 29(3):239–247, 2013.
- [58] A Hachiya, P Sriwiriyanont, E Kaiho, T Kitahara, Y Takema, and R Tsuboi. An in vivo mouse model of human skin substitute containing spontaneously sorted melanocytes demonstrates physiological changes after UVB irradiation. *J Invest Dermatol*, 125(2):364–372, 2005.
- [59] T Biedermann, A S Klar, S Bottcher-Haberzeth, T Michalczyk, C Schiestl, E Reichmann, and M Meuli. Long-term expression pattern of melanocyte markers in light-

and dark-pigmented dermo-epidermal cultured human skin substitutes. *Pediatr Surg Int*, 31(1):69–76, 2015.

- [60] A Iman, M A Akbar, K M Mohsen, F Ali, A Armin, A Sajjad, M Ahmad, M Ghavipisheh, and R Leila. Comparison of intradermal injection of autologous epidermal cell suspension vs. spraying of these cells on dermabraded surface of skin of patients with post-burn hypopigmentation. *Indian journal of dermatology*, 58(3):240, may 2013.
- [61] S. V. Mulekar, B. Ghwish, A. Al Issa, and A. Al Eisa. Treatment of vitiligo lesions by ReCell vs. conventional melanocyte-keratinocyte transplantation: A pilot study. *British Journal of Dermatology*, 158(1):45–49, 2008.
- [62] R H Huggins, M D Henderson, S V Mulekar, D M Ozog, H A Kerr, G Jabobsen, H W Lim, and I H Hamzavi. Melanocyte-keratinocyte transplantation procedure in the treatment of vitiligo: the experience of an academic medical center in the United States. *J Am Acad Dermatol*, 66(5):785–793, 2012.
- [63] P Toossi, M Shahidi-Dadras, M Mahmoudi Rad, and R J Fesharaki. Non-cultured melanocyte-keratinocyte transplantation for the treatment of vitiligo: a clinical trial in an Iranian population. *J Eur Acad Dermatol Venereol*, 25(10):1182–1186, 2011.
- [64] P A Golinski, N Zoller, S Kippenberger, H Menke, J Bereiter-Hahn, and A Bernd. [Development of an engraftable skin equivalent based on matriderm with human keratinocytes and fibroblasts]. *Handchir Mikrochir Plast Chir*, 41(6):327–332, 2009.
- [65] T D Sargeant, A P Desai, S Banerjee, A Agawu, and J B Stopek. An in situ forming collagen-PEG hydrogel for tissue regeneration. *Acta Biomater*, 8(1):124–132, 2012.
- [66] X Zhang, J Li, P Ye, G Gao, K Hubbell, and X Cui. Coculture of mesenchymal stem cells and endothelial cells enhances host tissue integration and epidermis maturation through AKT activation in gelatin methacryloyl hydrogel-based skin model. *Acta Biomaterialia*, 59:317–326, 2017.
- [67] S P Huang, C C Hsu, S C Chang, C H Wang, S C Deng, N T Dai, T M Chen, J Y Chan, S G Chen, and S M Huang. Adipose-derived stem cells seeded on acellular dermal matrix grafts enhance wound healing in a murine model of a full-thickness defect. *Ann Plast Surg*, 69(6):656–662, 2012.
- [68] M P Ribeiro, P I Morgado, S P Miguel, P Coutinho, and I J Correia. Dextran-based hydrogel containing chitosan microparticles loaded with growth factors to be used in wound healing. *Mater Sci Eng C Mater Biol Appl*, 33(5):2958–2966, 2013.

- [69] S J Gwak, S S Kim, K Sung, J Han, C Y Choi, and B S Kim. Synergistic effect of keratinocyte transplantation and epidermal growth factor delivery on epidermal regeneration. *Cell Transplantation*, 14(10):809–817, 2005.
- [70] D M Supp, A P Supp, S M Bell, and S T Boyce. Enhanced vascularization of cultured skin substitutes genetically modified to overexpress vascular endothelial growth factor. *J Invest Dermatol*, 114(1):5–13, 2000.
- [71] D M Supp and S T Boyce. Overexpression of vascular endothelial growth factor accelerates early vascularization and improves healing of genetically modified cultured skin substitutes. *J Burn Care Rehabil*, 23(1):10–20, 2002.
- [72] D M Supp, A C Karpinski, and S T Boyce. Vascular endothelial growth factor overexpression increases vascularization by murine but not human endothelial cells in cultured skin substitutes grafted to athymic mice. *J Burn Care Rehabil*, 25(4):337–345, 2004.
- [73] P Aramwit, S Palapinyo, T Srichana, S Chottanapund, and P Muangman. Silk sericin ameliorates wound healing and its clinical efficacy in burn wounds. *Archives of Dermatological Research*, 305(7):585–594, 2013.
- [74] M Vernez, W Raffoul, M C Gailloud-Matthieu, D Egloff, I Senechaud, R G Panizzon, and M Benathan. Quantitative assessment of cell viability and apoptosis in cultured epidermal autografts: application to burn therapy. *Int J Artif Organs*, 26(9):793–803, 2003.
- [75] F. A. Navarro, M. L. Stoner, C. S. Park, J. C. Huertas, H. B. Lee, F. M. Wood, and D. P. Orgill. Sprayed keratinocyte suspensions accelerate epidermal coverage in a porcine microwound model. *Journal of Burn Care and Rehabilitation*, 21(6):513–518, 2000.
- [76] G Dupuytren. Clinical lectures on surgery : delivered at Hotel Dieu, in 1832 : Dupuytren, Guillaume, 1777-1835. Free Download, Borrow, and Streaming : Internet Archive, 1833.
- [77] N S Moiemien, K C Lee, and K Joory. History of burns: The past, present and the future. *Burns & Trauma*, 2(4):169, 2014.
- [78] H S Kim, X Sun, J Lee, H Kim, X Fu, and K W Leong. Advanced drug delivery systems and artificial skin grafts for skin wound healing. *Advanced Drug Delivery Reviews*, 2018.

- [79] D Kadam. Novel expansion techniques for skin grafts. *Indian Journal of Plastic Surgery*, 49(1):5, 2016.
- [80] M Singh, K Nuutlia, A S Chauhan, and E Eriksson. Invasive Squamous Cell Carcinoma in Full-thickness Burn Wounds After Treatment with Cultured Epithelial Autografts. *Plast Reconstr Surg Glob Open*, 3(7):e460, 2015.
- [81] R Esteban-Vives, M T Young, T Zhu, J Beiriger, C Pekor, J Ziembicki, A Corcos, P Rubin, and J C Gerlach. Calculations for reproducible autologous skin cell-spray grafting. *Burns*, 42(8):1756–1765, 2016.
- [82] G. Gregory Gallico, Nicholas E. O'Connor, Carolyn C. Compton, Olaniyi Kehinde, and Howard Green. Permanent Coverage of Large Burn Wounds with Autologous Cultured Human Epithelium. *New England Journal of Medicine*, 311(7):448–451, aug 1984.
- [83] C Cuono, R Langdon, and J Mcguire. USE OF CULTURED EPIDERMAL AUTOGRAFTS AND DERMAL ALLOGRAFTS AS SKIN REPLACEMENT AFTER BURN INJURY. *The Lancet*, 1:1123–1124, 1986.
- [84] C Pham, J Greenwood, H Cleland, P Woodruff, and G Maddern. Bioengineered skin substitutes for the management of burns: a systematic review. *Burns*, 33(8):946–957, 2007.
- [85] J P Barret, S E Wolf, M H Desai, and D N Herndon. Cost-efficacy of cultured epidermal autografts in massive pediatric burns. *Annals of Surgery*, 231(6):869–876, 2000.
- [86] F M Wood, M L Kolybaba, and P Allen. The use of cultured epithelial autograft in the treatment of major burn wounds: eleven years of clinical experience. *Burns*, 32(5):538–544, 2006.
- [87] B S Atiyeh and M Costagliola. Cultured epithelial autograft (CEA) in burn treatment: Three decades later, 2007.
- [88] A M Munster. Cultured skin for massive burns. A prospective, controlled trial. *Ann Surg*, 224(3):372–377, 1996.
- [89] C Auxenfans, V Menet, Z Catherine, H Shipkov, P Lacroix, M Bertin-Maghit, O Damour, and F Braye. Cultured autologous keratinocytes in the treatment of large and deep burns: A retrospective study over 15 years. *Burns*, 41(1):71–79, 2015.

- [90] L Shi, Z J Lei, C Y Zhao, X X Lv, L Jiang, J Li, and X Y Li. A modified culture strategy of human keratinocytes to shorten the primary culture time. *Cell Biol Int*, 39(9):1073–1079, 2015.
- [91] R Sood, D Roggy, M Zieger, J Balledux, S Chaudhari, D J Koumanis, H S Mir, A Cohen, C Knipe, K Gabehart, and J J Coleman. Cultured epithelial autografts for coverage of large burn wounds in eighty-eight patients: The Indiana university experience. *Journal of Burn Care and Research*, 31(4):559–568, jul 2010.
- [92] M H Desai, J M Mlakar, R L McCauley, K M Abdullah, R L Rutan, P J Waymack, M C Robson, and D N Herndon. Lack of long-term durability of cultured keratinocyte burn-wound coverage: A case report. *Journal of Burn Care and Rehabilitation*, 12(6):540–545, 1991.
- [93] P A Clugston, C F Snelling, I B Macdonald, H L Maledy, J C Boyle, E Germann, A D Courtemanche, P Wirtz, D J Fitzpatrick, and D A Kester. Cultured epithelial autografts: three years of clinical experience with eighteen patients. *The Journal of burn care & rehabilitation*, 12(6):533–9, 1991.
- [94] H Matsumura, A Matsushima, M Ueyama, and N Kumagai. Application of the cultured epidermal autograft ”JACE for treatment of severe burns: Results of a 6-year multicenter surveillance in Japan. *Burns*, 2016.
- [95] K I Hata. Current issues regarding skin substitutes using living cells as industrial materials. *Journal of Artificial Organs*, 10(3):129–132, 2007.
- [96] C Theopold, D Hoeller, P Velander, R Demling, and E Eriksson. Graft site malignancy following treatment of full-thickness burn with cultured epidermal autograft. *Plast Reconstr Surg*, 114(5):1215–1219, 2004.
- [97] M Singh, K Nuutlia, A S Chauhan, and E Eriksson. Invasive Squamous Cell Carcinoma in Full-thickness Burn Wounds After Treatment with Cultured Epithelial Autografts. *Plast Reconstr Surg Glob Open*, 3(7):e460, 2015.
- [98] T J Phillips, S M Salman, J Bhawan, and G S Rogers. Burn scar carcinoma. Diagnosis and management. *Dermatol Surg*, 24(5):561–565, 1998.
- [99] J F Hansbrough, S T Boyce, M L Cooper, and T J Foreman. Burn wound closure with cultured autologous keratinocytes and fibroblasts attached to a collagen-glycosaminoglycan substrate. *Jama*, 262(15):2125–2130, 1989.

- [100] N Ojeh, I Pastar, M Tomic-Canic, and O Stojadinovic. Stem Cells in Skin Regeneration, Wound Healing, and Their Clinical Applications. *Int J Mol Sci*, 16(10):25476–25501, 2015.
- [101] J N McHeik, C Barrault, G Levard, F Morel, F X Bernard, and J C Lecron. Epidermal healing in burns: autologous keratinocyte transplantation as a standard procedure: update and perspective. *Plast Reconstr Surg Glob Open*, 2, 2014.
- [102] H Yim, H T Yang, Y S Cho, C H Seo, B C Lee, J H Ko, I S Kwak, D Kim, J Hur, J H Kim, and W Chun. Clinical study of cultured epithelial autografts in liquid suspension in severe burn patients. *Burns*, 37(6):1067–1071, 2011.
- [103] H Lee. Outcomes of sprayed cultured epithelial autografts for full-thickness wounds: A single-centre experience. *Burns*, 38(6):931–936, 2012.
- [104] B Hartmann, A Ekkernkamp, C Johnen, J C Gerlach, C Belfekroun, and M V Küntscher. Sprayed cultured epithelial autografts for deep dermal burns of the face and neck. *Annals of Plastic Surgery*, 58(1):70–73, 2007.
- [105] J C Gerlach, C Johnen, C Ottoman, K Bräutigam, J Plettig, C Belfekroun, S Münch, and B Hartmann. Method for autologous single skin cell isolation for regenerative cell spray transplantation with non-cultured cells. *International Journal of Artificial Organs*, 34(3):271–279, 2011.
- [106] F M Wood, N Giles, A Stevenson, S Rea, and M Fear. Characterisation of the cell suspension harvested from the dermal epidermal junction using a ReCell® kit. *Burns*, 38(1):44–51, 2012.
- [107] G Gravante, M. C. Di Fede, A Araco, M Grimaldi, B De Angelis, A Arpino, V Cervelli, and A Montone. A randomized trial comparing ReCell® system of epidermal cells delivery versus classic skin grafts for the treatment of deep partial thickness burns. *Burns*, 33(8):966–972, 2007.
- [108] V Cervelli, D Spallone, L Lucarini, Ludovico Palla, L Brinci, and B De Angelis. Treatment of stable vitiligo hands by ReCell® system: A preliminary report. *European Review for Medical and Pharmacological Sciences*, 14(8):691–694, aug 2010.
- [109] M Hivelin, Colin MacIver, J L Heusse, M Atlan, and L Lantieri. Improving the colour match of free tissue transfers to the face with non-cultured autologous cellular spray - A case report on a chin reconstruction. *Journal of Plastic, Reconstructive and Aesthetic Surgery*, 65(8):1103–1106, 2012.

- [110] J H Park, K M Heggie, D W Edgar, M K Bulsara, and F M Wood. Does the type of skin replacement surgery influence the rate of infection in acute burn injured patients? *Burns*, 39(7):1386–1390, 2013.
- [111] R Sood, D E Roggy, M J Zieger, M Nazim, B C Hartman, and J T Gibbs. A comparative study of spray keratinocytes and autologous meshed split-thickness skin graft in the treatment of acute burn injuries. *Wounds : a compendium of clinical research and practice*, 27(2):31–40, feb 2015.
- [112] J C. Gerlach, C Johnen, E McCoy, K Bräutigam, J Plettig, and A Corcos. Autologous skin cell spray-transplantation for a deep dermal burn patient in an ambulant treatment room setting. *Burns*, 37(4):e19–e23, 2011.
- [113] NHS England. The ReCell Spray-On Skin system for treating skin loss, scarring and depigmentation after burn injury — Guidance and guidelines — NICE, 2014.
- [114] K C Lee, J Dretzke, L Grover, A Logan, and N Moiemmen. A systematic review of objective burn scar measurements. *Burns & Trauma*, 4(1):14, 2016.
- [115] R Goedkoop, R Juliet, P H K You, J Daroczy, K P De Roos, R Lijnen, E Roland, and T Hunziker. Wound stimulation by growth-arrested human keratinocytes and fibroblasts: HP802-247, a new-generation allogeneic tissue engineering product. *Dermatology*, 220(2):114–120, 2010.
- [116] R S Kirsner, W A Marston, R J Snyder, T D Lee, D I Cargill, and H B Slade. Spray-applied cell therapy with human allogeneic fibroblasts and keratinocytes for the treatment of chronic venous leg ulcers: A phase 2, multicentre, double-blind, randomised, placebo-controlled trial. *The Lancet*, 380(9846):977–985, 2012.
- [117] R S Kirsner, W A Marston, R J Snyder, T D Lee, D I Cargill, Y Zhang, J E Dickerson, and H B Slade. Durability of healing from spray-applied cell therapy with human allogeneic fibroblasts and keratinocytes for the treatment of chronic venous leg ulcers: A 6-month follow-up. *Wound Repair and Regeneration*, 21(5):682–687, 2013.
- [118] J C Lantis, W A Marston, A Farber, R S Kirsner, Y Zhang, T D Lee, D I Cargill, and H B Slade. The influence of patient and wound variables on healing of venous leg ulcers in a randomized controlled trial of growth-arrested allogeneic keratinocytes and fibroblasts. *Journal of Vascular Surgery*, 58(2):433–439, 2013.

- [119] H. Slade W. Marston, R. Kirsner, R. Snyder, T. Lee, I. Cargill. Variables Affecting Healing of Venous Leg Ulcers In a Randomized, Vehicle-Controlled Trial of Topical Cellular Therapy. Technical report, 2011.
- [120] R S Kirsner, W Vanscheidt, D H Keast, J C Lantis, C R Dove, S M Cazzell, Mher Vartivarian, Matthias Augustin, William A. Marston, Nicholas D. McCoy, D. Innes Cargill, Tommy D. Lee, Jaime E. Dickerson, and Herbert B. Slade. Phase 3 evaluation of HP802-247 in the treatment of chronic venous leg ulcers. *Wound Repair and Regeneration*, 24(5):894–903, 2016.
- [121] M S Hu, M R Borrelli, H P Lorenz, M T Longaker, and D C Wan. Mesenchymal Stromal Cells and Cutaneous Wound Healing: A Comprehensive Review of the Background, Role, and Therapeutic Potential. *Stem Cells International*, 2018:1–13, 2018.
- [122] M F Rasulov, A V Vasilchenkov, N A Onishchenko, M E Krashennnikov, V I Kravchenko, T L Gorshenin, R E Pidtsan, and I V Potapov. First experience of the use bone marrow mesenchymal stem cells for the treatment of a patient with deep skin burns. *Bulletin of experimental biology and medicine*, 139(1):141–144, jan 2005.
- [123] V Falanga, S Iwamoto, M Chartier, T Yufit, J Butmarc, N Koultab, G Colvin, and P Carson. Autologous bone marrow-derived cultured mesenchymal stem cells delivered in a fibrin spray accelerate healing in murine and human cutaneous wounds. *Journal of Investigative Dermatology*, 127:S49–S49, 2007.
- [124] E Mansilla, G H Marín, M Berges, S Scafatti, J Rivas, A Núñez, M Menvielle, R Lamonega, C Gardiner, H Drago, F Sturla, M Portas, S Bossi, M V Castuma, S Peña Luengas, G Roque, K Martire, J M Tau, G Orlandi, and A Tarditti. Cadaveric bone marrow mesenchymal stem cells: first experience treating a patient with large severe burns. *Burns & Trauma*, 3(1):17, 2015.
- [125] M Ueda. Sprayed cultured mucosal epithelial cell for deep dermal burns. *Journal of Craniofacial Surgery*, 21(6):1729–1732, 2010.
- [126] I Grant, K Warwick, J Marshall, C Green, and R Martin. The co-application of sprayed cultured autologous keratinocytes and autologous fibrin sealant in a porcine wound model. *British Journal of Plastic Surgery*, 55(3):219–227, 2002.
- [127] M Madaghiele, A Sannino, L Ambrosio, and C Demitri. Polymeric hydrogels for burn wound care: Advanced skin wound dressings and regenerative templates. *Burns & Trauma*, 2(4):153–161, 2015.

- [128] E M Ahmed. Hydrogel: Preparation, characterization, and applications: A review. *Journal of Advanced Research*, 6(2):105–121, 2015.
- [129] V K Thakur and M K Thakur. Recent trends in hydrogels based on psyllium polysaccharide: a review. *Journal of Cleaner Production*, 82:1–15, 2014.
- [130] T Osmalek, A Froelich, and S Tasarek. Application of gellan gum in pharmacy and medicine. *International Journal of Pharmaceutics*, 466(1-2):328–340, 2014.
- [131] A Aravamudhan, D M Ramos, A A. Nada, and S G Kumbar. Chapter 4 – Natural Polymers: Polysaccharides and Their Derivatives for Biomedical Applications. In *Natural and Synthetic Biomedical Polymers*, pages 67–89. Elsevier, 2014.
- [132] A D Augst, H J Kong, and D J Mooney. Alginate hydrogels as biomaterials. *Macromol Biosci*, 6(8):623–633, 2006.
- [133] K A Smeds and M W Grinstaff. Photocrosslinkable polysaccharides for in situ hydrogel formation. *Journal of Biomedical Materials Research*, 54(1):115–121, jan 2001.
- [134] O Jeon, C Powell, S M Ahmed, and E Alsberg. Biodegradable, photocrosslinked alginate hydrogels with independently tailorable physical properties and cell adhesivity. *Tissue Eng Part A*, 16(9):2915–2925, 2010.
- [135] T Andersen, P Auk-Emblem, M Dornish, M R Lornejad-Schä, and C Schä. 3D Cell Culture in Alginate Hydrogels. *Microarrays*, 4:133–161, 2015.
- [136] O Jeon, D S Alt, S M Ahmed, and E Alsberg. The effect of oxidation on the degradation of photocrosslinkable alginate hydrogels. *Biomaterials*, 33(13):3503–3514, 2012.
- [137] J M O’Donoghue, S T O’Sullivan, E S Beausang, J I Panchal, M O’Shaughnessy, and T P O’Connor. Calcium alginate dressings promote healing of split skin graft donor sites., 1997.
- [138] M Brenner, C Hilliard, G Peel, G Crispino, R Geraghty, and G O’Callaghan. Management of pediatric skin-graft donor sites: a randomized controlled trial of three wound care products. *J Burn Care Res*, 36(1):159–166, 2015.
- [139] S O’Meara, M Martyn-st James, and UJ Adderley. Alginate dressings for venous leg ulcers (Review). *Cochrane Database Syst Rev*, Jun 25(6):77, 2013.

- [140] J C Dumville, N Stubbs, S J Keogh, and R M Walker. Hydrogel dressings for treating pressure ulcers. *Cochrane Database of Systematic Reviews*, 2014(7), 2014.
- [141] J Wasiak, H Cleland, F Campbell, and A Spinks. Dressings for superficial and partial thickness burns. *Cochrane Database Syst Rev*, 3:Cd002106, 2013.
- [142] J F Mano, L Gasperini, and R L Reis. Natural polymers for the microencapsulation of cells. *J. R. Soc. Interface*, 2014.
- [143] A Khoshzaban, P Keyhanvar, E Delrish, F Najafi, S H Keshel, I Watanabe, A Valanezhad, and T J Kashi. Alginate Microcapsules as Nutrient Suppliers: An In Vitro Study. *Cell Journal*, 20(1):25–30, apr 2018.
- [144] K G Chen, B S Mallon, R D G Mckay, and P G Robey. Human Pluripotent Stem Cell Culture: Considerations for Maintenance, Expansion, and Therapeutics. *Cell Stem Cell*, 14(1):13–26, 2014.
- [145] N C Hunt, R M Shelton, and L Grover. An alginate hydrogel matrix for the localised delivery of a fibroblast/keratinocyte co-culture. *Biotechnol J*, 4(5):730–737, 2009.
- [146] F Lim and A M Sun. Microencapsulated islets as bioartificial endocrine pancreas. *Science*, 210(21):908–10, 1980.
- [147] W Czaja, D Romanovicz, and R M Brown. Structural investigations of microbial cellulose produced in stationary and agitated culture. *Cellulose*, 11:403–411, 2004.
- [148] G Guhados, W Wan, and J L Hutter. Measurement of the Elastic Modulus of Single Bacterial Cellulose Fibers Using Atomic Force Microscopy. *Langmuir*, 21:6642–6646, 2005.
- [149] A Basu, K Heitz, M Strømme, K Welch, and N Ferraz. Ion-crosslinked wood-derived nanocellulose hydrogels with tunable antibacterial properties: Candidate materials for advanced wound care applications. *Carbohydrate Polymers*, 181:345–350, 2017.
- [150] N Lavoine, I Desloges, A Dufresne, and J Bras. Microfibrillated cellulose - Its barrier properties and applications in cellulosic materials: A review, 2012.
- [151] A Sannino, C Demitri, and M Madaghiele. Biodegradable Cellulose-based Hydrogels: Design and Applications. *materials*, 2:353–373, 2009.
- [152] H Dong, J F Snyder, K S Williams, and J W Andzelm. Cation-Induced Hydrogels of Cellulose Nanofibrils with Tunable Moduli. *Biomacromolecules*, 14:3338–3345, 2013.

- [153] J C Courtenay, M A Johns, F Galembeck, C Deneke, E M Lanzoni, A C Costa, J L Scott, and R I Sharma. Surface modified cellulose scaffolds for tissue engineering. *Cellulose*, 24:253–267, 2017.
- [154] P Muangman, S Opananon, S Suwanchot, and O Thangthed. Efficiency of microbial cellulose dressing in partial-thickness burn wounds. *Journal of the American College of Certified Wound Specialists*, 3(1):16–19, 2011.
- [155] L Fu, J Zhang, and G Yang. Present status and applications of bacterial cellulose-based materials for skin tissue repair. *Carbohydrate Polymers*, 92(2):1432–1442, 2013.
- [156] E Yun, X Loh, N Mohamad, M B Fauzi, M H Ng, S F Ng, M Cairul, and I M Amin. Development of a bacterial cellulose-based hydrogel cell carrier containing keratinocytes and fibroblasts for full-thickness wound healing. *Scientific Reports*, 2018.
- [157] F Ahmadi, Z Oveisi, S M Samani, and Z Amoozgar. Chitosan based hydrogels: characteristics and pharmaceutical applications. *Res Pharm Sci*, 10(1):1–16, 2015.
- [158] W Yu, X Ma, J Bao, Xi Liu, Y Ren, and H Xie. Comparative investigation of the binding characteristics of poly-l-lysine and chitosan on alginate hydrogel. *International Journal of Biological Macromolecules*, 84:135–141, 2015.
- [159] W Gao, J C Lai, and S W Leung. Functional enhancement of chitosan and nanoparticles in cell culture, tissue engineering, and pharmaceutical applications. *Front Physiol*, 3:321, 2012.
- [160] K Y Lee, W S Ha, and W H Park. Blood compatibility and biodegradability of partially N-acetylated chitosan derivatives. *Biomaterials*, 16:1211–1216, 1995.
- [161] E. M. Varoni, S. Vijayakumar, E. Canciani, A. Cochis, L. De Nardo, G. Lodi, L. Rimondini, and M. Cerruti. Chitosan-Based Trilayer Scaffold for Multitissue Periodontal Regeneration. *Journal of Dental Research*, 97(3):303–311, 2018.
- [162] T Kean and M Thanou. Biodegradation, biodistribution and toxicity of chitosan. *Advanced Drug Delivery Reviews*, 62(1):3–11, 2010.
- [163] A Hasanovic, M Zehl, G Reznicek, and C Valenta. Chitosan-tripolyphosphate nanoparticles as a possible skin drug delivery system for aciclovir with enhanced stability. *Journal of Pharmacy & Pharmacology*, 61(12):1609–1616, 2009.

- [164] J Berger, M Reist, A Chenite, O Felt-Baeyens, J M Mayer, and R Gurny. Pseudo-thermosetting chitosan hydrogels for biomedical application. *Int J Pharm*, 288(1):17–25, 2005.
- [165] A Montembault, C Viton, and A Domard. Rheometric study of the gelation of chitosan in aqueous solution without cross-linking agent. *Biomacromolecules*, 6(2):653–662, 2005.
- [166] T A Rickett, Z Amoozgar, C A Tucheck, J Park, Y Yeo, and R Shi. Rapidly photo-cross-linkable chitosan hydrogel for peripheral neurosurgeries. *Biomacromolecules*, 12(1):57–65, 2011.
- [167] Y Hayashi, S Yamada, K Y Guchi, Z Koyama, and T Ikeda. Chitosan and Fish Collagen as Biomaterials for Regenerative Medicine. *Marine Medicinal Foods*, 65:107–120, 2012.
- [168] N Charernsriwilaiwat, P Opanasopit, T Rojanarata, and T Ngawhirunpat. Lysozyme-loaded, electrospun chitosan-based nanofiber mats for wound healing. *Int J Pharm*, 427(2):379–384, 2012.
- [169] Tianhong Dai, Masamitsu Tanaka, Ying Ying Huang, and Michael R Hamblin. Chitosan preparations for wounds and burns: Antimicrobial and wound-healing effects, 2011.
- [170] H Liu, Y Du, X Wang, and L Sun. Chitosan kills bacteria through cell membrane damage. *International Journal of Food Microbiology*, 2004.
- [171] M H Periyah, A S Halim, A R Hussein, A Z Mat Saad, A H Abdul Rashid, and K Noorsal. In vitro capacity of different grades of chitosan derivatives to induce platelet adhesion and aggregation. *International Journal of Biological Macromolecules*, 52(1):244–249, 2013.
- [172] B L Bennett. Bleeding Control Using Hemostatic Dressings: Lessons Learned. *WILDERNESS & ENVIRONMENTAL MEDICINE*, 28:39–49, 2017.
- [173] M Rodriguez-Vazquez, B Vega-Ruiz, R Ramos-Zuniga, D A Saldana-Koppel, and L F Quinones-Olvera. Chitosan and Its Potential Use as a Scaffold for Tissue Engineering in Regenerative Medicine. *Biomed Res Int*, 2015:821279, 2015.
- [174] A B M Hilmi, A S Halim, A Hassan, C K Lim, K Noorsal, and I Zainol. In vitro characterization of a chitosan skin regenerating template as a scaffold for cells cultivation. *SpringerPlus*, 2(1):1–9, 2013.

- [175] C Chatelet, O Damour, and A Domard. Influence of the degree of acetylation on some biological properties of chitosan films. *Biomaterials*, 22(3):261–268, 2001.
- [176] K S Kang, G T Veeder, P J Mirrasoul, T Kaneko, and I W Cottrell. Agar-like polysaccharide produced by a pseudomonas species: production and basic properties. *Appl Environ Microbiol*, 43(5):1086–1091, 1982.
- [177] B N Singh, L D Trombetta, and K H Kim. Pharmaceutical Development and Technology Biodegradation Behavior of Gellan Gum in Simulated Colonic Media Biodegradation Behavior of Gellan Gum in Simulated Colonic Media. *Pharmaceutical Development and Technology*, 94(4):399–407, 2005.
- [178] S. Suri and R. Banerjee. In vitro evaluation of in situ gels as short term vitreous substitutes. *Journal of Biomedical Materials Research - Part A*, 79(3):650–664, dec 2006.
- [179] H Lee, S Fisher, M S Kallos, and C J Hunter. Optimizing gelling parameters of gellan gum for fibrocartilage tissue engineering. *Journal of Biomedical Materials Research - Part B Applied Biomaterials*, 98 B(2):238–245, 2011.
- [180] C J Ferris, K J Gilmore, S Beirne, D McCallum, G G Wallace, and M in het Panhuis. Bio-ink for on-demand printing of living cells. *Biomater. Sci.*, 1(2):224–230, jan 2013.
- [181] J T Oliveira, L S Gardel, T Rada, L Martins, M E Gomes, and R L Reis. Injectable gellan gum hydrogels with autologous cells for the treatment of rabbit articular cartilage defects. *J Orthop Res*, 28(9):1193–1199, 2010.
- [182] S R Moxon and A M Smith. Controlling the rheology of gellan gum hydrogels in cell culture conditions. *International Journal of Biological Macromolecules*, 84:79–86, 2016.
- [183] M W Lee, H F Tsai, S M Wen, and C H Huang. Photocrosslinkable gellan gum film as an anti-adhesion barrier. *Carbohydr Polym*, 90(2):1132–1138, 2012.
- [184] R Mehvar. Dextran for targeted and sustained delivery of therapeutic and imaging agents. *J Control Release*, 69(1):1–25, 2000.
- [185] S P Massia and J Stark. Immobilized RGD peptides on surface-grafted dextran promote biospecific cell attachment. *J Biomed Mater Res*, 56(3):390–399, 2001.

- [186] G Sun, Y I Shen, C C Ho, S Kusuma, and S Gerecht. Functional groups affect physical and biological properties of dextran-based hydrogels. *J Biomed Mater Res A*, 93(3):1080–1090, 2010.
- [187] S Moller, J Weisser, S Bischoff, and M Schnabelrauch. Dextran and hyaluronan methacrylate based hydrogels as matrices for soft tissue reconstruction. *Biomol Eng*, 24(5):496–504, 2007.
- [188] G Sun, X Zhang, Y I Shen, R Sebastian, L E Dickinson, K Fox-Talbot, M Reinblatt, C Steenbergen, J W Harmon, and S Gerecht. Dextran hydrogel scaffolds enhance angiogenic responses and promote complete skin regeneration during burn wound healing. *Proc Natl Acad Sci U S A*, 108(52):20976–20981, 2011.
- [189] Y Shen, H G Song, A E Papa, J A Burke, S W Volk, and S Gerecht. Acellular Hydrogels for Regenerative Burn Wound Healing: Translation from a Porcine Model. *Journal of Investigative Dermatology*, 135(10):2519–2529, 2015.
- [190] K M Park, M R Blatchley, and S Gerecht. The design of dextran-based hypoxia-inducible hydrogels via in situ oxygen-consuming reaction. *Macromol Rapid Commun*, 35(22):1968–1975, 2014.
- [191] M Voigt, M Schauer, D J Schaefer, C Andree, R Horch, and G B Stark. Cultured epidermal keratinocytes on a microspherical transport system are feasible to reconstitute the epidermis in full-thickness wounds. *Tissue Eng*, 5(6):563–572, 1999.
- [192] G D Prestwich, D M Marecak, J F Marecek, K P Vercruyssen, and M R Ziebell. Controlled chemical modification of hyaluronic acid: Synthesis, applications, and biodegradation of hydrazide derivatives. In *Journal of Controlled Release*, volume 53, pages 93–103, 1998.
- [193] T J Brown, U B G Laurent, and J R E Fraser. Turnover of hyaluronan in synovial joints: elimination of labelled hyaluronan from the knee joint of the rabbit. *Experimental Physiology*, 76(1):125–134, 1991.
- [194] C E Schanté, G Zuber, C Herlin, and T F Vandamme. Chemical modifications of hyaluronic acid for the synthesis of derivatives for a broad range of biomedical applications. *Carbohydrate Polymers*, 85:469–489, 2011.
- [195] I P Monteiro, D Gabriel, B P Timko, M Hashimoto, S Karajanagi, R Tong, A P Marques, R L Reis, and D S Kohane. A two-component pre-seeded dermal-epidermal scaffold. *Acta Biomater*, 10(12):4928–4938, 2014.

- [196] R Bennett and M Taher. Restylane persists for 23 months found during Mohs Micrographic Surgery - a source of confusion with hyaluronic acid surrounding basal cell carcinoma. *Dermatol Surg*, 31:1366–1369, 2005.
- [197] S Bowman, M E Awad, M W Hamrick, M Hunter, and S Fulzele. Recent advances in hyaluronic acid based therapy for osteoarthritis. *Clinical and Translational Medicine*, 7(1):6, 2018.
- [198] K T Dicker, L A Gurski, S Pradhan-Bhatt, R L Witt, M C Farach-Carson, and X Jia. Hyaluronan: A simple polysaccharide with diverse biological functions. *Acta Biomaterialia*, 10:1558–1570, 2014.
- [199] C Law, J Li, H Chou, Y Chen, and H Chan. Hyaluronic acid-dependent protection in H9C2 cardiomyocytes: A cell model of heart ischemia–reperfusion injury and treatment. *Toxicology*, 303:54–71, 2013.
- [200] C L Wu, H C Chou, J M Li, Y W Chen, J H Chen, Y H Chen, and H L Chan. Hyaluronic acid-dependent protection against alkali-burned human corneal cells. *Electrophoresis*, 34(3):388–396, 2013.
- [201] A D’Agostino, A Stellavato, L Corsuto, P Diana, R Filosa, A La Gatta, M De Rosa, and C Schiraldi. Is molecular size a discriminating factor in hyaluronan interaction with human cells? *Carbohydrate Polymers*, 157(157):21–30, 2017.
- [202] S Misra, V C Hascall, R R Markwald, and S Ghatak. Interactions between hyaluronan and its receptors (CD44, RHAMM) regulate the activities of inflammation and cancer, may 2015.
- [203] S R King, W L Hickerson, and K G Proctor. Beneficial actions of exogenous hyaluronic acid on wound healing. *Surgery*, 109(1):76–84, jan 1991.
- [204] M T Cerqueira, L P da Silva, T C Santos, R P Pirraco, V M Correlo, R L Reis, and A P Marques. Gellan gum-hyaluronic acid spongy-like hydrogels and cells from adipose tissue synergize promoting neoskin vascularization. *ACS Appl Mater Interfaces*, 6(22):19668–19679, 2014.
- [205] Z Wu, L Fan, B Xu, Y Lin, P Zhang, and X Wei. Use of Decellularized Scaffolds Combined with Hyaluronic Acid and Basic Fibroblast Growth Factor for Skin Tissue Engineering. *Tissue Engineering Part A*, 21(1-2):390–402, 2015.
- [206] H Wang, M Ho, C Chen, Y Chou, Z Wen, and Z Wang. Novel Biodegradable Porous Scaffold Applied to Skin Regeneration. *PLoS ONE*, 8(6):e56330, 2013.

- [207] M Kuroyanagi, A Yamamoto, N Shimizu, A Toi, T Inomata, A Takeda, and Y Kuroyanagi. Development of anti-adhesive spongy sheet composed of hyaluronic acid and collagen containing epidermal growth factor. *Journal of Biomaterials Science, Polymer Edition*, 25(12):1253–1265, 2014.
- [208] Y K Lin, Y Matsumoto, Y Kuroyanagi, and S Kagawa. A bilayer hyaluronic acid wound dressing to promote wound healing in diabetic ulcer. *Journal of Bioactive and Compatible Polymers*, 24(5):424–443, 2009.
- [209] R Simman, W Mari, S Younes, and M Wilson. Use of Hyaluronic Acid-Based Biological Bilaminar Matrix in Wound Bed Preparation: A Case Series. *Eplasty*, 18:e17, 2018.
- [210] A Faga, G Nicoletti, F Brenta, S Scevola, G Abatangelo, and P Brun. Hyaluronic acid three-dimensional scaffold for surgical revision of retracting scars: A human experimental study. *International Wound Journal*, 10(3):329–335, 2013.
- [211] G Gravante, D Delogu, N Giordan, G Morano, A Montone, and G Esposito. The use of hyalomatrix PA in the treatment of deep partial-thickness burns. *Journal of Burn Care and Research*, 28(2):269–274, 2007.
- [212] S K Han, S Y Kim, R J Choi, S H Jeong, and W K Kim. Comparison of tissue-engineered and artificial dermis grafts after removal of basal cell carcinoma on face - A pilot study. *Dermatologic Surgery*, 40(4):460–467, 2014.
- [213] S J Delatte, J Evans, A Hebra, W Adamson, H B Othersen, and E P Tagge. Effectiveness of beta-glucan collagen for treatment of partial-thickness burns in children. *Journal of Pediatric Surgery*, 36(1):113–118, 2001.
- [214] H Ismail, M Irani, and Z Ahmad. Starch-Based Hydrogels: Present Status and Applications. *International Journal of Polymeric Materials and Polymeric Biomaterials*, 62(7):411–420, 2013.
- [215] J Ngoenkam, A Faikrua, S Yasothornsrikul, and J Viyoch. Potential of an injectable chitosan/starch/beta-glycerol phosphate hydrogel for sustaining normal chondrocyte function. *Int J Pharm*, 391(1-2):115–124, 2010.
- [216] N Sperelakis. *Cell physiology sourcebook*, volume XXXIII. 2012.
- [217] S Van Vlierberghe, P Dubrueel, and E Schacht. Biopolymer-based hydrogels as scaffolds for tissue engineering applications: a review. *Biomacromolecules*, 12(5):1387–1408, 2011.

- [218] M Garcia-Fuentes, A J Meinel, M Hilbe, L Meinel, and H P Merkle. Silk fibroin/hyaluronan scaffolds for human mesenchymal stem cell culture in tissue engineering. *Biomaterials*, 30(28):5068–5076, 2009.
- [219] U J Kim, J Park, C Li, H J Jin, R Valluzzi, and D L Kaplan. Structure and properties of silk hydrogels. *Biomacromolecules*, 5(3):786–792, 2004.
- [220] S Kapoor and S C Kundu. Silk protein-based hydrogels: Promising advanced materials for biomedical applications. *Acta Biomater*, 31:17–32, 2016.
- [221] R Ghassemifar, S Redmond, Zainuddin, and T V Chirila. Advancing towards a tissue-engineered tympanic membrane: silk fibroin as a substratum for growing human eardrum keratinocytes. *J Biomater Appl*, 24(7):591–606, 2010.
- [222] B Kundu and S C Kundu. Silk sericin/polyacrylamide in situ forming hydrogels for dermal reconstruction. *Biomaterials*, 33(30):7456–7467, 2012.
- [223] H Teramoto, T Kameda, and Y Tamada. Preparation of gel film from Bombyx mori silk sericin and its characterization as a wound dressing. *Biosci Biotechnol Biochem*, 72(12):3189–3196, 2008.
- [224] Z Wang, Y Zhang, J Zhang, L Huang, J Liu, Y Li, G Zhang, S C Kundu, and L Wang. Exploring natural silk protein sericin for regenerative medicine: an injectable, photoluminescent, cell-adhesive 3D hydrogel. *Sci Rep*, 4:7064, 2014.
- [225] K Tsubouchi, Y Igarashi, Y Takasu, and H Yamada. Sericin enhances attachment of cultured human skin fibroblasts. *Biosci Biotechnol Biochem*, 69(2):403–405, 2005.
- [226] D S A Hickman, C L Pawlowski, U D S Sekhon, J Marks, and A S Gupta. Biomaterials and Advanced Technologies for Hemostatic Management of Bleeding. *Advanced Materials*, 30(4):1–40, 2018.
- [227] P J M Bouten, M Zonjee, J Bender, S T K Yauw, H Van Goor, J C M Van Hest, and R Hoogenboom. The chemistry of tissue adhesive materials. *Progress in Polymer Science*, 39:1375–1405, 2014.
- [228] K Foster, D Greenhalgh, R L Gamelli, D Mazingo, N Gibran, M Neumeister, S Z Abrams, E Hantak, L Grubbs, B Ploder, N Schofield, and L H Riina. Efficacy and Safety of a Fibrin Sealant for Adherence of Autologous Skin Grafts to Burn Wounds: Results of a Phase 3 Clinical Study. *Journal of Burn Care & Research*, 29(2):293–303, mar 2008.

- [229] L J Currie, R Martin, J R Sharpe, and S E James. A comparison of keratinocyte cell sprays with and without fibrin glue. *Burns*, 29(7):677–685, 2003.
- [230] CRYOSEAL ® FS SYSTEM, 2007.
- [231] K Yamamoto and L DeJoseph. Efficacy and Safety of Artiss Fibrin Tissue Sealant Use in Rhytidectomy: A Review of 120 Cases. *The Surgery Journal*, 03(02):e69–e74, 2017.
- [232] C M Bhamidipati, J S Coselli, and S A LeMaire. BioGlue in 2011: what is its role in cardiac surgery? *The Journal of extra-corporeal technology*, 44(1):P6–12, 2012.
- [233] H K Chenault, S K Bhatia, W G Dimaio, G L Vincent, W Camacho, and A Behrens. Sealing and healing of clear corneal incisions with an improved dextran aldehyde-PEG amine tissue adhesive. *Current Eye Research*, 36(11):997–1004, 2011.
- [234] D Miki, K Dastgheib, T Kim, A Pfister-Serres, K A Smeds, M Inoue, D L Hatchell, and M W Grinstaff. A photopolymerized sealant for corneal lacerations. *Cornea*, 21(4):393–399, 2002.
- [235] J M G Reyes, S Herretes, A Pirouzmanesh, D A Wang, J H Elisseeff, A Jun, P J McDonnell, R S Chuck, and A Behrens. A modified chondroitin sulfate aldehyde adhesive for sealing corneal incisions. *Investigative Ophthalmology and Visual Science*, 46(4):1247–1250, 2005.
- [236] D Eyrich, F Brandl, B Appel, H Wiese, G Maier, M Wenzel, R Staudenmaier, A Goepferich, and T Blunk. Long-term stable fibrin gels for cartilage engineering. *Biomaterials*, 28(1):55–65, jan 2007.
- [237] Y Li, H Meng, Y Liu, and B P Lee. Fibrin gel as an injectable biodegradable scaffold and cell carrier for tissue engineering. *Scientific World Journal*, 2015.
- [238] O Gsib, J Duval, M Goczkowski, M Deneufchatel, O Fichet, V Larreta-Garde, S Bencherif, and C Egles. Evaluation of Fibrin-Based Interpenetrating Polymer Networks as Potential Biomaterials for Tissue Engineering. *Nanomaterials*, 7(12):436, 2017.
- [239] F Lee and M Kurisawa. Formation and stability of interpenetrating polymer network hydrogels consisting of fibrin and hyaluronic acid for tissue engineering. *Acta Biomaterialia*, 9(2):5143–5152, 2013.

- [240] C Han, L Zhang, J Sun, H Shi, J Zhou, and C Gao. Application of collagen-chitosan/fibrin glue asymmetric scaffolds in skin tissue engineering. *Journal of Zhejiang University SCIENCE B*, 11(7):524–530, 2010.
- [241] S Cox, M Cole, and B Tawil. Behavior of human dermal fibroblasts in three-dimensional fibrin clots: dependence on fibrinogen and thrombin concentration. *Tissue Eng*, 10(5-6):942–954, 2004.
- [242] J Kopp, M G Jeschke, A D Bach, U Kneser, and R E Horch. Applied tissue engineering in the closure of severe burns and chronic wounds using cultured human autologous keratinocytes in a natural fibrin matrix. *Cell Tissue Bank*, 5(2):89–96, 2004.
- [243] P Langa, A Wardowska, J Zieliński, J Podolak-Popinigis, P Sass, P Sosnowski, K Kondej, A Renkielska, P Sachadyn, P Trzonkowski, and M Piķuła. Transcriptional profile of in vitro expanded human epidermal progenitor cells for the treatment of non-healing wounds. *Journal of Dermatological Science*, 89:272–281, 2017.
- [244] V Carriel, I Garzón, J M Jiménez, A C X Oliveira, S Arias-Santiago, A Campos, M C Sánchez-Quevedo, and M Alaminos. Epithelial and stromal developmental patterns in a novel substitute of the human skin generated with fibrin-agarose biomaterials. *Cells Tissues Organs*, 196(1):1–12, 2012.
- [245] A Meana, J Iglesias, M Del Rio, F Larcher, B Madrigal, M F Fresno, C Martin, F San Roman, and F Tevar. Large surface of cultured human epithelium obtained on a dermal matrix based on live fibroblast-containing fibrin gels. *Burns*, 24(7):621–630, 1998.
- [246] R Mittermayr, P Slezak, N Haffner, D Smolen, J Hartinger, A Hofmann, J Schense, D Spazierer, J Gampfer, A Goppelt, and H Redl. Controlled release of fibrin matrix-conjugated platelet derived growth factor improves ischemic tissue regeneration by functional angiogenesis. *Acta Biomater*, 29:11–20, 2016.
- [247] A Gugerell, W Pasteiner, S Nurnberger, J Kober, A Meinel, S Pfeifer, J Hartinger, S Wolbank, A Goppelt, H Redl, and R Mittermayr. Thrombin as important factor for cutaneous wound healing: Comparison of fibrin biomatrices in vitro and in a rat excisional wound healing model. *Wound Repair and Regeneration*, 22(6):740–748, 2014.
- [248] V R Sherman, W Yang, and M A Meyers. The materials science of collagen. *J Mech Behav Biomed Mater*, 52:22–50, 2015.

- [249] S Chattopadhyay and R T Raines. Collagen-based biomaterials for wound healing. *Biopolymers*, 101(8):821–833, 2014.
- [250] N Dagalakis, J Flink, P Stasikelis, J F Burke, and I V Yannas. Design of an artificial skin. Part III. Control of pore structure. *J Biomed Mater Res*, 14(4):511–528, 1980.
- [251] J F Burke, I V Yannas, W C Quinby Jr., C C Bondoc, and W K Jung. Successful use of a physiologically acceptable artificial skin in the treatment of extensive burn injury. *Ann Surg*, 194(4):413–428, 1981.
- [252] K R Chalimidi, Y Kumar, and U Anand Kini. Efficacy of collagen particles in chronic non healing ulcers. *Journal of Clinical and Diagnostic Research*, 2015.
- [253] D L N Snyder, B A Sullivan, M Karen, S M Schoelles, N Sullivan, and K M Schoelles. *Skin Substitutes for Treating Chronic Wounds*. Agency for Healthcare Research and Quality (US), dec 2012.
- [254] S Suzuki, K Matsuda, N Isshiki, Y Tamada, K Yoshioka, and Y Ikada. Clinical evaluation of a new bilayer “artificial skin” composed of collagen sponge and silicone layer. *British Journal of Plastic Surgery*, 43(1):47–54, 1990.
- [255] M. J. A. van Luyn, P. B. van Wachem, L. H. H. Olde Damink, P J Dijkstra, J Feijen, and P Nieuwenhuis. Secondary cytotoxicity of cross-linked dermal sheep collagens during repeated exposure to human fibroblasts. *Biomaterials*, 13(14):1017–1024, 1992.
- [256] M Kremer, E Lang, and A C Berger. Evaluation of dermal-epidermal skin equivalents (‘composite-skin’) of human keratinocytes in a collagen-glycosaminoglycan matrix(Integra artificial skin). *Br J Plast Surg*, 53(6):459–465, 2000.
- [257] V C van der Veen, M B A van der Wal, M C E van Leeuwen, M M W Ulrich, and E Middelkoop. Biological background of dermal substitutes. *Burns*, 36(3):305–321, 2010.
- [258] R S Kirsner. The use of Apligraf in acute wounds. *J Dermatol*, 25(12):805–811, 1998.
- [259] R J Kumar, R M Kimble, R Boots, and S P Pegg. Treatment of partial-thickness burns: a prospective, randomized trial using Transcyte. *ANZ J Surg*, 74(8):622–626, 2004.

- [260] K Vig, A Chaudhari, S Tripathi, S Dixit, R Sahu, S Pillai, V A Dennis, and S R Singh. Advances in Skin Regeneration Using Tissue Engineering. *International Journal of Molecular Sciences*, 2017.
- [261] S Natesan, D O Zamora, N L Wrice, D G Baer, and R J Christy. Bilayer hydrogel with autologous stem cells derived from debrided human burn skin for improved skin regeneration. *J Burn Care Res*, 34(1):18–30, 2013.
- [262] A Skardal, D Mack, E Kapetanovic, A Atala, J D Jackson, J Yoo, and S Soker. Bioprinted Amniotic Fluid-Derived Stem Cells Accelerate Healing of Large Skin Wounds. *STEM CELLS Translational Medicine*, 1(11):792–802, 2012.
- [263] Y B Lee, S Polio, W Lee, G Dai, L Menon, R S Carroll, and S S Yoo. Bio-printing of collagen and VEGF-releasing fibrin gel scaffolds for neural stem cell culture. *Exp Neurol*, 223(2):645–652, 2010.
- [264] D M Supp and S T Boyce. Engineered skin substitutes: practices and potentials. *Clin Dermatol*, 23(4):403–412, 2005.
- [265] J N Mansbridge. Tissue-engineered skin substitutes in regenerative medicine. *Current Opinion in Biotechnology*, 20(5):563–567, 2009.
- [266] A W C Chua, Y C Khoo, B K Tan, K C Tan, C L Foo, and S J Chong. Skin tissue engineering advances in severe burns: review and therapeutic applications. *Burns & Trauma*, 4(1):1–14, 2016.
- [267] S T Boyce and A L Lalley. Tissue engineering of skin and regenerative medicine for wound care. *Burns & Trauma*, 6(1):4, 2018.
- [268] A J Bullock, P Pickavance, D B Haddow, S Rimmer, and S MacNeil. Development of a calcium-chelating hydrogel for treatment of superficial burns and scalds. *Regen Med*, 5(1):55–64, 2010.
- [269] M E Cooke, S W Jones, B ter Horst, N Moiemmen, M Snow, G Chouhan, L J Hill, M Esmali, R J A Moakes, J Holton, R Nandra, R L Williams, A M Smith, and L M Grover. Structuring of Hydrogels across Multiple Length Scales for Biomedical Applications. *Advanced Materials*, 1705013:1–15, 2018.
- [270] M K Lee, M H Rich, K Baek, J Lee, and H Kong. Bioinspired tuning of hydrogel permeability-rigidity dependency for 3D cell culture. *Sci Rep*, 5:8948, 2015.
- [271] L Yuan, C Minghua, D Feifei, W Runxiu, L Ziqiang, M Chengyue, and J Wenbo. Study of the use of recombinant human granulocyte-macrophage colony-stimulating

- factor hydrogel externally to treat residual wounds of extensive deep partial-thickness burn. *Burns*, 41(5):1086–1091, 2015.
- [272] B Boonkaew, P M Barber, S Rengpipat, P Supaphol, M Kempf, J He, V T John, and L Cuttle. Development and characterization of a novel, antimicrobial, sterile hydrogel dressing for burn wounds: single-step production with gamma irradiation creates silver nanoparticles and radical polymerization. *J Pharm Sci*, 103(10):3244–3253, 2014.
- [273] S P Miguel, M P Ribeiro, H Brancal, P Coutinho, and I J Correia. Thermoresponsive chitosan-agarose hydrogel for skin regeneration. *Carbohydr Polym*, 111:366–373, 2014.
- [274] R Mohd Zohdi, Z Abu Bakar Zakaria, N Yusof, N Mohamed Mustapha, and M N Abdullah. Gelam (*Melaleuca* spp.) Honey-Based Hydrogel as Burn Wound Dressing. *Evid Based Complement Alternat Med*, 2012:843025, 2012.
- [275] K A Barbee. Mechanical cell injury. *Ann N Y Acad Sci*, 1066:67–84, 2005.
- [276] W S Veazey, K J Anusavice, and K Moore. Mammalian cell delivery via aerosol deposition. *Journal of Biomedical Materials Research. Part B, Applied Biomaterials*, 72(2):334–338, 2005.
- [277] J Hendriks, C Willem Visser, S Henke, J Leijten, D B F Saris, C Sun, D Lohse, and M Karperien. Optimizing cell viability in droplet-based cell deposition. *Scientific Reports*, 5(1):11304, 2015.
- [278] C Fredriksson, G Kratz, and F Huss. Transplantation of cultured human keratinocytes in single cell suspension: a comparative in vitro study of different application techniques. *Burns*, 34(2):212–219, 2008.
- [279] D G Harkin, R A Dawson, and Z Upton. Optimized delivery of skin keratinocytes by aerosolization and suspension in fibrin tissue adhesive. *Wound Repair & Regeneration*, 14(3):354–363, 2006.
- [280] W Veazey and K Moore. Delivery of tissue engineering media, 2003.
- [281] T R Sosnowski, A Kurowska, B Butruk, and K Jablczynska. Spraying of Cell Colloids in Medical Atomizers. In S Pierucci and J J Klemes, editors, *Icheap-11: 11th International Conference on Chemical and Process Engineering, Pts 1-4*, volume 32, pages 2257–2262. Aidic Servizi Srl, Milano, 2013.

- [282] K L Butler, J Goverman, H Ma, A Fischman, Y M Yu, M Bilodeau, A M Rad, A A Bonab, R G Tompkins, and S P Fagan. Stem cells and burns: Review and therapeutic implications. *Journal of Burn Care and Research*, 31(6):874–881, 2010.
- [283] S T Boyce, A P Supp, V B Swope, and G D Warden. Vitamin C regulates keratinocyte viability, epidermal barrier, and basement membrane in vitro, and reduces wound contraction after grafting of cultured skin substitutes. *J Invest Dermatol*, 118(4):565–572, 2002.
- [284] C E Butler and D P Orgill. Simultaneous in vivo regeneration of neodermis, epidermis, and basement membrane. *Adv Biochem Eng Biotechnol*, 94:23–41, 2005.
- [285] K Dijkstra, J Hendriks, M Karperien, L A Vonk, and D B F Saris. Arthroscopic Airbrush-Assisted Cell Spraying for Cartilage Repair: Design, Development, and Characterization of Custom-Made Arthroscopic Spray Nozzles. *Tissue Engineering Part C: Methods*, 23(9):505–515, 2017.
- [286] C D Marshall, M S Hu, T Leavitt, L A Barnes, H P Lorenz, and M T Longaker. Cutaneous Scarring: Basic Science, Current Treatments, and Future Directions. *Advances in Wound Care*, 7(2):29–45, 2018.
- [287] B Ter Horst, G Chouhan, N S Moiemien, and L M Grover. Advances in keratinocyte delivery in burn wound care. *Advanced Drug Delivery Reviews*, 123:18–32, 2018.
- [288] P Johnstone, J S Kwei, G Filobos, D Lewis, and S Jeffery. Successful application of keratinocyte suspension using autologous fibrin spray. *Burns*, 43(3):e27–e30, 2017.
- [289] A Allouni, R Papini, and D Lewis. Spray-on-skin cells in burns: a common practice with no agreed protocol. *Burns*, 39(7):1391–1394, 2013.
- [290] I. Fernández Farrés and I. T. Norton. Formation kinetics and rheology of alginate fluid gels produced by in-situ calcium release. *Food Hydrocolloids*, 40:76–84, 2014.
- [291] H A Barnes. The yield stress—a review or ‘greek’-everything flows? *Journal of Non-Newtonian Fluid Mechanics*, 81(1-2):133–178, 1999.
- [292] A Z Nelson and R H Ewoldt. Design of yield-stress fluids: A rheology-to-structure inverse problem. *Soft Matter*, 13(41):7578–7594, 2017.
- [293] Q D Nguyen and D V Boger. Measuring the Flow Properties of Yield Stress Fluids. *Annual Review of Fluid Mechanics*, 24(1):47–88, 1992.

- [294] E C Bingham and H Green. Paint, a plastic material and not a viscous liquid; the measurement of its mobility and yield value. *Proc. Am. Soc. Test. Mater.*, (20):640–75, 1920.
- [295] N E Fedorovich, J Alblas, J R. de Wijn, W E Hennink, A J Verbout, and W J A Dhert. Hydrogels as Extracellular Matrices for Skeletal Tissue Engineering: State-of-the-Art and Novel Application in Organ Printing. *Tissue Engineering*, 13(8):1905–1925, 2007.
- [296] D F Coutinho, S V Sant, H Shin, J T Oliveira, M E Gomes, N M Neves, A Khademhosseini, and R L Reis. Modified Gellan Gum hydrogels with tunable physical and mechanical properties. *Biomaterials*, 31(29):7494–7502, 2010.
- [297] D A Garrec and I T Norton. Understanding fluid gel formation and properties. *Journal of Food Engineering*, 112:175–182, 2012.
- [298] E R Morris, K Nishinari, and M Rinaudo. Gelation of gellan - A review, 2012.
- [299] WS Rasband. ImageJ: Image processing and analysis in Java. *Astrophysics Source Code Library*, 1:06013, 2012.
- [300] H Grasdalen and O Smidsrød. Gelation of gellan gum. *Carbohydrate Polymers*, 7(5):371–393, jan 1987.
- [301] A Gabriele, F Spyropoulos, and I T Norton. Kinetic study of fluid gel formation and viscoelastic response with kappa-carrageenan. *Food Hydrocolloids*, 23(8):2054–2061, 2009.
- [302] P A Williams and G O Phillips. *Gums and Stabilisers*. The Royal Society of Chemistry, 2002.
- [303] X Xin, A Borzacchiello, P A Netti, L Ambrosio, and L Nicolais. Hyaluronic-acid-based semi-interpenetrating materials. *Journal of Biomaterials Science, Polymer Edition*, 15(9):1223–1236, 2004.
- [304] A Borzacchiello and L Ambrosio. Structure-Property Relationships in Hydrogels. In *Hydrogels: Biological Properties and Applications*, pages 9–20. Springer Milan, Milano, 2009.
- [305] P Coussot. Yield stress fluid flows: A review of experimental data. *Journal of Non-Newtonian Fluid Mechanics*, 211:31–49, 2014.

- [306] S R Moxon and A M Smith. Controlling the rheology of gellan gum hydrogels in cell culture conditions. *International Journal of Biological Macromolecules*, 84:79–86, 2016.
- [307] J T Koivisto, T Joki, J E Parraga, R Paakkonen, L Yla-Outinen, L Salonen, I Jonkkari, M Peltola, T O Ihalainen, S Narkilahti, and M Kellomaki. Bioamine-crosslinked gellan gum hydrogel for neural tissue engineering. *Biomed Mater*, 12(2):25014, 2017.
- [308] J Silva-Correia, J M Oliveira, S G Caridade, J T Oliveira, R A Sousa, J F Mano, and R L Reis. Gellan gum-based hydrogels for intervertebral disc tissue-engineering applications. *J Tissue Eng Regen Med*, 5(6):e97–107, 2011.
- [309] M W Lee, H F Tsai, S M Wen, and C H Huang. Photocrosslinkable gellan gum film as an anti-adhesion barrier. *Carbohydr Polym*, 90(2):1132–1138, 2012.
- [310] K te Nijenhuis. *Thermoreversible Networks, Viscoelastic Properties and Structure of Gels*. 1997.
- [311] L R Stevens, K J Gilmore, G G Wallace, and M. In het Panhuis. Tissue engineering with gellan gum, 2016.
- [312] G Sworn, G R Sanderson, and W Gibson. Gellan gum fluid gels. *Topics in Catalysis*, 9(4):265–271, 1995.
- [313] I T Norton, D A Jarvis, and T J Foster. A molecular model for the formation and properties of fluid gels. *International Journal of Biological Macromolecules*, 26(4):255–261, 1999.
- [314] H Moritaka, H Fukuba, N Kkumeno', Nakahama, and K Nishinari. Effect of monovalent and divalent cations on the rheological properties of gellan gels. Technical report.
- [315] S. Adams, W. J. Frith, and J. R. Stokes. Influence of particle modulus on the rheological properties of agar microgel suspensions. *Journal of Rheology*, 48(6):1195–1213, nov 2004.
- [316] P Snabre and P Mills. Rheology of concentrated suspensions of viscoelastic particles. *Colloids and Surfaces A: Physicochemical and Engineering Aspects*, 152(1-2):79–88, 1999.

- [317] R J A Moakes, A Sullo, and I T Norton. Preparation and characterisation of whey protein fluid gels: The effects of shear and thermal history. *Food Hydrocolloids*, 45:227–235, 2015.
- [318] S B Ross-Murphy. Rheological characterization of polymer gels and networks. *Polymer Gels and Networks*, 2(3-4):229–237, 1994.
- [319] A M Grillet, N B Wyatt, and L M Gloe. Polymer Gel Rheology and Adhesion. *Rheology*, 2012.
- [320] N Altmann, J J Cooper-White, D E Dunstan, and J R Stokes. Strong through to weak 'sheared' gels. *Journal of Non-Newtonian Fluid Mechanics*, 124(1-3 SPEC. ISS.):129–136, 2004.
- [321] D A Garrec, B Guthrie, and I T Norton. Kappa carrageenan fluid gel material properties. Part 1: Rheology. *Food Hydrocolloids*, 33(1):151–159, 2013.
- [322] A B Metzner. Rheology of Suspensions in Polymeric Liquids. *Journal of Rheology*, 29(6):739–775, 1985.
- [323] D Li and A W Neumann. Equation of State for Interfacial Tensions of Solid-Liquid Systems. *Advances in Colloid and Interface Science*, 39:299–345, 1992.
- [324] B Ibsen. Treatment of shock with vasodilators measuring skin temperature on the big toe. Ten years' experience in 150 cases. *Dis Chest*, 52(4):425–429, 1967.
- [325] A M Kholoussy, S Sufian, C Pavlides, and T Matsumoto. Central peripheral temperature gradient. Its value and limitations in the management of critically ill surgical patients. *Am J Surg*, 140(5):609–612, 1980.
- [326] J C Ferguson, R G Chechetto, C C O'Donnell, B K Fritz, W C Hoffmann, C E Coleman, B S Chauhan, S W Adkins, G R Kruger, and A J Hewitt. Assessing a novel smartphone application - SnapCard, compared to five imaging systems to quantify droplet deposition on artificial collectors. *Computers and Electronics in Agriculture*, 128:193–198, 2016.
- [327] C Nansen, J C Ferguson, J Moore, L Groves, R Emery, N Garel, and A Hewitt. Optimizing pesticide spray coverage using a novel web and smartphone tool, SnapCard. *Agronomy for Sustainable Development*, 35(3):1075–1085, 2015.
- [328] J Silva-Correia, B Zavan, V Vindigni, T H Silva, J M Oliveira, G Abatangelo, and R L Reis. Biocompatibility evaluation of ionic- and photo-crosslinked methacrylated

- gellan gum hydrogels: in vitro and in vivo study. *Adv Healthc Mater*, 2(4):568–575, 2013.
- [329] M E Cooke, M J Pearson, R J A Moakes, C J Weston, E T Davis, S W Jones, and L M Grover. Geometric confinement is required for recovery and maintenance of chondrocyte phenotype in alginate. *APL Bioengineering*, 1(1):016104, dec 2017.
- [330] J H Holmes, J A Molnar, J E Carter, J Hwang, B A Cairns, B T King, D J Smith, Wayne C C, K N Foster, M D Peck, R Sood, M J Feldman, M H Jordan, D W Mozingo, D G Greenhalgh, T L Palmieri, J A Griswold, S Dissanaik, and W L Hickerson. A comparative study of the ReCell(R) device and autologous split-thickness meshed skin graft in the treatment of acute burn injuries. *Journal of Burn Care and Research*, 39(5):694–702, 2018.
- [331] J Howard. *Mechanics of Motor Proteins and the Cytoskeleton*. Sinauer Associates, Inc, 2001.
- [332] M B Ginzberg, R Kafri, and M Kirschner. On being the right (cell) size. *Science*, 348(6236), 2015.
- [333] S B Hopkinson, K J Hamill, Y Wu, J L Eisenberg, S Hiroyasu, and J C R Jones. Focal Contact and Hemidesmosomal Proteins in Keratinocyte Migration and Wound Repair. *Advances in Wound Care*, 3(3):247–263, 2014.
- [334] S A Agnihotri, S S Jawalkar, and T M Aminabhavi. Controlled release of cephalixin through gellan gum beads: Effect of formulation parameters on entrapment efficiency, size, and drug release. *European Journal of Pharmaceutics and Biopharmaceutics*, 63(3):249–261, 2006.
- [335] R Gorkin, M in het Panhuis, M Romero-Ortega, G G Wallace, E M Stewart, B C Thompson, L Stevens, R Lozano, and K J Gilmore. 3D printing of layered brain-like structures using peptide modified gellan gum substrates. *Biomaterials*, 67:264–273, 2015.
- [336] A B Dababneh and I T Ozbolat. Bioprinting Technology: A Current State-of-the-Art Review. *Journal of Manufacturing Science and Engineering*, 136(6):061016, 2014.
- [337] B Hopp. Femtosecond laser printing of living cells using absorbing film-assisted laser-induced forward transfer. *Optical Engineering*, 51(1):014302, jan 2012.

- [338] X Fu, N Liu, X Wu, J Xie, B Yao, and S Huang. 3D bioprinting matrices with controlled pore structure and release function guide in vitro self-organization of sweat gland. *Scientific Reports*, 6(1):1–8, 2016.
- [339] N Cubo, M Garcia, J F Del Cañizo, D Velasco, and J L Jorcano. 3D bioprinting of functional human skin: Production and in vivo analysis. *Biofabrication*, 9(1), 2017.
- [340] W L Ng, S Wang, W Y Yeong, and M W Naing. Skin Bioprinting: Impending Reality or Fantasy?, 2016.
- [341] K Nair, K Yan, and W Sun. A multilevel numerical model quantifying cell deformation in encapsulated alginate structures. *Journal of Mechanics of Materials and Structures*, 2(6):1121–1139, 2009.
- [342] K Chang Yan, K Nair, and W Sun. Three dimensional multi-scale modelling and analysis of cell damage in cell-encapsulated alginate constructs. *Journal of Biomechanics*, 43(6):1031–1038, 2010.
- [343] J Stricker, T Falzone, and M L Gardel. Mechanics of the F-actin cytoskeleton. *Journal of Biomechanics*, 43(1):9–14, 2010.
- [344] R Chang, J Nam, and W Sun. Effects of Dispensing Pressure and Nozzle Diameter on Cell Survival from Solid Freeform Fabrication–Based Direct Cell Writing. *Tissue Engineering Part A*, 14(1):41–48, 2008.
- [345] T Banno and M Blumenberg. Keratinocyte detachment-differentiation connection revisited, or Anoikis-Pityriasi Nexus Redux. *PLoS ONE*, 9(6), 2014.
- [346] K Miyazaki. Laminin-5 (laminin-332): Unique biological activity and role in tumor growth and invasion. *Cancer Science*, 97(2):91–98, 2006.
- [347] Y Shirakata. Regulation of epidermal keratinocytes by growth factors, 2010.
- [348] F. M. Watt and H. Green. Involucrin synthesis is correlated with cell size in human epidermal cultures. *Journal of Cell Biology*, 90(3):738–742, 1981.
- [349] F M Watt. Engineered Microenvironments to Direct Epidermal Stem Cell Behavior at Single-Cell Resolution, 2016.
- [350] H Green. Terminal differentiation of cultured human epidermal cells. *Cell*, 11(2):405–416, jun 1977.

- [351] F M Watt, P Boukamp, J Hornung, and N E Fusenig. Effect of growth environment on spatial expression of involucrin by human epidermal keratinocytes. *Archives of Dermatological Research*, 279(5):335–340, 1987.
- [352] C J Ferris, K J Gilmore, G G Wallace, and M in het Panhuis. Modified gellan gum hydrogels for tissue engineering applications. *Soft Matter*, 9 (14):3705–3711, 2013.
- [353] B A Pruitt, A T McManus, S H Kim, and C W Goodwin. Burn wound infections: Current status. *World Journal of Surgery*, 22(2):135–145, 1998.
- [354] A J Singer and S A McClain. Persistent wound infection delays epidermal maturation and increases scarring in thermal burns. *Wound Repair and Regeneration*, 10(6):372–377, 2002.
- [355] D Church, S Elsayed, O Reid, B Winston, and R Lindsay. Burn wound infections. *Clinical Microbiology Reviews*, 19(2):403–434, 2006.
- [356] B A Latenser, S G Miller, P Q Bessey, S M Browning, D M Caruso, M Gomez, J C Jeng, J A Krichbaum, C W Lentz, Je R Saffle, M J Schurr, D G Greenhalgh, and R J Kagan. National burn repository 2006: A ten-year review. *Journal of Burn Care and Research*, 28(5):635–658, 2007.
- [357] E Alp, A Coruh, G K Gunay, Y Yontar, and M Doganay. Risk Factors for Nosocomial Infection and Mortality in Burn Patients. *Journal of Burn Care & Research*, 33(3):379–385, 2012.
- [358] P Brychta. European Burns Association European Practice Guidelines for Burn Care Minimum level of Burn Care Provision in Europe. Technical report, 2017.
- [359] National Center for Biotechnology Information. Compound Summary for CID 176.
- [360] J E Bauman, R C Kolodny, and S K Webster. Vaginal organic acids and hormonal changes in the menstrual cycle. *Fertility and Sterility*, 38(5):572–579, 1982.
- [361] I Phillips, A Z Lobo, R Fernandes, and N S Gundara. ACETIC ACID IN THE TREATMENT OF SUPERFICIAL WOUNDS INFECTED BY PSEUDOMONAS AERUGINOSA. *Proc. Fedn Proc. Fedn Am. Soc. exp. Biol. J. Exp. Med. Nature J. exp. Med. Surgery, St. Louis J. surg. Res. Ann. N.Y. Acad. Sci. J. exp. Med. Ann. N.Y. Acad. Sci. Nature*, 24(209):621–267, 1963.
- [362] M Morgan, J R Deuis, M Frøsig-Jørgensen, R J Lewis, P J Cabot, P D Gray, and I Vetter. Burn pain: A systematic and critical review of epidemiology, pathophysiology, and treatment. *Pain Medicine (United States)*, 19(4):708–734, 2018.

- [363] J. M Sloss, N Cumberland, and S M Milner. Acetic acid used for the elimination of *Pseudomonas aeruginosa* from burn and soft tissue wounds. *Journal of the Royal Army Medical Corps*, 139(2):49–51, 1993.
- [364] W Doles, G Wilkerson, S Morrison, and R Richmond. Glacial Acetic Acid Adverse Events: Case Reports and Review of the Literature. *Hospital Pharmacy*, 50(4):304–309, 2015.
- [365] A P Fraise, M. A.C. Wilkinson, C R Bradley, B Oppenheim, and N Moiemmen. The antibacterial activity and stability of acetic acid. *Journal of Hospital Infection*, 84(4):329–331, 2013.
- [366] V L Madhusudhan. Efficacy of 1% acetic acid in the treatment of chronic wounds infected with *Pseudomonas aeruginosa*: prospective randomised controlled clinical trial. *International wound journal*, 13(6):1129–1136, 2016.
- [367] B S Nagoba, N M Suryawanshi, B Wadher, and S Selkar. Acidic Environment and Wound Healing: A Review. *Wiley Interdisciplinary Reviews: Nanomedicine and Nanobiotechnology*, 27(1):5–11, 2015.
- [368] T Bjarnsholt, M Alhede, P Ø Jensen, A K Nielsen, H K Johansen, P Homøe, N Høiby, M Givskov, and K Kirketerp-Møller. Antibiofilm Properties of Acetic Acid. *Advances in Wound Care*, 4(7):363–372, 2015.
- [369] B Kundukad, M Schussman, K Yang, T Seviour, L Yang, S A Rice, S Kjelleberg, and P S Doyle. Mechanistic action of weak acid drugs on biofilms. *Scientific Reports*, 7(1):4783, jul 2017.
- [370] O M Gomaa. The involvement of acetic acid in programmed cell death for the elimination of *Bacillus* sp. used in bioremediation. *Journal of Genetic Engineering and Biotechnology*, 10(2):185–192, 2012.
- [371] N Aminifarshidmehr. The management of chronic suppurative otitis media with acid media solution, 1996.
- [372] K B Waites, K C Canupp, J F Roper, S M Camp, and Y Chen. Evaluation of 3 methods of bladder irrigation to treat bacteriuria in persons with neurogenic bladder. *Journal of Spinal Cord Medicine*, 29(3):217–226, 2006.
- [373] J D Wilson, S M Shann, S K Brady, A G Mammen-Tobin, A L Evans, and R A Lee. Recurrent bacterial vaginosis: The use of maintenance acidic vaginal gel following treatment. *International Journal of STD and AIDS*, 16(11):736–738, nov 2005.

- [374] K H Yoo, S Lee, and S H Jeon. Simple renal cyst sclerotherapy with acetic acid: our 10-year experience. *J Endourol.*, 22(11):2559–63, 2008.
- [375] Y J Cho and J H Shin. Comparison of acetic acid and ethanol sclerotherapy for simple renal cysts: clinical experience with 86 patients. *SpringerPlus*, 5(1), 2016.
- [376] T Huo, Y H Huang, and J C Wu. Percutaneous ablation therapy for hepatocellular carcinoma: Current practice and future perspectives, 2005.
- [377] W J Trzaska, J N Correia, M T Villegas, R C May, and K Voelz. pH manipulation as a novel strategy for treating mucormycosis. *Antimicrobial Agents and Chemotherapy*, 59(11):6968–6974, 2015.
- [378] H. Ryssel, O. Kloeters, G. Germann, Th Schäfer, G. Wiedemann, and M. Oehlbauer. The antimicrobial effect of acetic acid—An alternative to common local antiseptics? *Burns*, 35(5):695–700, 2009.
- [379] S M Milner. Acetic acid to treat *Pseudomonas aeruginosa* in superficial wounds and burns. *The Lancet*, 340(8810):61, 1992.
- [380] W J Meyer, S Wiechman, L Woodson, M Jaco, and C R Thomas. *Chapter 64 – Management of pain and other discomforts in burned patients*. Elsevier Inc., fifth edit edition, 2012.
- [381] ASTM International. Standard test method for tensile properties of plastics. *ASTM International*, 08:46–58, 2003.
- [382] J M A Blair, M A Webber, A J Baylay, D O Ogbolu, and L J V Piddock. Molecular mechanisms of antibiotic resistance, 2015.
- [383] J Cambiaso-Daniel, J J Gallagher, W B Norbury, C C Finnerty, D N Herndon, and D M Culnan. Treatment of infection in burn patients. In *Total Burn Care: Fifth Edition*, pages 93–113.e4. Elsevier Inc., fifth edit edition, 2017.
- [384] F Zor, S Ozturk, F Bilgin, S Isik, and A Cosar. Pain relief during dressing changes of major adult burns: Ideal analgesic combination with ketamine. *Burns*, 36(4):501–505, 2010.
- [385] J Sun and Z Zhou. A novel ocular delivery of brinzolamide based on gellan gum: In vitro and in vivo evaluation. *Drug Design, Development and Therapy*, 12:383–389, 2018.

- [386] L J Hill, R J A Moakes, C Vareechon, G Butt, A Ng, K Brock, G Chouhan, R C Vincent, S Abbondante, R L Williams, N M Barnes, E Pearlman, G R Wallace, S Rauz, A Logan, and L M Grover. Sustained release of decorin to the surface of the eye enables scarless corneal regeneration. *npj Regenerative Medicine*, 3(1), 2018.
- [387] M W Lee, H J Chen, and S W Tsao. Preparation, characterization and biological properties of Gellan gum films with 1-ethyl-3-(3-dimethylaminopropyl)carbodiimide cross-linker. *Carbohydrate Polymers*, 82(3):920–926, 2010.
- [388] F Yamamoto and R L Cunha. Acid gelation of gellan: Effect of final pH and heat treatment conditions. *Carbohydrate Polymers*, 68(3):517–527, 2007.
- [389] C S F Picone and R L Cunha. Influence of pH on formation and properties of gellan gels. *Carbohydrate Polymers*, 84(1):662–668, 2011.
- [390] A B Norton, P W Cox, and F Spyropoulos. Acid gelation of low acyl gellan gum relevant to self-structuring in the human stomach. *Food Hydrocolloids*, 25(5):1105–1111, 2011.
- [391] J F Bradbeer, R Hancocks, F Spyropoulos, and I T Norton. Self-structuring foods based on acid-sensitive low and high acyl mixed gellan systems to impact on satiety. *Food Hydrocolloids*, 35:522–530, 2014.
- [392] R. Babu, S Sathigari, M. Kumar, and J. Pandit. Formulation of Controlled Release Gellan Gum Macro Beads of Amoxicillin. *Current Drug Delivery*, 7(1):36–43, 2010.
- [393] A S Hoffman. Hydrogels for biomedical applications. *Advanced Drug Delivery Reviews*, 64:18–23, 2012.
- [394] J Shen and D J Burgess. In vitro dissolution testing strategies for nanoparticulate drug delivery systems: Recent developments and challenges. *Drug Delivery and Translational Research*, 3(5):409–415, 2013.
- [395] A Lacci, K M and Dardik. Platelet-Rich Plasma : Support for Its Use in. *The Yale journal of biology and medicine.*, 83:1–9, 2010.
- [396] M J Martinez-Zapata, A J Martí-Carvajal, I Solà, S Bellmunt-Montoya, J Cid, and G Urrútia. Cochrane Database of Systematic Reviews Autologous platelet-rich plasma for treating surgical wounds (Protocol) Autologous platelet-rich plasma for treating surgical wounds (Protocol) i Autologous platelet-rich plasma for treating surgical wounds (Protoco. *Cochrane Database of Systematic Reviews*, 2013.

- [397] P. Harrison, J. Alsousou, I. Andia, T. Burnouf, D. Dohan Ehrenfest, P. Everts, H. Langer, J. Magalon, R. Marck, and P. Gresele. The use of platelets in regenerative medicine and proposal for a new classification system: guidance from the SSC of the ISTH. *Journal of Thrombosis and Haemostasis*, 16(9):1895–1900, 2018.
- [398] S B Lee, H Kim, S Lee, H Jang, H Myung, W Jang, S Shim, S Park, S Lee, M Kim, and J K Myung. A Method for the Activation of Platelet-Rich Plasma via Bead Mill Homogenizer for Mesenchymal Stem Cell Culture. *Tissue Engineering Part C: Methods*, 23(8):465–473, aug 2017.
- [399] E M Milford and M C Reade. Comprehensive review of platelet storage methods for use in the treatment of active hemorrhage. *Transfusion*, 56(April):S140–S148, 2016.
- [400] J. G. van der Bom, J. Jacobse, C. Caram-Deelder, R. A. Middelburg, A. L. Kreuger, and J.-L. Kerkhoffs. Effect of storage time of platelet products on clinical outcomes after transfusion: a systematic review and meta-analyses. *Vox Sanguinis*, 112(4):291–300, 2017.
- [401] C. Caram-Deelder, A. L. Kreuger, J. Jacobse, J. G. van der Bom, and R. A. Middelburg. Effect of platelet storage time on platelet measurements: a systematic review and meta-analyses. *Vox Sanguinis*, 111(4):374–382, 2016.
- [402] G. Michael Fitzpatrick. Novel platelet products under development for the treatment of thrombocytopenia or acute hemorrhage. *Transfusion and Apheresis Science*, 58(1):7–11, 2019.
- [403] P S Hartley, J Savill, and S B Brown. The death of human platelets during incubation in citrated plasma involves shedding of CD42b and aggregation of dead platelets. *Thrombosis and haemostasis*, 95:100–6, 2005.
- [404] A M Albanyan, P Harrison, and M F Murphy. Markers of platelet activation and apoptosis during storage of apheresis- and buffy coat-derived platelet concentrates for 7 days. *Transfusion*, 49(1):108–117, 2009.
- [405] R Ma, R Xie, C Yu, Y Si, X Wu, L Zhao, Z Yao, S Fang, H Chen, V Novakovic, C Gao, J Kou, Y Bi, H S Thatte, B Yu, S Yang, J Zhou, and J Shi. Phosphatidylserine-mediated platelet clearance by endothelium decreases platelet aggregates and procoagulant activity in sepsis. *Scientific Reports*, 7(1), 2017.
- [406] V Prochazka, H Klosova, J Stetinsky, J Gumulec, K Vitkova, D Salounova, J Dvorackova, H Bielnikova, P Klement, V Levakova, T Ocelka, L Pavliska, P Kovanic,

and G Klement. Addition of platelet concentrate to dermo-epidermal skin graft in deep burn trauma reduces scarring and need for revision surgeries. *Biomedical Papers*, 158(2):242–258, 2014.

- [407] K Düregger, A Gäble, and M Eblenkamp. Development and evaluation of a spray applicator for platelet-rich plasma. *Colloids and Surfaces B: Biointerfaces*, 171(June):214–223, 2018.
- [408] P F Van Der Meer and D De Korte. Platelet Additive Solutions: A Review of the Latest Developments and Their Clinical Implications. *Transfusion Medicine and Hemotherapy*, 45(2):98–102, 2018.

APPENDIX A

SUPPLEMENTARY MATERIAL CHAPTER 3

Supplementary Figure A.1:

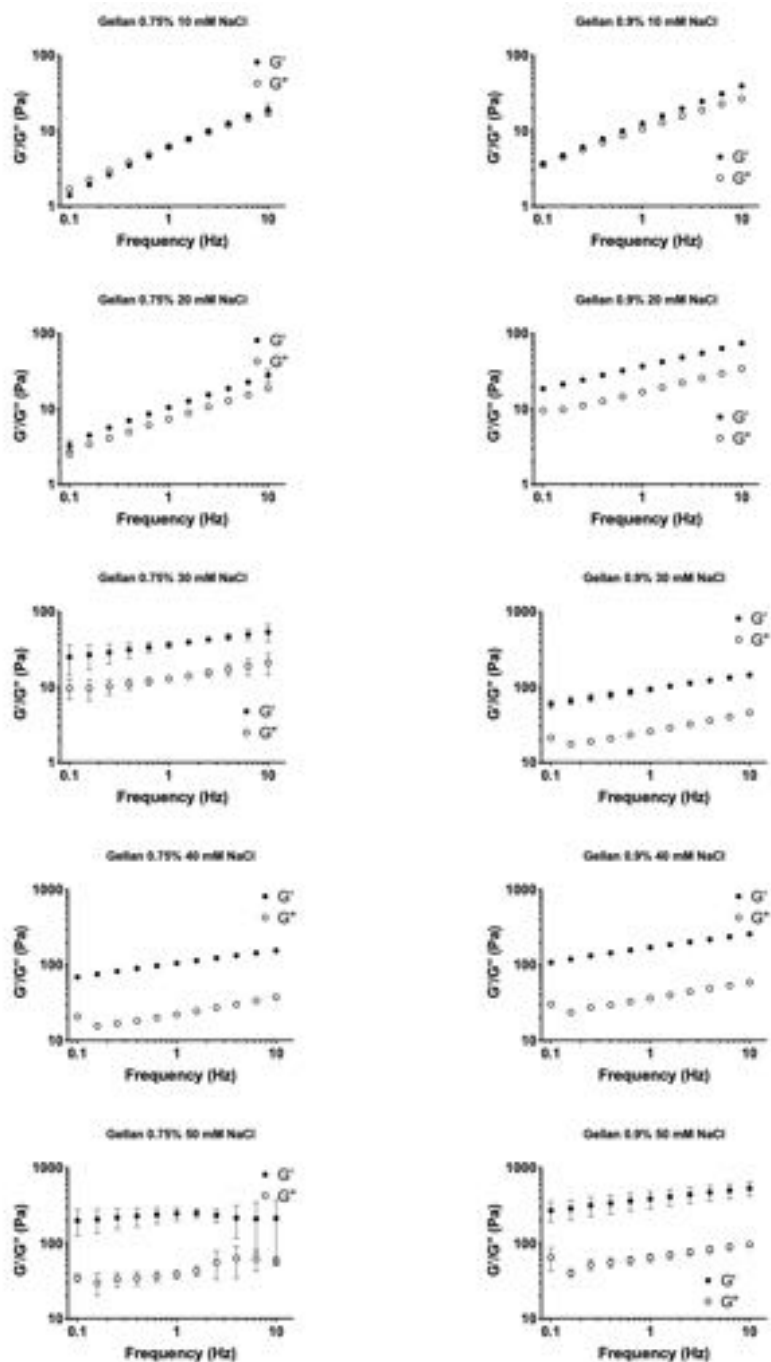


Figure A.1: Frequency dependence of a panel of gellan fluid gels. Frequency dependence of a panel of gellan fluid gels illustrates that all compositions behave as weak gels. In both polymer concentrations (0.75% and 0.9%) there is an evident increase in both  $G'$  and  $G''$  with increasing cross-linker concentration. Mean values of 3 individual measurements presented, error bars are SD (not visible when smaller than icon).

Supplementary Figure A.2:

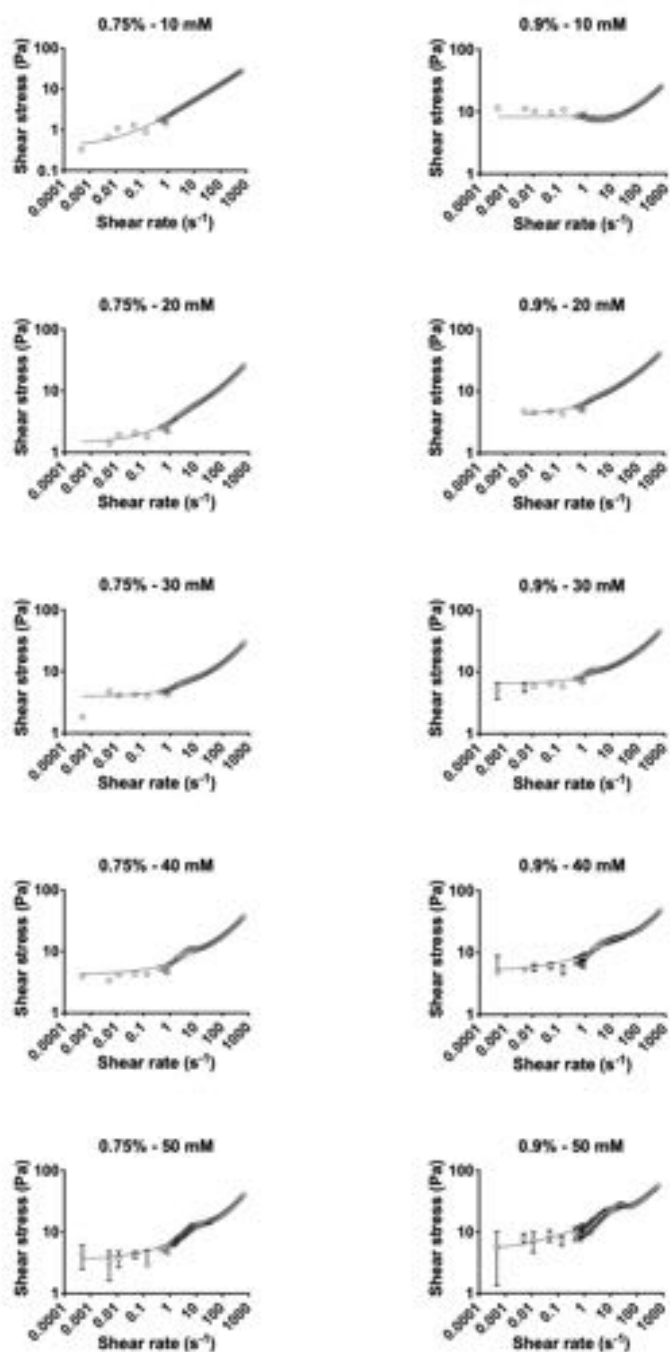


Figure A.2: Amplitude dependence of a panel of gellan fluid gels fitted for Herschel-Bulkley model. The shear rate dependence of gellan fluid gel plotted against shear stress fitted the Herschel-Bulkley equation good with a mean R square value of 0.98229 (range: 0.9387-0.9995). The individual fitting parameters and R<sup>2</sup> are shown in Table 2.2. Mean values of 3 individual measurements presented, error bars are SD (not visible when smaller than icon).

Supplementary Figure A.3:

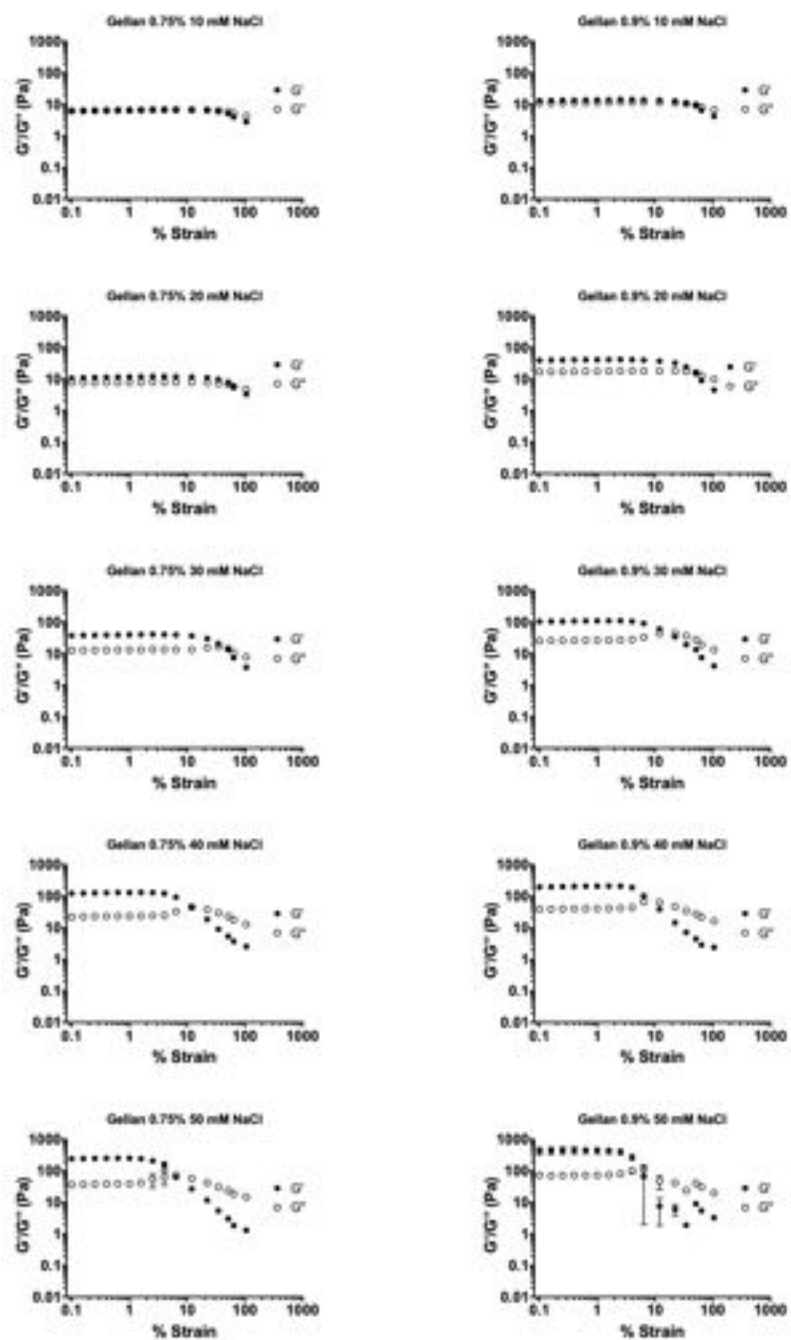


Figure A.3: Amplitude sweeps of a panel of gellan fluid gels. The elastic modulus of gellan fluid gels remains linear until about 10% strain, structure breakdown outside the LVR is indicated by decreasing  $G'$  in higher percentage strains. In both polymer concentration gels (0.75% and 0.9%) there is an earlier loss of elastic modulus with increasing cross-linker concentration. Mean values of 3 individual measurements presented, error bars are SD (not visible when smaller than icon).

## APPENDIX B

# SPRAY DELIVERY OF PRP

## B.1 Introduction

Platelet-Rich-Plasma (PRP) is derived from whole blood and gained increasing interest in regenerative medicine and has been used topically to enhance wound healing as it releases growth factors that stimulate tissue repair and can serve as a tissue sealant [395, 396]. PRP is prepared by centrifugation to concentrate platelets, since a variety of preparation methods are available, PRP can be classified based on several factors:

- Platelet concentration
- Leucocyte count
- Red blood cell count
- Activation
- Preparation technique

Recently, a new classification system has been proposed based on the above mentioned factors resulting in 4 main categories [397]:

- P-PRP (pure platelet-rich-plasma)
- L-PRP (leucocyte platelet-rich-plasma)
- P-PRF (pure platelet-rich-fibrin)
- L-PRF (leucocyte platelet-rich-fibrin)

PRP delivery is usually accompanied by activation via stimulus such as thrombin and calcium chloride in order to release their growth factors[396]. However, it is known that mechanical trauma can activate platelets as well, activation techniques based on this principle include: freeze-thawing cycles or use of tissue homogenizer [398]. It was hypothesised that spraying could induce a similar response and potentially pre-empt the activation via potential harmful exogenous calcium or thrombin. In this study, the effect of spraying on platelet activation and viability was investigated.

Besides topical application of concentrated platelets, transfusion of platelets has become an established practice in the treatment of active hemorrhage. Readily available donor platelets are required to meet the clinical need of treating trauma patients with major bleeding. Platelets can be stored under specific conditions (constant agitation at room temperature) for 5 days prior to transfusion, sometimes extended to 7 days[399]. During storage, changes occur in both platelets and medium, limiting the shelf life of platelet products. The negative impact of prolonged storage on platelet function and transfusion

outcomes have recently been highlighted [399–401]. Research into methods to prolong platelet storage and development of novel platelet products have not yet led to readily available platelets with extended shelf life [402]. The second aim of this study was to examine the effect of fluid gel encapsulation on platelets to investigate possible methods to prolong storage.

## **B.2 Methods**

This work was performed with the help of Dr P. Harrison for flowcytometry analysis and LTA assays, all the basic experimental work, imaging and results analysis has been performed by BTH.

### **B.2.1 Platelet rich plasma preparation**

Platelet rich plasma (P-PRP): whole blood from 1 healthy volunteer donor was collected in EDTA and citrate blood tubes (BD vacutainer, UK). Directly following collection, citrate tubes were agitated to allow mixing of anticoagulant and blood. Baseline platelet count was determined with Sysmex XN-1000 hematology analyzer (Sysmex UK, Milton Keynes, UK). Platelet rich plasma (PRP) was prepared by centrifugation of whole blood at 200 g for 10 min. PRP was carefully collected into fresh tubes without disturbing red blood cells underneath as illustrated in Figure B.1a.

Leucocyte rich PRP (L-PRP): was prepared from whole blood as described above, but centrifugation protocol adjusted to 1500 g for 20 min. The tube consisted of clear platelet-poor plasma at the top, a buffy coat containing white blood cells and platelets in the middle and red blood cells at the bottom as illustrated in Figure B.1b. The buffy coat was carefully obtained with minimal disturbance of the red blood cells. Full blood count including platelet count was performed with Sysmex XN-1000 (Sysmex UK, Milton Keynes, UK), for both PRP and L-PRP and platelet fold increase was calculated. Samples were kept at room temperature until testing.

### **B.2.2 PRP fluid gel encapsulation**

Platelet count of PRP was determined prior to mixing. A PRP to gel ratio of 1:5 was used to come to an approximate concentration of  $8 \times 10^4$  platelets/ $\mu\text{l}$ . Fresh PRP was gently mixed into the gellan fluid gel (0.9% gellan, 20 mM NaCl) with careful pipetting using a large orifice pipette tip to reduce mechanical cell stress. Samples were kept at room temperature until testing.

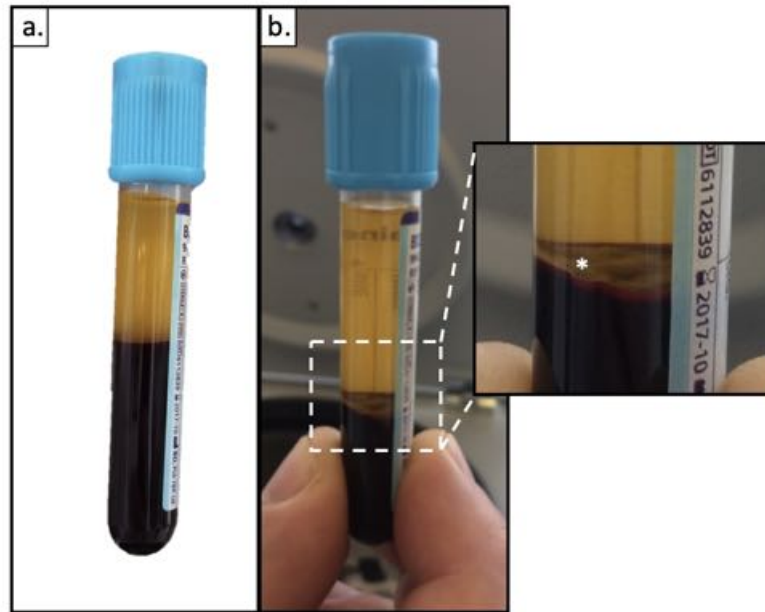


Figure B.1: Preparation of PRP. Two distinctive layers can be observed; a cloudy yellow layer of plasma including platelets on top and a deep red layer of erythrocytes at bottom (a). The L-PRP tube (b) has 3 distinct layers of clear yellow plasma on top, the buffy coat containing leucocytes and platelets in the middle indicated with (\*) and red blood cells at the bottom. [Source: Britt ter Horst].

### B.2.3 PRP viability

For this study, 4 conditions were compared: control PRP, sprayed PRP, encapsulated non sprayed PRP and encapsulated sprayed PRP. A volume of 0.5-1 ml of PRP was sprayed with an airbrush device (as described in section 2 ‘spray methods’ onto cover slips in a 6 well plate and 0.5-1 ml of control PRP was pipetted into the wells. All samples were immersed in PBS until testing. Live/dead assay was performed with calcein-acetoxymethyl ester (Calcein-AM), a cell permeable substrate that is not cell specific and stains viable cells. FM4-64 was used to stain non-viable platelets as previously described [403]. Stains were handled in a dark environment.

Encapsulated PRP: samples were immersed in a working solution of 100 nM Calcein-AM and 5  $\mu$ M FM4-64 in calcium-free Hanks’ balanced salt solution (HBSS) for 20 min. Coverslips were placed onto microscope slides and visualised using confocal microscopy (Olympus, Fluoview FV100), showing viable platelets green (Calcein AM) and non-viable platelets red (FM4-64).

Non-encapsulated PRP: platelets were diluted in HBSS (1:100) and 5  $\mu$ l of Calcein-AM (final concentration of 100 nM) and 5  $\mu$ l of FM4-64 (final concentration of 5  $\mu$ M) was added. Samples were incubated for 10 min at room temperature before analysing with

flowcytometry. Unstained samples were used as control for autofluorescence.

#### **B.2.4 Platelet activation**

Platelets were labeled with CD62P-FITC (P selectin) to measure activation before and after induced activation by the thrombin receptor activity peptide (TRAP). Sprayed PRP and non-sprayed PRP were diluted to  $100 \times 10^9/L$  in calcium free HBSS. IgG1 (mouse) FITC was used as control antibody and CD62P-FITC as platelet antibody. In non activated sample tubes, 5  $\mu l$  of platelet solution was added with 5  $\mu l$  of IgG1 (control) or 5  $\mu l$  of CD62-P (test) without mixing. Mixing of the solution was achieved by adding 40  $\mu l$  of PBS. In activated sample tubes, the mixing solution consisted of 5  $\mu l$  TRAP and 35  $\mu l$  PBS. All tubes were incubated for 15 min at room temperature prior to flowcytometric analysis. Accuri C6 flow cytometer equipped with CFlow software (BD Biosciences) was used for analysis. A minimum of 10.000 events were collected and a logarithmic gain was used. The platelet population was identified by their characteristic forward and side scatter signals and a manual gate drawn. Background fluorescence was set with the isotype control (IgG1 FITC) and the percentage and median fluorescence intensity of positive events recorded using the anti-CD62P FITC. Data is presented as percentage activation.

#### **B.2.5 Platelet aggregation**

Platelet aggregation of platelets encapsulated in fluid gel with flowcytometry is not possible due to higher viscosity of gel with risk of clogging. Therefore, platelet aggregation was assessed by Light Transmission Aggregometry, the addition of activation factors like thrombin, collagen, adenosine 5'-diphosphate (ADP), TRAP or von Willebrand factor (vWf) causes aggregation. Aggregated platelets allow more light to be transmitted compared non-aggregated platelets in suspension, light intensity is measured and presented as percentage light transmission. Samples were loaded on a PAP 8 aggregometer and TRAP was used as aggregation agonist. A total volume of 500  $\mu l$  per tube consisted of 50% PPP (Platelet poor plasma) and 50% PBS or gellan fluid gel as blank test. Test tubes consisted of 50% PRP and 50% PBS or gellan fluid gel.

## B.3 Results

### B.3.1 PRP preparation

P-PRP and L-PRP were prepared, the mean blood values obtained are presented in Table B.1. P-PRP was chosen for further spraying and encapsulation work as the addition of white blood cells was not needed at this stage.

Table B.1: Mean blood values of P-PRP and L-PRP preparations

	P-PRP		L-PRP			
	Mean	SD	N	Mean	SD	N
WBC ( $10^9/L$ )	0.248	0.468	6	32.535	2.100	2
RBC ( $10^{12}/L$ )	0.032	0.008	6	3.505	0.474	2
PLT-F ( $10^9/L$ )	408.833	53.019	6	1936.500	242.538	2

*WBC= white blood count, RBC= red blood count, PLT-F= platelet count (obtained with Sysmex), SD= standard deviation, N= number of preparations.*

### B.3.2 Spray delivery of PRP

#### Platelet activation

Platelet activation following spraying was measured by labeling activated platelets with P-selection, the sprayed and non-sprayed groups were compared and in a second group the response to induced activation by TRAP was measured by flowcytometry. It was found that sprayed platelets get slightly activated upon spraying, but do not respond well to induced activation (Figure B.2).

#### Platelet viability

Next, we examined whether this poor response of sprayed cells to activation is due to cell death by staining live platelets with Calcein AM and apoptotic/dead platelets by the plasma membrane binding FM4-64 stain as previously described [404]. Results of flowcytometry demonstrate a reduction of viable platelets from 97.6% (control) to 39.4% following spraying (Figure B.3A). When visualized with confocal microscopy it was indeed clear that sprayed platelets had a low percentage of viable cells. Furthermore, pseudopodia were noted on viable cells in both the sprayed and non-sprayed groups as shown in Figure

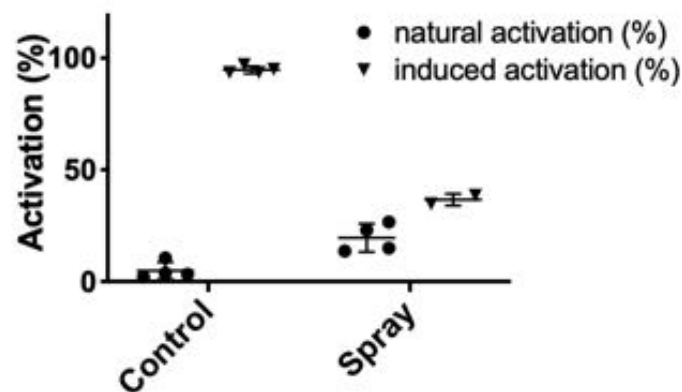


Figure B.2: Platelet activation following spray delivery. Natural and TRAP-induced platelets activation following spray delivery compared to control (non-spray delivery).

B.3B. Presence of pseudopodia indicates the start of platelets aggregation, these changes are irreversible.

### B.3.3 Fluid gel encapsulation of PRP

#### Platelet aggregation

Because flowcytometers are not equipped to run gel samples, activation of platelets was investigated by light transmission aggregometry (LTA). Aggregation of platelets was induced by adding an activation factor (TRAP). It was found that no spontaneous aggregation occurred when platelets were encapsulated in fluid gel. Furthermore, platelets responded to TRAP activation in 2 out of 3 experiments by aggregation (expressed by increased light transmission) when encapsulated in gellan fluid gel, as shown in Figure B.4.

#### Platelet viability

Clustering of platelets was also observed on day 1 with confocal microscopy where live cells were stained green and dead cells stained red. The cell clusters exhibited and although mainly stained green, a red 'shell' around individual cells was observed meaning that the aggregated cells take up FM4-64 early while potentially still viable (Figure B.5), this vesicle morphology is seen in apoptotic platelets[405]. Thus, encapsulation in fluid gel results in platelet activation in non-sprayed samples with some formation of pseudopodia and induces apoptosis. However, spontaneous aggregation was not observed in the LTA assay. This difference is potentially explained by the duration of encapsulation; platelets assessed for viability were kept in the gel for a longer period of time before imaging and

clustering might have occurred in that time frame, whereas LTA platelet aggregation was assessed immediately after mixing PRP and gel.

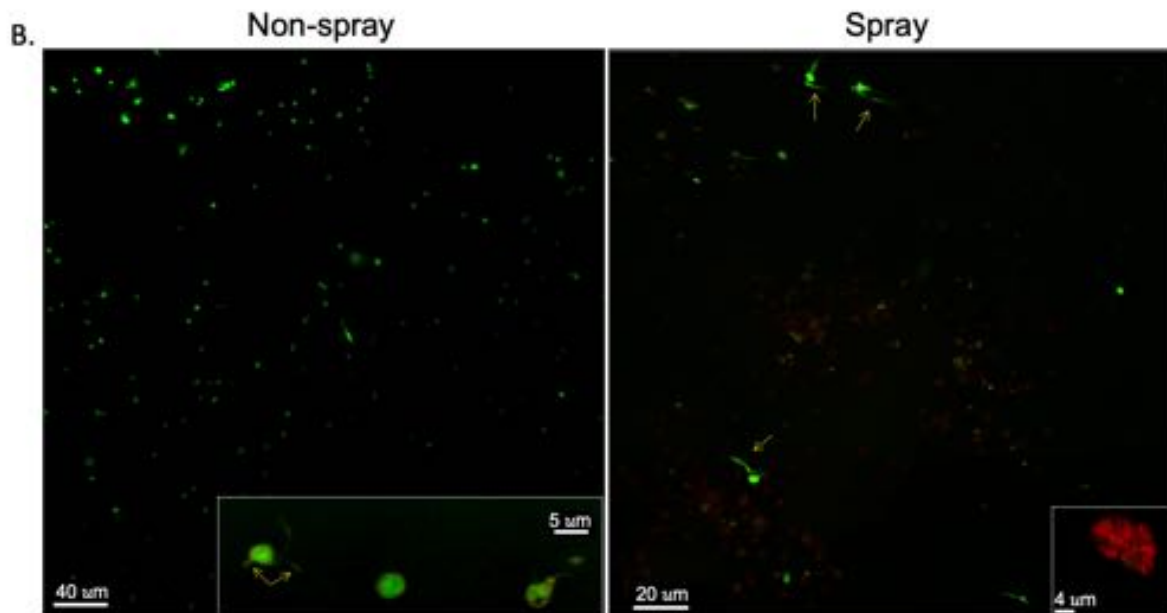
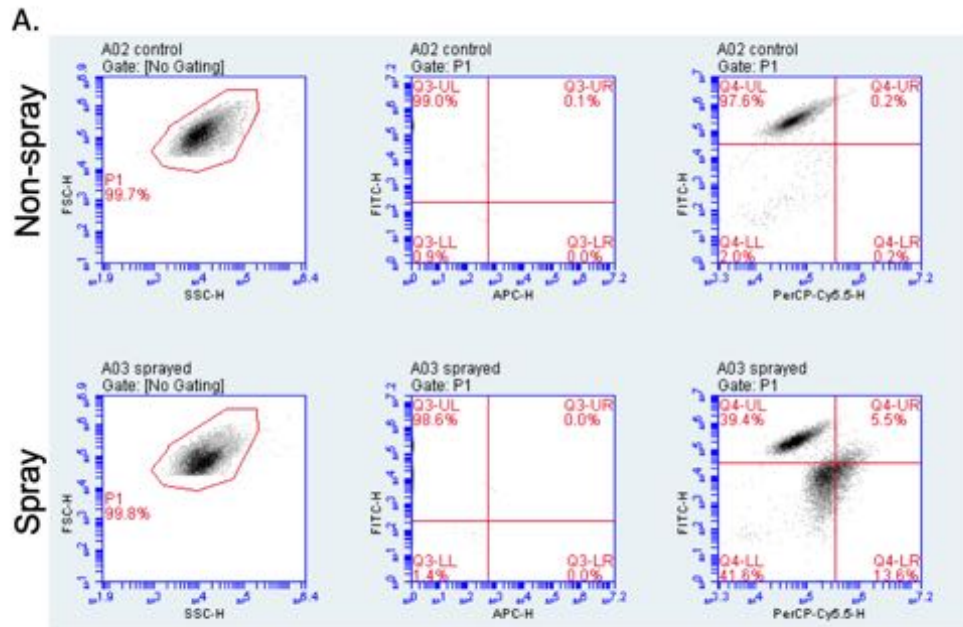


Figure B.3: Platelet viability following spray delivery. A) Flowcytometry results of live/dead stain of platelets following spray delivery compared to non-sprayed (pipetted) platelets. B) Confocal images of FM4-64 stained dead cells (red) and green viable platelets (stained by Calcein AM). Yellow arrows indicate pseudopodia, seen in both non-sprayed and sprayed cells.

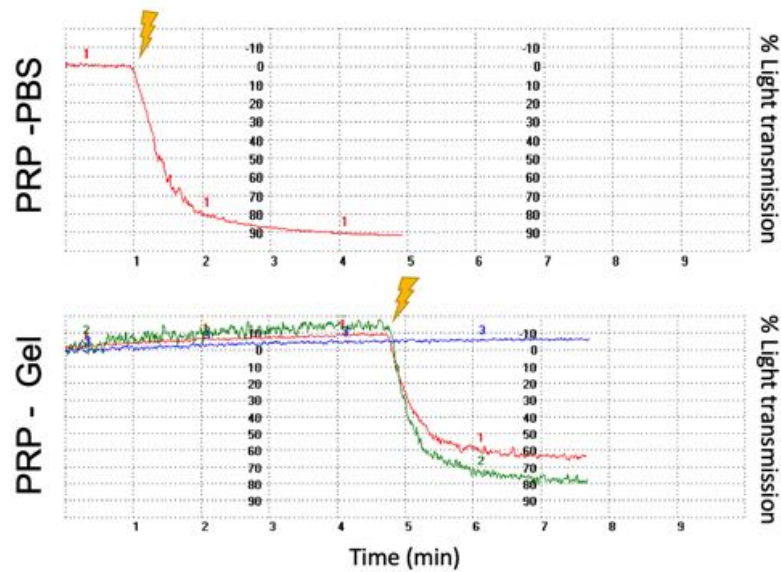


Figure B.4: Platelet aggregation in fluid gel. Control PRP in PBS showed activation upon activation with TRAP as indicated by ⚡. Percentage light transmission increases in 2 out of 3 PRP-gel samples upon stimulation by TRAP.

## B.4 Conclusion and future work

In this study, the effect of spraying concentrated platelets (P-PRP) on platelet activation, viability and morphology was investigated. Although, PRP spray devices are already used in clinic [406], but evidence on platelet viability following spraying is lacking[407]. The preliminary results showed that spraying induced platelet activation slightly, however, sprayed platelets were less receptive to induced activation (by TRAP) than non-sprayed platelets indicating a change in behaviour of sprayed cells. Airbrush spray systems allow for adjusting the airpressure at delivery; determining whether higher airpressure at delivery (increased mechanical stress) might be related to an increased rate of activation may help to understand the mechanism of platelet activation and be interesting for clinical applications. Furthermore, as platelet viability following spraying was reduced, the activation seen could be an early sign of apoptosis. It would be interesting to investigate whether this spray-induced activation would lead to similar growth factor release as non-sprayed platelets.

Secondly, encapsulation of platelets in gellan fluid gel was investigated in order to determine whether the gel could potentially be used as a storage medium. The results seem to indicate that platelets form clusters when encapsulated in the fluid gel. Interestingly, aggregation did not always occur when mixing platelets and gel in the LTA assay. This might be related by the duration of encapsulation. Current platelet storage medium includes additives such as glucose, acetate, potassium, magnesium, and phosphate in

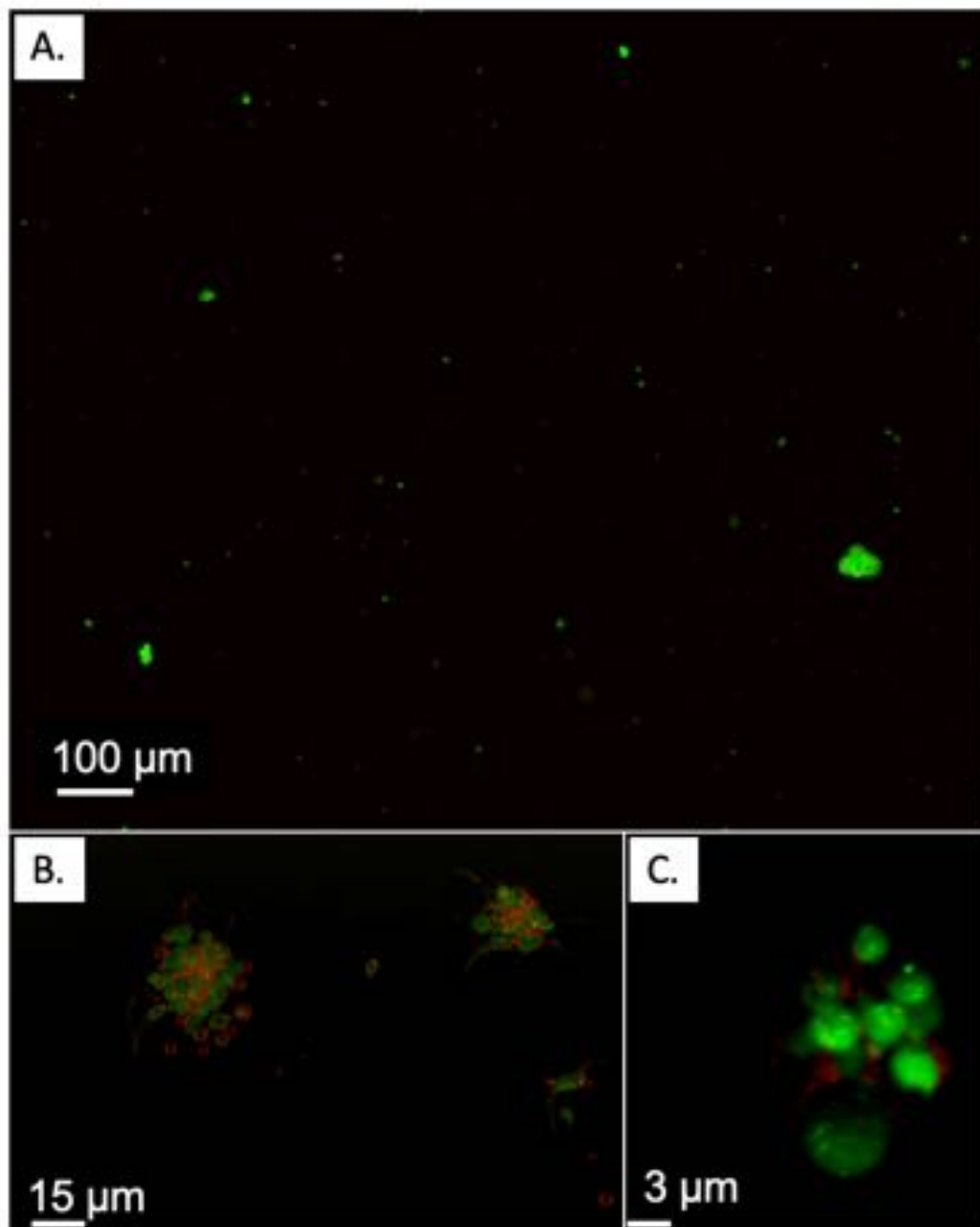


Figure B.5: Platelet viability following encapsulation in gellan fluid gel. FM4-64 stained dead cells red and green platelets are viable (stained by Calcein AM). Clustering of platelets was observed at all magnifications (A, B, C) and pseudopodia were observed (B).

order to inhibit the storage lesion (and activation)[408]. Future studies could aim to include these additives in the gel and engineer the fluid gel in such a way that it is closer to low viscosity fluids reducing aggregation and investigate platelet storage properties in more detail. This could be achieved by looking at activation, viability and growth factor release of the platelets.

APPENDIX C  
PUBLICATIONS



## Advances in keratinocyte delivery in burn wound care

Britt ter Horst<sup>a,b</sup>, Gurpreet Chouhan<sup>a</sup>, Naiem S. Moiem<sup>b</sup>, Liam M. Grover<sup>a,\*</sup>

<sup>a</sup> School of Chemical Engineering, University of Birmingham, Edgbaston B15 2TT, United Kingdom

<sup>b</sup> University Hospital Birmingham Foundation Trust, Burns Centre, Mindelsohn Way, B15 2TH Birmingham, United Kingdom

### ARTICLE INFO

#### Article history:

Received 11 April 2017

Received in revised form 14 June 2017

Accepted 23 June 2017

Available online 28 June 2017

#### Keywords:

Cell transplantation

Burn injury

Wound healing

Hydrogels

Spray application

### ABSTRACT

This review gives an updated overview on keratinocyte transplantation in burn wounds concentrating on application methods and future therapeutic cell delivery options with a special interest in hydrogels and spray devices for cell delivery.

To achieve faster re-epithelialisation of burn wounds, the original autologous keratinocyte culture and transplantation technique was introduced over 3 decades ago. Application types of keratinocytes transplantation have improved from cell sheets to single-cell solutions delivered with a spray system. However, further enhancement of cell culture, cell viability and function in vivo, cell carrier and cell delivery systems remain themes of interest. Hydrogels such as chitosan, alginate, fibrin and collagen are frequently used in burn wound care and have advantageous characteristics as cell carriers.

Future approaches of keratinocyte transplantation involve spray devices, but optimisation of application technique and carrier type is necessary.

© 2017 The Author(s). Published by Elsevier B.V. This is an open access article under the CC BY license (<http://creativecommons.org/licenses/by/4.0/>).

### Contents

1.	Introduction	19
2.	Skin	19
2.1.	Epidermis	19
2.1.1.	Keratinocyte differentiation and proliferation markers	19
2.1.2.	Factors promoting keratinocyte differentiation	20
2.1.3.	Keratinocyte interaction with other epidermal cells	20
2.2.	Dermis and basement membrane	20
3.	Wound healing and keratinocytes	21
3.1.	The role of keratinocytes in wound healing	21
3.1.1.	Angiogenesis	21
3.1.2.	Epithelialisation	21
3.2.	Pathophysiology of burn injury	22
3.3.	Rational for keratinocyte transplantation	22
4.	Cell transplantation technology	22
4.1.	Cell source	22
4.2.	Methods of human keratinocyte cell culture	23
4.2.1.	Historical development of keratinocyte culture	23
4.2.2.	Progress towards xenobiotic free culture techniques	23
4.2.3.	Additions to keratinocyte culture	23
4.3.	Keratinocyte viability after transplantation	24
5.	Application types of keratinocytes transplantation	24
5.1.	Introduction: grafting of burn wounds	24
5.2.	Cultured keratinocyte sheets	24
5.2.1.	Cultured autologous keratinocyte sheets	24
5.2.2.	Introduction of dermal substitutes including cultured keratinocytes	24
5.3.	Autologous keratinocyte transplantation in suspension	25

\* Corresponding author.

E-mail address: [L.M.Grover@bham.ac.uk](mailto:L.M.Grover@bham.ac.uk) (L.M. Grover).

5.3.1.	Pre-confluent keratinocytes suspension	25
5.3.2.	Uncultured keratinocytes suspension	26
5.3.3.	Allogeneic neonatal keratinocytes suspension	27
5.3.4.	Other clinical studies using cell sprays	27
5.4.	Hydrogels	27
5.4.1.	Hydrogels in burn care	27
6.	Methods of spray deposition	28
6.1.	Spray parameters and cell viability	28
6.2.	Spray systems	28
6.2.1.	Low and high pressure spray nozzle	28
6.2.2.	Liquid atomizer	29
7.	Potential therapeutic applications	29
7.1.	Future approaches keratinocyte transplantation	29
7.2.	Future spray cell delivery systems for burns wound care	29
Funding		29
Conflict of interest		29
Permission note		29
Acknowledgments		29
References		29

## 1. Introduction

Burn injuries are complicated wounds to manage with a relative high mortality rate in especially large area burns and elderly patients [1]. Substantial tissue damage and extensive fluid loss can cause impaired vital functions of the skin. Rapid epithelialisation is mandatory to restore the barrier function of the skin and enhance healing. Pathological scar formation (hypertrophic scarring) can occur as a long term sequelae of delayed wound healing. When healing is delayed, the potential short term common complications include wound infection affecting the local healing process or systemic inflammatory and immunological responses which subsequently can cause life threatening sepsis and multi-organ failure. In the United states, approximately 400,000 fire/burn injuries were recorded in 2014 in a population of about 300 million, including a total of 3196 (0.78%) fatal injuries (data from CDC in WISQARS Injury Mortality Report) [2].

Fortunately, survival rates have improved drastically over the last century due to advancements in burn care such as early surgical intervention, critical care support and wound care [3,4]. However, despite further technological advancements in the last 30 years, survival rates have not improved significantly over the last three decades and now seem to be plateauing in countries with high-standard burn care [5–7].

Furthermore, since modern standard burn care allows the majority of patients to survive thermal injury, other outcome measurements aiming to improve quality of life become more relevant. For example, shortening length of hospital stay, decreasing the number of trips to the operating theatre and optimizing the quality of restored tissue. Functional and aesthetic outcome of the restored tissue are reflected by scar quality in terms of pigmentation, pliability, sensation, hair growth and function (prevention of scar contraction).

All of these factors require a specialized approach aiming on regeneration of tissue instead of tissue repair. Progress in short term results (lifesaving wound coverage) remains essential. Subsequently, advances of long term results are desired to facilitate the need for quality of life improvement of the increasing population of burn survivors. Answers to these challenges are sought in the field of tissue engineering. Although, advances in engineered skin equivalents and cell-delivery to the wound bed are emerging in burn care, they currently do not meet the expected results and translation to clinical practice is challenging. Keratinocyte delivery was the first skin cell transplantation successfully translated to the clinical burn care. In the last four decades this method has been investigated widely and numerous researchers have contributed to a variety of improvements. This review gives an updated overview on applications of keratinocyte delivery in burns and wound healing and future therapeutic cell delivery options with a special interest in hydrogels and spray devices for cell delivery.

## 2. Skin

### 2.1. Epidermis

The skin is the largest organ of the body and has a barrier function, preventing the passage of water, electrolytes and pathogens (Fig. 1). The epidermis is predominantly formed from highly specialized epithelial cells called keratinocytes. Other cells which can be found in the epidermis include Langerhans' cells, melanocytes and Merkel cells, which are responsible for immune regulation, pigmentation and sensory function. Keratinocytes play a key role in epidermal restoration following injury through proliferation and re-epithelialisation (Fig. 2). Solely epidermal injuries will achieve re-epithelialisation from proliferated keratinocytes and heal by regeneration without scarring [8,9]. Differentiated keratinocytes perform their barrier function through the provision of a mechanical barrier in the formation of a keratinised layer and by reacting to invasion of pathogens via release of pro-inflammatory mediators which subsequently attract leukocytes to the site of invasion.

#### 2.1.1. Keratinocyte differentiation and proliferation markers

Keratinocytes proliferate from the basal cells of the innermost layer of the skin (*stratum basale*). The epidermal stem cells are attached by hemi-desmosomes to the *stratum basale* and can divide into either more stem cells, which persist indefinitely and to maintain the layer's regenerative capacity, or into transit amplifying cells which have limited division potential. As the transit amplifying cells continue to divide and proliferate, differentiation occurs. Throughout this differentiation process, the keratinocytes migrate upwards towards the *stratum spinosum* and *stratum granulosum* to eventually become corneocytes which form a relatively impermeable outer layer, the *stratum corneum*. Once fully differentiated, these corneocytes lose their nucleus and cytoplasmic organelles and will eventually be shed off via desquamation. The estimated time for turnover from epidermal stem cell to desquamation in healthy human skin is around 39 days [10].

During this process, keratinocytes express several differentiation proteins including keratins which are intermediate filament proteins in epithelial cells. Keratins play a host of important function including the provision of structural support, protection of epithelial cells from mechanical and non-mechanical stress and the regulation of apoptosis and protein synthesis [11]. There are 37 known functional human epithelial keratin genes, divided in type 1 and 2 genes. Mutations in these genes are associated with skin diseases such as epidermolysis bullosa simplex (keratin 5, 14) with structural weak epidermal basal cells or epidermolytic hyperkeratosis (keratin 1 and 10) [12]. Keratin expression is frequently used as a marker for epidermal proliferation and differentiation in cell culture, with keratin 14 (K14) being used for the

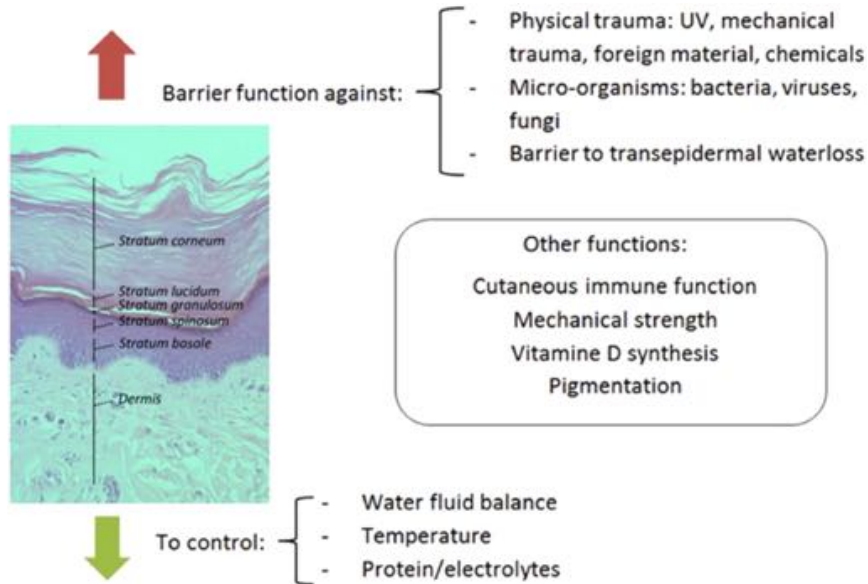


**Fig. 1.** Layers and function of the skin. The uppermost layer of the skin is the epidermis. The epidermis consists of 5 main layers described from deep to superficial: stratum basale, stratum spinosum, stratum granulosum, stratum lucidum and stratum corneum. The epidermis has two distinct functions: a protective barrier function against trauma and fighting off pathogens as well as a controlling function regulating body temperature, fluid and electrolyte balance. Other functions of the epidermis include production of vitamin D, pigmentation, providing mechanical strength and it has a role in cutaneous immune function.

[Source: histology image provided by Dr. G. M Reynolds PhD CSci FIBMS, Liver Unit of Queen Elizabeth Hospital Birmingham, UK. Image adapted by Britt ter Horst, with permission from G M Reynolds.]

basal layer and keratin 10 for the spinous layer. Other differentiation markers starting at the basal layer are K5, and K15, spinous layers K1 and K10, transglutaminase and involucrin, at the granular layer. Filaggrin, loricrin and caspase-14 activation are hypothesised to play a role in terminal keratinocyte differentiation [13–15]. (Fig. 2).

### 2.1.2. Factors promoting keratinocyte differentiation

A major regulator of keratinocyte differentiation is the calcium gradient. Extracellular calcium concentration is lowest in the stratum basale and gradually increases until the stratum granulosum. Elevated levels of extracellular calcium concentrations stimulate formation of intercellular contacts and the increase of intracellular free calcium concentrations via transmembrane calcium influx, which subsequently initiates differentiation via stimulation of the calcium receptor (CaR) [14]. This has consequences for the culture technique of keratinocytes *in vivo*, high calcium concentration induces differentiation, whereas in low calcium concentration keratinocytes remain proliferative [14–16].

E-cadherin provides adherens junctions for adhesion between cells which is crucial for keratinocyte differentiation. In addition, following a signalling pathway e-cadherin can increase the intracellular calcium concentration [14]. Furthermore, 1,25-Dihydroxyvitamin D3 (Vitamin D3) is known to influence keratinocyte differentiation by regulating gene expression and modulating calcium concentrations [17,18].

Logically, factors that promote proliferation will inhibit differentiation of keratinocytes. Factors known to promote proliferation are TGF- $\alpha$ , vitamin A, transcription factor p63 and epidermal growth factor (EGF).

### 2.1.3. Keratinocyte interaction with other epidermal cells

Within the epidermis, keratinocytes interact with other surrounding cell types for example, melanocytes. Melanin production (melanogenesis), occurs in the melanocytes and protects the DNA of melanocytes and keratinocytes from ultraviolet radiation and contributes to the colouration of the skin. Keratinocytes take up melanin via the melanin containing melanosomes produced by melanocytes [19].

The interactions between keratinocytes and fibroblasts in wound healing have been well described in literature, where a double paracrine signalling concept is proposed. Keratinocytes instruct fibroblasts to produce growth factors and cytokines such as keratinocyte growth factor, fibroblast growth factor-7, GM-CSF and IL-6 [20]. Consequently, expression of these growth factors initiates keratinocyte proliferation. The transcription factor activator protein-1 seems to play an important role in this process [21]. Furthermore, under the control of keratinocytes, fibroblasts can obtain a myofibroblast phenotype, which is important for wound contraction [20].

### 2.2. Dermis and basement membrane

Underneath the epidermis, the dermal layer acts a support network, providing strength and elasticity to the skin. Fibroblasts are the key cells of the dermis. Fibroblasts are responsible for the production and maintenance of the extracellular matrix which is formed by fibrous components (collagen and elastin) embedded in non-fibrous elements such as proteoglycans and glycosaminoglycans (GAGs). Collagens are the main structural element of the extracellular matrix (ECM) and provide tensile strength, regulate cell adhesion and

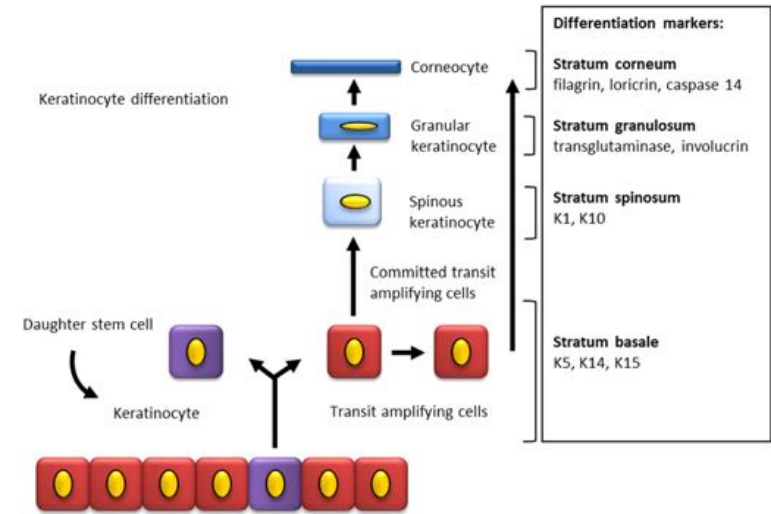


**Fig. 2.** Keratinocyte differentiation and markers. Diagram showing differentiation of keratinocytes in the epidermis with expression of stratification markers. Basal keratinocytes express Keratin 5, keratin 14 and keratin 15. When keratinocytes differentiate they move upwards into the suprabasal layers: stratum spinosum, stratum granulosum and finally stratum corneum. Differentiating keratinocytes express specific markers in each epidermal layer.

[Source: Britt ter Horst].

support migration. Other cellular components include endothelial cells, smooth muscle cells and mast cells [22]. The vascular deep and superficial plexus lie within the upper and lower part of the reticular dermis respectively and supply the dermis and epidermis. The epidermis and dermis are firmly connected by the basement membrane, and the epidermal-dermal junction is bordered and stabilized by the anchoring of keratinocyte-derived collagen (type VII) fibrils into the dermis. Additionally, collagen XVII, a structural component of hemidesmosomes, mediates the anchoring of basal epithelial cells to the basement membrane [23]. If this junction is disrupted, serious morbidity such as seen in epidermolysis bullosa can occur [12].

Several structures originate in the dermis and extend into the epidermis such as sensory nerves, sweat glands and hair follicles. Hair follicles are lined with epidermal keratinocytes and contain multipotent stem cells [24]. Therefore, if the dermis is only partially injured these adnexal structures can deliver cells that can proliferate, migrate and regenerate the epidermis. However, the dermis lacks the intrinsic capability of regeneration and heals by fibrosis and scar formation. Sensory nerves are responsible for mediating pain and itch, control inflammation and there is evidence that shows that they may also influence the remodeling phase [9]. After skin injury the body starts a remarkable healing process which often results in complete regeneration.

### 3. Wound healing and keratinocytes

#### 3.1. The role of keratinocytes in wound healing

The skin barrier function can be disrupted by trauma such as a thermal injury. Wound healing usually occurs via four overlapping phases; haemostasis, inflammation, proliferation and remodeling. Normally this process is sufficient to allow the skin to repair itself after injury. However, extensive skin loss, as seen in burn victims, requires intervention to allow for tissue restoration. Burn injuries are often caused by

heat, however, electricity, radiation, chemicals or friction can also result in similar injuries clinically [25]. Following thermal injury, a complex healing process will start with the involvement of numerous specialized and interacting cells, molecules and pathways. The cellular response involves macrophages, platelets, fibroblasts, epithelial and endothelial cells. In addition to the various cellular interactions, proteins and glycoproteins such as growth factors, cytokines, chemokines, inhibitors and their receptors can also influence healing. Although, burns heal differently from normal wound healing, the phases of healing remain the same [26]. Keratinocytes and fibroblasts play an important role in the proliferative phase which is focused on the replacement of the damaged ECM and restoration of tissue structure and function. Activation of keratinocytes and fibroblasts by macrophages via cytokine and growth factor release causes angiogenesis, collagen production, ECM production and epithelialisation [27].

#### 3.1.1. Angiogenesis

The restoration of the vascular network is essential as angiogenesis supports cell activity by providing oxygen and nutrients to the wound bed. Once endothelial cells are activated by macrophages, they loosen their cell to cell junctions in order to migrate. This process as well as endothelial proliferation is encouraged by a hypoxic and acidotic environment which is typically found in wounds. Finally, revascularisation occurs when sprouted vessels organise into capillary networks. Vascularisation consequently neutralizes the hypoxic and acidotic wound environment and leads to decreased production of angiogenic factors. This eventually results in reduction of endothelial cell migration and proliferation [8,28].

#### 3.1.2. Epithelialisation

Within hours of injury re-epithelialisation starts with a vital role being played by keratinocytes. The quantity of epidermal stem cells residing in stem cell niches such as in the hair follicles, sebaceous glands

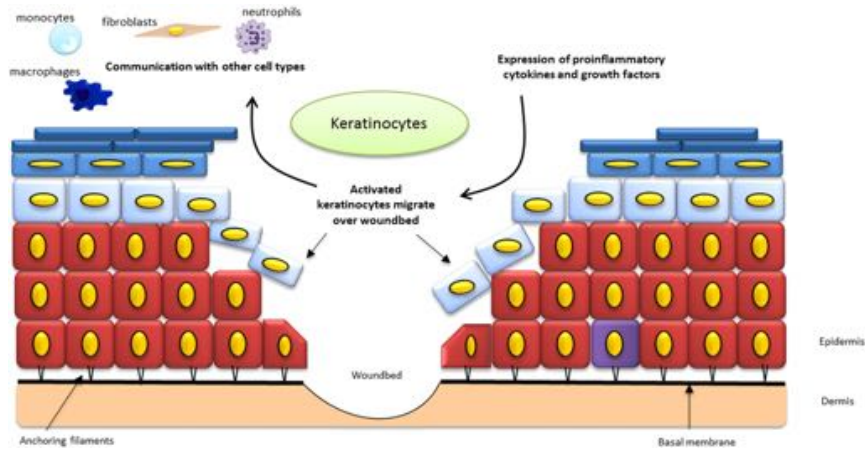


**Fig. 3.** Role of keratinocytes in re-epithelialisation. Schematic illustration of a skin injury with keratinocytes as key cells. Keratinocytes are activated via pro-inflammatory cytokines and growth factors released in the wound bed. Once activated, keratinocytes from the wound edges and dermal appendages migrate over the provisional matrix and finally close the defect in a process called epithelialization. When the basal layer is spared from injury, basal keratinocytes can support this process by upward migration as occurs in non-injured skin. Activated keratinocytes communicate with other cell types present in the epidermis. Epithelial cells proliferate and differentiate to achieve a stratified epithelium with restoration of the barrier function of the skin. Maturation of the wound continues over a period of several months with fibroblasts remodeling the underlying dermis. [Source: Britt ter Horst].

and basal layers of the interfollicular epidermis determines the regenerative capability of the skin [8,24].

Activated by growth factors released by macrophages, keratinocytes migrate to the wound bed and fill the defect (Fig. 3). In order for keratinocytes to start their migration they undergo phenotypical alterations by loosening of intercellular adhesions, although some desmosome contacts are sustained [8]. Furthermore, cells can separate from the basal layer once hemidesmosomes are disrupted which allows them to migrate laterally [8,29]. When integrin receptors are expressed, the keratinocytes flatten and the altered basal keratinocytes migrate over the granulation tissue to form a monolayer of epithelial cells, but remain under the non-viable eschar of the burn wound. While moving they secrete proteolytic enzymes that enable the degradation of provisional matrix and promotes further cell migration [30]. After a confluent sheet of cells covers the wound bed, the cells then divide to form a multi-layered stratified epithelium and mature under the influence of TGF- $\beta$ 1 and TGF- $\beta$ 2 [31].

Keratinocytes play a vital role in especially the proliferative phase of burn wound healing leading to epithelialisation and restoration of the vascular network. For this reason and the possibility of in vitro keratinocyte culture, keratinocytes are considered an excellent candidate for cell transplantation.

### 3.2. Pathophysiology of burn injury

Major burn injury, defined as approximately 20% of the total body surface area (TBSA) burned, causes burn shock due to severe haemodynamic and haematopoietic dysfunction [26] secondary to immediate evaporative and direct fluid losses [32], extensive loss of proteins, reduced colloid oncotic pressure and wound oedema development. Without intervention the fluid loss will result in desiccation of deeper tissues and further cell death leading to an increase in wound depth. A moist wound bed is necessary for epithelial cell movement and therefore for successful re-epithelialisation [9]. Furthermore, with disruption of the barrier function of the skin, microorganisms have easy access and when entering the microcirculation can cause systemic infection.

Presence of these acute systemic responses are related with increased morbidity and mortality numbers [33,34], especially in the elderly [1].

### 3.3. Rational for keratinocyte transplantation

Traditional therapy for severe burns is surgical debridement and autologous skin graft. However, with extensive burn injury healthy donor site is scarce and alternatives to restore skin function are necessary. When rapid epithelialisation can be achieved the skin barrier function is restored and this can determine a patient's likelihood of survival. Clearly, it is important in the treatment of a burn injury to focus on quick re-epithelialisation. Therefore, development of successful and efficient autologous skin replacement techniques is highly desirable. Wound closure will not occur without epithelialisation and epithelialisation will not occur without the presence of keratinocytes in the wound bed [8]. To achieve faster re-epithelialisation, keratinocyte transplantation was introduced as part of the burn wound care arsenal over 30 years ago. However, the original autologous keratinocyte transplantation technique has several disadvantages which has spurred researchers to seek for improvements in cell culture technique, delivery systems and also the optimisation of the timing of keratinocyte transplantation [35].

## 4. Cell transplantation technology

### 4.1. Cell source

Keratinocytes and their progenitor cells can be sourced locally from stem cell niches in hair follicles. Several stem cell niches are known: mesenchymal stem cells (MSC) resident in the dermal papilla and multipotent hair follicle stem cells (HFSC) and melanocyte stem cells in the superior bulge [36]. HFSCs are essential for normal morphogenesis of hair follicles, sebaceous glands and contribute to formation of the three epithelial cell lines [37]. Progenitor cells also reside in the bone marrow and could arise from embryonic cell lines [38].

### 4.2. Methods of human keratinocyte cell culture

#### 4.2.1. Historical development of keratinocyte culture

The first successful in vitro human keratinocyte expansion, achieved by Rheinwald and Green in 1975, paved the way towards autologous cell transplantation in burn care [39]. Keratinocytes were successfully cultured in the presence of fibroblast feeder cells. However, to prevent these fibroblasts from outgrowing the keratinocyte population, irradiated murine 3T3 fibroblast feeder cells, which have lost their mitotic ability but remain metabolically active, were used [39]. Besides the use of feeder cells, culture media often contains fetal calf serum with growth factors, hormones and antibiotics [39–41]. Keratinocytes are able to be grown into colonies and subsequently form a stratified epithelium and human keratinocyte stem cells were proven to have an enormous proliferation potential. Subsequently, small cell sheets of two or three layers of confluent keratinocytes were produced and not long after, the first human transplantation became a reality [42,43].

Keratinocytes cultured for clinical use must have the regenerative capability to form an effective epidermis after transplantation. It is thought that in vitro differentiating keratinocytes do not contribute significantly to regeneration in vivo [44]. Instead, keratinocyte stem cells and their transient amplifying cells seem to have excellent regenerative capacities [45]. Thus, culturing keratinocytes that keep the ability to produce progeny once transplanted, seems key for successful epidermis formation following transplantation.

The degree of differentiation in vitro can be controlled by the method of culture. Fully differentiated keratinocytes (confluent) multilayers as well as pre-confluent single cells can be produced and delivered to the wound bed [16,46]. In a histological comparison of cultured pre-confluent and uncultured keratinocytes seeded on a collagen-GAG matrix in a pig model, both provided a fully differentiated epidermis in 14 days. A thicker and confluent cell layer, however, was obtained more rapidly with the cultured cells [47]. The original culture method has been the subject of much debate, because the murine fibroblast feeder layers can potentially result in transplantation of animal components with the keratinocyte product. Due to the serious risk of animal-derived disease transmission to human epithelium in the transplantation process, it is not advised to use undefined xenogenic materials in the treatment of patients. Additionally, radioactive irradiation of murine fibroblasts in this technique is accompanied with higher costs and potential uptake of irradiated DNA via the murine fibroblasts into the transplanted keratinocytes might cause cell destruction [48].

#### 4.2.2. Progress towards xenobiotic free culture techniques

To limit or exclude the transmission risk, other keratinocyte culture protocols without feeder cells and limited or no use of xenogenic media products have been developed [16,49]. Jubin et al. showed that human keratinocytes can be successfully expanded in co-culture with non-irradiated autologous human fibroblasts in Rheinwald and Green but still required medium supplemented with fetal bovine serum (FBS) to maintain their proliferative phenotype in vitro [50]. A further approach to minimise xenogenic products in culture media was introduced when serum free medium was used for the expansion of keratinocytes with non-irradiated human fibroblasts on several substrates [49]. However, FBS still had to be used to expand the human fibroblasts initially.

Although the culture media are free of serum, often other products used in the culture media still contain animal-derived proteins. This could be solved by the use of only human material, however the risk of infection remains and high costs in an already expensive process makes this option less favourable. Successful culture of human keratinocytes in a serum-free and feeder-free culture was demonstrated in vitro in a skin equivalent model by Coolen et al. With the addition of collagen type IV, serum substitute and keratinocyte growth factor (KGF) a differentiated epidermis could be formed

[51]. Lamb et al. demonstrated that although keratinocytes grown in serum-free and feeder-free conditions did show sufficient propagation, these cells were not able to support mature epidermis formation in an in vitro skin model. However, when re-introduced to a serum-containing media they then did form a stratified epidermis. Moreover, when heat-inactivated serum was used an improved stratified epidermis was formed, indicating that serum-products also contains (heat-sensitive) factors that can inhibit in vitro epidermis formation [52].

Lenihan et al. compared three commercially available feeder-free media systems; CnT-07 medium (CellnTech, Bern, Switzerland), EDGS (Gibco), S7 (Gibco) with the original Rheinwald and Green method [39] for expansion of human keratinocytes for clinical usage. A maximum of 3 weeks culture time (passed twice) was allowed, as the ideal transplantation window was considered between 4 and 20 days. They found that all three feeder free culture media supported keratinocyte growth. However, the only fully xenobiotic free media (S7) had a low cumulative population doubling time and therefore did not reach sufficient cell numbers to be considered for clinical usage at day 21 and was therefore excluded from further analyses [53].

Using feeder free and serum free media is less labour intensive and beneficial for use in the clinical setting, further research will have to show whether keratinocytes maintain their proliferative potential in vivo. Besides elimination of xenobiotic materials from culture media, the elimination of antibiotics is a further goal to improve keratinocyte cell expansion for usage in the clinical setting [54].

#### 4.2.3. Additions to keratinocyte culture

To further encourage and optimise skin regeneration following burn injury, improvements have been made to the keratinocyte transplantation process. These have included the addition of multiple other cell types and growth factors during keratinocyte culture or transplantation.

The addition of melanocytes in the keratinocyte culturing process has been proposed to solve the problem of potential irregular pigmentation of the post burn scar. Co-culturing of keratinocytes with melanocytes has been investigated in patients with vitiligo and in full thickness wound healing in animal models [55–58]. In humans, more evidence is available for uncultured cell suspensions containing keratinocytes and melanocytes for the treatment of hypopigmented lesions [59–62]. However, these pilot studies are limited by small sample sizes and lack of controls. Controlled clinical studies are needed to support the findings before this technique can be accepted as standard clinical practice.

Cultured epithelial autografts lack a vascular plexus and burn wounds often have insufficient vascularisation due to the disruption of the dermal layer. Therefore, approaches to promote angiogenesis via the addition of autologous or allogenic endothelial cells into skin grafts have been proposed [63,64]. Also, adipose derived stem cells (ASCs) have received attention with respect to their potential to enhance wound healing. Huang et al. seeded human ASCs onto a dermal acellular skin substitute in vitro to enhance vascularisation. When transplanted to full thickness wounds in nude mice, an increase in blood vessel density was found two weeks post transplantation compared to controls [65]. Another approach is to add growth factors like epidermal growth factor (EGF) [66]. Additionally, co-delivery of cultured keratinocytes with EGF in a fibrin matrix demonstrated improvement of epidermal regeneration in full thickness wounds in a murine model [67]. Furthermore, Supp et al. genetically modified keratinocytes with an overexpression of vascular endothelial growth factor (VEGF) to stimulate angiogenesis in skin substitutes in animal studies [68,69]. Besides adding factors, modifications of the 3D structure of skin substitutes to stimulate faster ingrowth of vascular structures have also been proposed [70]. Of interest from a tissue engineering perspective, is whether transplanted cells actually survive and function in vivo.

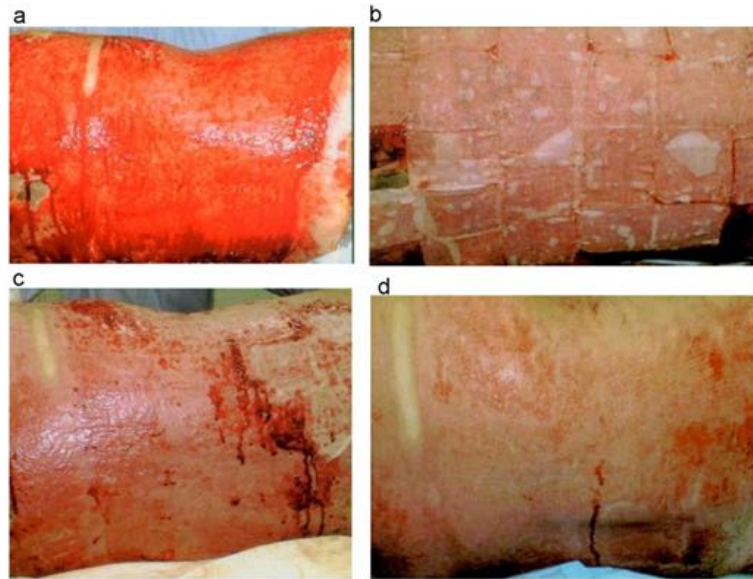


**Fig. 4.** Burn wound coverage with cultured epithelial autografts applied in sheets. In this example, successful burn wound healing in about 2 weeks was achieved when the sheets were removed a week after application. a) Deep second degree burn in the back of a 29-year old patient after excision of the burn b) application of cultured keratinocyte sheets c) removal of sheets 8 days after surgery and d) complete healing 16 days after surgery.

[Reprinted from Burns Volume 41, Issue 1, Pages 71–79, Cultured autologous keratinocytes in the treatment of large and deep burns: A retrospective study over 15 years, Celine Auxenfans, Veronique Menet, Zulma Catherine, Hristo Shipkov, Pierre Lacroix, Marc Bertin-Maghit, Odile Damour, Fabienne Braye, Copyright (2017), with permission from Elsevier.]

#### 4.3. Keratinocyte viability after transplantation

Cell survival of transplanted keratinocytes *in vivo* is of great interest for tissue engineering purposes. Vernez et al. evaluated the cell viability and apoptosis balance in clinical samples taken from cultured epidermal autografts prior to transplantation [71]. Although, all samples showed high levels of cell viability and low levels of apoptosis, variable biological activity of certain parameters between samples of different patients was observed. It was suggested that this could impact on therapeutic efficacy [71]. In a pig model Navarro et al. found no altered cell viability before and after spraying a suspension of cultured keratinocytes to full thickness wounds [72]. Duncan et al. examined cultured human keratinocyte proliferation measured with the MTT assay after spray delivery to a de-epidermalised dermis (DED) *in vitro* and found no significant cell death or reduced cell proliferation [73]. These studies seem to support that cells remain viable and maintain proliferative capability after spray cell delivery to a wound bed.

### 5. Application types of keratinocytes transplantation

#### 5.1. Introduction: grafting of burn wounds

Ambroise Paré (1510–1590 CE) was probably the first to describe the surgical intervention for early excision of burn wounds [74]. Surgical burn care has progressed tremendously since then and methods which have now become well established in burn care include early excision of burn wounds, the development of autologous and allogenic skin grafts and the use of skin substitutes [75].

Techniques involving transplantation of healthy human skin to damaged areas are still the gold standard in deep or full thickness burn

wounds. However, challenges arise when large areas are affected and donor sites are scarce. Subsequently, many skin graft expansion techniques have been developed to reduce donor site size, these techniques include meshing of the graft (maximum expansion ratio of 1:9), modified meek technique (expansion ratio of 1:9), epidermal blister grafting (expansion ratio of 1:1) and several techniques of micro grafting such as epidermal CelluTome™ micro-grafting (expansion ratio: 1:6), or Xpansion® micro-grafting (maximum expansion ratio: 1:100). Developers of cellular based techniques claim to deliver even higher expansion rates, such as cultured epithelial sheets (expansion rate 1:1000) and uncultured cell suspensions (maximum expansion rate 1:100) [76,77]. However, to the knowledge of the authors no other studies have been able to support these findings.

Furthermore, procedures to harvest skin are time consuming, can lead to longer healing times with prolonged hospital stay and can be accompanied by donor site complications. Additionally, skin grafts do not always meet the desired cosmetic outcomes.

Therefore, methods to enhance the results of skin grafting and alternatives to it have been subject of much research in the last few decades. Specifically, progress towards a permanent epidermal replacement or its improved regeneration is the main goal of cellular based therapy. In Fig. 6 different methods of autologous keratinocyte transplantation are schematically summarized.

#### 5.2. Cultured keratinocyte sheets

##### 5.2.1. Cultured autologous keratinocyte sheets

In 1981, O'Connor et al. reported the first transplant of cultured autologous keratinocytes to treat a burn injury [43]. Cultured epithelial autografts (CEA) were developed to replace the epidermis and restore the

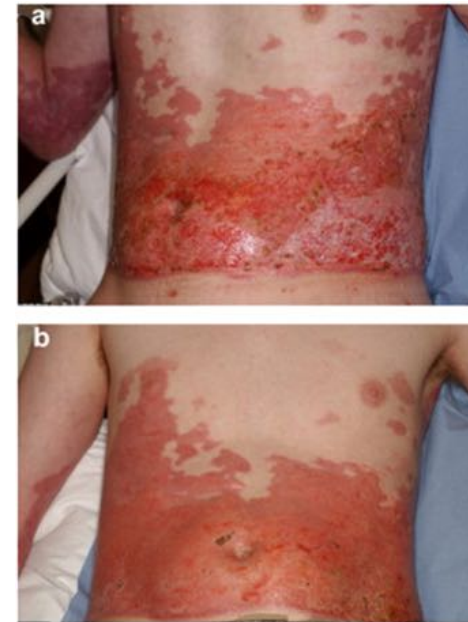


**Fig. 5.** Spray delivery of cultured keratinocytes to enhance burn wound healing. In this example, a mixed depth burn to the abdomen was treated with solely sprayed cultured keratinocytes (no additional mesh grafting) 27 days after injury. The wound was considered to have healed completely 10 days after treatment. Unfortunately, long term outcomes in terms of scar quality were not available for this patient.

[Reprinted from Burns Volume 36, Issue 3, Pages e10–e20, Sprayed cultured autologous keratinocytes used alone or in combination with meshed autografts to accelerate wound closure in difficult-to-heal burns patients, S. Elizabeth James, Simon Booth, Baljit Dheansa, Dawn J. Mann, Michael J. Reid, Rostislav V. Shevchenko, Philip M. Gilbert, Copyright (2017), with permission from Elsevier.]

barrier function of the skin [78,79]. In the last three decades CEAs have been adapted and introduced to the clinical setting (Fig. 4).

Nowadays, several commercialised bioengineered skin products derived from autologous cells are available. In general, clinicians harvest autologous skin and the company produces a graftable substrate seeded with the autologous cells for clinical use in approximately 2 weeks (Epicel, Genzyme, Cambridge, MA and Laserskin, Fidia, Italy). The timeframe wherein viability of the grafts can be ascertained (shelf-life) is 24–48 h. These services will often involve high costs and a certain waiting time and narrow application timeframe.

In 2007, the FDA approved the use of CEAs for use in patients with deep dermal or full thickness burns greater than, or equal to 30% TBSA (Epicel, Genzyme, Cambridge, MA) [43,80,81]. The main advantage of cultured epithelial autografts is that large areas of the body can be covered with autologous cells derived from a small biopsy and improvement in the speed of re-epithelialisation has been reported. In terms of cosmetic results, CEA seems to have better results when compared to wide mesh autograft in extensive burns [82]. However, several authors who have reviewed the use of cultured epithelial autografts in burn care have found variability in terms of graft take and cosmetic outcomes [46,83,84].

A major disadvantage of this technique is the long time-interval between biopsy and grafting. Although the average culture time has improved from 5 [43] to about 3 weeks [85,86], variability among patients

has been described, especially among different age groups [87]. Following burn excision, the wound can be temporary covered with allograft and/or xenograft dressings for several weeks until CEA is ready. However, this is related to a higher risk of wound colonization and infection [46]. The ideal timing for keratinocyte transplantation is difficult to determine as it is dependent on several factors including hospital facilities and patient conditions [86,88].

Furthermore, both short and long term clinical limitations such as the formation of bullae, poor take rates, fragility of the sheets and wound contractures have been reported [88–90]. These may be due to the lack of a dermal component that is necessary to support the new epidermal layer.

The restoration of the dermis is important for the skin to regain mechanical strength and to facilitate adherence of the new or transplanted epidermis [36]. Although in one study, an advanced application technique with allograft wound bed preparation and combination of CEA with wide meshed autograft seems to improve take rates up to 84% [91].

Cell culture is an expensive process and the cost/benefit relationship of this method is heavily debated [92]. Finally, the potential of graft site malignancy after keratinocyte transplantation has been highlighted [93, 94]. However, the type of malignancy reported, squamous cell carcinoma, is also known to occur in burn wounds and scars in the absence of keratinocyte transplantation [95].

#### 5.2.2. Introduction of dermal substitutes including cultured keratinocytes

With a complete absence of a dermal component, the cultured keratinocytes are thought to be of limited value in treating full-thickness burns due to the poor quality of the resulting epidermis. Consequently, this has led researchers to optimise the wound bed via the use of allogenic or artificial substitutes prior to keratinocyte transplantation. A further approach is to grow or seed the cultured keratinocytes on a (dermal) substitute to facilitate secure transplantation and improve healing potential [96]. This concept was introduced by Hansbrough and Boyce in 1989 [97]. Many types of delivery systems have since followed, and have been extensively discussed in the literature throughout the years [98–100].

Limitations in keratinocyte cell culture methods and transplantation have impeded the widespread use of this technique in the clinical setting. The use of single-cell suspension was introduced predominantly to shorten the culture time.

#### 5.3. Autologous keratinocyte transplantation in suspension

To overcome the main negative features of epidermal sheets which are the long culture times and poor cell adhesion to the wound bed, delivery of cells in suspension form has been investigated.

While epidermal sheets contain cultured confluent cells that are passed the phase of exponential growth, cell suspension delivery systems can be designed to contain pre-confluent cells. Ideally, these cells are harvested or passaged when reaching a 70–80% coverage of culture dishes to ensure their proliferative capability and avoid confluence, hence the term pre- or sub confluent cells. When a sufficient cell number is reached (after approximately 2 weeks of culture), the cells are detached and suspended in a saline solution for clinical use. As differentiation *in vitro* is not desirable, keratinocytes in a pre-confluent suspension form is often preferred for transplantation (Fig. 5).

Nowadays, several commercially available spray cell delivery products are used clinically to enhance burn wound healing. These techniques can be categorised by the type and level of confluence of the transplanted cells.

##### 5.3.1. Pre-confluent keratinocytes suspension

The use of pre-confluent cells can shorten culturing time and facilitate more rapidly available cellular grafts, which in theory is likely to

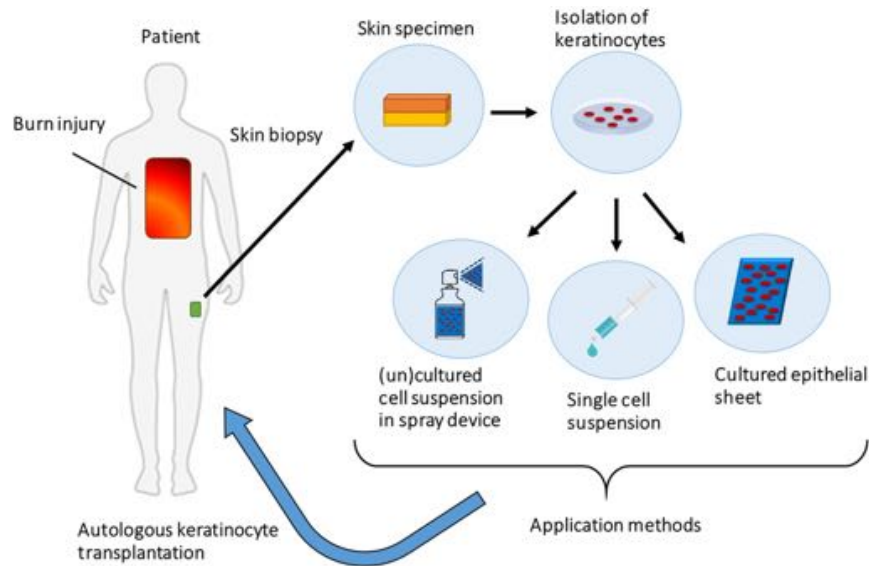


**Fig. 6.** Methods of autologous keratinocyte transplantation to burn wounds. In patients with burn injury keratinocytes can be isolated from a small skin biopsy as illustrated above. The autologous keratinocytes can be cultured and delivered to the wound bed of the patient by several methods. First to be developed was a sheet of cultured epithelial cells, thereafter a single cell suspension applied to the wound by dripping from a syringe and latest development is application of cultured or uncultured cells in single-suspension with a spray device. [Source: Britt ter Horst].

reduce the risk of wound infections and consequently the length of hospital stay [101,102]. A commercial suspension consisting of autologous pre-confluent keratinocytes has been available since 2007 for aerosol delivery. Hartman et al. treated 19 patients with deep dermal face and neck burns with a spray apparatus with an estimated spray pressure of 8.2 mm Hg, which seems to be a surprisingly low delivery pressure using autologous cultured epithelial cells of 80–90% confluence at the end of passage 0 [103].

An alternative commercially available cell spray system is Keraheal<sup>™</sup>, which was developed by MCTT, Korea. This system utilizes an autologous non-differentiated pre-confluent keratinocyte suspension, which is sprayed to the burn wound followed by fibrin spray application. The Keraheal<sup>™</sup> methodology is similar to conventional CEA and requires 2–3 weeks of culture time, but the cells are provided in a suspension instead of sheet. To date, two single centre retrospective studies have evaluated the clinical outcomes of the sprayed cell suspension in combination with wide meshed skin grafts in a total of 39 (6 patients who died or were lost to follow up were excluded from follow up analyses) patients with severe burns. Graft take rate two weeks after application is surprisingly different between the studies, but after 8 weeks the take rates are both above 90%. A follow up of 1–2 years was achieved in both studies with a Vancouver scar scale (VSS) assessment. Scar evaluation 12 months after surgery was lower in Lee et al. with an average VSS of 3 compared to an average VSS of 5 in Yim et al. [101,102].

Various developers have introduced adjustments to the technique in terms of the application device, cell detachment process, confluency of transplanted cell and application setting in order to meet clinical needs.

### 5.3.2. Uncultured keratinocytes suspension

A further approach is the use of uncultured autologous cells for direct application onto burn wounds without pre-processing in a tissue

culture lab. In a single procedure, a small piece (2 × 2 cm) of skin is harvested by the surgeon and then placed in an enzymatic solution followed by manual scraping of the epidermal layer, the skin specimen is placed in a buffer solution and subsequently filtered before use. The company provides a kit which allows the clinical team to process the cells in a single treatment session without the need for a lab technician or transport of the cells elsewhere [83,104]. The use of an uncultured mixture of autologous epidermal cells (keratinocytes, melanocytes, dermal fibroblasts and Langerhans cells) was introduced to clinical practice in 2005 as a standardized spray device under the name ReCell (Avita Medical Europe Ltd., Melbourne, UK).

The purported benefits of this system are the elimination of lengthy culture times and the delivery of a mixture of autologous epidermal cells.

Since its introduction, several studies have demonstrated promising outcomes with the use of ReCell for acute burn wounds or in the treatment of hypopigmentation. These studies ranged from case reports to larger comparative studies [105,60,106–109]. Although most papers have shown promising results, the potential value of spray cell transplantation in burns is difficult to evaluate due to the heterogeneity of the studies in terms of clinical outcomes explored, patient population, wound characteristics, type of treatment and study design [99]. Gerlach et al. used a similar approach with direct application of an uncultured autologous epidermal suspension on the wound bed using a fine needle spray in a single treatment session. Although, a small number of patients was treated and results were not compared to controls [110, 111]. The question arises whether a large wound area can be covered by the harvest of cells without expansion from a small skin specimen. In an *in vitro* study an expansion ratio of over 1:100 was calculated for uncultured cells sprayed with a density of 10<sup>6</sup> cells/cm<sup>2</sup> for an estimated surface coverage [112]. However, there is no other literature to support the claimed expansion rate.

To allow the comparison of clinical data, it has been recommended by the National Institute for Health and Clinical Excellence (NICE) that studies evaluating spray delivery of uncultured cells need to include at least: the time to 95% healing of the burn wound, length of hospital stay, scar assessment, physical function and cosmetic appearance of the burned area and compare these results with the current standard of care [69]. To date, randomized controlled clinical trials and non-commercial studies investigating effectiveness compared to conventional treatment are lacking. Challenges arise in consistent assessment for burn wound healing as objective non-invasive assessment tools have not yet been incorporated widely in routine burn care and might not be superior to visual expert assessment [26]. Therefore, researchers rely on subjective clinical assessments for acute burn wound healing and late outcomes in terms of scarring [113].

### 5.3.3. Allogeneic neonatal keratinocytes suspension

Several research groups have explored the possibility of the transplantation of fetal allogeneic cells with the purpose of stimulating regeneration of residual cells in the wound. Neonatal foreskin derived allogeneic cells have low immunogenic properties which is preferred in tissue transplantation. This work has resulted in the creation of skin substitutes that have been seeded with allogeneic cells such as Apligraf (Organogenesis, Canton, MA) and OrCel (Ortec International, Inc., New York, New York).

Similar to the developments in autologous cells delivery, allogeneic cell suspensions have also been investigated as an alternative method of cell delivery. A cell suspension, code named HP802–47, which contains allogeneic neonatal non-proliferating human keratinocytes and fibroblasts in thrombin was developed for the use in chronic wounds. Multi-centre randomized controlled phase IIa and IIb studies were conducted and have demonstrated promising outcomes in wound closure of venous leg ulcers [114–118]. Subsequently, a double blinded Phase III study followed in North America and Europe comparing wound closure after HP802–247 treatment or placebo in venous leg ulcers. However, the study was unexpectedly halted in the preliminary stages due to disappointing results [119]. To the knowledge of the authors, no clinical studies have been conducted for the treatment of burn wounds with HP802–247.

### 5.3.4. Other clinical studies using cell sprays

Delivery of mesenchymal stem cell (MSC) to (burn) wounds is considered very promising due their capacity to differentiate into multiple lineages and potential beneficial effects on the immune response [54]. However, only few clinical studies investigated the use of mesenchymal stem cells to treat burn wounds have been performed so far [120–122]. Ueda conducted a pilot study of 10 patients treated with cultured epithelial autograft (CMEA) delivered to deep dermal burn wounds without adverse events and a healing time of approximately 12 days (range 7–14 days) [123].

Iman et al. compared spray delivery versus intradermal injection of autologous cultured keratinocyte-melanocyte suspension to treat hypopigmented burn scars in a total of 28 patients. Although patients might show a beneficial result with pigmentation, no statistical difference in type of application was found [59].

Cell transplantation techniques have changed significantly after the introduction of different cell-carriers and various forms of cell spray techniques. Nevertheless, some shortcomings of the suspension application technique have yet to be addressed.

For example, spraying on an uneven wound bed that often also occurs on a curved body contour, can result in uneven spreading of the cell suspension or dripping off the wound bed [46,124]. A potentially useful development of keratinocyte transplantation is to improve the method of delivery in order to optimise cell delivery to the designated area and stimulate cell adherence to the wound bed. More recently, cell transplantation exploiting hydrogel carriers have gain interest among researchers. In the past decade

biomaterials to mediate cell delivery and accommodate cells in a 3D microenvironment have been investigated. A plethora of synthetic and natural polymers which may form hydrogels have been studied as potential cell delivery vehicles due to their ability to integrate with healthy tissue.

## 5.4. Hydrogels

Hydrogels are defined as polymer networks with the ability to swell and absorb water within their structure. Due to their hydrophilic nature and flexibility they are very similar mechanically to human soft-tissue. Both natural and synthetic hydrogels could be considered for tissue engineering. Natural hydrogels benefit from high biological affinity and are often easily degradable, but the risk of infection transmission and difficulties with purification has increased the popularity of synthetic hydrogels.

[125,126] Biopolymer gels can be formed out of polysaccharides or proteins. For example, polysaccharides obtained from plants (gum acacia, guar gum, starch, psyllium [127]), seaweeds (alginate, agarose, carrageenans), micro-organisms (dextran, gellan gum) or animal derived (chitosan, chitin) (hyaluronic acid) and proteins gained from animal or human tissue (collagen, fibrin, gelatin, elastin) or animal products (silk sericin, silk fibroin) [128].

### 5.4.1. Hydrogels in burn care

Hydrogels currently available for patient care have been reviewed by many clinicians, but a skin substitute that is able to achieve complete skin regeneration has not yet been reported [79,129–131]. However, hydrogels play a promising role in the development of next generation skin substitutes in burn care and are often used as wound dressings [132,133], regenerative scaffolds or delivery devices for cells and therapeutic e.g. drugs, growth factors etc. Hydrogels have several characteristics to promote skin healing such as the ability to absorb and release water, which is useful in regulating burn wound exudate. Furthermore, the architecture of hydrogels can be modified to mimic the body's own extracellular matrix and their tunable mechanical properties can provide customised elasticity and flexibility [125] and make them suitable candidates for skin regeneration [66,134–139].

**5.4.1.1. Chitosan.** Chitosan is a hydrophilic, non-toxic polysaccharide derived from de-acetylated chitin, obtained from crustaceans or fungi [140]. Due to its numerous advantageous characteristics such as the ability to encourage haemostasis, the ability to be modified so that it can be degraded by human enzymes and availability of a variety of formulation forms [141], chitosan hydrogels have been widely used in many biomedical applications. Topical forms of chitosan are used as wound healing stimulating dressings, for haemostasis [142–143] and specifically for use in the treatment of burn wounds [144–145].

Furthermore, the positive influence of chitosan on keratinocyte proliferation and adhesion has been described previously [146] and chitosan as a bio-active polymer is suggested as a promising candidate for tissue regeneration [147].

**5.4.1.2. Alginate.** Alginate is a negatively charged polysaccharide derived from the cell walls of brown algae (seaweed) and has hydrophilic properties. Besides its widespread use in the food and paper-printing industry, it has gained much popularity as a biomaterial due to its non-immunogenicity, low cost, and simple gelation method. Alginate is FDA approved for medical applications and is commercially available as alginate based dressings such as Kaltostat<sup>®</sup> which are widely used in burn treatment [9,148] Alginate dressings are also commonly used for the coverage of donor sites post-skin harvest and has also been successful in the treatment of paediatric burn patients [149].

**5.4.1.3. Fibrin.** Fibrin is a protein which can be derived from human or animal blood. It can naturally form a gel and acts as a haemostatic

agent in the body after tissue injury. For this reason, fibrin has been used as a sealant (fibrin glue) in the medical field [150]. For wound healing, fibrin sealants and gels have been used for the delivery of several cell types such as fibroblasts [151–152], mesenchymal stem cells [121] and keratinocytes [153–155]. Specifically, in keratinocyte spray delivery, additional fibrin sealant seems beneficial for adhesion of the suspension to the (artificial) wound bed [40,124,156]. In contrast, Currie et al. performed a histological and immunohistological analysis and did not show a difference when adding fibrin glue to a keratinocyte spray delivery system in terms of epithelialisation [157].

Furthermore, fibrin has also been explored for keratinocyte transplantation in combination with a dermal substitute. For example, encapsulated keratinocytes seeded in alloderm [158], keratinocytes seeded on a fibrin based dermal matrix containing fibroblasts [153, 159] or as a glue to enhance adhesion of human dermis [160] or Integra [161]. More recently, angiogenesis stimulating factors have been added to fibrin scaffolds to improve regeneration of ischemic tissue [162].

**5.4.1.4. Collagen.** Collagen is the most abundant protein in the human body, it is the main structural protein of the extracellular matrix and has a key role in wound healing [163]. Therefore, many tissue engineered collagen based products have been developed. In 1981, Burke and Yannas developed an artificial dermal replacement based on collagen, which has eventually led to the production of the commercialised dermal substitute Integra [164]. In the same decade, Hansbrough et al. used a collagen-glycosaminoglycan scaffold with attached cultured autologous keratinocytes and fibroblasts in burn wound treatment [97]. Since then, collagen matrices in different forms have been investigated thoroughly in wound healing; as (a) cellular dermal replacements [163–168] or as a bilayered skin substitutes such as OrCel [166], Transcyte [169], Apligraf [170], Integra [171] and Matriderm [63]. Also, collagen hydrogels have been developed for tissue regeneration [64] with autologous cells incorporated to improve burn wound healing [139]. Although widely investigated and used in clinical practice, collagen matrices and hydrogels have a fast degradation when applied to human tissue which can have an undesirable effect. However, the rapid degradation of collagen-based biomaterials can be stabilized through chemical cross-linking [172].

Examples of other hydrogels used for cell delivery in wound healing or specifically burn care are gelatin [173], hyaluronic acid [81,174], silk sericin [70,175] and dextran [66,176].

All the above mentioned hydrogels have been successfully translated to clinical practice and some are part of the standard burn wound treatment arsenal. Hydrogels have advanced burn care as part of tissue engineered skin substitutes, incorporated in dressings, topical creams or as sprayable substance.

## 6. Methods of spray deposition

### 6.1. Spray parameters and cell viability

Cell transplantation can be achieved by several techniques. In this chapter the focus lies on cell transplantation to the tissue via aerosol or spray delivery.

Sprayed cells are expected to be damaged at time of impact to the receiving surface. Following impact, the cell membrane can elongate and deform. Cell rupture and subsequently cell death can occur in largely overstretched cell membranes [177]. More precisely, cells can tolerate a cell membrane area stretch of up to 5% before it becomes detrimental to cell survival. Cell elongation, deformation and subsequent cell survival depends on many variables such as target surface characteristics, viscosity of the transporting fluid/media and velocity of the delivered cell containing droplet, nozzle distance and diameter.

Veazey et al. investigated the cell viability of xenogeneic 70% confluence fibroblasts immediately after aerosol delivery with a support system and their growth behaviour in a culture model [178]. The airbrush

system used could be adjusted for different nozzle diameters (312, 494, 746  $\mu\text{m}$ ) and air pressure at delivery (ranging from 41 kPa to 124 kPa). It was found that cell viability directly measured post aerosol delivery significantly decreased with higher pressure and smaller nozzle diameter. For cell proliferation studies, only the highest pressure with smallest nozzle diameter combination showed a delayed population doubling time and the time to reach confluence was doubled [178].

In another in vitro study with 80% confluence neonatal dermal rat fibroblasts an analytical model was proposed to describe the impact of several spray parameters in a droplet-based spray application to the cell viability. Stiffness of the tissue surface, high cell-viscosity and cell-velocity had a negative influence on cell viability post spray impact, whereas a larger cell-containing droplet diameter had a positive effect on cell viability. The latter was explained as a cushioning effect of the droplet to the surface protecting the cell within the droplet [179].

In other words, cell viability is expected to be highest in large and low-viscosity single cell-containing droplets sprayed with low-velocity onto a soft tissue surface.

Wounds would serve as a soft receiving surface for cell transplantation and can be expected to be highly viscous when hydrogels are used. Hence, tailored spray devices, with pressures and nozzle diameters optimized for cell survival can play an important role in improving cell delivery.

### 6.2. Spray systems

Spray systems are being widely used in many industries. Surprisingly little research has focused on the influence of the type of aerosol device on mammalian cell survival after transplantation.

#### 6.2.1. Low and high pressure spray nozzle

Fredriksson et al. evaluated 7 different application techniques for cell transplantation on cell viability and proliferation in an in vitro study. Based on current clinical practice they included commercially available spray systems: spray nozzle systems such as the Harvest SK/S Spray Applicator Kit®, high and low pressure Tissomat applicator in combination with a Duploject™ spray nozzle, a Duploject™ spray nozzle without additional pressure control and two non-spray systems: pipetting and paintbrushing. This study showed an approximate 50% drop in viable cell count immediately after transplantation when using a high pressure device (200 kPa) and a further decline to nearly 40% viable cell count after 2 weeks of culturing, which was comparable to the paintbrush [180]. In contrast, Harkin et al. measured a 20% higher post aerosol delivery cell survival with similar pressures [156]. The immediate cell survival is comparable with other studies utilising low pressure delivery methods/systems [178]. Although no statistically significant differences were displayed, the poorest cell viability after 2 weeks was seen in the high pressure device and paintbrush [180]. Fredriksson et al. hypothesised that an additional application of fibrin sealant might improve cell survival. Furthermore, the authors emphasized the importance of measuring the proliferation capacity of cells post aerosolisation, since a large difference was seen in their data among the different devices. Interestingly, the delivery pressure and nozzle diameter of clinically used manual cell spray devices is unclear and might impact on cell viability and proliferation capacity.

Aerosol delivery with handheld airbrush systems with adjustable air pressure supply have also been previously investigated and studies have demonstrated consistent acceptable cell viability of above 80% with low delivery pressure (below 69 kPa) [171,178]. According to Veazey et al., this system should also be compatible with alginate-, gellan, hyaluronic and hyaluronate-based hydrogel cell carriers [68]. However, to date, there is no published data to support this statement.

#### 6.2.2. Liquid atomizer

Liquid atomizers or nebulizers originally designed for aerosol drug delivery to the trachea have also been explored for cell delivery. In burns, inhalation injury can occur with damage to the trachea and drug- or cell delivery could be used to improve the healing of these injured areas. Sosnowski et al. investigated the use of 5 different atomizers for cell delivery to the trachea in terms of cell viability. However, a droplet size below 20  $\mu\text{m}$  was found to be incompatible for fibroblast encapsulation and 3 nebulizer devices had to be excluded. The nasal atomizer (NA) and Microsprayer Aerosolizer (MSA) had above 90% viable cells post spraying, but the viable cell count in the NA group declined to 65% 48 h after spraying, indicating that it was a more destructive aerosol technique [181].

All spray cell delivery techniques have been investigated in vitro or rodent studies, which has led to the development of commercial spray devices that are now available in clinical practice for burn wound treatment.

## 7. Potential therapeutic applications

### 7.1. Future approaches keratinocyte transplantation

Several reviews in the last decade have discussed the future implications of skin tissue engineering and/or specifically keratinocyte cell transplantation in the treatment of burns [35,36,54,131,182].

Larger burn wounds often require mesh grafting. Autologous epidermal cell transplantation can complement mesh grafting by stimulating rapid epithelialization, which is highly desirable to improve patient's chance of survival and eventually improve scarring. Burns specific clinical studies investigating keratinocyte transplantation are available, but due to heterogeneity of the studies and different outcome parameters the evidence remains low. Comparative trials with standardized outcomes and ideally randomized treatment for available cell transplantation techniques are required.

Due to the disadvantages of CEA sheets, future research is focused on optimizing keratinocyte proliferation by transplantation of pre- or sub confluence cells. Further improvement of keratinocyte culture method in terms of culture time, reducing infection risk and elimination of xenobiotic products and also antibiotics needs to be further investigated.

Graft attachment in keratinocyte transplantation remains an important focus for research. Boyce and Supp developed a cultured skin substitute containing cultured human keratinocytes and fibroblasts attached to a collagen-glycosaminoglycan matrix which seems to form a basement membrane at the dermal-epidermal junction in vitro [183]. Importance of basement membrane formation and rapid epithelialisation has to be taken into account in novel cell spray or carrier delivery methods [183,184].

### 7.2. Future spray cell delivery systems for burns wound care

Spray cell delivery to burn wounds can overcome the major issues of conventional grafting techniques by reducing donor site and enhance fast re-epithelialisation. The available delivery systems can be improved by optimizing spray features to aim for high cell viability and proliferation. This should be tailored according to cell type and receiver surface. Spray features to optimise might be: air delivery pressure, nozzle designs, carrier type and depending on technique of delivery, cell containing droplet size [178,179,181]. Further research should take into account the importance of preventing cell damage, since this could reflect poor proliferation [178,180]. Hydrogels could potentially serve as a mechanical protection for the cells during transplantation and provide structural support once transplanted. Although in vitro studies have shown good short term cell survival post aerosol delivery, clinical studies have not been able to show similar results as yet. The challenge for researchers is to develop a feasible spray delivery system with acceptable cell viability and proliferation which can be translated to clinical

studies. Also, current clinical cell spray devices could potentially benefit from these optimized features.

## Funding

This work was supported by the Scar Free foundation, formally known as the Healing Foundation. The funding source had no involvement in designing the study, data collection, interpretation of data and decision to submit the article for publication. None of the authors has a financial interest in any of the products, devices, or drugs mentioned in this manuscript.

## Conflict of interest

The authors state no conflict of interest.

## Permission note

Permission to publish Fig. 4 and Fig. 5 have been received from Elsevier.

## Acknowledgments

The authors would like to thank Dr. K.C. Lee and Dr. K. Al-Tarrah for proof reading the manuscript.

## References

- [1] P.C. Jackson, J. Hardwicke, A. Bamford, P. Nightingale, Y. Wilson, R. Papini, et al., Revised estimates of mortality from the Birmingham Burn Centre, 2001–2010: a continuing analysis over 65 years, *Ann. Surg.* 259 (5) (2014) 979–984.
- [2] Web-based injury statistics query and reporting system [Internet] cited 06/10/2016. Available from: <https://www.cdc.gov/injury/wisqars/> 2014.
- [3] T. Osler, L.G. Glance, D.W. Hosmer, Simplified estimates of the probability of death after burn injuries: extending and updating the Baux score, *J. Trauma* 68 (3) (2010) 690–697.
- [4] J. Tobiasen, J.M. Hiebert, R.F. Edlich, The abbreviated burn severity index, *Ann. Emerg. Med.* 11 (5) (1982) 260–262.
- [5] M.J. Muller, D.N. Herndon, The challenge of burns, *Lancet (London, England)* 343 (8891) (1994) 216–220.
- [6] G. McGwin Jr., J.M. Cross, J.W. Ford, L.W. Rue 3rd, Long-term trends in mortality according to age among adult burn patients, *J. Burn Care Rehabil.* 24 (1) (2003) 21–25.
- [7] N.A. Forster, M. Zingg, S.R. Haile, W. Kunzi, P. Giovanoli, M. Guggenheim, 30 years later—does the ABSI need revision? *Burns* 37 (6) (2011) 958–963.
- [8] I. Pastar, C. Stojadinovic, N.C. Yin, H. Ramirez, A.G. Nusbaum, A. Sawaya, et al., Epithelialization in wound healing: a comprehensive review, *Adv. Wound Care* 3 (7) (2014) 445–464.
- [9] D.N. Herndon, Total Burn Care, Saunders Elsevier, Edinburgh, 2012.
- [10] G.D. Weinstein, J.L. McCullough, P. Ross, Cell proliferation in normal epidermis, *J. Invest. Dermatol.* 82 (6) (1984) 623–628.
- [11] L.H. Gu, P.A. Coulombe, Keratin function in skin epithelia: a broadening palette with surprising shades, *Curr. Opin. Cell Biol.* 19 (1) (2007) 13–23.
- [12] M.B. Omary, P.A. Coulombe, W.H. McLean, Intermediate filament proteins and their associated diseases, *N. Engl. J. Med.* 351 (20) (2004) 2087–2100.
- [13] A.C. Steven, M.E. Bisher, D.R. Roop, P.M. Slemer, Biosynthetic pathways of filaggrin and loritricin—two major proteins expressed by terminally differentiated epidermal keratinocytes, *J. Struct. Biol.* 104 (1–3) (1990) 150–162.
- [14] D.D. Bikle, Z. Xie, C.L. Tu, Calcium regulation of keratinocyte differentiation, *Expert. Rev. Endocrinol. Metab.* 7 (4) (2012) 461–472.
- [15] G. Dencker, P. Ovaere, P. Vandenaebale, W. Declercq, Caspase-14 reveals its secrets, *J. Cell Biol.* 180 (3) (2008) 451–458.
- [16] S.T. Boyce, R.G. Ham, Calcium-regulated differentiation of normal human epidermal keratinocytes in chemically defined clonal culture and serum-free serial culture, *J. Invest. Dermatol.* 81 (1 Suppl) (1983) 335–405.
- [17] M.J. Su, D.D. Bikle, M.L. Mancianti, S. Pillai, 1,25-Dihydroxyvitamin D3 potentiates the keratinocyte response to calcium, *J. Biol. Chem.* 269 (20) (1994) 14723–14729.
- [18] Y. Oda, C.L. Tu, A. Menendez, T. Nguyen, D.D. Bikle, Vitamin D and calcium regulation of epidermal wound healing, *J. Steroid Biochem. Mol. Biol.* 164 (2016) 379–385.
- [19] M. Chihorek, M. Wachulska, A. Stasiewicz, A. Tymianska, Skin melanocytes: biology and development, *Postep. Dermatol. Alergol.* 30 (1) (2013) 30–41.
- [20] S. Werner, T. Krieg, H. Smola, Keratinocyte-fibroblast interactions in wound healing, *J. Invest. Dermatol.* 127 (5) (2007) 998–1008.
- [21] A. Szabowski, N. Maas-Szabowski, S. Andrich, A. Kolbus, M. Schorpp-Kistner, N.E. Fusingen, et al., c-Jun and JunB antagonistically control cytokine-regulated mesenchymal-epidermal interaction in skin, *Cell* 103 (5) (2000) 745–755.

- [22] T. Rozario, D.W. DeSimone, The extracellular matrix in development and morphogenesis: a dynamic view, *Dev. Biol.* 341 (1) (2010) 126–140.
- [23] C. Has, J.S. Kern, *Collagen XVII*, *Dermatol. Clin.* 28 (1) (2010) 61–66.
- [24] V. Levy, C. Lindon, Y. Zheng, B.D. Harfe, B.A. Morgan, Epidermal stem cells arise from the hair follicle after wounding, *FASEB J.* 21 (7) (2007) 1358–1366.
- [25] (WHO) WHO, Burns – fact sheet 2016 [updated September 2016]. Available from: <http://www.who.int/mediacentre/factsheets/fs365/en/>.
- [26] M.P. Rowan, L.C. Cancio, E.A. Elster, D.M. Burmeister, L.F. Rose, S. Natesan, et al., Burn wound healing and treatment: review and advancements, *Crit. Care* 19 (2015) 243.
- [27] G.C. Gurtner, S. Werner, Y. Barrandon, M.T. Longaker, Wound repair and regeneration, *Nature* 453 (7193) (2008) 314–321.
- [28] R. Grose, S. Werner, Wound-healing studies in transgenic and knockout mice, *Mol. Biotechnol.* 28 (2) (2004) 147–166.
- [29] S.H. Lijems, J.M. de Pereda, A. Sonnenberg, Current insights into the formation and breakdown of hemidesmosomes, *Trends Cell Biol.* 16 (7) (2006) 376–383.
- [30] P. Chen, W.C. Parks, Role of matrix metalloproteinases in epithelial migration, *J. Cell. Biochem.* 108 (6) (2009) 1233–1243.
- [31] C.K. Jiang, M. Tomic-Canic, D.J. Lucas, M. Simon, M. Blumenberg, TGF beta promotes the basal phenotype of epidermal keratinocytes: transcriptional induction of K65 and K14 keratin genes, *Growth Factors (Chur, Switzerland)* 12 (2) (1995) 87–97.
- [32] B.E. Zawacki, K.W. Spitzer, A.D. Mason Jr., L.A. Johns, Does increased evaporative water loss cause hypermetabolism in burned patients? *Ann. Surg.* 171 (2) (1970) 236–240.
- [33] T.N. Pham, L.C. Cancio, N.S. Gibran, American Burn Association practice guidelines burn shock resuscitation, *J. Burn Care Res.* 29 (1) (2008) 257–266.
- [34] E.V. Robins, Burn shock, *Crit. Care Nurs. Clin. North Am.* 2 (2) (1990) 299–307.
- [35] L. Lootens, N. Brusseleers, H. Beele, S. Monstrey, Keratinocytes in the treatment of severe burn injury: an update, *Int. Wound J.* 10 (1) (2013) 6–12.
- [36] A.D. Metcalfe, M.W. Ferguson, Tissue engineering of replacement skin: the crossroads of biomaterials, wound healing, embryonic development, stem cells and regeneration, *J. R. Soc. Interface* 4 (14) (2007) 413–437.
- [37] J.A. Nowak, L. Polak, H.A. Pasolli, E. Fuchs, Hair follicle stem cells are specified and function in early skin morphogenesis, *Cell Stem Cell* 3 (1) (2008) 33–43.
- [38] A.B. Mohd Hilmi, A.S. Halim, Vital roles of stem cells and biomaterials in skin tissue engineering, *World J. Stem Cells* 7 (2) (2015) 428–436.
- [39] J.C. Rheinwald, H. Green, Serial cultivation of strains of human epidermal keratinocytes: the formation of keratinizing colonies from single cells, *Cell* 6 (3) (1975) 331–343.
- [40] C.O. Duncan, R.M. Shelton, H. Navsaria, D.S. Balderson, R.P. Papiñi, J.E. Barralet, In vitro transfer of keratinocytes: comparison of transfer from fibrin membrane and delivery by aerosol spray, *J. Biomed Mater Res B Appl Biomater* 73 (2) (2005) 221–228.
- [41] C. Rasmussen, C. Thomas-Virmig, B.L. Allen-Hoffmann, et al., *Methods Mol. Biol. (Clifton, NJ)* 945 (2013) 161–175.
- [42] H. Green, O. Kehinde, J. Thomas, Growth of cultured human epidermal cells into multiple epithelia suitable for grafting, *Proc. Natl. Acad. Sci. U. S. A.* 76 (11) (1979) 5665–5668.
- [43] N.E. O'Connor, J.B. Mulliken, S. Banks-Schlegel, O. Kehinde, H. Green, Grafting of burns with cultured epithelium prepared from autologous epidermal cells, *Lancet* 1 (8211) (1981) 75–78.
- [44] Y. Pournay, M.R. Pittelkow, Cell density and culture factors regulate keratinocyte commitment to differentiation and expression of suprabasal K1/K10 keratins, *J. Invest. Dermatol.* 104 (2) (1995) 271–276.
- [45] Y. Barrandon, N. Grasset, A. Zaffaroni, F. Gorostidi, S. Claudinot, S.L. Droz-Georget, et al., Capturing epidermal stemness for regenerative medicine, *Semin. Cell Dev. Biol.* 23 (8) (2012) 937–944.
- [46] D.L. Chester, D.S. Balderson, R.P. Papiñi, A review of keratinocyte delivery to the wound bed, *J. Burn Care Rehabil.* 25 (3) (2004) 266–275.
- [47] C.E. Butler, I.V. Yannas, C.C. Compton, C.A. Cornea, D.P. Orgill, Comparison of cultured and uncultured keratinocytes seeded into a collagen-GAG matrix for skin replacements, *Br. J. Plast. Surg.* 52 (2) (1999) 127–132.
- [48] A. Heiskanen, T. Satomaa, S. Tittinen, A. Laitinen, S. Mannelin, U. Impola, et al., N-glycolylneuraminic acid xenotransplantation contamination of human embryonic and mesenchymal stem cells is substantially reversible, *Stem Cells* 25 (1) (2007) 197–202.
- [49] T. Sun, M. Higham, C. Layton, J. Haycock, R. Short, S. MacNeil, Developments in xenobiotic-free culture of human keratinocytes for clinical use, *Wound Repair Regen.* 12 (6) (2004) 626–634.
- [50] K. Jubin, Y. Martin, D.J. Lawrence-Watt, J.R. Sharpe, A fully autologous co-culture system utilising non-irradiated autologous fibroblasts to support the expansion of human keratinocytes for clinical use, *Cytotherapy* 63 (6) (2011) 655–662.
- [51] N.A. Coolen, M. Verkerk, L. Reijnen, M. Vlig, A.J. van den Bogerdt, M. Breeveld, et al., Culture of keratinocytes for transplantation without the need of feeder layer cells, *Cell Transplant.* 16 (6) (2007) 649–661.
- [52] R. Lamb, C.A. Ambler, Keratinocytes propagated in serum-free, feeder-free culture conditions fail to form stratified epidermis in a reconstituted skin model, *PLoS One* 8 (1) (2013), e52494.
- [53] C. Lenihan, C. Rogers, A.D. Metcalfe, Y.H. Martin, The effect of isolation and culture methods on epithelial stem cell populations and their progeny toward an improved cell expansion protocol for clinical application, *Cytotherapy* 16 (12) (2014) 1750–1759.
- [54] K.I. Gardien, E. Middelkoop, M.M. Ulrich, Progress towards cell-based burn wound treatments, *Regen. Med.* 9 (2) (2014) 201–218.
- [55] L. Guerra, S. Capurro, F. Melchi, G. Primavera, S. Bondanza, R. Cancedda, et al., Treatment of “stable” vitiligo by Timsurgery and transplantation of cultured epidermal autografts, *Arch. Dermatol.* 136 (11) (2000) 1380–1389.
- [56] S. Bottcher-Haberzeth, A.S. Klar, T. Biedermann, C. Schiestl, C. Meuli-Simmen, E. Reichmann, et al., “Troping the color”: restoring the original donor skin color by addition of melanocytes to bioengineered skin analogs, *Pediatr. Res.* 29 (3) (2013) 239–247.
- [57] T. Biedermann, A.S. Klar, S. Bottcher-Haberzeth, T. Michalczyc, C. Schiestl, E. Reichmann, et al., Long-term expression pattern of melanocyte markers in light-and dark-pigmented dermo-epidermal cultured human skin substitutes, *Pediatr. Surg. Int.* 31 (1) (2015) 69–76.
- [58] A. Hachiya, P. Sriwriyanont, E. Kaiho, T. Kitahara, Y. Takema, R. Tsuboi, An in vivo mouse model of human skin substitute containing spontaneously stored melanocytes demonstrates physiological changes after UVB irradiation, *J. Invest. Dermatol.* 125 (2) (2005) 364–372.
- [59] A. Iman, M.A. Akbar, K.M. Mohsen, F. Ali, A. Armin, A. Sajjad, et al., Comparison of intradermal injection of autologous epidermal cell suspension vs. spraying of these cells on dermabraded surface of skin of patients with post-burn hypopigmentation, *Indian J. Dermatol.* 58 (3) (2013) 240.
- [60] S.V. Mulekar, B. Chwis, A. Al Issa, Eisa A. Al, Treatment of vitiligo lesions by ReCell vs. conventional melanocyte-keratinocyte transplantation: a pilot study, *Br. J. Dermatol.* 158 (1) (2008) 45–49.
- [61] R.H. Huggins, M.D. Henderson, S.V. Mulekar, D.M. Ozog, H.A. Kerr, G. Jabobsen, et al., Melanocyte-keratinocyte transplantation procedure in the treatment of vitiligo: the experience of an academic medical center in the United States, *J. Am. Acad. Dermatol.* 66 (5) (2012) 785–793.
- [62] P. Toossi, M. Shahidi-Dadras, M. Mahmoodi Rad, R.J. Fesharaki, Non-cultured melanocyte-keratinocyte transplantation for the treatment of vitiligo: a clinical trial in an Iranian population, *J. Eur. Acad. Dermatol. Venerol.* 25 (10) (2011) 1182–1186.
- [63] P.A. Golinski, N. Zoller, S. Kippenberger, H. Menke, J. Beretier-Hahn, A. Bernd, Development of an engraftable skin equivalent based on matrigel with human keratinocytes and fibroblasts, *Handchir. Mikrochir. Plast. Chir.* 41 (6) (2009) 327–332.
- [64] T.D. Sargeant, A.P. Desai, S. Banerjee, A. Agawu, J.B. Stopek, An in situ forming collagen-PEG hydrogel for tissue regeneration, *Acta Biomater.* 8 (1) (2012) 124–132.
- [65] S.P. Huang, C.C. Hsu, S.C. Chang, C.H. Wang, S.C. Deng, N.T. Dai, et al., Adipose-derived stem cells seeded on acellular dermal matrix grafts enhance wound healing in a murine model of a full-thickness defect, *Ann. Plast. Surg.* 69 (6) (2012) 656–662.
- [66] M.P. Ribeiro, P.I. Morgado, S.P. Miguel, P. Coutinho, J.J. Correia, Dextran-based hydrogel containing chitosan microparticles loaded with growth factors to be used in wound healing, *Mater Sci Eng Mater Biol Appl* 33 (5) (2013) 2958–2966.
- [67] S.J. Gwak, S.S. Kim, K. Sung, J. Han, Y.C. Choi, B.S. Kim, Synergistic effect of keratinocyte transplantation and epidermal growth factor delivery on epidermal regeneration, *Cell Transplant.* 14 (10) (2005) 809–817.
- [68] Veazey W, Moore K. Delivery of tissue engineering media. Google Patents; 2003.
- [69] (NICE) NiHacE, The ReCell Spray-On Skin system for treating skin loss, scarring and depigmentation after burn injury 2014 [updated November 2014]. Medical technologies guidance [MTG21] Available from: <https://www.nice.org.uk/guidance/mtg21>.
- [70] P. Aramwit, S. Palapinyo, T. Srihana, S. Chottanapund, P. Muangman, Silk sericin ameliorates wound healing and its clinical efficacy in burn wounds, *Arch. Dermatol. Res.* 305 (7) (2013) 585–594.
- [71] M. Vernez, W. Raffoul, M.C. Gailloud-Matthieu, D. Eglhoff, I. Senechaut, R.G. Panizon, et al., Quantitative assessment of cell viability and apoptosis in cultured epidermal autografts: application to burn therapy, *Int. J. Artif. Organs* 26 (9) (2003) 793–802.
- [72] F.A. Navarro, M.L. Stoner, C.S. Park, J.C. Huertas, H.B. Lee, F.M. Wood, et al., Sprayed keratinocyte suspensions accelerate epidermal closure in a porcine wound model, *Br. J. Burn Care Rehabil.* 21 (6) (2000) 513–518.
- [73] C.O. Duncan, R.M. Shelton, H. Navsaria, D.S. Balderson, R.P.G. Papiñi, J.E. Barralet, In vitro transfer of keratinocytes: comparison of transfer fibrin membrane and delivery by aerosol spray, *J. Biomed Mater Res B Appl Biomater* 73B (2) (2005) 221–228.
- [74] G. Dupuytren, A.L.M.P. BDBA, Oral Lessons of Clinical Surgery, faites à l'Hôtel-Dieu de Paris, Baillière, Paris, 1839.
- [75] K.C. Lee, K. Joory, N.S. Moiemien, History of burns: the past, present and the future, *Burns Trauma* 2 (4) (2015) 169–180.
- [76] D. Kadam, Novel expansion techniques for skin grafts, *Indian J. Plast. Surg.* 49 (1) (2016) 5–15.
- [77] M. Singh, K. Nautliya, C. Kruse, M.C. Robson, E. Caterson, E. Eriksson, Challenging the conventional therapy: emerging skin graft techniques for wound healing, *Plast. Reconstr. Surg.* 136 (4) (2015) 524e–530e.
- [78] H. Liu, Y. Yin, K. Yao, Construction of chitosan-gelatin-hyaluronic acid artificial skin in vitro, *J. Biomater. Appl.* 21 (4) (2007) 413–430.
- [79] C. Pham, J. Greenwood, H. Cleland, P. Woodruff, G. Maddern, Bioengineered skin substitutes for the management of burns: a systematic review, *Burns* 33 (2007).
- [80] G.G. Gallico 3rd, N.E. O'Connor, C.C. Compton, O. Kehinde, H. Green, Permanent coverage of large burn wounds with autologous cultured human epithelium, *N. Engl. J. Med.* 311 (7) (1984) 448–451.
- [81] D. Hanjaya-Putra, Y.I. Shen, A. Wilson, K. Fox-Talbot, S. Khetan, J.A. Burdick, et al., Integration and regression of implanted engineered human vascular networks during deep wound healing, *Stem Cells Transl. Med.* 2 (4) (2013) 297–306.
- [82] J.P. Barret, S.E. Wolf, M.H. Desai, D.N. Herndon, Cost-efficacy of cultured epidermal autografts in massive pediatric burns, *Ann. Surg.* 231 (6) (2000) 869–876.
- [83] F.M. Wood, M.L. Kolybaba, P. Allen, The use of cultured epidermal autograft in the treatment of major burn wounds: eleven years of clinical experience, *Burns* 32 (5) (2006) 538–544.
- [84] B.S. Atiyeh, M. Costagliola, Cultured epithelial autograft (CEA) in burn treatment: three decades later, *Burns* 33 (4) (2007) 405–413.
- [85] A.M. Munster, Cultured skin for massive burns. A prospective, controlled trial, *Ann. Surg.* 224 (3) (1996) 372–375 (discussion 5–7).
- [86] C. Auzanfans, V. Menet, Z. Catherine, H. Shipkov, P. Lacroix, M. Bertin-Maghit, et al., Cultured autologous keratinocytes in the treatment of large and deep burns: a retrospective study over 15 years, *Burns* 41 (1) (2015) 71–79.
- [87] L. Shi, Z.J. Lei, C.Y. Zhao, X.X. Lv, L. Jiang, J. Li, et al., A modified culture strategy of human keratinocytes to shorten the primary culture time, *Cell Biol. Int.* 39 (9) (2015) 1073–1079.
- [88] R. Sood, D. Roggy, M. Zieger, J. Balleud, S. Chaudhari, D.J. Koumanis, et al., Cultured epithelial autografts for coverage of large burn wounds in eighty-eight patients: the Indiana University experience, *J. Burn Care Res.* 31 (4) (2010) 559–568.
- [89] M.H. Desai, J.M. Mlakar, R.L. McCauley, K.M. Abdullah, R.L. Rutan, J.P. Waymack, et al., Lack of long-term durability of cultured keratinocyte burn-wound coverage: a case report, *J. Burn Care Rehabil.* 12 (6) (1991) 540–545.
- [90] P.A. Clugston, C.F. Snelling, I.B. Macdonald, H.L. Maloney, J.C. Boyle, E. Germann, et al., Cultured epithelial autografts: three years of clinical experience with eighteen patients, *J. Burn Care Rehabil.* 12 (6) (1991) 533–539.
- [91] H. Matsumura, A. Matsushima, M. Ueyama, N. Kumagai, Application of the cultured epidermal autograft “JACEE(R)” for treatment of severe burns: results of a 6-year multicenter surveillance in Japan, *Burns* 42 (4) (2016) 769–776.
- [92] K. Hata, Current issues regarding skin substitutes using living cells as industrial materials, *J. Artif. Organs* 10 (3) (2007) 129–132.
- [93] C. Theopold, D. Hoeller, P. Velander, R. Demling, E. Eriksson, Graft site malignancy following treatment of full-thickness burn with cultured epidermal autograft, *Plast. Reconstr. Surg.* 114 (5) (2004) 1215–1219.
- [94] M. Singh, K. Nautliya, A.S. Chauhan, E. Eriksson, Invasive squamous cell carcinoma in full-thickness burn wounds after treatment with cultured epithelial autografts, *Plast. Reconstr. Surg. Global Open* 3 (7) (2015), e460.
- [95] T.J. Phillips, S.M. Salmán, J. Bhawan, G.S. Rogers, Burn scar carcinoma. Diagnosis and management, *Dermatol. Surg.* 45 (1998) 561–565.
- [96] C. Cuono, R. Langdon, J. McGuire, Use of cultured epidermal autografts and dermal allografts as skin replacement after burn injury, *Lancet* 1 (8490) (1986) 1123–1124.
- [97] J.F. Hansbrough, S.T. Boyce, M.L. Cooper, T.J. Foreman, Burn wound closure with cultured autologous keratinocytes and fibroblasts attached to a collagen-glycosaminoglycan substrate, *JAMA* 262 (15) (1989) 2125–2130.
- [98] N. Ojeh, I. Pastar, M. Tomic-Canic, O. Stojadinovic, Stem cells in skin regeneration, wound healing, and their clinical applications, *Int. J. Mol. Sci.* 16 (10) (2015) 25476–25501.
- [99] J.N. McHeik, C. Barraud, E. Levard, F. Morel, F.X. Bernard, J.C. Lecon, Epidermal healing in burns: autologous keratinocyte transplantation as a standard procedure: update and perspective, *Plast. Reconstr. Surg. Global Open* 2 (2014).
- [100] C. Pham, J. Greenwood, H. Cleland, P. Woodruff, G. Maddern, Bioengineered skin substitutes for the management of burns: a systematic review, *Burns* 33 (8) (2007) 946–957.
- [101] H. Yim, H.T. Yang, Y.S. Cho, C.H. Seo, B.C. Lee, J.H. Ko, et al., Clinical study of cultured epithelial autografts in liquid suspension in severe burn patients, *Burns* 37 (6) (2011) 1067–1071.
- [102] H. Lee, Outcomes of sprayed cultured epithelial autografts for full-thickness wounds: a single-centre experience, *Burns* 38 (6) (2012) 931–936.
- [103] B. Hartmann, A. Ekkemkamp, C. Johnen, J.C. Gerlach, C. Belfekroun, M.V. Kuntscher, Sprayed cultured epithelial autografts for deep dermal burns of the face and neck, *Ann. Plast. Surg.* 58 (1) (2007) 70–73.
- [104] J.C. Gerlach, C. Johnen, C. Ottmann, K. Brautigam, J. Plettig, C. Belfekroun, et al., Method for autologous single skin cell isolation for regenerative cell spray transplantation with non-cultured cells (vol 34, pg 271, 2011), *Int. J. Artif. Organs* 34 (2) (2014) 184.
- [105] G. Gravante, M.C. Di Fede, A. Araco, M. Grimaldi, B. De Angelis, A. Arpino, et al., A randomized trial comparing ReCell (R) system of epidermal cells delivery versus classic skin grafts for the treatment of deep partial thickness burns, *Burns* 33 (8) (2007) 966–972.
- [106] V. Cervelli, B. De Angelis, A. Balzani, G. Colicchia, D. Spallone, M. Grimaldi, Treatment of stable vitiligo by ReCell system, *Acta Dermatovenerol.* 38 (17) (4) (2009) 273–278.
- [107] M. Hivelin, C. MacIver, J.L. Heusse, M. Atlan, L. Lantieri, Improving the colour match of free tissue transfers to the face with non-cultured autologous cellular spray - a case report on a chin reconstruction, *J. Plast. Reconstr. Aesthet. Surg.* 65 (8) (2012) 1103–1106.
- [108] J.H. Park, K.M. Heggie, D.W. Edgar, M.K. Bulsara, F.M. Wood, Does the type of skin replacement surgery influence the rate of infection in acute burn injured patients? *Burns* 39 (7) (2013) 1386–1390.
- [109] R. Sood, D.E. Roggy, M.J. Zieger, M. Nazim, B.C. Hartman, J.T. Gibbs, A comparative study of spray keratinocytes and autologous meshed split-thickness skin graft in the treatment of acute burn injuries, *Wounds* 27 (2) (2015) 31–40.
- [110] J.C. Gerlach, C. Johnen, C. Ottmann, K. Brautigam, J. Plettig, C. Belfekroun, et al., Method for autologous single skin cell isolation for regenerative cell spray transplantation with non-cultured cells, *Int. J. Artif. Organs* 34 (3) (2011) 271–279.
- [111] J.C. Gerlach, C. Johnen, E. McCoy, K. Brautigam, J. Plettig, A. Corcos, Autologous skin cell spray-transplantation for a deep dermal burn patient in an ambulant treatment room setting, *Burns* 37 (4) (2011) e19–e23.
- [112] R. Esteban-Vives, M.T. Young, T. Zhu, J. Berjiger, C. Pekor, J. Ziembicki, et al., Calculations for reproducible autologous skin cell-spray grafting, *Burns* 42 (8) (2016) 1756–1765.
- [113] K.C. Lee, J. Dretzke, L. Grover, A. Logan, N. Moiemien, A systematic review of objective burn scar measurements, *Burns Trauma* 4 (2016) 14.
- [114] R. Goedkoop, R. Juliet, P.H.K. You, J. Daroczy, K.P. de Roos, R.L.P. Lijnen, et al., Wound stimulation by growth-arrested human keratinocytes and fibroblasts: HPB02-247, a new-generation allogeneic tissue engineering product, *Dermatology* 220 (2) (2010) 114–120.
- [115] R.S. Kirsner, W.A. Marston, R.J. Snyder, T.D. Lee, D.J. Cargill, H.B. Slade, et al., Spray-applied cell therapy with human allogeneic fibroblasts and keratinocytes for the treatment of chronic venous leg ulcers: a phase 2, multicentre, double-blind, randomised, placebo-controlled trial, *Lancet* 380 (9846) (2012) 977–985.
- [116] R.S. Kirsner, W.A. Marston, R.J. Snyder, T.D. Lee, D.I. Cargill, Y.X. Zhang, et al., Durability of healing from spray-applied cell therapy with human allogeneic fibroblasts and keratinocytes for the treatment of chronic venous leg ulcers: a 6-month follow-up, *Wound Repair Regen.* 21 (5) (2013) 682–687.
- [117] J.C. Lantis, W.A. Marston, A. Farber, R.S. Kirsner, Y.X. Zhang, T.D. Lee, et al., The influence of patient and wound variables on healing of venous leg ulcers in a randomized controlled trial of growth-arrested allogeneic keratinocytes and fibroblasts, *J. Vasc. Med. Biol.* 25 (2) (2013) 433–439.
- [118] W. Marston, R. Kirsner, R. Snyder, T. Lee, J. Cargill, H. Slade, Variables affecting healing of venous leg ulcers in a randomized, vehicle-controlled trial of topical cellular therapy, *J. Vasc. Med. [Internet]* 55 (1) (2012) 303 Available from: <http://onlinelibrary.wiley.com/doi/cochrane/central/articles/743/CN-00830743/frame.html>.
- [119] R.S. Kirsner, W. Vanscheidt, D.H. Keast, J.C. Lantis 2nd, C.R. Dove, S.M. Cazzell, et al., Phase 3 evaluation of HPB02-247 in the treatment of chronic venous leg ulcers, *Wound Repair Regen.* 24 (5) (2016) 894–903.
- [120] M.F. Rasulov, A.V. Vasilenchenko, N.A. Onishchenko, M.E. Krashennnikov, V.I. Kravchenko, T.L. Gorshenin, et al., First experience of the use bone marrow mesenchymal stem cells for the treatment of a patient with deep skin burns, *Bull. Exp. Biol. Med.* 139 (1) (2005) 141–144.
- [121] V. Falanga, S. Iwamoto, M. Chartier, T. Yufit, J. Butmarc, N. Kouttab, et al., Autologous bone marrow-derived cultured mesenchymal stem cells delivered in a fibrin spray accelerate healing in murine and human cutaneous wounds, *J. Investig. Dermatol.* 127 (2007) 549-S.
- [122] E. Mansilla, G.H. Marin, M. Berges, S. Scafatti, J. Rivas, A. Nunez, et al., Cadaveric bone marrow mesenchymal stem cells: first experience treating a patient with large severe burns, *Burns Trauma* 3 (2015) 9.
- [123] M. Ueda, Sprayed cultured mucosal epithelial cell for deep dermal burns, *J. Craniofac. Surg.* 21 (6) (2010) 1729–1732.
- [124] I. Grant, K. Warwick, J. Marshall, C. Green, R. Martin, The co-application of sprayed cultured autologous keratinocytes and autologous fibrin sealant in a porcine wound model, *Br. J. Plast. Surg.* 55 (3) (2002) 219–227.
- [125] M. Madaghiele, C. Demitri, A. Sannino, L. Ambrosio, Polymeric hydrogels for burn wound care: advanced skin wound dressings and regenerative templates, *Burns Trauma* 2 (4) (2015) 153–161.
- [126] E.M. Ahmed, Hydrogel: preparation, characterization, and applications: a review, *J. Adv. Res.* 6 (2) (2015) 105–121.
- [127] V.K. Thakur, M.K. Thakur, Recent trends in hydrogels based on psyllium polysaccharide: a review, *J. Clean. Prod.* 82 (2014) 1–15.
- [128] T. Osmalek, A. Froelich, S. Tasarek, Application of gellan gum in pharmacy and medicine, *Int. J. Pharm.* 466 (1–2) (2014) 328–340.
- [129] D.M. Supp, S.T. Boyce, Engineered skin substitutes: practices and potentials, *Clin. Dermatol.* 23 (2005).
- [130] J.N. Mansbridge, Tissue-engineered skin substitutes in regenerative medicine, *Curr. Opin. Biotechnol.* 20 (5) (2009) 563–567.
- [131] A.W.C. Chua, Y.C. Khoo, B.K. Tan, K.C. Tan, C.L. Foo, S.J. Chong, Skin tissue engineering advances in severe burns: review and therapeutic applications, *Burns Trauma* 4 (1) (2016) 1–14.
- [132] A.J. Bullock, P. Pickavance, D.B. Haddow, S. Rimmer, S. MacNeil, Development of a calcium-chelating hydrogel for treatment of superficial burns and scalds, *Regen. Med.* 5 (1) (2010) 56–64.
- [133] J. Wasiak, H. Cleland, F. Campbell, A. Spinks, Dressings for superficial and partial thickness burns, *Cochrane Database Syst. Rev.* 3 (2013) Cd002106.
- [134] M.K. Lee, M.H. Rich, K. Baek, J. Lee, H. Kong, Biopsprinted tuning of hydrogel permeability-rigidity dependency for 3D cell culture, *Sci Rep* 5 (2015) 8948.
- [135] L. Yuan, C. Minghua, D. Feifei, W. Runxian, L. Ziqiang, M. Chengyue, et al., Study of the use of recombinant human granulocyte-macrophage colony-stimulating factor hydrogel externally to treat residual wounds of extensive deep partial-thickness burn, *Burns* 41 (5) (2015) 1086–1091.
- [136] B. Boonkew, P.M. Barber, S. Rengpipat, P. Supaphol, M. Kempf, J. He, et al., Development and characterization of a novel, antimicrobial, sterile hydrogel dressing for burn wounds: single-step production with gamma irradiation creates silver nanoparticles and radical polymerization, *J. Pharm. Sci.* 103 (10) (2014) 3244–3253.
- [137] S.P. Miguel, M.P. Ribeiro, H. Brancel, P. Coutinho, J.J. Correia, Thermoresponsive chitosan-agarose hydrogel for skin regeneration, *Carbohydr. Polym.* 111 (2014) 366–373.
- [138] R. Mohd Zohdi, Z. Abu Bakar Zakaria, N. Yusof, N. Mohamed Mustapha, M.N. Abdullah, Helan (*Melaleuca spp.*) honey-based hydrogel as burn wound dressing, *Evid. Based Complement. Alternat. Med.* 2012 (2012) 843025.
- [139] S. Natesan, D.O. Zamora, N.L. Wrice, D.G. Baer, R.J. Christy, Bilayer hydrogel with autologous stem cells derived from debried human burn skin for improved skin regeneration, *J. Burn Care Res.* 34 (1) (2013) 18–30.
- [140] F. Ahmadi, Z. Oveis, S.M. Samani, Z. Amoozgar, Chitosan based hydrogels: characteristics and pharmaceutical applications, *Res. Pharm. Sci.* 10 (1) (2015) 1–16.
- [141] W. Gao, J.C. Lai, S.W. Leung, Functional enhancement of chitosan and nanoparticles in cell culture, tissue engineering, and pharmaceutical applications, *Front. Physiol.* 3 (2012) 321.

- [142] N. Charernsriwilaiwat, P. Opanasopit, T. Rojanarata, T. Ngawhirunpat, Lysozyme-loaded, electrospun chitosan-based nanofiber mats for wound healing, *Int. J. Pharm.* 427 (2) (2012) 379–384.
- [143] T. Wang, X.K. Zhu, X.T. Xue, D.Y. Wu, Hydrogel sheets of chitosan, honey and gelatin as burn wound dressings, *Carbohydr. Polym.* 88 (1) (2012) 75–83.
- [144] T.H. Dai, M. Tanaka, Y.Y. Huang, M.R. Hamblin, Chitosan preparations for wounds and burns: antimicrobial and wound-healing effects, *Expert Rev. Anti-Infect. Ther.* 9 (7) (2011) 857–879.
- [145] I.A. Alsarra, Chitosan topical gel formulation in the management of burn wounds, *Int. J. Biol. Macromol.* 45 (1) (2009) 16–21.
- [146] C. Chatelet, O. Damour, A. Domard, Influence of the degree of acetylation on some biological properties of chitosan films, *Biomaterials* 22 (3) (2001) 261–268.
- [147] M. Rodriguez-Vazquez, B. Vega-Ruiz, R. Ramos-Zuniga, D.A. Saldana-Koppel, L.F. Quinones-Olvera, Chitosan and its potential use as a scaffold for tissue engineering in regenerative medicine, *Biomed. Res. Int.* 2015 (2015) 821279.
- [148] J. Wasiaik, H. Cleland, Burns: dressings, *BMJ Clin. Evid.* 2015 (2015).
- [149] M. Brenner, C. Hilliard, G. Peel, C. Crispino, R. Geraghty, G. O'Callaghan, Management of pediatric skin-graft donor sites: a randomized controlled trial of three wound care products, *J. Burn Care Res.* 36 (1) (2015) 159–166.
- [150] A. Gugerell, W. Pastiner, S. Nurnberger, J. Kober, A. Meinel, S. Pfeifer, et al., Thrombin as important factor for cutaneous wound healing: comparison of fibrin biomaterials in vitro and in a rat excisional wound healing model, *Wound Repair Regen.* 22 (6) (2014) 740–748.
- [151] R. Gorodetsky, R.A. Clark, J. An, J. Gailit, L. Levdansky, A. Vexler, et al., Fibrin microbeads (FMB) as biodegradable carriers for culturing cells and for accelerating wound healing, *J. Invest. Dermatol.* 112 (6) (1999) 866–872.
- [152] S. Cox, M. Cole, B. Tawil, Behavior of human dermal fibroblasts in three-dimensional fibrin clots: dependence on fibrinogen and thrombin concentration, *Tissue Eng.* 10 (5–6) (2004) 942–954.
- [153] A. Meana, J. Iglesias, M. Del Rio, F. Larcher, B. Madrigal, M.F. Fresno, et al., Large surface of cultured human epithelium obtained on a dermal matrix based on live fibroblast-containing fibrin gels, *Burns* 24 (7) (1998) 621–630.
- [154] J. Kopp, M.G. Jeschke, A.D. Bach, U. Kneser, R.E. Horch, Applied tissue engineering in the closure of severe burns and chronic wounds using cultured human autologous keratinocytes in a natural fibrin matrix, *Cell Tissue Bank.* 5 (2) (2004) 89–96.
- [155] E. Taghlabadi, P. Mohammadi, N. Aghdami, N. Falah, Z. Orouji, A. Nazari, et al., Treatment of hypertrophic scar in human with autologous transplantation of cultured keratinocytes and fibroblasts along with fibrin glue, *Cell J.* 17 (1) (2015) 49–58.
- [156] D.G. Harkin, R.A. Dawson, Z. Upton, Optimized delivery of skin keratinocytes by aerosolization and suspension in fibrin tissue adhesive, *Wound Repair Regen.* 14 (3) (2006) 354–363.
- [157] L.J. Currie, R. Martin, J.R. Sharpe, S.E. James, A comparison of keratinocyte cell sprays with and without fibrin glue, *Burns* 29 (7) (2003) 677–685.
- [158] H. Bannasch, T. Unterberg, M. Fohn, B. Weyand, R.E. Horch, G.B. Stark, Cultured keratinocytes in fibrin with decellularised dermis close porcine full-thickness wounds in a single step, *Burns* 34 (7) (2008) 1015–1021.
- [159] L.P. Kamolz, M. Luegmair, N. Wick, B. Eisenbock, S. Burjak, R. Koller, et al., The Viennese culture method: cultured human epithelium obtained on a dermal matrix based on fibroblast containing fibrin glue gels, *Burns* 31 (1) (2005) 25–29.
- [160] P.K. Lam, E.S. Chan, R.S. Yen, H.C. Lau, W.W. King, A new system for the cultivation of keratinocytes on acellular human dermis with the use of fibrin glue and 3T3 feeder cells, *J. Burn Care Rehabil.* 21 (1 Pt 1) (2000) 1–4.
- [161] M.M. Melendez, R.R. Martinez, A.B. Dagum, S.A. McClain, M. Simon, J. Sobanko, et al., Porcine wound healing in full-thickness skin defects using Integra™ with and without fibrin glue with keratinocytes, *Can. J. Plast. Surg.* 16 (3) (2008) 147–152.
- [162] R. Mittermayr, P. Slezak, N. Halffner, D. Smolen, J. Hartinger, A. Hofmann, et al., Controlled release of fibrin matrix-conjugated platelet derived growth factor improves ischemic tissue regeneration by functional angiogenesis, *Acta Biomater.* 29 (2016) 11–20.
- [163] I.V. Yannas, D. Tzeranis, P.T. So, Surface biology of collagen scaffold explains blocking of wound contraction and regeneration of skin and peripheral nerves, *Biomed. Mater. (Bristol, England)* 11 (1) (2016) 014106.
- [164] N. Dagalakis, J. Flink, P. Stasikelis, J.F. Burke, I.V. Yannas, Design of an artificial skin. Part III. Control of pore structure, *J. Biomed. Mater. Res.* 14 (4) (1980) 511–528.
- [165] S.A. Kolenik 3rd, T.W. McGovern, D.J. Leffell, Use of a lyophilized bovine collagen matrix in postoperative wound healing, *Dermatol. Surg.* 25 (4) (1999) 303–307.
- [166] Z. Ruzszzak, Effect of collagen matrices on dermal wound healing, *Adv. Drug Deliv. Rev.* 55 (12) (2003) 1595–1611.
- [167] S.R. Slivka, L.K. Landeen, F. Zeigler, M.P. Zimmer, R.L. Bartel, Characterization, barrier function, and drug metabolism of an in vitro skin model, *J. Invest. Dermatol.* 100 (1) (1993) 40–46.
- [168] D.Y. Chau, R.J. Collighan, E.A. Verderio, V.L. Addy, M. Griffin, The cellular response to transglutaminase-cross-linked collagen, *Biomaterials* 26 (33) (2005) 6518–6529.
- [169] R.J. Kumar, R.M. Kimble, R. Boots, S.P. Pegg, Treatment of partial-thickness burns: a prospective, randomized trial using Transcyte, *ANZ J. Surg.* 74 (8) (2004) 622–626.
- [170] R.S. Kirsner, The use of Apligraf in acute wounds, *J. Dermatol.* 25 (12) (1998) 805–811.
- [171] M. Kremer, E. Lang, A.C. Berger, Evaluation of dermal-epidermal skin equivalents ('composite-skin') of human keratinocytes in a collagen-glycosaminoglycan matrix (Integra artificial skin), *Br. J. Plast. Surg.* 53 (6) (2000) 459–465.
- [172] P. Angele, J. Abke, R. Kujat, H. Faltermeier, D. Schumann, M. Nerlich, et al., Influence of different collagen species on physico-chemical properties of crosslinked collagen matrices, *Biomaterials* 25 (14) (2004) 2831–2841.
- [173] C.J. Gustafson, A. Birgisson, J. Junker, F. Huss, L. Salemark, H. Johnson, et al., Employing human keratinocytes cultured on macroporous gelatin spheres to treat full thickness-wounds: an in vivo study on athymic rats, *Burns* 33 (6) (2007) 726–735.
- [174] A. Skardal, S.V. Murphy, K. Crowell, D. Mack, A. Atala, S. Soker, A tunable hydrogel system for long-term release of cell-secreted cytokines and bioprinted in situ wound cell delivery, *J. Biomed Mater Res B Appl Biomater* (2016).
- [175] Z. Wang, Y. Zhang, J. Zhang, L. Huang, J. Liu, Y. Li, et al., Exploring natural silk protein sericin for regenerative medicine: an injectable, photoluminescent, cell-adhesive 3D hydrogel, *Sci Rep* 4 (2014) 7064.
- [176] G. Sun, X. Zhang, Y.L. Shen, R. Sebastian, L.E. Dickinson, K. Fox-Talbot, et al., Dextran hydrogel scaffolds enhance angiogenic responses and promote complete skin regeneration during burn wound healing, *Proc. Natl. Acad. Sci. U. S. A.* 108 (52) (2011) 20976–20981.
- [177] Y. Garcia, B. Wilkins, R.J. Collighan, M. Griffin, A. Pandit, Towards development of a dermal rudiment for enhanced wound healing response, *Biomaterials* 29 (7) (2008) 857–868.
- [178] W.S. Veazey, K.J. Anusavice, K. Moore, Mammalian cell delivery via aerosol deposition, *J. Biomed Mater Res B Appl Biomater* 72 (2) (2005) 334–338.
- [179] J. Hendriks, C. Willem Visser, S. Henke, J. Leijten, D.B. Saris, C. Sun, et al., Optimizing cell viability in droplet-based cell deposition, *Sci Rep* 5 (2015) 11304.
- [180] C. Fredriksson, G. Kratz, F. Huss, Transplantation of cultured human keratinocytes in single cell suspension: a comparative in vitro study of different application techniques, *Burns* 34 (2) (2008) 212–219.
- [181] T.R. Sosnowski, A. Kurowska, B. Butruk, K. Jablczynska, Spraying of cell colloids in medical atomizers, in: S. Pierucci, J.J. Klems (Eds.), *Icheap-11: 11th International Conference on Chemical and Process Engineering*, Pts 1–4, Chemical Engineering Transactions, 32, Aidi Servizi Srl, Milano 2013, pp. 2257–2262.
- [182] K.L. Butler, J. Goverman, H. Ma, A. Fischman, Y.M. Yu, M. Bilodeau, Stem cells and burns: review and therapeutic implications, *J. Burn Care Res.* 31 (2010).
- [183] S.T. Boyce, A.P. Supp, V.B. Swope, G.D. Warden, Vitamin C regulates keratinocyte viability, epidermal barrier, and basement membrane in vitro, and reduces wound contraction after grafting of cultured skin substitutes, *J. Invest. Dermatol.* 118 (4) (2002) 565–572.
- [184] C.E. Butler, D.P. Orgill, Simultaneous in vivo regeneration of neodermis, epidermis, and basement membrane, *Adv. Biochem. Eng. Biotechnol.* 94 (2005) 23–41.



Contents lists available at ScienceDirect

Acta Biomaterialia

journal homepage: www.elsevier.com/locate/actabiomat



Full length article

## A gellan-based fluid gel carrier to enhance topical spray delivery

B. ter Horst<sup>a,b,c,\*</sup>, R.J.A. Moakes<sup>a</sup>, G. Chouhan<sup>a</sup>, R.L. Williams<sup>a</sup>, N.S. Moiemien<sup>b</sup>, L.M. Grover<sup>a</sup><sup>a</sup>School of Chemical Engineering, University of Birmingham, Edgbaston, B15 2TT, United Kingdom<sup>b</sup>University Hospital Birmingham Foundation Trust, Burns Centre, Mindelsohn Way, B15 2TH Birmingham, United Kingdom<sup>c</sup>The Scar Free Foundation Birmingham Burn Research Centre, United Kingdom

## ARTICLE INFO

## Article history:

Received 2 August 2018

Received in revised form 10 March 2019

Accepted 19 March 2019

Available online 20 March 2019

## Keywords:

Cell transplantation

Gellan gum

Fluid gel

Yield-stress fluid

Spray therapies

## ABSTRACT

Autologous cell transplantation was introduced to clinical practice nearly four decades ago to enhance burn wound re-epithelialisation. Autologous cultured or uncultured cells are often delivered to the surface in saline-like suspensions. This delivery method is limited because droplets of the sprayed suspension form upon deposition and run across the wound bed, leading to uneven coverage and cell loss. One way to circumvent this problem would be to use a gel-based material to enhance surface retention. Fibrin systems have been explored as co-delivery system with keratinocytes or as adjunct to ‘seal’ the cells following spray delivery, but the high costs and need for autologous blood has impeded its widespread use. Aside from fibrin gel, which can exhibit variable properties, it has not been possible to develop a gel-based carrier that solidifies on the skin surface. This is because it is challenging to develop a material that is sprayable but gels on contact with the skin surface. The manuscript reports the use of an engineered carrier device to deliver cells via spraying, to enhance retention upon a wound. The device involves shear-structuring of a gelling biopolymer, gellan, during the gelation process; forming a yield-stress fluid with shear-sensitive behaviours, known as a fluid gel. In this study, a formulation of gellan gum fluid gels are reported, formed with from 0.75 or 0.9% (w/v) polymer and varying the salt concentrations. The rheological properties and the propensity of the material to wet a surface were determined for polymer modified and non-polymer modified cell suspensions. The gellan fluid gels had a significantly higher viscosity and contact angle when compared to the non-polymer carrier. Viability of cells was not impeded by encapsulation in the gellan fluid gel or spraying. The shear thinning property of the material enabled it to be applied using an airbrush and spray angle, distance and air pressure were optimised for coverage and viability.

## Statement of significance

Spray delivery of skin cells has successfully translated to clinical practice. However, it has not yet been widely accepted due to limited retention and disputable cell viability in the wound. Here, we report a method for delivering cells onto wound surfaces using a gellan-based shear-thinning gel system. The viscoelastic properties allow the material to liquefy upon spraying and restructure rapidly on the surface. Our results demonstrate reduced run-off from the surface compared to currently used low-viscosity cell carriers. Moreover, encapsulated cells remain viable throughout the process. Although this paper studies the encapsulation of one cell type, a similar approach could potentially be adopted for other cell types. Our data supports further studies to confirm these results in *in vivo* models.

Crown Copyright © 2019 Published by Elsevier Ltd on behalf of Acta Materialia Inc. All rights reserved.

## 1. Introduction

Large surface area wounds, such as those seen in burns patients, compromise the barrier function of skin. When coupled with

extensive fluid loss, an impairment of vital bodily functions can arise, which can result in death. Rapid epithelialisation is essential to restoring the function of the skin and in the longer-term, to reduce the likelihood of scarring [1]. Current clinical practice includes transplantation of autologous skin from a healthy site of the body, however, challenges arise when a limited number of donor sites are available.

One approach to overcome this issue is to deliver autologous skin cells (usually keratinocytes) to the wound; either in suspension following a period of culture, or directly after harvest from the patient [2]. Over recent years, cell transplantation techniques have evolved from syringe-dripping to spraying systems [3]. The major advantage of the spray techniques is the rapid delivery to large and geometrically complex areas of the body. For medical applications, a minimum distance of 10 cm from the body is necessary to allow safe application without the risk of an air embolus, this is easily achieved in topical application (in comparison with endoscopic surgery). Even though spraying presents great potential for topically applying cells in suspension, there are still many drawbacks, including: spillage of cells from the wound bed and uneven spreading [3,4]. This results in the application of dressing materials around the wound as a means to retain as many cells on the wound bed as possible [5]. Although poor retention is considered a critical disadvantage of the cell spraying methodology amongst clinicians, it has not as of yet received much attention within the published literature. Autologous fibrin sprays, similar to fibrin glue, have been proposed to retain sprayed epithelial cells at the wound [4,6]. However, high costs and the need for patient's own blood-derived fibrin, have impeded widespread use of this technique to date. While hydrogels have gained huge and sustained interest for therapeutic delivery systems, development of a practical system for topical spray delivery is technically challenging; requiring either *in-situ* gelation on the surface of the wound or a sufficiently high viscosity to be retained on the wound but not clog the spray nozzle.

Fluid gels have shown continued promise to address these issues, whereby at rest act in a pseudo-solid fashion but can be made to flow under shear [7] This is derived through the processing of a hydrogel during its sol to gel transition. The application of shear during the sol-gel transition has been previously shown to support the formation of discrete gel particles, which in close proximity interact with one another in suspension to give reversible shear thinning and solid-like behaviours. Furthermore, fluid gels have been previously shown to demonstrate yield stresses once at rest [8]. The presence of yield stresses and yielding behaviours has generated much debate within the rheological literature, due to a long understanding that “everything flows” [9]. However, it is generally accepted that in practise, within timescales relevant to the material in question, a material has a yield stress if it does not flow below a defined threshold [10]. The importance of engineering yield-stresses into fluids has been recently highlighted by Nelson and Ewoldt [10] demonstrating a clear set of design principles for such materials. Here they have highlighted the synergistic link between customer need/material specification and the materials microstructure, allowing for its application, an example of this would be paint where the presence of a dynamic yield stress allows it to “stick” to the wall without running [11,12]. Such principles were used to design a biopolymer hydrogel with viscoelastic properties that allow the material to liquefy when passing through the nozzle, but restructure to a weak gel on the receiving surface. Thus, facilitating retention of cells on the receiving surface without impairing the spraying process itself (Fig. 3).

Biopolymer hydrogels are widely used in burn wound care as dressings, and tissue-engineered scaffolds with or without bioactive compounds [13]. Hydrogels offer ideal systems often mimicking the 3D architecture of native extracellular matrix (ECM) [13]. The ability of these gels to entrap relatively large volumes of water at low percentages (%wt) of polymer is beneficial for maintaining a moist wound environment, allowing rapid diffusion of nutrients and metabolites [14]. Gellan gum was used as the biopolymer of choice in this study due to its highly tuneable mechanical properties [13]. Gellan gum hydrogels can be designed for many biomedical applications [15] using many forms including fluid gels [16,17].

To date, surprisingly little research has focused on quantifying the uniformity of sprayed solutions for wound coverage and the influence of spraying on mammalian cell survival after transplantation [18,19]. This study addresses some of the problems of current spray delivery systems and proposes gellan fluid gel as a material that could be utilised to enhance cell retention upon a surface following spraying.

## 2. Material and methods

## 2.1. Fluid gel preparation

Low acyl gellan gum stock solutions (1% (w/v) and 0.83% (w/v)) were prepared by the addition of gellan powder [Kelcogel<sup>®</sup> obtained from Azelis, Hertford, UK] to sterile water at 65 °C under constant agitation. Following, stocks of NaCl cross-linker solutions were prepared to concentrations of 0.1, 0.2, 0.3, 0.4 and 0.5 M in sterile water. Final polymer sols were subsequently formed by mixing aliquots of both gellan with cross-linker stock solutions (9:1) at 65 °C, resulting in final concentrations of either 0.9% (w/v) or 0.75% (w/v) polymer – 10 mM, 20 mM, 30 mM 40 mM and 50 mM NaCl. Gellan sols were then added to the cup of a couette (Cup diameter 28 mm, vane diameter, 26 mm) rheometry set-up (Kinexus Ultra, Malvern Pananalytical, UK) at 60 °C. After allowing thermal equilibrium to be reached, the system was cooled at a rate of 1 °C min<sup>-1</sup> to 20 °C under constant shearing, 450 s<sup>-1</sup>; unless stated otherwise. Post-production shear was removed, and fluid gels stored at 4 °C until further testing/use.

## 2.2. Rheological measurements

All rheological measurements were performed at 25 °C using a Kinexus Ultra rheometer (Malvern Pananalytical, UK) equipped with 40 mm parallel plates (1 mm gap height), 48 h post-processing.

Small deformation rheometry was undertaken varying both amplitude and frequency. Amplitude data was obtained in strain-controlled mode, ranging from 0.1 to 500% logarithmically at a constant frequency of 1 Hz. Linear viscoelastic regions (LVRs) were determined and a common strain of 0.5% was found to be common across all systems. This strain was then used for all frequency sweeps ranging between 0.1 and 10 Hz. Single frequency data was collected as a function of temperature at 0.5% strain and 1 Hz. Temperature ramps were applied at 1 °C min<sup>-1</sup> and moduli (G' and G'') obtained.

Non-linear rheology was determined using shear ramps in shear rate mode. Ramps were undertaken from 0.1 to 600 s<sup>-1</sup> logarithmically over 3-minute timescale. Hysteresis of the systems was probed by undertaking a second sweep immediately after the first, from 600 s<sup>-1</sup> back to 0.1 s<sup>-1</sup>. Data from the second ramp was fitted to the Herschel-Bulkley model (Equation (1)) to determine the dynamic yield stress ( $\sigma_y$ ).

$$\sigma = \sigma_y + K\dot{\gamma}^n \quad (1)$$

where  $\sigma_y$  is the yield stress,  $K$  is the consistency factor,  $\dot{\gamma}$  is the shear rate and  $n$  is the flow index.

The yield stress was compared to the maximum stress on the material at an inclining substrate to investigate whether flow is induced. Maximum stress was determined by the following formula:

$$\sigma_{max} = \rho gh(\sin\beta) \quad (2)$$

where  $\sigma_{max}$  is the maximum stress on the material,  $\rho$  the material density (kg m<sup>-3</sup>),  $g$  the gravitational acceleration of 9.807 m s<sup>-2</sup>,  $h$  is the height (m) and  $\beta$  the angle of inclined substrate.

\* Corresponding author at: Institute of Translational Medicine (Heritage building, 3rd Floor), Mindelsohn Way, Edgbaston, Birmingham B15 2TH, UK.  
E-mail address: bxt564@bham.ac.uk (B. ter Horst).

<https://doi.org/10.1016/j.actbio.2019.03.036>

1742-7061/Crown Copyright © 2019 Published by Elsevier Ltd on behalf of Acta Materialia Inc. All rights reserved.

### 2.3. Microscopy of fluid gels

Micrographs of the fluid gel systems were undertaken using a Leica DM6000 microscope (Leica Microsystems, UK). Firstly, fluid gels were diluted at a ratio of 4:1 in PEG400, via slow addition of the PEG under constant agitation. Post-dilution, one drop of the system was dispensed onto a microscope slide and coverslip placed over the top. Images were obtained at x20 magnification using phase contrast to distinguish between the continuous and particulate phases. ImageJ was used to add scale bars. Images presented are typical representations of the systems, compared against a minimum of 5 other micrographs.

### 2.4. Contact angle measurements

The static contact angle of sodium chloride and gellan fluid gel droplets on a variety of surfaces at room temperature were determined by imaging and subsequent measurement with ImageJ software using the DropSnake Plugin [20]. A 60  $\mu$ l droplet was dropped onto the test surfaces and imaged. Three repetitions were performed, each sample was measured three times and the mean contact angle was calculated. Substrates used included: gelatin 5% (w/v) (prepared with deionized water and bovine gelatin, stirred and allowed to set at 4 °C for a minimum of 60 min), alumina ceramic (referred to as ceramic in this paper), porcine epidermis and porcine subcutis. Porcine skin (Arun Meats & Livestock LTD, UK) was kept frozen and thawed before use.

### 2.5. Spray methods

Materials were delivered through an airbrush with external mixture and a standard medium size nozzle of 750  $\mu$ m in diameter (Badger, Universal 360 model, US) as illustrated in Fig. 5a. An oil-free air compressor (Badger BA1100, US) was used as the air source with air pressure regulator. Air pressure at delivery (15 psi), nozzle diameter (750  $\mu$ m), application distance (10–15 cm) and spray angle from spray tip to receiving surface (45°) were standardised (Fig. 5b). The airbrush system was cleaned and the nozzle rinsed thoroughly with ethanol 70% and allowed to air dry in the laminate flow hood before each spray cell experiment. Between experiments the nozzle was purged with 1 ml ethanol 70% and 1 ml culture media to ensure no cells from a previous application remained.

### 2.6. Spray analysis using water sensitive paper

For investigation of uniform distribution following spraying the individual droplet size, droplet size distribution and area covered by the gel was compared to control liquid (water or sodium chloride) (Fig. 5). Water-sensitive paper (WSP) of 26 mm  $\times$  76 mm (John Rhodes AS Ltd, Evesham, UK) was utilized to compare gellan fluid gel to the control liquid in a standardized fashion (Fig. 5c). Yellow coloured spray cards coated with bromoethyl blue dye turn blue when in contact with water. Measurements included: the percentage area covered by sprayed volume (%coverage), droplet size and droplet size distribution. Volumes of 50  $\mu$ l or 25  $\mu$ l were sprayed with an airbrush onto the WSP and allowed to dry for up to 60 min. A minimum of 3 repetitions was performed. Images were obtained directly following spray application, dried spray cards were scanned at 600x600 dpi (Konica Minolta scanner, bizhub c3350). Images were analysed with ImageJ Software, a colour threshold was set and the image was converted to a binary image. Then, percentage of coverage was calculated by the ratio of original (white pixels) to covered area (black pixels) (%coverage = (Area<sub>covered</sub>/Area<sub>original</sub>)\*100). For droplet size the 'Particle Analysis plugin' was used. Obtained parameters include droplet diameter (D) in mm, droplet area (A) in mm<sup>2</sup> and total

sprayed area (TSA) in mm<sup>2</sup>. A value where 50% of the total sprayed volume consists of drops with diameter larger than the median value and 50% smaller than the median value (DA50) could be obtained from the data. Next, DA10 and DA90 were obtained, similar to DA50, but for 10% and 90%. Relative Span factor (RSF), a single number reflecting the uniformity of the droplet size distribution was calculated in accordance with Eq. (3):

$$RSF = \frac{(DA90 - DA10)}{DA50} \quad (3)$$

### 2.7. Cell culture

Human Dermal Fibroblasts (HDFs) were used for all experiments. Fibroblast culture media was prepared from Dulbecco's modified Eagle's medium – high glucose (DMEM) (Sigma, UK), supplemented with 10% fetal bovine serum (FBS), 1.5% penicillin-streptomycin and 2.5% L-glutamine. Cultures were maintained in the incubator (5% CO<sub>2</sub>, temperature 37 °C, 100% humidity) and culture media changed every 2–3 days. Cells were harvested when they reached approximately 80% confluence.

### 2.8. Encapsulation of human dermal fibroblasts

HDFs were detached from cell culture flask using TrypLE solution (Sigma, UK), buffered with fibroblast culture media and centrifuged at 1000 rpm for 3 min. Cells were suspended in gellan fluid gels (0.9% or 0.75% (w/v)) at a concentration of 1–2  $\times$  10<sup>6</sup> cells/ml. Cell solutions were pipetted on culture petri dishes or sprayed with the airbrush device into cell culture treated 24-well plates and fresh culture media was added before samples were incubated (at 5% CO<sub>2</sub>, temperature 37 °C, 100% humidity) for later experiments or directly stained for imaging.

### 2.9. Live/Dead assay

Calcein acetocymethylester (Calcein AM) (Invitrogen, UK) was used to stain live cells and Propidium iodide (PI) (Invitrogen, UK) was used to stain dead cells. Calcein AM/PI stain was added to 1 ml of DMEM, samples were immersed in 100  $\mu$ l/ml of this solution for 20 min in the incubator. Samples were visualized using confocal microscopy (Olympus, Fluoview FV100), showing viable cells green (Calcein AM) and non-viable cells red (PI). Laser setting 488 nm and 543 nm for Calcein AM and PI respectively. Cell viability was measured with ImageJ software, images were split in the colour channels red (dead cells) and green (live cells). For each sample, cells were automatically counted by using the particle size plugin of ImageJ. Percentage of viable cells were calculated by the following formula (Eq. (4)):

$$viable\ cells\ (\%) = \frac{number\ of\ viable\ cells}{total\ number\ of\ cells\ (live + dead\ cells)} \times 100 \quad (4)$$

### 2.10. Alamar blue metabolic activity

Encapsulated and control HDFs were seeded or sprayed into 24-well tissue cultured plates at a density of 5  $\times$  10<sup>4</sup> per well for cells in gel and 1  $\times$  10<sup>4</sup> for cells in medium. Fresh growth medium at a volume of 1 ml was added, cells were then incubated for a minimum of 24 hr (at 5% CO<sub>2</sub>, temperature 37°, 100% humidity) together with negative control wells including medium and gellan fluid gel. Metabolic activity was assessed at day 1, 3 and 7 for all 4 conditions by incorporating 10% Alamar Blue reagent (Life Technologies, UK) into the culture medium. After an incubation time of 4 h,

absorbance was read at 570 nm and 600 nm using a microplate reader (Multiskan FC, Thermo Scientific, UK). Percentage reduction was calculated by comparing absorbance to negative control wells with the following equation:

$$percentage\ reduced\ (\%) = \frac{(\epsilon_{ox2} \times A1) - (\epsilon_{ox1} \times A2)}{(\epsilon_{red1} \times B2) - (\epsilon_{red2} \times B1)} \times 100 \quad (5)$$

A1 = absorbance at 570 nm test well; A2 = absorbance at 600 nm test well; B1 = absorbance at 570 nm control well and B2 = absorbance at 600 nm control well.

Standard molar extinction coefficients for oxidized ( $\epsilon_{ox}$ ) and reduced ( $\epsilon_{red}$ ) form of alamarBlue<sup>®</sup> were used:

$\epsilon_{ox1}$  = 80,586 at 570 nm;  $\epsilon_{ox2}$  = 117,216 at 600 nm;  $\epsilon_{red1}$  = 155,677 at 570 nm and  $\epsilon_{red2}$  = 14,652 at 600 nm

### 2.11. Statistical methods

Mean values and standard deviations are plotted unless stated otherwise. Unpaired t-tests and two-way ANOVA were performed using Prism 7 (GraphPad software, CA, USA) with a significance of  $p < 0.05$ .

## 3. Results

### 3.1. Fluid gel material and characterisation

#### 3.1.1. Fluid gel production

The preparation of fluid gels has been depicted in Fig. 1a using a schematic of the cup and vane set-up. Here a constant shearing force is applied to a gellan sol as it is forced, thermally as the system is cooled, through a sol-gel transition: as such the gelation

becomes confined by degree of shear applied, resulting in the formation of a particulate suspension of microgel particles (Fig. 1b and c) [16]. The formation of such systems was monitored via changes in viscosity as a function of temperature (Fig. 1d). Fig. 1d highlights that at a critical temperature an increase in the system viscosity was observed, dependent on the concentration of crosslinker in agreement with data published for quiescent gels [21]. The increase in viscosity results from the formation of particles which trap the continuous aqueous phase resulting in an effective change in the particle volume until a plateau is reached [22,23]. Such particles were studied using optical microscopy, showing anisotropic particles with varying length to width ratios (visually observed) dependent on the salt concentration (Fig. 1b and c, 50 and 10 mM NaCl respectively).

Mechanical responses have been shown in Fig. 1e and f, demonstrating the typical viscoelastic properties of the fluid gel. Fig. 1e compares the flow profile of the fluid gel against that of the current standard used for cell spraying (0.9% saline solution). The saline solution demonstrated a linear relationship between the shear stress and rate, typical of a Newtonian system where the viscosity is independent of the shear rate. In contrast, the fluid gel exhibited a shear thinning profile, typical of such systems [16], with a much greater viscosity in comparison to the saline. Linear rheology was further probed using frequency dependent measurements to better understand the materials behaviour at rest (Fig. 1f). Data suggests the formation of a weakly gelled network, both dependent on frequency and displaying large values of Tan  $\delta$  (ratio of loss to storage modulus;  $G''/G'$ ) [24,25], again previously reported as typical characteristics of such systems [7,16,24] (The calculated loss tangent was  $>0.1$  for all gels, as shown in Table 1).

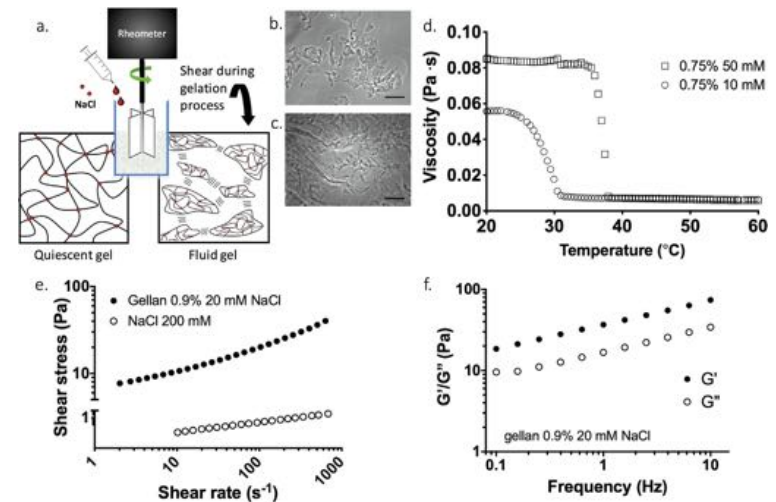


**Fig. 1.** Manufacture process and characteristics of gellan fluid gel. a) fluid gel manufacture process as adapted from Cooke et al. 2018 with permission [17]. Micrographs of diluted 0.75% fluid gels in 4:1 PEG:gellan ratio, manufactured with 50 mM NaCl (b) and 10 mM NaCl (c), scale bar = 100  $\mu$ m. d) Flow profiles for the formation of gellan fluid gel (0.75% (w/v), 10 mM and 50 mM NaCl) gelation of fluid gel occurs as temperature is decreasing under a constant shear rate of 450 s<sup>-1</sup>. Values presented are of one representative measurement. e) Flow profiles of post-production of gellan 0.9%, 20 mM NaCl demonstrated a non-Newtonian shear thinning behaviour with higher viscosity at low shear compared to 200 mM sodium chloride showing a linear relationship typical of a Newtonian fluid. N = 3 for gellan and N = 2 for NaCl. Mean values presented, error bars are SD (smaller than icon and therefore not visible). f) Frequency dependence of 0.9% (w/v) gellan fluid gel (20 mM NaCl) with gradually increasing G' and G'' modulus under increasing frequency typical of a weak gel system. Mean values of 3 individual measurements presented, error bars are SD (smaller than icon and therefore not visible).

**Table 1**  
Rheological properties of gellan fluid gels. All gels were fabricated with low acyl gellan gum powder and cross-linked with sodium chloride (NaCl) until a final concentration of 0.75% (w/v) or 0.9% (w/v) with a constant shear rate ( $450 \text{ s}^{-1}$ ) during the gelation process. Flow profiles for 3 individual samples per gel composition was measured at  $25^\circ \text{C}$  and viscosity at a shear rate of  $205 \text{ s}^{-1}$  shown, mean with standard deviation (SD) is presented. Viscosity of all gels is higher than control liquid (NaCl) and dependent on cross-linker and polymer concentration.  $G'$  at frequency of 1 Hz is presented, %strain at which loss of storage modulus occurs indicating the end of the LVR, loss tangent ( $G''/G'$ ), a loss tangent of  $> 0.1$  indicates a weak gel [1], as shown here all fluid gels compositions can be considered weak gels. \*1 sample of 200 mM NaCl was tested, viscosity measured at shear rate of  $205 \text{ s}^{-1}$ .

Material	Solution concentration	Cross-linker concentration (mM)	Mean viscosity (Pa.s) (SD)	$G'$ (Pa) (SD)	Strain end LVR (%)	Loss tangent ( $G''/G'$ )
Gellan	0.75% (w/v)	10	0.085 (0.001)	5.99 (0.17)	15.87	1.03
		20	0.076 (0.000)	10.45 (0.42)	12.00	0.70
		30	0.086 (0.002)	36.46 (3.42)	6.39	0.35
		40	0.110 (0.002)	105.74 (5.48)	4.02	0.21
		50	0.118 (0.005)	215.03 (35.89)	2.52	0.16
	0.90% (w/v)	10	0.117 (0.001)	12.54 (0.29)	12.00	0.84
		20	0.125 (0.003)	36.81 (1.28)	22.26	0.45
		30	0.135 (0.006)	94.45 (7.97)	6.39	0.27
		40	0.143 (0.002)	171.23 (10.36)	4.02	0.21
		50	0.177 (0.011)	388.47 (100.14)	2.52	0.17
Sodium chloride	200 mM	-	0.004*	-	-	-

### 3.1.2. Modulation of fluid gel properties

Manipulation over the material properties of the fluid gels was probed systematically as a function of both polymer and cross-linker concentrations; with a view to improve the characteristics required for enhanced “spray-ability”. Flow behaviour and viscosity for the fluid gel systems have been shown in Fig. 2a and b. All systems showed a high degree of shear thinning as the shear rate was increased from  $0.1$  to  $600 \text{ s}^{-1}$  (Fig. 2a). Shear profiles were used to estimate the behaviour of the fluid during spraying. This was achieved by comparing data. As previously described by Hendriks et al. [26] the expected shear rate ( $\dot{\gamma}$ ) encountered during spraying can be estimated by calculating the nozzle-induced shear rate ( $\dot{\gamma}$ ) in  $\text{s}^{-1}$  during spraying with the following formula:

$$\dot{\gamma} = \frac{V}{D_N} \quad (6)$$

( $\dot{\gamma}$  = shear rate in  $\text{s}^{-1}$ ,  $V$  = velocity ( $\text{m s}^{-1}$ ) of liquid and  $D_N$  = diameter of nozzle ( $\text{m}$ ). Standard nozzle diameter of the airbrush is  $750 \mu\text{m}$  ( $7.5 \times 10^{-4} \text{ m}$ ). Flow velocity ( $v$ ) was calculated by the following equation:

$$Q = v \times A \quad (7)$$

Volumetric flow rate ( $Q$ ) in  $\text{m}^3 \text{ s}^{-1}$ , flow velocity ( $v$ ) in  $\text{m/s}$ , column cross-sectional area ( $A$ ) in  $\text{m}^2$ .

For the standard nozzle size of  $750 \mu\text{m}$ , the nozzle induced shear rate of gellan 0.9% hydrogel was estimated at  $223 \text{ s}^{-1}$ . Viscosities were obtained and compared at the calculated shear rate were derived from rheology testing (Fig. 2b). For airbrush application, the estimated viscosity of the material was shown to be a function of both polymer and NaCl concentration. At comparative cross-linking concentrations, the higher polymer systems resulted in increased fluid gel viscosities. Additionally, a linear correlation between cross-linker concentration and viscosity was observed, again where higher concentrations of the cross-linker formed more viscous suspensions. However, ultimately all systems were characterised by a low spraying viscosity,  $8.4 \times 10^{-2} \text{ Pa.s}$  ( $\pm 6.7 \times 10^{-4}$ ) to  $1.8 \times 10^{-1} \text{ Pa.s}$  ( $\pm 1.2 \times 10^{-2}$ ). Although such viscosities are considered in this case low, they are still over an order of magnitude greater than the viscosity of the current standard delivery medium used for cell spraying.

The amplitude dependence (reflected in percentage strain) of the storage and viscous moduli are presented in Fig. 2c. Under increasing strain all tested compositions of gellan fluid gels eventually underwent a cross over showing a transition in  $G'$  domi-

nance to systems governed by  $G''$  (full data range shown in Supplementary Data: panel of gels). The data highlights one of the important properties of the fluid gels, where at large deformations the suspensions act as liquid-like materials, enabling flow. Changes in the degree of bulk suspension elasticity ( $G'$ ) as a function of the polymer and salt concentration has been demonstrated in Fig. 2d and e. Here both the magnitude of  $G'$  and length of the LVR were observed to be a function of the polymer and cross-linker concentrations, with the LVR shortening and modulus increasing with elevated salt concentrations.

Frequency data obtained for the fluid gel formulations highlighted a change in mechanical behaviour with frequency sweeps of 10 mM NaCl systems demonstrating initial  $G'$  dominated systems with clear cross-overs to  $G''$  domination (Fig. 2f and g). However, at higher salt concentrations ( $> 20 \text{ mM}$  to  $50 \text{ mM}$ ) plots showed  $G''$  dominance over the whole frequency range studied, with both  $G'$  and  $G''$  demonstrating some frequency dependence, typical of viscoelastic gel-like fluids. Gel strength was observed to increase, described by a reduction in  $\tan \delta$  (Table 1 and Supplementary Fig. 2) as a function of both salt and polymer concentration.

A simple experiment to demonstrate the clinical challenge of spray run-off has been shown in Fig. 3a, in which the control (sodium chloride) instantly flows on vertical tilted porcine skin surface in comparison to the retained fluid gel. Fluid gel hysteresis was probed to study the time dependent behaviours of the systems post spraying, using consecutive shear ramps: increasing and decreasing in shear rate ( $0.1$ – $600 \text{ s}^{-1}$  and  $600$  to  $0.1 \text{ s}^{-1}$ ). Direct comparison of the flow profiles suggests little change, with a large degree of the initial viscosity of the system is recovered almost instantaneously. Fig. 3b. The rheological phenomenon known as the dynamic yield stress was examined to describe the ability of the fluid gel to be maintained upon the skin without flowing. The Herschel-Bulkley model can be used to determine the yield stress of a fluid [27]. Data fitted to the model presented for the second sweep (example shown in Fig. 3c and Supplementary Fig. 3). Yield stress plotted as a function of the fluid gel formulations have been presented in Fig. 3d (full data presented in Table 2). Fitting to the 10 mM NaCl systems for both polymer concentrations resulted in negative values, indicating an inadequate means of describing the yield-stress fluid. However, a linear correlation between NaCl concentration and yield stress was observed for the higher concentrations. A simple gravitational model described for “sagging” was used to assess fluid gel resistance to flow on an inclined plane. The

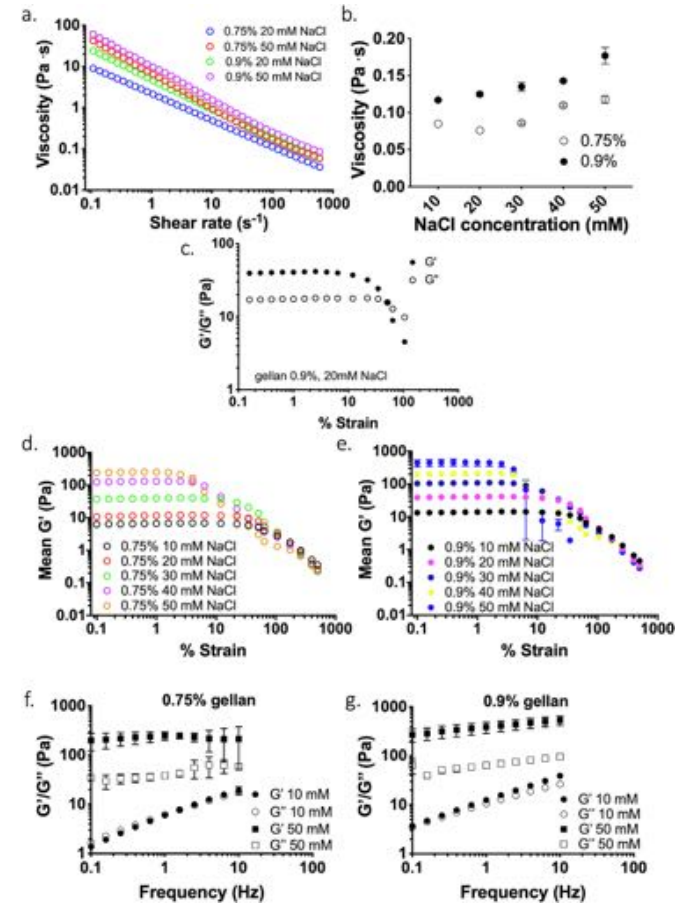


**Fig. 2.** Modulation of fluid gel properties. a) demonstrates that gellan fluid gels behave as shear-thinning materials (non-Newtonian), since viscosity decreased as shear rate increased. Four compositions of gellan fluid gel (0.9% (w/v), 20 mM and 50 mM NaCl and 0.75% (w/v), 20 mM and 50 mM NaCl) presented. b) Increasing crosslinker or polymer concentration results in higher viscosity as demonstrated here. Data is mean viscosity at shear rate  $205 \text{ s}^{-1}$  c) Amplitude dependence of storage and loss moduli in gellan 0.9%, 20 mM as representative gel shows that under increasing strain eventually  $G'$  and  $G''$  will cross-over resulting in a  $G''$  dominated system indicating more liquid like behaviour under high strain. Storage modulus as a function of the polymer and salt concentration of 0.75% fluid gels (d) and 0.9% fluid gels (e) shows an earlier loss of storage modulus (shorter LVR's) in higher salt-concentrations. f) Frequency dependence of four systems is shown here to illustrate influence of salt-concentration on viscoelastic-properties, from viscoelastic-solids at 10 mM NaCl concentrations to gel-like behaviours at 50 mM NaCl concentrations.  $G''$  (open signs) and  $G'$  (closed signs) values are presented. Unless stated otherwise, mean values of three independent measurements are presented, error bars represent the standard deviation. Mean values of 3 individual measurements presented, error bars are SD (smaller than icon and therefore not visible).

gravitational forces, described as ‘maximum stress on the material at an inclined surface’ were calculated with Eq. (2) using the following values: material density of  $1020 \text{ kg m}^{-3}$  for fluid gel (0.9%, 20 mM NaCl), assuming a fluid gel thickness of  $1.0 \times 10^{-4} \text{ m}$  and a substrate angle of  $45^\circ$ . The calculated maximum stress was observed to be lower than the yield stress of the gel, with values of  $0.85 \text{ Pa}$  and  $1.777 \text{ Pa}$  respectively.

### 3.1.3. Spray-ability of the fluid gel carrier

Spreading properties of the fluid gels in comparison to saline solution were investigated to gain further information of both cov-

erage and run-off. The contact angles for the fluid gel and control (NaCl) were measured on a variety of substrates, comparing their wetting ability. Gellan fluid gels exhibited a significantly higher mean contact angle than NaCl on gelatin ( $63.3^\circ$  vs  $44.4^\circ$ ,  $p < 0.001$ ), porcine epidermis ( $54.8^\circ$  vs  $25.37^\circ$ ,  $p < 0.001$ ) and porcine dermis ( $59.7^\circ$  vs  $36.6^\circ$ ,  $p < 0.001$ ) describing lower wettability, resulting in reduced spreading. There was no significant difference found for contact angles on ceramic, with a mean contact angle of  $37.5^\circ$  for gellan fluid gel and  $35.8^\circ$  for NaCl (Fig. 4a).

Flow and spreading due to the thermos-responsive properties of the gellan was also investigated. The effect of increasing tempera-

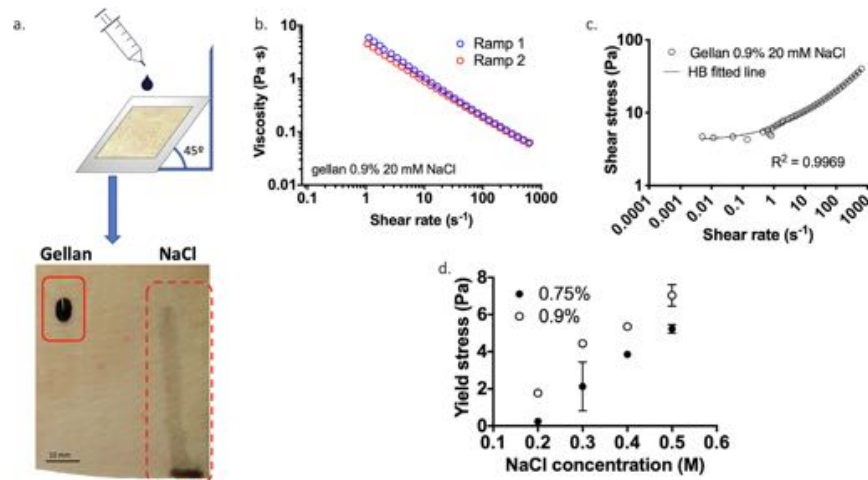


**Fig. 3.** Determination of fluid gel retention. a) gellan fluid gel (0.9% (w/v), 20 mM NaCl) and sodium chloride (200 mM) were dyed with acrylic black ink (Daler Rowney Bracknell, UK). Gellan fluid gel (left) and sodium chloride (right) droplets applied to tilted porcine skin at the same time. A low rate of spreading of the gellan fluid gel compared to sodium chloride was macroscopically observed. b) Viscosity of gellan fluid gel under increasing (ramp 1) and decreasing (ramp 2) shear rates over a known time frame. Plotted data includes mean viscosity of 0.9% (w/v), 20 mM NaCl prepared under same conditions, error bars represent SD. Increase in shear rate leads to shear thinning (decrease in viscosity) and decreasing the shear rate allows the gellan fluid gel to recover, demonstrated as increased viscosity resulting in a small thixotropy. Mean values of 3 individual measurements presented, error bars are SD (smaller than icon and therefore not visible). c) Herschel-Bulkley model fitted for 0.9%, 20 mM NaCl gel showing an excellent fit to the model represented in a  $R^2$  of 0.9969. d) Yield stresses determined using the Herschel-Bulkley model for 0.75% and 0.9% fluid gels with 20, 30, 40 and 50 mM NaCl. Yield stress was found to increase in higher polymer concentration gels and in higher salt-concentrations. Mean values of 3 individual measurements presented, error bars are SD.

**Table 2**  
Fitting parameters from the Herschel-Bulkley model for gellan fluid gels. Values presented are mean of 3 individual measurements, yield stress (+SD), K is the consistency index, n is the flow index. E is standard error, presented for each fitting value and R square as value for goodness of fit.

Gellan concentration (% w/v)	Final NaCl concentration (mM)	Mean Yield Stress (SD)	$E_y$	K	$E_K$	n	$E_n$	$R^2$
0.75%	10	-0.655 (0.005)	0.072	2.508	0.049	0.360	0.004	0.9995
	20	0.250 (0.018)	0.156	1.945	0.108	0.377	0.010	0.9965
	30	2.130 (1.306)	0.208	1.657	0.125	0.409	0.016	0.9928
	40	3.854 (0.084)	0.436	1.405	0.302	0.466	0.021	0.9848
	50	5.231 (0.227)	0.608	1.247	0.461	0.496	0.023	0.9804
0.90%	10	-0.848 (0.016)	0.291	3.844	0.060	0.340	0.070	0.9387
	20	1.777 (0.091)	0.226	2.860	0.156	0.383	0.010	0.9969
	30	4.446 (0.098)	0.305	2.508	0.184	0.413	0.015	0.9934
	40	5.357 (0.072)	0.806	2.166	0.653	0.441	0.023	0.9775
	50	7.036 (0.572)	1.600	2.921	1.454	0.423	0.030	0.9624

ture on the degree of structure within the fluid gels system was investigated as a function of  $G'$  and  $G''$  (Fig. 4b). Increasing temperature resulted in a reduction in the storage modulus, as the junction zones that create the 3D matrix began to break down, resulting in fluid-like behaviour of the gels. In general, a reduction in storage modulus appeared to occur between 30 and 40 °C for all gels, as shown in Fig. 4c, this range includes peripheral skin temperature. Based on the rheological data, gellan fluid gel with 0.9% polymer concentration and 20 mM NaCl cross-linker concentration was considered most suitable for the cell spray application (further discussed later), and thus used for further studies.

Spray coverage (% coverage) is the proportional area of receiving surface covered by sprayed material (gellan hydrogel or control liquid). A higher percentage of area was covered with water compared to gellan hydrogel, although these differences were not statistically significant (Fig. 5c and d). As expected, a higher percentage coverage was achieved when sprayed volume was increased, however,

this was not proportional, i.e. doubling the volume did not double the area covered (Fig. 5d). There was a non-statistically significant positive correlation between sprayed volume and percentage coverage for gellan hydrogel ( $p = 0.301$ , 95%CI: 33.09, 11.86; Pearson correlation 0.820) and water ( $p = 0.065$ , CI95%: -34.066, 1.308; Pearson correlation 0.723). This could be explained by the observed accumulation of droplets (especially in the centre of the sprayed area) with increasing volumes.

Individual droplet size was determined for all sprayed cards with ImageJ Software. The minimum cut off droplet size was set at 0.01 mm<sup>2</sup>. Mean droplet size of water ( $5.5 \times 10^{-2}$  mm<sup>2</sup>) and gellan fluid gel ( $5.2 \times 10^{-2}$  mm<sup>2</sup>) was not found to be significantly different ( $p = 0.326$ , 95%CI: -0.011, 0.004). On the other hand, the gellan fluid gel has a lower mean relative span factor (RSF) of 8.57 indicating a more uniform drop size distribution compared to the water (11.84). However, this difference was not found statistically different ( $P = 0.457$ , 95% CI: -8.77, 2.23). Droplet size

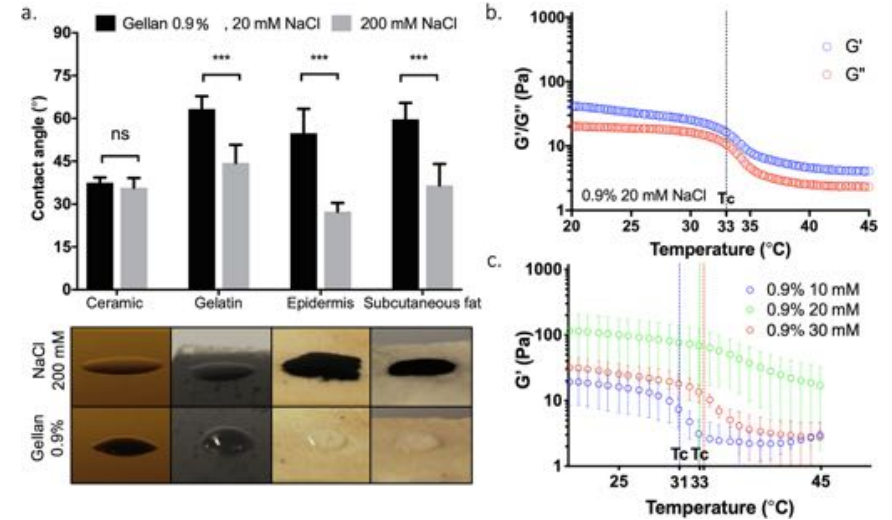


**Fig. 4.** Structural stability on the receiving surface. a) Mean contact angles of gellan fluid gel (0.9% (w/v), 20 mM) compared with control liquid (sodium chloride, 200 mM) on a variety of surfaces. Three repetitions for each surface and three measurements per repetition were performed. Error bars represent SD. Gellan fluid gel demonstrates larger contact angles on all tested surfaces compared to control liquid. b) Thermo-responsive properties of gellan (0.9%, 20 mM NaCl) was probed by investigating viscoelastic properties under increasing temperature. Increasing temperature resulted in a reduction in the storage modulus, resulting in fluid-like behaviour of the gel.  $T_c$  denotes the critical temperature at which the elastic structure starts to rapidly break down. Values presented are of one representative measurement. c) The storage modulus against rising temperatures in a panel of gellan fluid gels is presented. Gels with higher cross-linker concentrations de-structure (show fluid like behaviour) at higher temperature levels. Mean values of 2 individual measurements presented, error bars are SD.

distribution dependence on sprayed volume was investigated by comparing the RSF of two sprayed volumes per material. Gellan fluid gel showed a smaller decline in RSF when a smaller volume is sprayed compared to water, but this difference was not found significant ( $p = 0.854$ , 95% CI: -12.00, 4.62 for 25  $\mu$ l and  $p = 0.654$ , 95%CI: -33.24889, -4.89256 for 50  $\mu$ l). (Fig. 5e and f).

### 3.2. Biological response to fluid gel spray delivery

#### 3.2.1. Cell viability

Limited evidence of airbrush cell spray systems has been published, with most data presenting moderate cell viability (69–70% survival) following spraying in Hank's Balanced Salt Solution [28] or cell culture media [29]. As investigated by Hendriks et al. [26] certain spray conditions impact on cell viability such as receiving tissue/substrate stiffness, viscosity of cell carrier, nozzle-surface distant and delivery pressure. Therefore, all these conditions were standardised to reduce bias as described in section 2.4. The study aimed to develop a cell carrier with maintaining a cell viability comparable to current spray systems. Cell viability of sprayed encapsulated human dermal fibroblasts was evaluated at days 1, 3, and 7 using live/dead assay as demonstrated in Fig. 6. Cells remained viable in the gellan fluid gel up to at least day 7, with a mean cell viability of 88.0% (range 80.6% – 96.9%). Encapsulated HDFs attached to the bottom of the culture disks at day 7 (Fig. 7c) and spreading of the cells was observed at day 14 (Fig. 7d). Therefore, it can be assumed that cells are able to diffuse out of the gel, whether this is by active migration or passive sedimentation needs to be confirmed. Sprayed HDFs encapsulated in gellan fluid gel maintained similar high viability throughout the

studied period, there was no statistically significant difference between the application methods (Fig. 6b).

Alamar blue, a non-toxic reagent used to quantify the cellular metabolic activity, was used to investigate metabolic activity of encapsulated and sprayed cells. Data shown in Fig. 7 shows that metabolic activity directly measured via absorbance and is expressed by percentage of reduction. Percentage reduction of encapsulated cells remained stable over the tested period of 7 days. Whereas cells in culture medium showed a significant increase in percentage reduction indicating a proliferation of the cells following delivery (Fig. 7d). No statistically significant differences of sprayed cells compared to non-sprayed cells were found. Data implies that proliferation capacity of encapsulated cells is limited, while cell viability remains high.

### 4. Discussion

Cell spraying techniques have been translated to clinical practice, but limited success finds them not routinely used within burns care [30]. Several features of the cell solution could be compromising the full potential of the technology: e.g. cell-spillage, non-uniform distribution [3] and decrease in cell viability following transplantation [18].

This study aimed to remedy this clinical problem by engineering a sprayable gellan-based fluid gel, to enable cells to be transplanted to the receiving surface without spillage and/or loss of cell viability. The polymer used to prepare the hydrogel was gellan gum, a polysaccharide derived from the bacterium *Pseudomonas elodea*, comprised of D-glucuronic acid, L-rhamnose and D-glucose subunits. This natural polymer is FDA approved as a food additive, however, has also found its way to the pharmaceutical

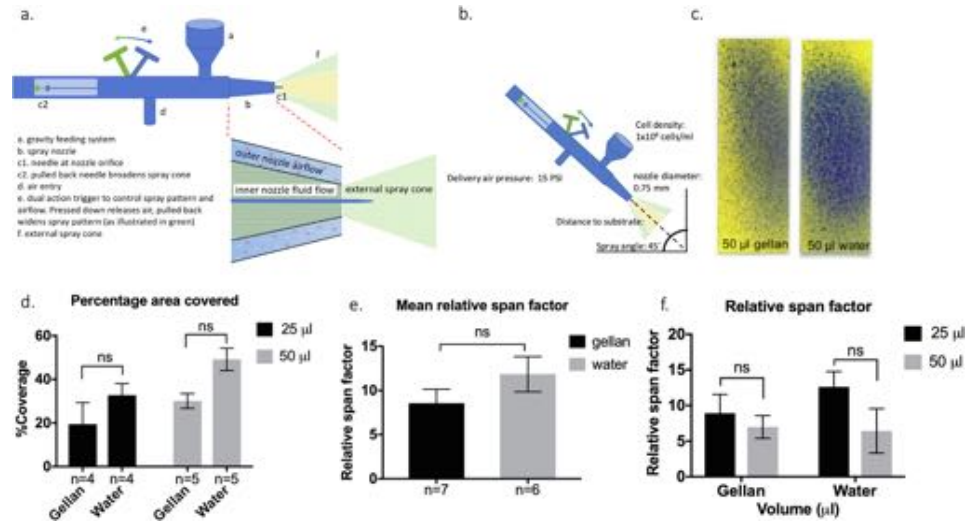


**Fig. 5.** Spray features of gellan gum fluid gel. 0.9% (w/v) gellan fluid gel with 20 mM NaCl cross-linker was used for all spray experiments presented in this figure. Mean values are presented, error bars represent SD. a) Schematic illustration of airbrush and its nozzle. b) Schematic of standardized airbrush spray experiment set up. c) Illustration of water-sensitive paper with area coverage demonstrated for sprayed gellan fluid gel and control (volume of 50 µl). d) percentage of area covered seems higher with sprayed water compared to gellan fluid gel, but no statistically significant difference was found. e-f) A lower mean relative span factor was calculated for gellan fluid gels (gellan) in comparison to control liquid (water) for both sprayed volumes together (e) and separated (f) This difference was more profound when looking at low sprayed volumes of 25 µl, indicating a more uniformly spray distribution for the gel, but no statistical difference was found.

and biomedical industry due to its biocompatibility in a range of tissues - demonstrating non-cytotoxic behaviour. A plethora of biomedical applications for gellan gum have been reported, such as regeneration of cartilage [31,32], neural tissue [33] or intervertebral discs [34] and topical applications to enhance wound healing [35], have arisen from its diverse nature lending it to applications such as injectables, films/dressings, eye drops and cell culture matrices [31].

Cross-linking of gellan gum can be achieved using ionic cross-linkers with monovalent cations ( $\text{Na}^+$  or  $\text{K}^+$ ) resulting in the formation of weaker gels than comparative divalent cations [211736]. Strong gels, although they do not disintegrate easily upon the wound bed like weak gels, do not easily conform to the body resulting in poor bioavailability. Even though on a bulk scale weaker gels are prone to breaking-up, the ability to get them to conform and disintegrate on a microscale presents an advantage for sprayed cell applications; as a gradual form of degradation is desired to release the cells and eventually remove the foreign material. The lack of cell binding capacity of gellan also means that cells do not necessarily attach to the material readily [37], which is again beneficial for rapid cell migration from the gel to tissue. Furthermore, adhesive cells such as fibroblasts and keratinocytes are dependent on adhesion to exhibit differentiation, therefore adhesive cells can be encapsulated in gellan hydrogel while potentially preserving their differentiation potential.

Fluid gels formulated with gellan therefore propose an ideal matrix for cell delivery, via spraying; demonstrating key rheological properties needed for both spraying and contouring to the wound surface for the release of cells *in situ* (Fig. 1). Fluid gels are formed via the application of constant confinement (mechanical shear) to a biopolymer undergoing a sol-gel transition [16,38]. Applying this technique to gellan results in the restriction of order-

ing during the random coil to helix transition, preventing the formation of a continuous gelled network, and forming a particulate suspension; where particle growth is governed ultimately by the interplay between gelation kinetics and degree of confinement acting within the system [39] (Fig. 1a). This was demonstrated by the change in gelling profiles for the 0.75% (w/v) fluid gels prepared using either 10 or 50 mM NaCl. Here, for the same degree of confinement applied (a shear rate of  $450 \text{ s}^{-1}$ ), systems resulted in very different gelling temperatures and final viscosities (although it is key to note that these viscosities are found well within the systems shear thinning region). In this case the heightened concentration of crosslinker has prompted gelation at higher temperatures, as expected from literature, as the salt ions promote the formation of helices with tighter binding and stronger junction zones [40]. Changes in the viscosity of the two systems is described in a similar way, where tighter binding and stronger junction zones between polymer chains results in more rigid particles [40] and a subsequent increase in suspension viscosity as demonstrated by Adams *et al.* [41] in accordance with Snabre and Mills [42]. Micrographs of the systems suggested changes in particle morphology (Fig. 1b and c). Differences in particles formed under the same degree of shear are likely to reflect a change in the mechanism of formation, as detailed by Fernández Farrés *et al.* [8]: who demonstrated that at faster gelation kinetics large gelled entities were initially formed that became broken down in flow, whereas as when gelation is much slower, particles were formed within the elongation flow itself - within the rheometer geometry [8,16,43] (although further characterisation of the systems here is needed to qualitatively address key parameters including particle size and degree of anisotropy to draw stronger conclusions on this area).

Systematic modulation of the fluid gel properties, in order to optimise the system for spray applications was achieved through

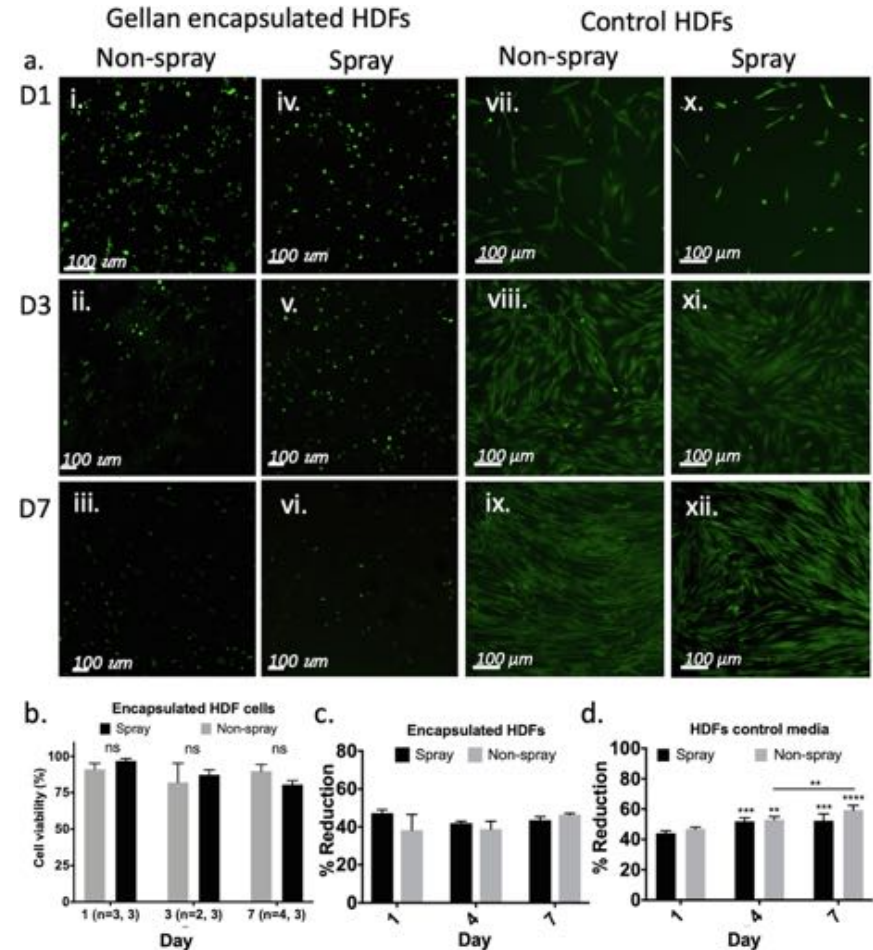


**Fig. 6.** Human dermal fibroblast response to fluid gel spray delivery. ai-axii) Fluorescence cell viability assay of encapsulated human dermal fibroblasts (HDF) before (iii) and after (iv-vi) spraying shows similar high cell viability. Similar for good viability is seen in sprayed cells (x-xii) in control medium compared to non-sprayed cells (vii-ix). b) No significant differences between the two groups on each timepoint was found. Presenting data is mean cell viability and SD. Airbrush spray set up was standardized with air pressure at delivery of 15 psi, nozzle diameter (750 µm), consistent angle and distance to receiving surface. cd) Alamar blue assay of encapsulated and control HDFs. % Reduction of encapsulated sprayed and control cells did not change significantly over the studied period. Statistically significant differences were found for cells sprayed in medium, comparing day 1 to day 4 and day 7 and in non-sprayed cells also between day 4 and day 7. Significant differences found by two-way ANOVA and post-hoc statistical testing is indicated by \* ( $p < 0.05$ ), \*\* ( $p < 0.01$ ), and \*\*\* ( $p < 0.001$ ), which correspond to p values in brackets. Data are presented as the means ( $\pm$ SD) from one experiment, performed in triplicate. (For interpretation of the references to colour in this figure legend, the reader is referred to the web version of this article.)

careful control over the formulation; varying both the biopolymer and cross-linker concentrations. Changes in the microstructure were probed using small deformation rheology. Frequency dependence sweeps of low salt concentration systems demonstrated an initial  $G'$  domination with a clear cross-over to  $G''$  domination. Whereas at higher salt concentrations, these cross-overs did not occur and  $G'$  dominated over the whole frequency range studied, but both  $G'$  and  $G''$  are demonstrating some frequency dependence,

with decreasing values for the loss tangent ( $\tan \delta$ ) as a function of increasing salt concentrations. Gel-like mechanical spectra arise from the restriction of polymer movement preventing the polymers from relaxing. However, within the gel systems, polymer re-arrangement results in viscous dissipation of energy ( $G''$ ) [44,45]. The reduction in  $\tan \delta$  suggested increased hinderance within the gelled matrix, as polymer re-arrangement becomes increasing prohibited, due to a higher crosslink density at higher

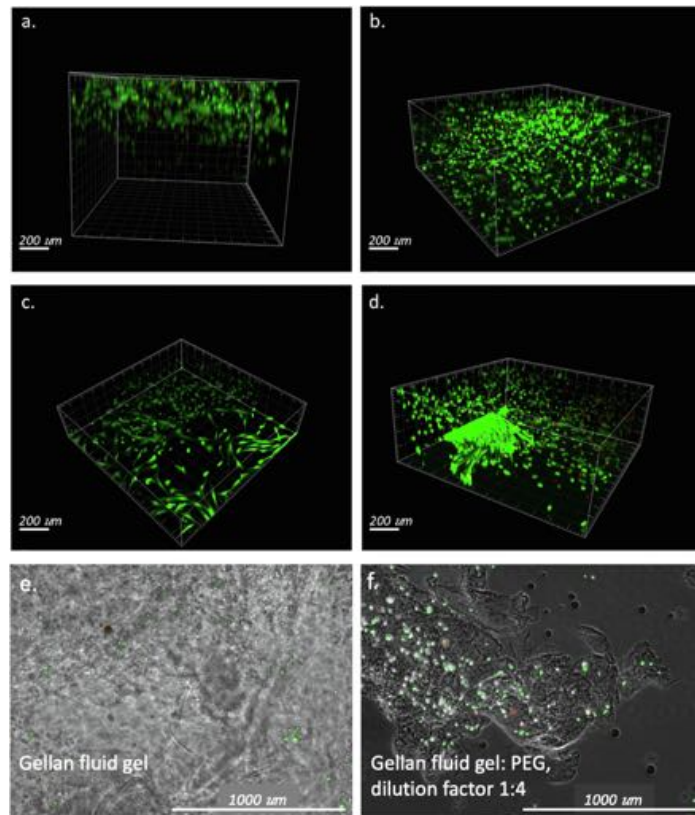


**Fig. 7.** Live/dead assay of HDFs encapsulated in gellan fluid gel. Z-stack image of fluorescence cell viability assay of human dermal fibroblasts (HDF) after 1 day (Fig. a), 3 days (Fig. b), 7 days (Fig. c) and 14 days (Fig. d) of encapsulation in gellan fluid gel (livecells stained green, dead cells stained red). Cells are viable and attach to the bottom of the well and seem to migrate out of the gel. Position of cells within the gel is shown in micrographs of encapsulated cells in gellan fluid gel (e) stained with fluorescence live/dead dye and in PEG diluted fluid gel (f). Images were obtained at day of encapsulation. (For interpretation of the references to colour in this figure legend, the reader is referred to the web version of this article.)

salt concentrations. This has also been seen in the frequency dependence data which indicates that the fluid gels became stiffer at a high frequency due to the rapid relaxation time of short chain segments. On a bulk scale, this results in the formation of stiffer particles, with suspensions exhibiting increased storage moduli [41]. Meanwhile  $G''$  also increased with increasing frequency, contributing to recoverable deformation and energy dissipation, especially in fluid gels with a low crosslinking degree (10 mM NaCl). However, it is key to note that although the suspension rheology is governed primarily through the stiffness of the particles, weak interactions between particles [7,8,16,39] effectively resulted in the suspensions demonstrating mechanical spectra which fall somewhat between those typical of entangled polymers and strong-gels [16].

Strain sweeps were used to explore the nature of the weak forces between suspended particles. It has previously been proposed that during the conformational change of the biopolymer

during cooling (coil to helix formation) complete polymerisation at the particle interface becomes prevented [16,39]. This results in points of weak association between particles. On deformation the fluid gel suspensions reached a critical strain at which they no longer act linearly. This critical strain is principally related to the proximity of gellan chains to each other and the number of weak interactions (hydrogen bonds etc.) at both the particle interfaces, and interstitial gellan remaining within the aqueous phase [46]. At larger deformations physical debonding between particle-particle and particle-interstitial gellan can occur resulting in a reduction in storage modulus. Reduced deformation of the fluid gel particles as a function of the increased stiffness (at higher salt concentrations) results in a shortening of the contact zones between particles, effectively reducing the degree of interactions between polymer chains [41]. This explains the reduction in LVR with increasing salt concentrations. Furthermore, it is hypothesised that changes in particle morphology (smaller discrete

through to long ribbon-like particles) may also play a role within the particle contact time; as the longer “ribbon-like” particles remain in contact across much larger strains (deformations) before the systems begin to breakdown [43,47]. Again, such inferences require further quantification of the micrographs obtained.

The effects of formulation on suspension viscosity were studied in respect to spray-ability. The effect of salt concentration has been previously described within the manuscript, however, viscosity modulation was also achieved by changing the concentration of polymer. Once gelled under shear, the formation of particulates resulted in entrapment of the continuous aqueous phase, effectively increasing the volume occupied by the particles. In correspondence with work published by Adams *et al.* [41], a direct correlation between the initial polymer weight fraction and particle phase volume can be assumed, as such the increase in viscosity thus becomes a function of the particle packing fraction; with rheologies typical of highly concentrated systems [48]. However, at shear rates comparable to those expected during spraying, all systems resulted in a degree of shear thinning that allowed application.

Fluid gel systems exhibited very little thixotropy, recovering much of their original viscosity once shear had been removed. Flow profiles were compared to the Herschel-Bulkley equation, which highlighted the presence of a yield stress for all systems formulated with >20 mM NaCl. Again, similar trends to the small deformation rheology were observed, where increases in both salt and polymer concentrations, tended towards larger yield stresses. Such overlap implies a common mechanism, whereby increased cross-link density and subsequent interactions (increased  $G'$ ), results in connected particles that require a critical stress in order to induce flow. Yielding values were compared to gravitational stresses, as a simple force balance. In all cases where yielding behaviour was observed, the fluid gel yield stress surpassed that of the gravitational stress, suggesting long residence times on the skin, where many of the surfaces are contoured. Clinically this means the finite gelled layer would remain *in situ* until mechanically removed, likely during dressing changes or other cleaning processes.

Following the ability to spray, spreading of the material post-application is also important: as large degrees of spreading lead to vast amounts of run-off and too little prevents the formation of a continuous layer. Complete wetting of a material to the surface occurs when the contact angle is near to  $0^\circ$  as high wetting requires small contact angles  $<90^\circ$ , while large contact angles refer to low wettability  $>90^\circ$  [49]. Contact angles obtained for the fluid gel systems across a variety of materials including biological substrates encountered within a burn environment: epidermis and subcutaneous fat (Fig. 4a). The gellan-based systems showed a significant increase in contact angle ( $p < 0.001$ ) across the gelatin, epidermis and subcutaneous fat substrates. This is a result of enhanced viscosity which strongly influences the liquid-surface. Fluid gels are enriched with the presence of polar groups, long polymer chains and possibly additional side chains causing a slower spreading, and less spillage. Whereas the low-viscosity saline solutions (such as sodium lactate and sodium chloride solutions), currently used as the delivery vehicle of choice in sprayed cell systems, exhibit low cohesive forces suggesting stronger adhesive forces to the substrate resulting in high wettability.

Spreading as a result of the thermo-reversible nature of the gellan gels was also probed, in respect to temperatures associated with burns wounds. Average peripheral skin temperatures lie around  $34^\circ\text{C}$  [50], but can vary greatly in critically ill patients, especially following burn injuries  $p < 0.001$  when room and body temperatures are deliberately increased [50,51]. Upon heating, the gels showed weakening of the interactions between the particles as demonstrated by a reduction in  $G'$  at a critical temperature,  $T_c$  (Fig. 4b). This loss of storage modulus is caused by the gel melt-

ing (initially by melting of residual unaggregated helices and secondly by melting of the aggregated double helices [17]), with  $T_c$  correlating closely with literature obtained using as differential scanning calorimetry (DSC) [52]. Structural weakening was shown to be influenced by salt concentration as expected from literature. As such, delayed onset of gel breakdown could be achieved by increasing the cross-linker concentration (Fig. 4c), corresponding to data by Morris *et al.* [17]. Ultimately the balance between the mechanical behaviour of the gels and weakening is important as a certain degree gel breakdown is desired, so cells are easily able to be released from the gel. Also, to improve patient experience the remaining polymer can be taken off the skin with cleaning solution warmed to skin temperature. The fluid gel composition can be tuned to these specific needs and highlighted the 0.9% (w/v), 20 mM NaCl formulation as the optimal system to trial as the cell delivery vehicle.

Current cell spray delivery systems have been used clinically by manufacturers guidance only. Quantifying the total area covered by the cell sprays has been investigated sparsely [53]. Furthermore, uniformity of the sprayed solutions could provide information on even cell distribution indirectly informing on required cell density. In this study, spray coverage and uniformity of distribution was quantified using water-sensitive paper (WSP) (Fig. 5). The technique was used to quantify sprayed gellan fluid gel in terms of percentage coverage and droplet size by a similar method utilizing ImageJ software described by Ferguson *et al.* [54,55]. A trend towards lower coverage of the gellan hydrogel was seen (Fig. 5d), likely explained by preserved droplet stability (shape) as a result of larger contact angles, however, such differences were not statistically significant.

The high cell viability following encapsulation in this study is supported by the current literature, with successful encapsulation of numerous cell types reported in quiescent gellan hydrogels [15,32,33,56]. After 7 days of culturing within the fluid gel, cell attachment to the bottom of the well was noted, suggesting movement of the fibroblasts (Fig. 7). Adherence, elongation and spreading of the fibroblasts over the plastic was also observed. Data suggested that the fluid gel support migration of the cells whilst preserving their cell function. Such observation correspond to the findings by Ferris *et al.* reporting cell settling of mouse myoblasts in gellan fluid gel [57]. It is proposed that such movement is facilitated either by passive sedimentation through the gelled particles or active migration of the cells out of the gel as seen in alginate-based fluid gels [58]; however, further study on environmental conditions that might influence this migration needs to be further addressed.

Cell viability post-spraying is an important factor to consider, as numerous mechanical stresses during the spraying process can be detrimental to the cell's integrity [18]; causing structural cell damage such as membrane elongation, adverse cell responses (e.g. some cell differentiation processes are mechanically activated) or diminished cell viability after deposition. Several parameters influence the shear stresses exerted on the cell systems during spraying such as nozzle diameter, viscosity of the material and velocity at delivery [26]. Previous studies based on saline carrier systems demonstrate a survival rate of  $>90\%$  when a low air pressure and large nozzle sizes were used [19]. This study demonstrates a comparable level of viability when spray nozzles with similar diameters and air pressure were used, compared to current commercially available spray systems. Modification of viscosity provided by the fluid gel system can be crucial to protecting the cells, providing a cushioning effect during delivery [26]. Data has shown that metabolic activity of encapsulated sprayed cells is similar to non-encapsulated cells at day 1 and remains stable for 7 days (tested period). Because the metabolic activity of non-encapsulated cells increases over time following spraying whereas

encapsulated cells expressed a steady level metabolic activity, it is possible that the proliferation capacity of encapsulated cells is restricted in the fluid gel. But the introduction of a structured fluid gel has not compromised cell viability following spraying in an *in vitro* setting. Although demonstrated *in vitro*, within a clinical setting, cells are sprayed into a hostile wound environment, potentially exposed to further mechanical trauma by wound dressings. It is suggested that the fluid gel carrier may provide extended shielding, enhancing the potential of the cells by allowing time for migration and adhesion within the local tissues. The findings of this study support that gellan fluid gel is a promising cell carrier for cell spray delivery, but further research is needed to investigate this technique in an *in vivo* model.

## 5. Conclusions

The work presented here demonstrates the development of a gellan-based fluid gel system, with flexible viscoelastic properties that can be tuned to facilitate spray delivery requirements such as: liquefying at high shear during spraying, self-structuring post-spraying and resistance to flow once *in situ*. Spray assessment of the gellan fluid gel demonstrated higher contact angles and limited runoff of the receiving surfaces when compared to a current clinically available cell carrier. Furthermore, cell compatibility to the gellan fluid gel was high, with good cell viability over a 7-day timescale. Additionally, viability of the encapsulated cells was not compromised following the spraying process. Therefore, gellan fluid gels provide a promising candidate for cell encapsulation, bridging the clinical need for sprayed systems and allowing retention to the wound site. However, future work will need to focus on functional and proliferation behaviour of transplanted epithelial cells with a view to translation of the technique within *in vivo* models.

## Permission Note

Permission to publish an adapted version of Fig. 1a has been received from John Wiley and Sons.

## Funding

This work was supported by the Scar Free foundation. The funding source had no involvement in designing the study, data collection, interpretation of data and decision to submit the article for publication. None of the authors has a financial interest in any of the products, devices, or drugs mentioned in this manuscript.

## Disclosures

The authors state no conflict of interest.

## Acknowledgements

This study was funded by a Medical Research Council Developmental Pathway Funding 517 Scheme (MR/N019016/1) and by the Scar Free Foundation Birmingham Burn Research Centre.

## Appendix A. Supplementary data

Supplementary data to this article can be found online at <https://doi.org/10.1016/j.actbio.2019.03.036>.

## References

- [1] C.D. Marshall, M.S. Hu, T. Leavitt, L.A. Barnes, H.P. Lorenz, M.T. Longaker, Cutaneous Scarring: Basic Science, Current Treatments, and Future Directions, *Adv. Wound Care*. 7 (2018) 29–45, <https://doi.org/10.1089/wound.2016.0696>.
- [2] B. Ter Horst, G. Chouhan, N.S. Moiemien, L.M. Grover, Advances in keratinocyte delivery in burn wound care, *Adv. Drug Deliv. Rev.* (2017), <https://doi.org/10.1016/j.addr.2017.06.012>.
- [3] D.L. Chester, D.S. Balderson, R.P. Papini, A review of keratinocyte delivery to the wound bed, *J. Burn Care Rehabil.* 25 (2004) 266–275.
- [4] P. Johnstone, J.S. Kwei, G. Filobos, D. Lewis, S. Jeffery, Successful application of keratinocyte suspension using autologous fibrin spray, *Burns* 43 (2017) e27–e30, <https://doi.org/10.1016/j.burns.2016.05.010>.
- [5] A. Alloumi, R. Papini, D. Lewis, Spray-on-skin cells in burns: a common practice with no agreed protocol, *Burns* 39 (2013) 1391–1394, <https://doi.org/10.1016/j.burns.2013.03.017>.
- [6] L.J. Currie, R. Martin, J.R. Sharpe, S.E. James, E. James, A comparison of keratinocyte cell sprays with and without fibrin glue, *Burns* 29 (2003) 677–685, [https://doi.org/10.1016/S0305-4179\(03\)00155-4](https://doi.org/10.1016/S0305-4179(03)00155-4).
- [7] M.E. Cooke, S.W. Jones, B. ter Horst, N. Moiemien, M. Snow, G. Chouhan, L.J. Hill, M. Esmaeli, R.J.A. Moakes, J. Holton, R. Nandra, R.L. Williams, A.M. Smith, L.M. Grover, Structuring of Hydrogels across Multiple Length Scales for Biomedical Applications, *Adv. Mater.* 30 (2018), <https://doi.org/10.1002/adma.201705013>.
- [8] I. Fernández Farrés, R.J.A. Moakes, I.T. Norton, Designing biopolymer fluid gels: A microstructural approach, *Food Hydrocoll.* 42 (2014) 362–372, <https://doi.org/10.1016/j.foodhyd.2014.03.014>.
- [9] H.A. Barnes, The yield stress-a review or 'greek'-everything flows?, *J. Nonnewton. Fluid Mech.* 81 (1999) 133–178, [https://doi.org/10.1016/S0377-0257\(98\)00094-9](https://doi.org/10.1016/S0377-0257(98)00094-9).
- [10] A.Z. Nelson, R.H. Ewoldt, Design of yield-stress fluids: a rheology-to-structure inverse problem, *Soft Matter* 13 (2017) 7578–7594, <https://doi.org/10.1039/c7sm00758b>.
- [11] Q.D. Nguyen, D.V. Boger, Measuring the Flow Properties of Yield Stress Fluids, *Annu. Rev. Fluid Mech.* 24 (1992) 47–88, <https://doi.org/10.1146/annurev.fl.24.010192.000403>.
- [12] E.C. Bingham, H. Green, Paint, a plastic material and not a viscous liquid; the measurement of its mobility and yield value, *Proc. Am. Soc. Test. Mater.* (1920) 640–675.
- [13] M. Madaghiele, C. Demitri, A. Sannino, L. Ambrosio, Polymeric hydrogels for burn wound care: advanced skin wound dressings and regenerative templates, *Burn. Trauma* 2 (2015) 153–161, <https://doi.org/10.4103/2321-3868.143616>.
- [14] N.E. Fedorovich, J. Alblas, J.R. de Wijn, W.E. Hennink, A.J. Verboom, W.J.A. Dhert, Hydrogels as Extracellular Matrices for Skeletal Tissue Engineering: State-of-the-Art and Novel Application in Organ Printing, *Tissue Eng.* 13 (2007) 1905–1925, <https://doi.org/10.1089/ten.2006.0175>.
- [15] D.F. Coutinho, S. Sant, H. Shin, J.T. Oliveira, M.E. Gomes, N.M. Neves, A. Khademhosseini, R.L. Reis, Modified Gellan Gum hydrogels with tunable physical and mechanical properties, *Biomaterials* 31 (2010) 7494–7502, <https://doi.org/10.1016/j.biomaterials.2010.06.035>.
- [16] D.A. Garrec, I.T. Norton, Understanding fluid gel formation and properties, *J. Food Eng.* 112 (2012) 175–182, <https://doi.org/10.1016/j.jfoodeng.2012.04.001>.
- [17] E.R. Morris, K. Nishinari, M. Rinaudo, Gelation of gellan – a review, *Food Hydrocoll.* 28 (2012) 373–411, <https://doi.org/10.1016/j.foodhyd.2012.01.004>.
- [18] C. Fredriksson, G. Kratz, F. Huss, Transplantation of cultured human keratinocytes in single cell suspension: a comparative *in vitro* study of different application techniques, *Burns* 34 (2008) 212–219, <https://doi.org/10.1016/j.burns.2007.03.008>.
- [19] W.S. Veazey, K.J. Anusavice, K. Moore, Mammalian cell delivery via aerosol deposition, *J. Biomed. Mater. Res. Part B Appl. Biomater.* 72B (2005) 334–338, <https://doi.org/10.1002/jbm.b.30159>.
- [20] W. Rasband, ImageJ: Image processing and analysis in Java, *Astrophys. Source Code Libr.* 1 (2012) 06013, <https://doi.org/10.1016/j.molcel.2006.04.003>.
- [21] H. Grasdalen, O. Smidsrød, Gelation of gellan gum, *Carbohydr. Polym.* 7 (1987) 371–393, [https://doi.org/10.1016/0144-8617\(87\)90004-X](https://doi.org/10.1016/0144-8617(87)90004-X).
- [22] A. Gabriele, F. Spyropoulos, I.T. Norton, Kinetic study of fluid gel formation and viscoelastic response with kappa-carrageenan, *Food Hydrocoll.* 23 (2009) 2054–2061, <https://doi.org/10.1016/j.foodhyd.2009.03.018>.
- [23] P.A. Williams, *Gums and Stabilisers* (2002) 384.
- [24] Assunta Borzacchiello, Luigi Ambrosio, *In: Hydrogels*, Springer Milan, Milano, 2009, pp. 9–20, [https://doi.org/10.1007/978-89-470-1104-5\\_2](https://doi.org/10.1007/978-89-470-1104-5_2).
- [25] X. Xin, A. Borzacchiello, P.A. Netti, L. Ambrosio, L. Nicolais, Hyaluronic-acid-based semi-interpenetrating materials, *J. Biomater. Sci. Polym. Ed.* 15 (2004) 1223–1236, <https://doi.org/10.1163/1568562041753025>.
- [26] J. Hendriks, C. Willem Visser, S. Henke, J. Leijten, D.B.F. Saris, C. Sun, D. Lohse, M. Karperien, Optimizing cell viability in droplet-based cell deposition, *Sci. Rep.* 5 (2015) 11304, <https://doi.org/10.1038/srep11304>.
- [27] P. Coussot, Yield stress fluid flows: a review of experimental data, *J. Nonnewton. Fluid Mech.* 211 (2014) 31–49, <https://doi.org/10.1016/j.jnnfm.2014.05.006>.
- [28] W.S. Veazey, K. Moore, K.J. Anusavice, K. Moore, Mammalian cell delivery via aerosol deposition, *J. Biomed. Mater. Res. B Appl. Biomater.* 72 (2003) 334–338.
- [29] F.A. Navarro, M.L. Stoner, C.S. Park, J.C. Huertas, H.B. Lee, F.M. Wood, D.P. Orgill, Sprayed keratinocyte suspensions accelerate epidermal coverage in a porcine microwound model, *J. Burn Care Rehabil.* 21 (2000) 513–518, <https://doi.org/10.1097/00004630-200021060-00007>.
- [30] J.N. McHeik, C. Barrault, G. Levard, F. Morel, F.X. Bernard, J.C. Lecron, Epidermal healing in burns: autologous keratinocyte transplantation as a standard procedure: update and perspective, *Plast Reconstr Surg Glob Open*. 2 (2014), <https://doi.org/10.1097/gox.0000000000000176>.
- [31] S.R. Moxon, A.M. Smith, Controlling the rheology of gellan gum hydrogels in cell culture conditions, *Int. J. Biol. Macromol.* 84 (2016) 79–86, <https://doi.org/10.1016/j.ijbiomac.2015.12.007>.
- [32] J.T. Oliveira, L.S. Gardel, T. Rada, L. Martins, M.E. Gomes, R.L. Reis, Injectable gellan gum hydrogels with autologous cells for the treatment of rabbit articular cartilage defects, *J. Orthop. Res.* 28 (2010) 1193–1199, <https://doi.org/10.1002/jor.21114>.
- [33] J.T. Koivisto, T. Joki, J.E. Parraga, R. Paakkonen, L. Ylä-Outinen, L. Salonen, I. Jonkkari, M. Peltola, T.O. Ihalainen, S. Narkilahti, M. Kellomaki, Bioamine-crosslinked gellan gum hydrogel for neural tissue engineering, *Biomed. Mater.* 12 (2017) 25014, <https://doi.org/10.1088/1748-605X/aa62b0>.
- [34] J. Silva-Correia, J.M. Oliveira, S.G. Caridade, J.T. Oliveira, R.A. Sousa, J.F. Mano, R. L. Reis, Gellan gum-based hydrogels for intervertebral disc tissue-engineering applications, *J. Tissue Eng Regen. Med.* 5 (2011) e97–e107, <https://doi.org/10.1002/term.363>.
- [35] M.W. Lee, H.F. Tsai, S.M. Wen, C.H. Huang, Photocrosslinkable gellan gum film as an anti-adhesion barrier, *Carbohydr. Polym.* 90 (2012) 1132–1138, <https://doi.org/10.1016/j.carbpol.2012.06.064>.
- [36] K. te Nijenhuis, Thermoreversible Networks, Viscoelastic Properties and Structure of Gels (1997).
- [37] *Biomater. Sci.* 4 (9) (2016) 1276–1290, <https://doi.org/10.1039/C6BM00322B>.
- [38] G. Sworn, G.R. Sanderson, W. Gibson, Gellan gum fluid gels, *Top. Catal.* 9 (1995) 265–271, [https://doi.org/10.1016/S0268-005X\(09\)80257-9](https://doi.org/10.1016/S0268-005X(09)80257-9).
- [39] I.T. Norton, D.A. Jarvis, T.J. Foster, A macromolecular model for the formation and properties of fluid gels, *Int. J. Biol. Macromol.* 26 (1999) 255–261, [https://doi.org/10.1016/S0141-8130\(99\)00091-4](https://doi.org/10.1016/S0141-8130(99)00091-4).
- [40] *Food Hydrocoll.* 4 (6) (1991) 495–507, [https://doi.org/10.1016/S0268-005X\(09\)80200-2](https://doi.org/10.1016/S0268-005X(09)80200-2).
- [41] J. Rheol. 48 (6) (2004) 1195–1213, <https://doi.org/10.1122/1.1795193>.
- [42] P. Snabre, P. Mills, Rheology of concentrated suspensions of viscoelastic particles, *Colloids Surf. A Physicochem. Eng. Asp.* 152 (1999) 79–88, [https://doi.org/10.1016/S0927-7757\(98\)00619-0](https://doi.org/10.1016/S0927-7757(98)00619-0).
- [43] R.J.A. Moakes, A. Sullio, I.T. Norton, Preparation and characterisation of whey protein fluid gels: the effects of shear and thermal history, *Food Hydrocoll.* 45 (2015) 227–235, <https://doi.org/10.1016/j.foodhyd.2014.11.024>.
- [44] S.B. Ross-Murphy, Rheological characterization of polymer gels and networks, *Polym. Gels Networks* 2 (1994) 229–237, [https://doi.org/10.1016/0966-7822\(94\)90007-8](https://doi.org/10.1016/0966-7822(94)90007-8).
- [45] A.M. Grillet, N.B. Wyatt, L.M. Gloe, Polymer Gel Rheology and Adhesion, *Rheology* (2012), <https://doi.org/10.5772/36975>.
- [46] N. Altmann, J.J. Cooper-White, D.E. Dunstan, J.R. Stokes, Strong through to weak “sheared” gels, *J. Nonnewton. Fluid Mech.* 124 (2004) 129–136, <https://doi.org/10.1016/j.jnnfm.2004.07.013>.
- [47] D.A. Garrec, B. Guthrie, I.T. Norton, Kappa carrageenan fluid gel material properties. Part 1: Rheology, *Food Hydrocoll.* 33 (2013) 151–159, <https://doi.org/10.1016/j.foodhyd.2013.02.014>.
- [48] J. Rheol. 29 (6) (1985) 739–775, <https://doi.org/10.1122/1.549808>.
- [49] D. Li, A.W. Neumann, Equation of State for Interfacial Tensions of Solid-Liquid Systems, *Adv. Colloid Interface Sci.* 39 (1992) 299–345.
- [50] B. Ibsen, Treatment of shock with vasodilators measuring skin temperature on the big toe. Ten years' experience in 150 cases, *Dis. Chest.* 52 (1967) 425–429.
- [51] A.M. Kholoussy, S. Sufian, C. Pavlides, T. Matsumoto, Central peripheral temperature gradient. Its value and limitations in the management of critically ill surgical patients, *Am J Surg.* 140 (1980) 609–612.
- [52] E. Dickinson, Food polymers, gels and colloids (1991).
- [53] R. Esteban-Vives, M.T. Young, T. Zhu, J. Beiriger, C. Pekor, J. Ziembski, A. Corcos, P. Rubin, J.C. Gerlach, Calculations for reproducible autologous skin cell-spray grafting, *Burns* 42 (2016) 1756–1765, <https://doi.org/10.1016/j.burns.2016.06.013>.
- [54] J.C. Ferguson, R.G. Chechetto, C.C. O'Donnell, B.K. Fritz, W.C. Hoffmann, C.E. Coleman, B.S. Chauhan, S.W. Adkins, G.R. Kruger, A.J. Hewitt, Assessing a novel smartphone application - SnapCard, compared to five imaging systems to quantify droplet deposition on artificial collectors, *Comput. Electron. Agric.* 128 (2016) 193–198, <https://doi.org/10.1016/j.compag.2016.08.022>.
- [55] C. Nansen, J.C. Ferguson, J. Moore, L. Groves, R. Emery, N. Garel, A. Hewitt, Optimizing pesticide spray coverage using a novel web and smartphone tool, *SnapCard, Agron. Sustain. Dev.* 35 (2015) 1075–1085, <https://doi.org/10.1007/s13593-015-0309-y>.
- [56] J. Silva-Correia, B. Zavan, V. Vindigni, T.H. Silva, J.M. Oliveira, G. Abatangelo, R. L. Reis, Biocompatibility evaluation of ionic- and photo-crosslinked methacrylated gellan gum hydrogels: *In vitro* and *in vivo* study, *Adv. Healthc. Mater.* 2 (2013) 568–575, <https://doi.org/10.1002/adhm.201200256>.
- [57] C.J. Ferris, K.J. Gilmore, S. Beirne, D. McCullum, G.G. Wallace, M., in *het Panhuis*, Bio-ink for on-demand printing of living cells, *Biomater. Sci.* 1 (2013) 224–230, <https://doi.org/10.1039/C2BM00114D>.
- [58] M.E. Cooke, M.J. Pearson, R.J.A. Moakes, C.J. Weston, E.T. Davis, S.W. Jones, L.M. Grover, Geometric confinement is required for recovery and maintenance of chondrocyte phenotype in alginate, *APL Bioeng.* 1 (2017), <https://doi.org/10.1063/1.5006752> 016104.

# Natural polymers: biomaterials for skin scaffolds

## 6

Britt ter Horst<sup>1,2,3</sup>, Naiem S. Moiemem<sup>2</sup>, Liam M. Grover<sup>4</sup>

<sup>1</sup>School of Chemical Engineering, University of Birmingham, Birmingham, United Kingdom;

<sup>2</sup>University Hospital Birmingham Foundation Trust, Birmingham, United Kingdom;

<sup>3</sup>The Scar Free Foundation Birmingham Burn Research Centre, Birmingham, United Kingdom;

<sup>4</sup>University of Birmingham, Birmingham, United Kingdom

### 6.1 Introduction

Polymer-based biomaterials are widely used in wound treatment as wound dressings and regenerative scaffolds. Polymers are commonly used to form hydrogels, as the ability of hydrogels to absorb and release water is very useful in regulating excessive wound exudates while maintaining a moist wound environment to allow healing [1]. Polymers derived from natural sources have most frequently been used for the development of next generation skin substitutes due to their similarities with the extracellular matrix. In contrast with some of their synthetic counterparts, natural hydrogels are biocompatible, biodegradable, and of low cytotoxicity. However, effort into modifying synthetic polymers has resulted in promising biomaterials for wound healing [2,3]. Natural polymers can support several aspects of wound healing: some natural hydrogels are known for their hemostatic properties (chitosan, fibrin), others for their antimicrobial properties [4] or for stimulation of reepithelization when seeded with skin cells. Some disadvantages of natural hydrogels such as structural weakness and rapid degradation have been addressed by researchers. For example, strength of a cellulose hydrogel was increased by introducing carboxyl and aldehyde groups to the surface of cellulose nanofibrils [5] and degradation of collagen can be slowed down by chemical cross-linking [6]. Source variability is another disadvantage that is difficult to address, but Gomez et al. showed that selecting the appropriate alginate purification method can optimize the yield and can influence polymer properties [7].

However, care must be taken with products derived from natural materials, since they may be immunogenic, transmit pathogens, and difficult to purify and sterilize. Modifications to natural hydrogels to make them suitable for clinical use have been widely investigated over the last decades, and this has resulted in an increased availability of hydrogel systems for skin repair and regeneration purposes. To date, however, no natural polymer-based skin substitute has been able to achieve complete skin regeneration.

### 6.2 Definition and classification of natural polymer-derived materials

Hydrogels are polymer networks with high water holding capabilities [8] with an ability to absorb and release water. The polymer chains in a hydrogel can be held together through weak ionic interactions, physical entanglement, or through covalent binding between the polymer chains within the gel structure. The “cross-linked” structure enables the hydrogel to swell with water and create a solid that will eventually fail if placed under increasing loads.

Hydrogels can be classified according to their source, as being either natural or synthetic. Natural hydrogels are those hydrogels that consist of a polymer network based on natural products such as proteins (e.g., collagen or gelatin) and polysaccharides (e.g., starch, alginate, or agarose). When a single polymer is cross-linked, a homopolymeric hydrogel can be formed. A blend of two and multiple polymers are named *copolymeric* and *multipolymeric* hydrogels, respectively. Mixing two or more polymers can result in several types of bonds; polymers can bond back to back (block copolymers), bonding of end of polymer 1 to a portion of the backbone of polymer 2 (graft copolymer), and if no bonding occurs a polymer blend is formed. A mixture of two or more polymers with partially interlacing networks without covalent bonds are interpenetrating polymeric network (IPN) or semiIPN (consisting of a cross-linked polymer and a non cross-linked polymer) [9].

Frequently used natural polymers are negatively charged (alginate, hyaluronic acid) due to their carboxyl or sulfate groups. Although cell interactions based on electrostatic charge of polymers is not fully understood, it has been postulated that positively charged polymers allow for cell attachment. Brodaczewska et al. have shown that chitosan (a cationic polymer) attracted inflammatory cells in vivo [10]. Baxter et al. found that a chitosan dressing initially stimulated the expression of TGF- $\beta$ 1 in mice, but that the expression was decreased after the initial inflammatory phase in a burn wound model [11]. Several classification systems for hydrogels are available as shown in Table 6.1 [8].

**Table 6.1** Polymers can be classified using different systems depending on source, physical properties, and chemical properties.

Classification system	
Source	Natural Synthetic
Polymeric composition	Homopolymeric Copolymeric Multipolymeric
Polymeric bonding	Polymer blend Graft copolymer Block copolymer Interpenetrating polymeric network (IPN) Semi-IPN (cross-linked polymer and noncross-linked polymer).

**Table 6.1 Continued**

Classification system	
Configuration	Amorphous (noncrystalline) Semicrystalline (mixture of amorphous and crystalline phases) Crystalline
Type of cross-linking	Chemical Physical
Electronical charge	Nonionic (neutral) Ionic (anionic or cationic groups) Amphoteric (both acid and basic groups) Polybetaines (both anionic and cationic groups)
Physical appearance	Film Gel Sponge Foam Powder

Natural polymers can be designed to enable wound healing as bioactive materials (fibrin glue), or as vehicles for cell or drug delivery, 3D networks that stimulate and/or organize local tissue to recover or regenerate. An overview of applications is given in Fig. 6.1. The selection of polymer materials for biomedical applications is based on features such as solubility, architecture, pore size, water absorption capacity, degradability, electrical charge, etc. In this chapter the importance of these features for the development of scaffolds aimed to heal wounds will be discussed, as well as the currently available or promising natural polymer-based materials for skin repair and regeneration.

## 6.3 Natural polymers in wound healing

### 6.3.1 Polysaccharides

Polysaccharides are often used in wound dressings as shown in Table 6.2, examples are calcium alginate, cellulose, and chitosan-based dressings. The use of polysaccharides has also found its way in tissue engineering for wound healing. Polysaccharides consist of linked monosaccharides and are sourced from renewable resources such as plants and animals. As these resources are widely available in nature, polysaccharides are an attractive candidate for researchers. The most commonly used polysaccharides and proteins for skin repair applications are listed in Table 6.2.

#### 6.3.1.1 Alginate

Alginate is a linear anionic polymer that consists of mannuronic acid, referred to as *M blocks*, and guluronic acid (G block) units. Alginates with a high proportion of

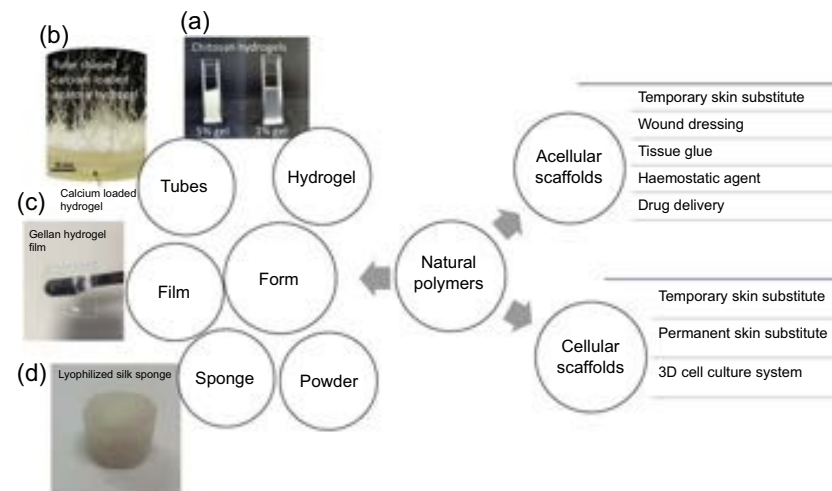


**Figure 6.1** Applications of natural polymer scaffolds in skin repair and regeneration. Permission to publish obtained from (a) author (unpublished work) (b) John Wiley and Sons, E.A.B. Hughes, S.C. Cox, M.E. Cooke, O.G. Davies, R.L. Williams, T.J. Hall, L.M. Grover, Interfacial mineral fusion and tubule entanglement as a means to harden a bone augmentation material, *Adv Healthc Mater* 7 (2018) 1–9. doi:10.1002/adhm.201701166. (c) author's own work (d) American Chemical Society, J. Rnjak-Kovacina, L.S. Wray, K.A. Burke, T. Torregrosa, J.M. Golinski, W. Huang, D.L. Kaplan, Lyophilized silk sponges: a versatile biomaterial platform for soft tissue engineering, *ACS Biomater Sci Eng* 1 (2015) 260–270. doi: 10.1021/ab500149p.

G blocks are easier to process and seem to have lower immunogenicity and therefore are more suitable for biomaterials [14]. Alginate is usually sourced from the cell wall of brown algae but can also be synthesized by certain bacteria. Its widespread use in biomedical applications is due to beneficial properties like biocompatibility, nonimmunogenicity, simple gelation process, ability to control its degradation, and relatively low cost. Alginate is a versatile polymer; its mechanical properties can be tuned by the type and concentration of cross-linker [15]. Alginate can form hydrogels by ionic cross-linking with cations such as  $\text{Ca}^{2+}$ . The divalent cations will bind exclusively to the G blocks. Covalent cross-linking is another approach, but as the reagent can be cytotoxic a secondary cleaning step is often required. While covalent cross-linking is permanent, ionic cross-linking can be reversed. Also, photo-cross-linking under mild conditions has been introduced for in vivo gelation of alginate onto the eye [16]. Lack of cell adhesion ligands and its poorly controlled natural degradation have limited its suitability for some applications. However, alginate can be modified to gain higher cell adhesivity by peptide coupling such as arginyl-glycyl-aspartic acid (RGD) to the polymer [17,18]. Degradation can be influenced by the amount of G blocks present, with higher content resulting in slower degradation. Oxidation

**Table 6.2** Natural polymers and their properties commonly used for skin repair and regeneration.

Type	Polymer	Source	Degradation	Biodegradable	Cell binding
Polysaccharides	Agarose	Red algae	Nondegradable	No	Low
	Alginate	Brown algae	Ion exchange	No <sup>a</sup>	Low
	Carrageenan	Red algae	Ion exchange, enzymatic cleavage	No	Low
	Starch	Plants	Enzymatic cleavage	Yes	High <sup>b</sup>
	Cellulose	Plants, wood	Enzymatic cleavage	No	Low
	Chitosan	Crustaceans, fungi	Ion exchange	Yes	High
	Hyaluronic acid	ECM (animal derived), bacterial fermentation	Enzymatic cleavage	Yes	High
	Gellan gum	Bacteria	Thermal, enzymatic cleavage, ion exchange (hydrolytic degradation)	Yes	High
	Dextran	Bacteria	Phagocytosis	Yes <sup>c</sup>	Low
	Bacterial cellulose	Bacteria	Enzymatic cleavage	No	Low
	Proteins	Collagen	ECM (animal derived)	Enzymatic cleavage	Yes
Fibrin		Blood (heterologous, autologous)	Enzymatic cleavage	Yes	High
Gelatin		ECM, collagen	Enzymatic cleavage	Yes	High
Elastin		ECM	Enzymatic cleavage	Yes	High
Silk sericin		<i>Bombyx mori</i>	Thermal, pH responsive	Yes	High
Silk fibroin		<i>Bombyx mori</i>	Proteolytic	Yes	High

ECM, extracellular matrix.

<sup>a</sup>Polymer can be modified to be biodegradable.<sup>b</sup>Starch derivatives have cell binding capacities.<sup>c</sup>Derivates are biodegradable.

Natural polymers: biomaterials for skin scaffolds

155

of photo-cross-linked alginate prior to methacrylation has shown to speed up biodegradation due to a higher susceptibility to hydrolysis [19].

Commercially available alginate-based wound dressings such as Kaltostat and AlgiSite are widely used in acute burn care, donor wound site coverage [20,21], venous leg ulcers [22], and pressure ulcers [23]. Although (calcium) alginate dressings have been used for many years in wound care, clinical data is still poor as not many well-designed clinical trials have been conducted [24].

Numerous researchers have demonstrated that cells can be successfully encapsulated in alginate hydrogels [25,26]. Alginate as culture matrix can improve proliferation of microencapsulated human pluripotent stem cells [27] and supports viability and function of other cell types [15,18,28]. Alginate-based macroporous systems for cell culture are now commercially available with different pore sizes to suit specific cell types. These sterile scaffolds are ionically gelled and then dried. After rehydration and cell seeding they turn into hydrogels [18]. The first transplantation of alginate beads with encapsulated pancreatic cells into the human body happened in the 1980s [29]. Despite attempts to encapsulate skin cells into alginate scaffolds [28], a similar development for alginate-based cellular regenerative scaffolds to treat wounds has not been established.

### 6.3.1.2 Cellulose

Cellulose is the most abundant biopolymer in nature and can be derived from a variety of organisms such as plants (vascular plants or algae) and bacteria (*Acetobacter xylinum*). Biosynthesis of bacterial cellulose fibrils eventually results in the development of a large nanofibrous network on the outer side of the bacterium with a macroscopically gelatinous appearance [30]. These fibers are around 20–100 nm thick and oriented in a unidirectional fashion [31]. Cellulose derived from plants or specifically wood generally have a smaller diameter (3–5 nm) forming bundles of 20–50 nm thick [32,33]. Other differences are the higher water holding capacity and lower crystallinity of bacterial cellulose [30]. Cellulose hydrogels can be formed by cross-linking solutions of cellulose derivatives such as methylcellulose and sodium carboxymethylcellulose [34].

Hydrogels can also be formed by ion-cross-linking of negatively charged nanofibrillated cellulose (wood-derived) with divalent or trivalent cations [32,35]. Bacterial cellulose has gained interest for the development of skin replacement therapy because of its 3D architecture with high mechanical strength, high water holding capacity, and biocompatibility. Interestingly, its natural negatively charged surface can be altered with or without [36] the use of matrix ligands to improve cell attachment.

Clinically available acellular products such as Biofill (Fibrocel) or Nanocell (Thai Nano Cellulose Co Ltd.) are available for the treatment of a variety of wounds (burns, chronic ulcers, following excision of skin cancers, and as donor site dressing) [37,38].

Recently, a bacterial cellulose hydrogel was proposed as cell carrier and wound dressing to stimulate wound healing in a full thickness mice model. Bacterial cellulose

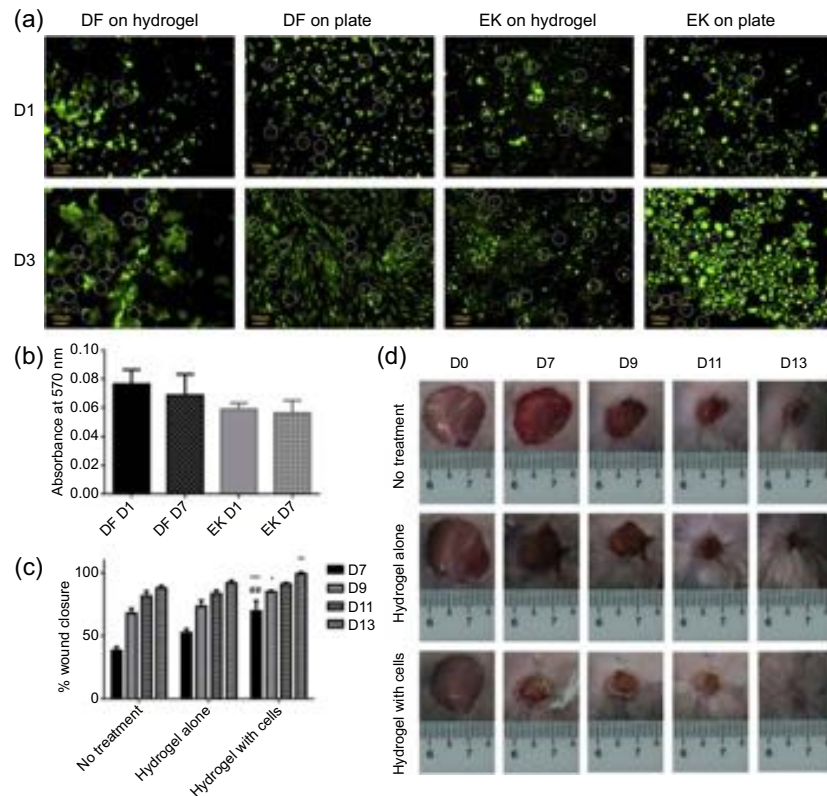


**Figure 6.2** Bacterial cellulose cellular scaffold. Live and dead stain of dermal fibroblasts (DF) and epidermal keratinocytes (EK) on the bacterial cellulose hydrogel and on culture plastic at day 1 and day 3 (a). MTT assay results for proliferation of cells on the hydrogel at day 1 and day 7 showed no significant differences between any of the groups (b). Percentage of wound healing of full thickness punch biopsy wounds in rats treated with bacterial cellulose hydrogel with and without cells and no treatment control. Significant differences with the no treatment group are marked with (\*), (\*\*), (\*\*\*) for ( $P < .05$ ), ( $P < .01$ ), and ( $P < .001$ ), respectively. (c). Clinical photos were taken at day 0, 7, 9, 11, 13 (d).

Figures were adapted from E. Yun, X. Loh, N. Mohamad, M.B. Fauzi, M.H. Ng, S.F. Ng, M. Cairul, I.M. Amin, Development of a bacterial cellulose-based hydrogel cell carrier containing keratinocytes and fibroblasts for full-thickness wound healing, *Sci Rep* (2018). doi:10.1038/s41598-018-21174-7, open access article, published under Creative Commons Attribution 4.0 International License (<http://creativecommons.org/licenses/by/4.0/>).

hydrogel was mixed with an acrylic acid solution and cells (human keratinocytes and dermal fibroblasts) were seeded into the hydrogel. The results, as shown in Fig. 6.2, indicate that this scaffold seems to be suitable as cell carrier and full thickness wound healing in a mice model was achieved, but no compare treatment was given [39].

### 6.3.1.3 Chitosan

Chitosan is a polysaccharide obtained from deacetylated chitin which is the structural component in the exoskeleton of crustaceans or fungi [40]. The polymer is named chitosan when over 50% of chitin is deacetylated. It is a weak base that can be dissolved in acidic solutions; this could be a limitation for applications where solubility in a pH neutral environment is desired. Chitosan has unique characteristics, as it is one of few cationic natural polymers and can form polyelectrolyte complexes with polymers of the opposite charge [41]. Chitosan has gained interest for tissue engineering purposes due to its many advantageous properties: it is nontoxic, promotes hemostasis, high cell adhesivity, and is biodegradable [14,42]. A relatively rapid biodegradation in vitro has been described with the use of lysozyme [43]. Degradability of chitosan can be influenced by a higher degree of deacetylation [43] and molecular weight [44], resulting in slower degradation in the body. However, its degradation in the body is not yet fully understood [45].

Cross-linking techniques that successfully formed hydrogels include ionic [46], chemical [47], physical cross-linker [48] and photopolymerization [49]. But chitosan on its own has weak mechanical properties and modifications or blending with other polymers is often required.

The positive charge of chitosan is of particular interest for researchers as adherence to negatively charged surfaces or cells is increased [50].

As a wound dressing chitosan has shown to be hemostatic and antimicrobial and improves wound healing [51], especially in burn wounds [52]. Its antimicrobial properties are thought to be caused by the ionic bonding of chitosan onto negatively charged bacteria surfaces leading to altered permeability with intracellular content being released and ultimately cell death [53]. The influence of chitosan on platelets is not well understood, but platelets seem to adhere to chitosan derivatives and aggregates causing a thrombogenic effect [54].

The hemostatic effect of chitosan has led to commercially available dressings such as HemCon bandage (HemConMedical Technologies, Inc.) and Celox gauze (MedTrade) marketed for the local treatment of bleeding wounds [55]. Chitosan is a bioactive polymer that has a promise as scaffold for tissue regeneration as it is cytocompatible toward many cell types [56]. Hilmi et al. described the use of a chitosan 3D culture scaffold with incorporation of human dermal fibroblasts and reported cell survival up to 14 days. The interconnected pores that were formed were considered to support fibroblast attachment to the scaffold (Fig. 6.3B–D) [58]. Keratinocytes and especially fibroblasts seem to adhere better onto chitosan with a lower degree of deacetylation as shown in Fig. 6.3A [59].

### 6.3.1.4 Gellan

Gellan gum is an FDA approved product that is regularly used in the food industry as a thickener. It is a hydrophilic anionic polysaccharide produced by the bacterium *Pseudomonas elodea* [60]. The favorable physicochemical features of gellan has generated much interest for its use in pharmaceutical and biomedical applications [61]. The enzyme galactomannanase can degrade gellan [62], but also common human

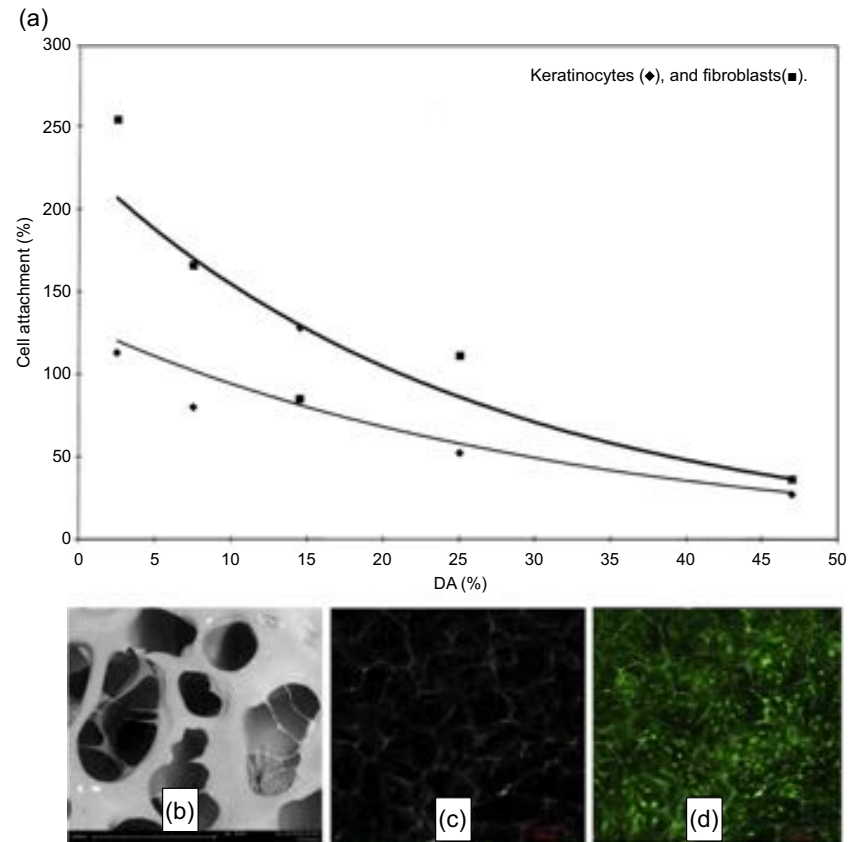


**Figure 6.3** Cell compatibility of chitosan scaffolds. Cell adhesion of keratinocytes and fibroblasts to chitosan decreases when degree of acetylation (DA%) increases (a). Scanning electron microscope of a porous chitosan scaffold with interconnected pores, scale bars 140  $\mu\text{m}$  (b). Confocal microscopy images of the scaffold used as 3D templates for human dermal fibroblasts culture showed homogeneously spread and viable cells, scale bars 100  $\mu\text{m}$  (c,d).

Permission to publish adapted figures obtained from Elsevier, (a) C. Chatelet, O. Damour, A. Domard, C. Chatelet, O. Damour, A. Domard, Influence of the degree of acetylation on some biological properties of chitosan films, *Biomaterials*. 22 (2001) 261–268. Figures (b–d) were adapted from A.B.M. Hilmi, A.S. Halim, A. Hassan, C.K. Lim, K. Noorsal, I. Zainol, In vitro characterization of a chitosan skin regenerating template as a scaffold for cells cultivation, *SpringerPlus*. 2 (2013) 1–9. doi:10.1186/2193-1801-2-79, open access article published under Creative Commons Attribution License (<http://creativecommons.org/licenses/by/2.0>).

enzymes such as lysozyme or trypsin [63]. The rate of degradation is slower in low acyl group gellan as shown by Lee et al. [64]. However, it remains unclear whether gellan completely degrades in the body as Ferris et al. noted degradation in terms of mass loss up to 28 days, but no further degradation in the following 140 days [65].

In terms of tissue engineering, gellan-based injectable materials have previously been used for cartilage reconstruction [66]. Various autologous cell types such as preosteoblasts, fibroblasts, and chondrocytes were successfully encapsulated within a hydrogel [66,67]. Furthermore, a topical application of gellan in the form of an antiadhesive and nontoxic dressing was found to stimulate healing and improved the scarring outcome in a rodent study [68]. However, no gellan-based skin scaffolds are available for clinical use at the moment.

### 6.3.1.5 Dextran

Dextran is a hydrophilic natural polysaccharide produced by bacteria and its degradation occurs via phagocytosis [69]. Dextran-derived hydrogels can be formed by chemical or physical cross-linking or via radical polymerization. Since dextran-based hydrogels have a limited cell adhesivity and do not seem to affect cell viability, they have been used in drug delivery. These features in combination with slow degradation have limited its use for tissue engineering in wound healing. Therefore, research groups have attempted to tailor the properties of dextran hydrogels to improve its cell adhesion [70] and biocompatibility [71] and have modified its degradation profile [72] to ultimately enhance functionality in tissue engineered scaffolds for burn wound healing [73]. The application of an acellular dextran hydrogel has been investigated in full thickness burns in mice and was found to stimulate angiogenesis and skin regeneration [73]. Similar results were seen in a full thickness porcine model, and additionally an improved dermal reconstruction and reinnervation were observed [74]. More recently, a hypoxia-inducible dextran hydrogel promoting neovascularization has been proposed by the same research group [75].

In terms of cell delivery to wounds, keratinocytes have been seeded into collagen-coated dextran microspheres transplanted as micrografts to full thickness wounds in athymic nude mouse model, but intradermal epithelial cysts were formed possibly due to high carrier adhesivity and slow degradation of the microspheres [76].

### 6.3.1.6 Hyaluronic acid

Hyaluronic acid (HA) is an anionic, linear polymer that is present in all living organisms and can be found in connective tissue especially in the dermis of the skin, but it is also abundant in vitreous humor of the eye and synovial fluid. It can be derived from many tissues via extraction and enzyme digestion methods or by bacterial synthesis. HA is an important glycosaminoglycan consisting of D-glucuronic acid and N-acetyl-D-glucosamine. Degradation in natural tissue occurs by enzymatic cleavage with different types of enzymes among tissues [77]. Rapid biodegradation is found to be problematic in certain biomedical applications, for example, in a rodent study a half-life of only 24 h following joint and skin injection was found [78]. Hence,

for biomedical applications HA requires modification to be able to form a hydrogel and also to reduce biodegradation *in vivo* [79] which then can be administered by injection or incorporated in dressings [80]. Examples of HA hydrogels formed by chemical cross-linking are dermal fillers with prolonged durability; histological studies have reported HA presence in the skin for up to 9–23 months [81]. As a highly hydrophilic polymer, its use as lubricant and biological absorber injected to deteriorating joints has been widely explored [82]. A variety of biological functions of HA have been recognized such as its role in cell motility, adhesion, and regulation [83].

The chain length and molecular weight of hyaluronic acid plays an important role in its biological function. In an *in vitro* cell study, rat cardiomyocytes underwent ischemic-reperfusion injury and were incubated with low molecular weight HA (LMW-HA, 100 kDa) or high molecular weight HA (HMW-HA 1000 kDa), and it was found that cell viability and wound healing (scratch wound assay) of HMW-HA pretreated cells were significantly improved. Proteomic expression assays demonstrated a significant recovery of cytoskeleton regulation proteins in samples following injury when pretreated with HMW-HA and not with LMW-HA, suggesting cytoskeletal rearrangement by HMW-HA [84]. Likewise, Wu et al. investigated the effect of HA in chemically burned (alkali) human corneal cells and suggested superior cell viability and more rapid wound healing in cells treated with HMW-HA (1525 kDa) when compared to LMW-HA (127 kDa) [85].

However, in other studies focusing on wound healing, small HA fragments seem to have a beneficial effect on wound healing [86], potentially due to its role in stimulating proinflammatory mediators [87]. Advantages of LMW-HA is its solubility in serum, making it suitable for systemic distribution. Furthermore, HA can bind to CD44 and receptor for HA-mediated motility (RHAMM) cell surface receptors. Binding of HA to CD44 triggers internalization; because CD44 is overexpressed in cancer cells it can be used in anticancer drug delivery [87].

Cell surface RHAMM is implicated in mediation of cell migration and cell focal adhesion in response to degraded HA activation [9].

HA interaction with RHAMM is linked to cell motility and cell focal adhesion and interplays with CD44. HA can be functionalized with cell adhesion peptides to enhance cell attachment to other cell types [80]. The diversity in chemical modification techniques offers opportunities for copolymeric biomaterials and makes HA a versatile polymer for use in tissue engineering.

Cells that are naturally surrounded by HA rich connective tissue in the body have commonly been encapsulated into HA scaffolds such as chondrocytes and dermal fibroblasts. A plethora of biomedical materials based on hyaluronic acid derivatives has been commercialized for deteriorating joints, (commercial) skincare, and wound healing purposes.

For wound healing specifically, rodent full thickness skin wound models have suggested a beneficial effect of HA to wound healing [88] using scaffolds containing HA [89–93]. A scaffold available for human use is Hyalomatrix (Anika therapeutics, former Fidia Advanced Biopolymers, Padua, Italy), a sterilized matrix based on hyaluronic acid derivative (benzyl ester of hyaluronic acid) with an outer layer of

semipermeable silicone. The scaffold can be directly delivered to the wound bed and aims to attract cellular ingrowth of fibroblasts and ECM components and promote vascular ingrowth. It has been used as dermal replacement in serious surgical wounds [94] and following scar release in adult patients with final autologous skin graft applied to most patients in 2–4 weeks after scaffold placement [95]. Gravante et al. used Hyalomatrix in pediatric burn patients as dermal replacement therapy following dermabrasion debridement and considered it safe to use and reported no adverse events [96]. However, no large good quality control studies in humans are available that focus on wound healing.

Hyalograft is an HA scaffold seeded with autologous human dermal fibroblasts.

Han et al. compared the use of an acellular HA scaffold (Hyalomatrix) to the same scaffold seeded with human dermal fibroblasts (Hyalograft) in terms of wound healing in 35 patients with a soft tissue defect to the face following basal cell carcinoma removal. Although the study lacks statistical power, the outcomes were in favor of the cellular scaffold with less scar contracture and a flatter scar compared to the acellular scaffold [97].

#### 6.3.1.7 Starch

Starches can be derived from widespread available plant sources such as potato, corn, rice, oat [98], or wheat [99]. Thermosensitive starch hydrogels can be formed by  $\beta$ -glycerol phosphate cross-linking [100]. Chemically modified starches have been used for drug delivery and tissue engineering. For example, an injectable starch-chitosan hydrogel was developed for the delivery of chondrocytes by Vioych et al. Due to the nonionic nature of starch, it can easily blend with other polymers and in this study, starch was found to increase the pore size and water absorption ability of the resulting polymer blend [100]. Although starch-based hydrogels are easily available and degraded by enzymatic degradation, it has not been widely explored for wound healing purposes [99].

#### 6.3.2 Proteins

A protein is a linear polymer made up from amino acids. DNA in cells produce proteins, the type and composition of the amino acids determine its final structure and function [101]. Proteins can be derived from blood products (fibrin), mammalian tissue (collagen, gelatin, and elastin), or other animal products (silk fibroin and silk sericin). Advantages in using proteins are that they are biodegradable and usually enhance cell adhesion to the scaffold. Some disadvantages are a low mechanical strength of protein skin scaffolds and the availability and costs of human/animal products. The properties of proteins for the use in skin scaffolds are listed in Table 6.2. The most abundant protein in the human body and the main structural component of the dermal layer of the skin is collagen. Therefore, many bioengineered skin scaffolds consist of collagen. However, researchers have been exploring other proteins for the development of skin scaffolds. Here, we describe those proteins that have most commonly been incorporated in cellular and acellular skin scaffolds.

### 6.3.2.1 Silk proteins

Silk produced by the silk worm *Bombyx mori* contains two major proteins named silk sericin and silk fibroin. Due to its mechanical strength and biocompatibility, fibroin has been widely used in textiles, drug delivery, and as a biomaterial [102]. For example, a fibroin/hyaluron scaffold supporting mesenchymal stem cell adhesion has been developed [103].

Alterations to fibroin degradability and surface modification have been successfully performed to meet biomedical needs [104]. Fibroin fiber ropes have been used as suture material for closure of surgical wounds for many years, and this clinical success has paved the way for its use in other different biomedical applications such as solubilized fibers to produce sponges, films, and hydrogels used in wound healing and tissue engineering [105]. For example, in the development of a tympanic membrane replacement, a fibroin substrate that stimulates human keratinocyte growth was engineered [106].

In contrast, silk sericin has not yet been explored that extensively, and for many years silk sericin was discarded as a waste product in the derivation of fibroin. Sericin is the glue that is found between the fibroin fibers. Its positive features such as non-immunogenicity; serum-dependent cell-adhesivity; and its specific antioxidant, antibacterial, and anticoagulative features make sericin a promising candidate for biomedical applications such as in skin regeneration [107–109]. Teramoto et al. described a low cell adhesivity where other studies have shown a high cell adhesivity in different cell types [108–110]. These contrasting results might be explained by a serum-dependent cell adhesivity of sericin.

### 6.3.2.2 Fibrin

Fibrin is an insoluble protein, a product from fibrinogen found in blood plasma. Upon tissue injury the proteolytic thrombin is activated which cleaves the soluble fibrinogen into the insoluble protein fibrin. Because it naturally forms a fibrous mesh that acts as blood clotting agent, it has been widely investigated for wound healing applications. Especially, as a hemostatic tissue sealant [111] in surgical wound closure where a hydrogel can be dripped or sprayed onto a wound surface to enhance healing or as glue when subsequently a skin graft is applied on top. Fibrin has been translated to clinical practice successfully in the form of a spray, powder, or sheet consisting of fibrin, thrombin, calcium ions, factor VIII, and a protease [112]. This tissue sealant has shown to enforce engraftment of autologous skin grafts in burn wound care [113] and skin substitutes [114]. Because activation by thrombin is required; these products are usually provided in a dual syringe system that can mix upon application to the body. Some products such as Cryoseal (Thermogenesis, US) [115] and Vivostat (Vivolution A/S, Denmark) utilize autologous blood plasma for onsite preparation of the sealant; however, this can be a disadvantage in patients that are potentially hemodynamic unstable. An alternative is the use of FDA approved human pooled plasma (Artiss). However, the high costs of the system limit its widespread use globally [113,116]. Other proteins that have been used as tissue sealants are gelatin and albumin; however, gelatin has not been

used for skin wounds. Although albumin-based tissue adhesives are FDA approved for cardiac and vascular surgery [117], no reports in skin wounds have been found. Also polysaccharides like chitosan, chitin, dextran, chondroitin sulfate, hyaluronic acid can be used to form tissue adhesives [112]. Chitosan as a positively charged polymer is thought to attract red blood cells which accelerate blood clotting. A sponge form of chitosan is on the market as hemostatic, adhesive material in acute wound care [55]. Although dextran, chondroitin sulfate, and hyaluronic acid show promise as tissue adhesive in corneal [118–120] defects, their use in skin wounds has not been explored yet.

Fibrin is easily degraded by proteolytic enzymes in the body and therefore fibrin hydrogels or scaffolds usually have weak mechanical properties. Improving these mechanical properties can be achieved by optimizing cross-linker concentration and pH [121], or utilizing degradation regulators and fibrin stabilizers such as aprotinin and tranexamic acid [122]. Additionally, to reinforce fibrin scaffolds they can be combined with other polymers to form interpenetrating polymer networks (IPN) [123]. Encouraging results have been established by a fibrin-hyaluronic network with increasing structural stability of the gel, but decreased proliferation of encapsulated fibroblasts occurred in stiffer materials [124].

Besides its role in blood clotting, the fibrin network is also a nest for cells to attach, proliferate, and migrate through. Fibrin as a sealant has also been used to coat scaffolds for improved cell adhesion [125] and in bilayered substitutes as a natural barrier to separate the epidermal and dermal layer. Due to its high biocompatibility and high affinity to cells, a variety of cell types have been encapsulated in fibrin carriers such as fibroblasts [126], keratinocytes [127,128], mesenchymal stem cells [129], and combinations of cells seeded into or onto fibrin scaffold [130] or gels [80,131].

Although, degradation of autologous fibrin is rapid, no toxic byproducts are released in the natural degradation process and no rejection occurs upon transplantation. Fibrin gel in its natural form seems most suitable for applications that do not require a high mechanical strength or long duration in situ.

Recently, the addition of angiogenesis stimulating factors to fibrin scaffolds has been developed to improve the regeneration of ischemic tissue [132]. Interestingly, higher thrombin concentration in fibrin matrices appears to diminish neovascularization and epithelization time [133]. This is potentially due to slow scaffold degradation as thrombin activates factor XIII which induces the cross-linking of fibrin monomers and consequently reduces the natural degradation process.

### 6.3.2.3 Collagen

Collagen is the most abundant protein in the human body and the main component of the extracellular matrix [134]. It is the main structural protein in the dermal layer of the skin with an essential role in wound healing. Therefore, many skin scaffolds have been developed based on collagen as primary component [135]. A total of 29 collagen types have been described. Collagen type I is most frequently used in skin scaffolds, as it is the abundant protein in native dermal tissue. In the early 80s Burke and Yannas published their first clinical study of a permanent artificial dermal template based on

bovine collagen and shark chondroitin 6-sulfate which led to the development of the commercialized dermal substitute Integra [136,137]. At the same time, the first burn patient was treated by grafting of their wounds with cultured autologous keratinocytes [138] following the method that Rheinwald and Green had developed just a few years before [139,140]. Based on the developments in that decade Hansbrough and Boyce were able to develop a collagen-glycosaminoglycan scaffold seeded with viable cultured autologous keratinocytes and fibroblasts and published successful engraftment into burns patient [141].

Ever since, collagen-based materials in different forms have been developed for wound healing and translated to clinical practice, such as hydrogels for hydration of dry wounds (Woun'Dres Collagen Hydrogel), as injectable scaffold [142], collagen sponges [143] (SkinTemp II dressings for superficial wound and blisters), powder [144], and an extensive list of collagen films/dressings [145]. The natural mechanical strength of collagen is weakened by its extraction process. To reinforce the collagen and control its in vivo degradation, new bonds can be formed by in vitro cross-linking. Collagen hydrogels are typically formed by chemical, physical, or enzymatic cross-linking [135], such as in Pelnac, a lyophilized porcine atelocollagen porous sponge that is cross-linked by 0.05 M acetic acid containing 0.2 wt% glutaraldehyde [146]. For biomaterials, chemical cross-linking is usually less suitable as cytotoxicity can occur upon degradation in vivo [147].

Other forms include composite acellular skin substitutes such as Biobrane, Integra [148], and Matriderm [149]. In Matriderm collagen types III and V are incorporated in combination with type I collagen and coated with elastin hydroxylate [150].

The majority of cellular skin scaffolds available on the market are based on animal-derived collagen. Collagen-based cellular skin substitutes include OrCel, StrataGraft, Apligraf [151,152], DenovoSkin, Transcyte [153], and Engineered Skin Substitute (ESS) [154]. These substitutes are incorporated with autologous cells from a healthy part of the patient's skin or allogenic cells. More recently, the incorporation of adipose-derived stem cells in a collagen hydrogel was investigated and seem to improve wound healing in a rodent burn model [155].

Collagen gels as bio-ink [156] and in cell-laden bioprinted scaffolds have also been studied. For example, in an attempt to stimulate vascularization in neural tissue, Lee et al. conducted an experimental study where cells, collagen, and VEGF-releasing fibrin gel were bioprinted to form a scaffold [157].

## 6.4 Applications of natural polymers in skin repair and regeneration

### 6.4.1 Wound dressings for partial thickness skin wounds

A wound is a lesion of the skin that can occur following several types of trauma such as thermal injury, laceration, ulceration, skin de-gloving, and certain skin diseases that result in severe skin loss (skin blistering diseases: SJS/TEN; epidermal bullosa; and bacterial, fungal, or viral-related skin diseases).

The depth of a wound can be described by the layers affected, from superficial (purely epidermal damage such as a sunburn), to partial thickness (epidermis and dermis involved), and finally full thickness (epidermis, dermis, and subcutaneous fat and/or underlying tissues are involved) injuries.

Wounds can also be divided into acute or chronic wounds. Design of effective polymer-based dressings relies on knowledge of wound etiology, wound healing, patient condition and the desired effects of the material used on the wound.

Current polymer-based dressings for wounds include:

- Temporary applications with elements that may accelerate healing and reduce complications such as infection and scarring.
- Temporary or definite (partial) replacement of skin to restore skin function rapidly.

#### 6.4.1.1 Important properties for wound dressings

Polymer-based scaffolds are appealing for biomedical purposes due to their mechanical tunability. However, it is important for researchers to understand which properties are crucial for their application. Many natural polymer-based materials have been introduced as wound dressings into clinical practice often as hemostatic and/or absorbent wound dressings.

For superficial wounds that lack the epidermis but have a supporting healthy dermis, a dressing can be designed to act as temporary barrier until the autologous epidermis has healed, meanwhile supporting the wound by facilitating nutrient supply and controlling fluid loss. For chronic wounds, more emphasis on debridement of unhealthy tissue, antimicrobial effects, and attraction of nutrients is desired. Examples are Intrasite gel and Purilon gel, both based on carboxymethylcellulose, which aim to debride superficial wounds and provide a moist wound environment.

In acute wounds the emphasis lies on reducing blood loss and supporting the underlying healthy tissue to recover and start regenerating. Hemostatic features of chitosan have been recognized in the treatment of acute wounds that require rapid hemostasis and resulted in chitosan-based products such as HemCon Bandage and Xstat that are used for both civilian and combat medicine [55,158]. Also, calcium alginate-based products such as Kaltostat and Curasorb are widely used in superficial wounds as they form a hydrophilic gel at application creating a moist environment [159]. The calcium from these dressings is exchanged for sodium in the wound bed which then interacts with procoagulant proteins that participate in the clotting cascade. The main dressing features for the treatment of acute wounds are summarized in Table 6.3 and an overview of acellular applications based on natural polymers for healing of superficial wounds is shown in Table 6.4.

### 6.4.2 Scaffolds for repair and regeneration of full thickness wounds

#### 6.4.2.1 Temporary scaffolds

Deeper wounds usually lack epidermal adnexa (hair follicles, sweat glands, and sebaceous glands) that have their roots in the dermis. Without these adnexa, regeneration of

**Table 6.3** Desirable wound dressing properties.

Biocompatible
Non-toxic
Control of wound fluid (absorb exudate, keep moist wound environment, and reduce fluid loss)
Antimicrobial
Pain reducing
Biodegradable
Cost-effective
Mechanical properties (strong, elastic, transparent)
Easy application and removal
Available in a variety of sizes and thicknesses

the skin is unlikely to occur or occurs very slowly resulting in severe contractures. To avoid these complications, a partial thickness skin graft (epidermal layer with a variable thickness of dermis) is transplanted from either autologous skin from a healthy part of the patient's body or a skin substitute. Skin substitutes can be temporary or permanent. Temporary skin substitutes are used as short-term wound coverage and aim to boost healing and prepare the wound bed for optimizing engraftment of autologous skin grafting. It is usually removed after a few weeks before final grafting takes place. Examples of temporary skin substitutes are cadaver allograft, porcine xenograft, Apligraf, and Oasis wound matrix.

#### 6.4.2.2 Permanent scaffolds

Traditional tissue engineering with natural polymers for wound healing applications involves the encapsulation of autologous cells within a polymer scaffold, which then can be transplanted to the patient's wound. For wound repair and regeneration, the matrix should either degrade while releasing bioactive components that stimulate extracellular matrix (ECM) production or the matrix permanently integrates into the host tissue supporting the bodies' tissue architecture and stimulating cells to infiltrate the matrix such as seen in Matriderm and Integra [168].

Scaffolds containing natural components are typically well tolerated which minimizes the risk of developing undesirable responses such as inflammation or rejection upon transplantation to the human body. Therefore, components that naturally exist in extracellular matrix such as collagen and hyaluronic acid seem obvious materials for scaffold formation and have been widely used. However, other natural polymers have also been extensively investigated for this purpose due to their unique characteristics that could provide the structure for a regenerative template to enhance wound healing. Commonly used natural polymers for tissue engineered cellular scaffolds are alginate

**Table 6.4** Acellular natural polymer-based dressings for superficial to partial thickness wounds.

Superficial partial thickness wounds			
Name (company)	Components	Action	References
Intrasite gel (Smith and Nephew, US)	Modified carboxymethylcellulose (2.3%) and propylene glycol (20%)	Amorphous sterile hydrogel dressing for use in shallow and deep open wounds	[160,161]
Purilon gel (coloplast, humleback, Denmark)	Sodium carboxy methylcellulose, calcium alginate	Necrotic and sloughy wounds + first and second degree burns. Secondary dressing needed	[162,163]
Granugel (ConvaTec)	Pectin, carboxymethylcellulose and propylene glycol	Provide a moist wound environment for dry partial and full thickness wounds. (Transparent for wound review)	[164]
HemCon bandage (HemCon medical technologies inc., portland, OR, US)	Lyophilized chitosan dressing	Hemostatic, cross-links RBCs to form a mucoadhesive barrier	[165]
XStat (RevMedx inc, wilsonville, OR, US)	Cellulose sponges coated with chitosan to assist with a mucoadhesive barrier	Hemostatic, cross-links RBCs to form a mucoadhesive barrier	[166]
Celox gauze (MedTrade Products Ltd, crew, UK)	Chitosan granules	Hemostatic, cross-links RBCs to form a mucoadhesive barrier	[165]
Calcium alginate dressings: Algosteril (johnson & johnson), comfeel alginate dressing (coloplast), CarrasorbH (Carrington laboratories), kaltostat (ConvaTec), Nu-Derm (johnson and johnson, USA), Curasorb (kendall), and AlgiSite (smith and nephew)	Calcium alginate	Hemostatic, calcium alginate dressings are designed to interact with sodium in wounds to create an ionic exchange and help enhance the epithelialization process	[24]
Woun'Dres Collagen hydrogel (coloplast, humleback, Denmark)	Collagen gel	Hydrates dry wounds and eschar	[167]

[28], agarose [169], collagen [151], chitosan [56], fibrin [80], gelatin [170], hyaluronic acid [97], or blends of the above mentioned polymers. Besides the collagen and hyaluronic-based cellular scaffolds, no other natural polymer-based cellular scaffold has been translated to a commercial product available for skin regeneration.

Some can be derived from abundant marine sources (alginate) or from material that otherwise would have been discarded such as silk sericin, usually a waste product during the production of silk fibroin for textile manufacture [109]. Others are derived from animal or human tissue and blood (collagen, fibrin, hyaluronic acid). Importantly, most of these materials have mild preparation conditions well-suited for cell encapsulation.

### Important properties for polymer scaffolds as regenerative templates

Many researchers have summarized currently available skin substitutes, their sources, and (dis)advantages [154,171,172]. Some have suggested that the ideal skin substitute or replacement should be durable, autologous, vascularized, and consist of all skin adnexa and stem cells. Such a skin substitute does not yet exist [173], but recent advances in regulation and genetically modification of skin (stem) cells could bring us a step closer to developing fully functional skin regeneration templates [174]. As described by Nicholas et al. five major criteria are thought to be important for a skin substitute scaffold [175].

1. Barrier function
2. Cell compatibility
3. Biocompatibility
4. Biodegradability
5. Cost-effectiveness

**Barrier function** Following skin injury the barrier function of epidermal layer is destroyed allowing pathogens to freely enter the body. A well-designed scaffold should block or decrease the influx of pathogens. This can be achieved by creating a favorable bed for early application of an autologous epidermal layer (skin graft) onto the substitute. Success depends on early vascularization of the scaffold which in turn depends on, among other things, a pore size suitable for fibroblast and endothelial cell infiltration.

Another approach includes a synthetic layer on top of the scaffold that mimics the properties of the epidermis as seen in commercially available substitutes (Integra [176], Renoskin, Hyalomatrix and Pelnac [146,177–179]).

Meanwhile, hydrogel scaffolds should maintain a moist wound environment to encourage healing [180,181] while preventing extensive fluid loss as seen in burn patients. However, very wet wounds can stimulate bacterial growth which can reduce healing as well.

**Cell compatibility** The currently available noncellular polymer scaffolds do not aim to fully replace the host tissue but have a more supporting function. These scaffolds can stimulate cell influx by their material design; important features are thickness, pore size, and (surface) morphology.

Fibroblasts and keratinocytes are the most common cell types to be incorporated in polymer-based scaffolds designed to replace or regenerate skin [154]. However, in order to fully restore all skin structures also other cell types have been under the attention of researchers. For example, melanocytes [182], adipose cells [183], amniotic fluid-derived cells (AFS) [156], and mesenchymal stem cells [184] have been incorporated in polymer scaffolds [185]. Preliminary in vitro and animal studies [156,183] are promising, but still far from translation to human.

Epidermal cells are anchor-dependent cells that will need to attach and spread out over a substrate in order to proliferate and differentiate. Material pretreated with- or consistent of extracellular matrix constituents like collagen and fibronectin are more likely to bind cells as cell adhesion is mediated by specific cell surface receptors for molecules in the extracellular matrix. Epithelial cells, like keratinocytes, also require cell to cell adhesion in order to proliferate [186]. Proliferation and/or differentiation prior to transplantation are not always desired. When designing a scaffold, this should be taken into account so that cells are entrapped within an optimal environment before transplantation to the skin. Cells should remain viable in the scaffold prior to transplantation, integrate homogeneously, and their proliferation and/or differentiation capacity after transplantation to the wound bed should not be compromised [173].

### Biocompatibility (non-toxic, non-immunogenic, and non-inflammatory)

Failure of a scaffold to integrate into the body is often caused by rejection due to a foreign body response. This basically means that the body recognizes the new tissue as foreign and initiates the immune reaction, resulting in excess inflammation and rapid degradation of the scaffold structure together with the transplanted cells. Besides losing the cellular matrix, this intense inflammatory response triggers the release of more proinflammatory cytokines that increase fibrosis and ultimately scarring. In wound care treatment of burns the traditional autologous skin grafts have a very high take rate without rejection, but they can fail due to infection or an unfavorable wound bed preparation. When allogenic or xenogenic skin grafts are used, rejection is a common result. Therefore, when designing scaffolds, the focus must lie on modifying the scaffold so that the host tissue recognizes it as its own.

Natural polymers are known for their low toxicity [14]. They usually undergo degradation by cleavage of enzymes present in the human body or through hydrolytic degradation resulting in body friendly degradation products. Biodegradable materials are attractive for implantation in the body, but rapid degradation can also be undesirable. Polymers can be modified to reduce this degradation process, but care must be taken to avoid production of toxic byproducts or induce toxic effects of the modified material. An example is chitosan, a polymer with overall low toxicity, but when the charge density is modified into a higher charge molecule, this is related to increased toxicity [45].

Blending of polymers can optimize scaffold biocompatibility as seen in blends of fibrin and hyaluronic acid [124]. Another example is the use of fibrin to coat a collagen-chitosan scaffold to improve cell adherence [125].

Several approaches to optimize biocompatibility can be considered:

- To include natural components that can easily be recognized by the body
- Use natural polymers that are known for their low toxicity
- Use mild processing conditions to minimize toxic byproducts

**Biodegradable, long-lasting, flexible** Polymer scaffolds functioning as regenerative templates should be firm enough to resist tear during surgical application and have some resistance against shearing of applied dressings and movement of patient. However, the ability to stretch over joint regions is desired.

Early vascularization is key to ensure successful engraftment. Some scaffolds are expected to initially support the transplantation of cells and promote healing but eventually degrade and are replaced by autologous tissue. Duration of degradation time should be adapted by speed of vascularization, as the supporting skeleton should last until the graft is sufficiently integrated. Up to 3 weeks is usually described for scaffold vascularization *in vivo* but this duration has been shortened to about 1 week in a noncross-linked bovine collagen scaffold coated with elastin hydrolysate (Matriderm) [187]. The collagen scaffold with skin graft on top was compared to conventional skin graft in a full thickness pig wound model. More endothelial cells were detected with a positive Von Willebrand factor stain in the scaffold group after 1 week of treatment indicating neovascularization compared to less positively stained cells in the control arm. Lamme et al. postulate that the collagen matrix acts as an ECM facilitating cell attachment and deposition of fibronectin along the collagen fibers, which might attract endothelial cells resulting in faster vascularization [187]. Also, the presence of elastin hydroxylate might speed up vascularization as elastin-derived peptides are known to promote endothelial cell migration and angiogenesis [188]. Interestingly, when the skin substitute with elastin hydrolysate incorporated was compared to Integra in a rat study, both substitutes performed well in terms of take rate, vascularization, and inflammatory response. As shown in Fig. 6.4 the key differences were that the collagen-elastin skin substitute, Matriderm, formed a thinner neodermis, but had been populated with more cells compared to single-layer Integra [190]. Matriderm is a noncross-linked collagen-based matrix, which might have encouraged faster degradation in comparison to Integra single-layer, which is a cross-linked bovine tendon collagen matrix. This reflects the importance of critical scaffold design to meet clinical needs.

**Cost-effective** In order to translate promising scaffolds to clinical practice and be adopted for widespread use, low-cost designs are preferred. When designing a scaffold, attempts to reduce final costs can be sought in reducing labor intensity, use of low-cost materials, short manufacture time with minimal use of specialized equipment, and an efficient sterilization process.

In 1998 the FDA approved the first bioengineered skin scaffold for use in clinical practice, Apligraf (Organogenesis), which is a collagen-based bilayered product incorporated with human fibroblasts in the lower layer and human keratinocytes in the upper layer. The development of many other cellularized scaffolds followed, but only a few have been commercialized and fully approved by the FDA [191]. A commonly

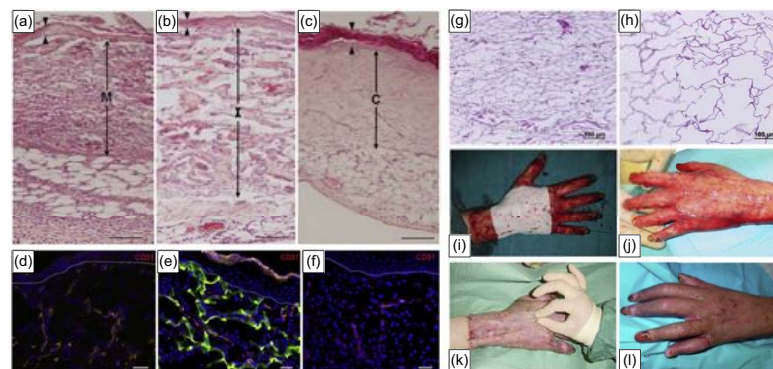


**Figure 6.4** Comparison of Matriderm and Integra acellular scaffolds. HE stain 14 days after single stage application of Matriderm (1 mm thickness) (a), Integra single-layer (1.3 mm) (b) and control (c) to full thickness skin defects in rats. Successful formation of epidermis (between markers) and populated neodermis (arrows) in all transplants, with highest cell density seen in Matriderm neodermis. Both substitutes formed a thicker neodermis than the control; however, Integra formed a thicker neodermis than Matriderm. Scale bars 100  $\mu$ m. CD31 stain (red) to visualize endothelial cells and Hoechst (blue) for cell nuclei and autofluorescent collagen (green) in Integra 14 days after single stage application of Matriderm (1 mm thickness) (d), Integra single-layer (1.3 mm) (e) and control (f) to full thickness skin defects in rats. All transplants show comparable development of a capillary network in the superficial neodermis. Scale bars 50  $\mu$ m. HE stain of Matriderm (g) and Integra (h) shows a more dense network of collagen fibers formed in Matriderm compared to Integra. Clinical application of Matriderm (i) and Integra at day 7 after injury (j) with results of treatment after 11 and 55 days of application for Matriderm (k) and Integra (l), respectively. Permission to publish adapted figures obtained from ©Springer-Verlag 2011 (a–f), Elsevier (g,h) V.C. van der Veen, M.B.A. van der Wal, M.C.E. van Leeuwen, M.M.W. Ulrich, E. Middelkoop, Biological background of dermal substitutes, *Burns*. 36 (2010) 305–321. doi:10.1016/j.burns.2009.07.012, (i,k) M. Madaghiele, C. Demitri, A. Sannino, L. Ambrosio, Polymeric hydrogels for burn wound care: advanced skin wound dressings and regenerative templates, *Burn Trauma* 2 (2015) 153–161. doi:10.4103/2321-3868.143616 and (j,l) A. Danin, G. Georgesco, A. Le Touze, A. Penaud, R. Quignon, G. Zakine, Assessment of burned hands reconstructed with Integra W by ultrasonography and elastometry, *Burns*. 38 (2012) 998–1004. doi:10.1016/j.burns.2012.02.017.

mentioned limitation is the high costs of these scaffolds, which can vary widely per product [192]. The cost-effectiveness of advanced cellular and acellular scaffolds in venous ulcers [193] was not proven, but lack of comparable studies makes it difficult to draw valid conclusions. However, Bradfords et al. suggest that in diabetic foot ulcers the use of cellular scaffold may lower overall costs by reducing clinic visits burden on healthcare systems [194].

It is important to realize that most regenerative templates available in clinical care have not been investigated thoroughly in randomized controlled trials. Snyder et al. noted that in only 7 out of 57 skin substitutes, investigated for the use in chronic wounds, this was the case [145]. Furthermore, most studies selected patients that are more likely to heal and exclude those with poor healing conditions. Care must be taken when interpreting outcomes of these studies and extrapolating findings as the effect in a general population in a representable setting is yet to be examined [195].

#### Permanent acellular scaffolds

Permanent engraftment of scaffolds for wound regeneration requires more complicated material features. Currently available acellular scaffolds aim to create a stable dermal layer by stimulating neovascularization and reformation of the basement membrane to secure the transplanted material to underlying tissue. The formation of an adequate basement membrane is a challenge in acellular scaffolds [150]. Boyce et al. addressed the issue by surfacing their porous collagen-GAG dermal substitute with a flat layer of nonporous collagen-GAG to facilitate keratinocyte adherence and spreading [196]. Also, Lamme et al. [187] have shown that their collagen-elastin scaffold had positive chondroitin sulfate and laminin labeling 6 weeks after application in a pig model, indicating formation of the basement membrane. Some substitutes provide a (temporary) epidermal layer as well, but once the dermal templates are engrafted they usually require autologous epidermal (split-skin) grafts for definite coverage [174]. Furthermore, these materials can promote cellular ingrowth and may model scar development [73,74]. Commonly used permanent scaffolds are Integra, Matriderm, Pelnac, and Alloderm.

An overview of acellular applications based on natural polymers for healing of superficial to partial thickness wounds is shown in Table 6.5 and full thickness wounds in Table 6.6.

#### Permanent cellular scaffolds

Although the ingrowth of fibrovascular tissue might be promoted by acellular scaffolds, cellular scaffolds aim to provide a more rapid and complete regeneration of the skin by incorporating skin cells such as fibroblasts and keratinocytes to the matrix. However, regeneration of many other skin components that contribute to the full function of the skin is still lacking. Deficiencies such as hypopigmentation, absence of adnexa, and nerve innervation reduce the quality of the reconstructed skin. An overview of available cellular scaffolds to date is given in Table 6.6.

**Table 6.5** Acellular natural polymer–based scaffolds for regeneration of deep dermal to full thickness wounds.

Deep dermal to full thickness wounds - dermal substitutes						
Name (manufacturer)	Main components	Application	Thickness	Pore size	Cross-linking	Clinical studies
Integra Dermal Regeneration Template (integra LifeSciences, plainsboro, NJ, USA)	Bovine collagen and chondroitin-sulfate coated with outer layer of semipermeable silicone	Partial and full thickness wounds as dermal replacement	0.79–2.03, 2.06–3.30 mm	30–120 $\mu$ m	Yes	[176,197,198]
Matriderm (Skin and Health Care AG, billerbeck, Germany)	Bovine collagen and elastin	Partial and full-thickness wounds as dermal replacement	1 or 2 mm	75 $\mu$ m	No	[199,200]
Pelnac (gunze medical Materials center, kyoto, Japan)	Porcine atelocollagen with (fortified pelnac) or without (single layer) silicone outer layer	Partial and full-thickness wounds	3 mm	70–110 $\mu$ m	Yes	[146]
Hyalomatrix (anika Therapeutics, bedford, MA, US former fidia Advanced Biopolymers, padua, Italy)	Derivative of hyaluronic acid with outer layer of semipermeable silicone	Partial and full-thickness wounds as dermal replacement	1.2 mm	n.k.	No	[95,96]
AlloDerm (lifeCell, corporation, brachburg, NJ, USA)	Decellularized human dermis	Partial and full-thickness wounds as dermal replacement	0.8–1.2, 1.2–2.8, 2.8–4.0 mm	n.a.	No	[201–203]

Strattice (lifecell corporation, branchburg, NJ, US)	Decellularized porcine dermis (alpha-gal removed)	Soft tissue (hernia repairs etc)	1.5–2.0 mm	n.a.	No	[202,204]
Dermamatrix (Synthes, Westchester, PA, US)	Decellularized human dermis	Soft tissue replacement	0.2–0.4, 0.4–0.8, 0.8–1.7, 1.7 > mm	n.a.	No	[203]
Oasis wound matrix (healthpoint ltd., fort worth, TX, US)	Porcine small intestine submucosa	Partial to full thickness burn wounds and chronic wounds	0.30 mm	20–30 nm	No	[205]
Permacol (covedien, mansfield MA, US)	Decellularized porcine dermis	Full thickness wounds	0.4 or 1.5 mm	n.a.	Yes	[206]
Glyaderm (Euro Skin bank, beverwijk, netherlands)	Decellularized human dermis	Full thickness wounds	0.2–0.6 mm	n.a.	No	[207]
Renoskin (groupe perouse, bornel, France)	Bovine collagen 1 with GAG with outerlayer of silicone	Burn wounds, tissue defects	1.5–2.5 mm	100 µm	Yes	No clinical studies in skin wounds
Graftjacket (wright medical technology, inc, arlington, TN, USA healthpoint)	Decellularized pre-meshed human dermis	Soft tissue replacement, chronic wounds, and ligament repair	1, 1.4, or 2 mm	n.a.	No	[208–210]

*n.a.*, not applicable; *n.k.*, not known.

**Table 6.6** Cellular natural polymer–based scaffolds for wound healing and regeneration of deep dermal to full thickness wounds.

Deep dermal to full thickness wounds—cellular scaffolds							
Name (manufacturer)	Main components	Cells	Thickness	Pore size	Cross-linked	Application	Clinical studies
Apligraf (organogenesis, canton, MA, USA)	Bilayered scaffold of bovine type I collagen gel	Neonatal allogenic human fibroblasts (dermal layer) neonatal allogenic human keratinocytes (epidermal layer)	0.4–0.75 mm	n.a.	No	Partial and full thickness (burn) wounds, skin graft donor sites, chronic wounds, epidermolysis bullosa	[151,211,212]
StrataGraft (stratatech corporation, madison, WI)	Nonbovine purified type I collagen	Allogenic human dermal fibroblasts and NIKS cells <sup>a</sup>	n.d.	n.d.	n.d.	Partial and full thickness (burn) wounds	[213,214]
Tiscover (a-skin B.V., amsterdam, netherlands)	Acellular human dermis	Autologous human fibroblasts	1–2 mm	n.a.	No	Chronic wounds	[215]
Orcel (forticell bioscience New York, USA)	Bovine collagen type 1 sponge and gel	Allogenic fibroblasts and keratinocytes in gel	1 mm	50–250 $\mu$ m	Yes	Chronic wounds and donor sites	[216,217]

DenovoSkin (Euroskingraft)	Compressed bovine collagen type I hydrogel [218]	Autologous dermal fibroblasts seeded into scaffold and keratinocytes seeded onto scaffold	n.d.	n.d.	Yes	Full thickness burns, other large full thickness skin defects	Phase IIb trial running in Europe
DenovoDerm (Euroskingraft)	Compressed bovine collagen type 1 hydrogel [218]	Autologous dermal fibroblasts	n.d.	n.d.	Yes	Deep to full thickness (burn) wounds	Phase I trial running in Europe
Engineered Skin Substitute (ESS) (amarantus BioScience holdings, inc.)	Collagen-glycosaminoglycan	Autologous fibroblasts and stratified keratinocytes	<400 µm	n.d.	n.d.	Partial and full thickness burn wounds	[219]
TissueTech autograft System, hyalograft 3D and laserskin combined (fidia Advanced Biopolymers, padua, Italy)	Derivative of hyaluronan (HYAFF) scaffold (dermal layer and microperforated hyaluronan acid membrane (epidermal layer)	Autologous human fibroblasts (dermal layer) and keratinocytes (epidermal layer)	n.d.	n.d.	n.d.	Deep to full thickness (burn) wounds	[220]

*n.a.*, not applicable; *n.k.* = not known.

<sup>†</sup>pathogen-free human keratinocyte progenitor formed in stratified epidermis.

## 6.5 Conclusion

Natural polymers have been exploited widely for repair and reconstruction of the skin and have transitioned to a number of successful commercial products. Despite this success, there still remain some very significant challenges to overcome. None of the existing materials allow for full regeneration of the skin adnexa, meaning that functional and esthetic outcome is often poor. Furthermore, although materials exist that integrate well into the host tissue without causing rejection, none of the skin scaffolds to date fully support or degrade following the natural regeneration process. Future challenges exist to redesign natural polymeric materials so that they facilitate the bodies' own regenerative processes and degrade at a consistent and appropriate rate. Ultimately, such scaffolds should support regeneration of all functions of the skin while allowing a scarfree wound closure.

## List of abbreviations

<b>ECM</b>	extracellular matrix
<b>CD44</b>	cluster of differentiation 44
<b>IPN</b>	interpenetrating polymeric network
<b>Semi-IPN</b>	semi-interpenetrating polymeric network
<b>TGF-<math>\beta</math>1</b>	transforming growth factor beta one
<b>SJS</b>	Stevens—Johnson syndrome
<b>TEN</b>	toxic epidermal necrolysis
<b>FDA</b>	food and drug administration
<b>RGD</b>	arginyl-glycyl-aspartic acid
<b>HA</b>	hyaluronic acid
<b>LMW</b>	low molecular weight
<b>HMW</b>	high molecular weight
<b>kDa</b>	kilodaltons
<b>RHAMM</b>	receptor for hyaluronic acid mediated motility
<b>VEGF</b>	vascular endothelial growth factor.

## References

- [1] M. Madaghiele, C. Demitri, A. Sannino, L. Ambrosio, Polymeric hydrogels for burn wound care: advanced skin wound dressings and regenerative templates, *Burn Trauma* 2 (2015) 153–161, <https://doi.org/10.4103/2321-3868.143616>.
- [2] A. Li, B.L. Dearman, K.E. Crompton, T.G. Moore, J.E. Greenwood, Evaluation of a novel biodegradable polymer for the generation of a dermal matrix, *J Burn Care Res* 30 (2009) 717–728, <https://doi.org/10.1097/BCR.0b013e3181abffca>.
- [3] M. Rottmar, M. Richter, X. Mäder, K. Grieder, K. Nuss, A. Karol, B. Von Rechenberg, E. Zimmermann, S. Buser, A. Dobmann, J. Blume, A. Bruinink, In vitro investigations of a novel wound dressing concept based on biodegradable polyurethane, *Sci Technol Adv Mater* 16 (2015) 10, <https://doi.org/10.1088/1468-6996/16/3/034606>.

- [4] M. Kong, X.G. Chen, K. Xing, H.J. Park, Antimicrobial properties of chitosan and mode of action: a state of the art review, *Int J Food Microbiol* 144 (2010) 51–63, <https://doi.org/10.1016/j.ijfoodmicro.2010.09.012>.
- [5] K. Syverud, S.R. Pettersen, K. Draget, G. Chinga-Carrasco, Controlling the elastic modulus of cellulose nanofibril hydrogels-scaffolds with potential in tissue engineering, *Cellulose* 22 (2015) 473–481, <https://doi.org/10.1007/s10570-014-0470-5>.
- [6] W. Friess, Collagen-biomaterial for drug delivery 1, *Eur J Pharm Biopharm* (1998) 113–136.
- [7] C.G. Gomez, M.V. Pérez Lambrecht, J.E. Lozano, M. Rinaudo, M.A. Villar, Influence of the extraction-purification conditions on final properties of alginates obtained from brown algae (*Macrocystis pyrifera*), *Int J Biol Macromol* 44 (2009) 365–371, <https://doi.org/10.1016/j.ijbiomac.2009.02.005>.
- [8] E.M. Ahmed, Hydrogel: preparation, characterization, and applications: a review, *J Adv Res* 6 (2015) 105–121, <https://doi.org/10.1016/j.jare.2013.07.006>.
- [9] L.H. Sperling, Interpenetrating Polymer Networks: An Overview, 1994. <https://pubs.acs.org/sharingguidelines>.
- [10] K. Brodaczewska, N. Wolaniuk, K. Lewandowska, K. Donskow-Iysoniewska, M. Doligalska, Biodegradable chitosan decreases the immune response to *Trichinella spiralis* in mice, *Molecules* 22 (2017) 1–16, <https://doi.org/10.3390/molecules22112008>.
- [11] R.M. Baxter, T. Dai, J. Kimball, E. Wang, M.R. Hamblin, W.P. Wiesmann, S.J. McCarthy, S.M. Baker, Chitosan dressing promotes healing in third degree burns in mice: gene expression analysis shows biphasic effects for rapid tissue regeneration and decreased fibrotic signaling, *J Biomed Mater Res* 101 A (2013) 340–348, <https://doi.org/10.1002/jbm.a.34328>.
- [12] E.A.B. Hughes, S.C. Cox, M.E. Cooke, O.G. Davies, R.L. Williams, T.J. Hall, L.M. Grover, Interfacial mineral fusion and tubule entanglement as a means to harden a bone augmentation material, *Adv Healthc Mater* 7 (2018) 1–9, <https://doi.org/10.1002/adhm.201701166>.
- [13] J. Rnjak-Kovacina, L.S. Wray, K.A. Burke, T. Torregrosa, J.M. Golinski, W. Huang, D.L. Kaplan, Lyophilized silk sponges: a versatile biomaterial platform for soft tissue engineering, *ACS Biomater Sci Eng* 1 (2015) 260–270, <https://doi.org/10.1021/ab500149p>.
- [14] A. Aravamudhan, D.M. Ramos, A.A. Nada, S.G. Kumbar, Chapter 4 – natural polymers: polysaccharides and their derivatives for biomedical applications, in: *Nat. Synth. Biomed. Polym.*, Elsevier, 2014, pp. 67–89, <https://doi.org/10.1016/B978-0-12-396983-5.00004-1>.
- [15] A.D. Augst, H.J. Kong, D.J. Mooney, Alginate hydrogels as biomaterials, *Macromol Biosci* 6 (2006) 623–633, <https://doi.org/10.1002/mabi.200600069>.
- [16] K.A. Smeds, A. Pfister-Serres, D. Miki, K. Dastgheib, M. Inoue, D.L. Hatchell, M.W. Grinstaff, Photocrosslinkable polysaccharides for in situ hydrogel formation, *J Biomed Mater Res* 54 (2001) 115–121.
- [17] O. Jeon, C. Powell, S.M. Ahmed, E. Alsberg, Biodegradable, photocrosslinked alginate hydrogels with independently tailorable physical properties and cell adhesivity, *Tissue Eng* 16 (2010) 2915–2925, <https://doi.org/10.1089/ten.TEA.2010.0096>.
- [18] T. Andersen, P. Auk-Emblem, M. Dornish, M.R. Lornejad-Schä, C. Schä, 3D cell culture in alginate hydrogels, *Microarrays* 4 (2015) 133–161, <https://doi.org/10.3390/microarrays4020133>.
- [19] O. Jeon, D.S. Alt, S.M. Ahmed, E. Alsberg, The effect of oxidation on the degradation of photocrosslinkable alginate hydrogels, *Biomaterials* 33 (2012) 3503–3514, <https://doi.org/10.1016/j.biomaterials.2012.01.041>.
- [20] J.M. O'Donoghue, S.T. O'Sullivan, E.S. Beausang, J.I. Panchal, M. O'Shaughnessy, T.P. O'Connor, Calcium alginate dressings promote healing of split skin graft donor sites, *Acta Chir Plast* 39 (1997) 53–55.

- [21] M. Brenner, C. Hilliard, G. Peel, G. Crispino, R. Geraghty, G. O'Callaghan, Management of pediatric skin-graft donor sites: a randomized controlled trial of three wound care products, *J Burn Care Res* 36 (2015) 159–166, <https://doi.org/10.1097/bcr.000000000000161>.
- [22] S. O'Meara, M. Martyn-st James, Alginate dressings for venous leg ulcers (Review), *Cochrane Database Syst Rev* (June 25, 2013) 77, <https://doi.org/10.1002/14651858.CD010182.pub3>. [www.cochranelibrary.com](http://www.cochranelibrary.com).
- [23] D. Jc, K. Sj, Z. Liu, N. Stubbs, W. Rm, M. Fortnam, Alginate Dressings for Treating Pressure Ulcers (Review), 2015, <https://doi.org/10.1002/14651858.CD011277.pub2>. [www.cochranelibrary.com](http://www.cochranelibrary.com).
- [24] J. Wasiak, H. Cleland, F. Campbell, A. Spinks, Dressings for superficial and partial thickness burns, *Cochrane Database Syst Rev* 3 (2013) Cd002106, <https://doi.org/10.1002/14651858.CD002106.pub4>.
- [25] A. Khoshzaban, P. Keyhanvar, E. Delrish, F. Najafi, S. Heidari Keshel, I. Watanabe, A. Valanezhad, T. Jafarzadeh Kashi, Alginate microcapsules as nutrient suppliers: an in vitro study, *Cell J* 20 (2018) 25–30, <https://doi.org/10.22074/cellj.2018.4508>.
- [26] J.F. Mano, L. Gasperini, R.L. Reis, Natural polymers for the microencapsulation of cells, *J R Soc Interface* (2014), <https://doi.org/10.1098/rsif.2014.0817>.
- [27] K.G. Chen, B.S. Mallon, R.D.G. Mckay, P.G. Robey, Human pluripotent stem cell culture: considerations for maintenance, expansion, and therapeutics, *Cell Stem Cell* 14 (1) (2014) 13–26, <https://doi.org/10.1016/j.stem.2013.12.005>.
- [28] N.C. Hunt, R.M. Shelton, L. Grover, An alginate hydrogel matrix for the localised delivery of a fibroblast/keratinocyte co-culture, *Biotechnol J* 4 (2009) 730–737, <https://doi.org/10.1002/biot.200800292>.
- [29] F. Lim, A.M. Sun, Microencapsulated islets as bioartificial endocrine pancreas, *Sun Source Sci New Ser* 210 (1980) 908–910. <http://www.jstor.org/stable/1684447>.
- [30] W. Czaja, D. Romanovicz, R.M. Brown, Structural investigations of microbial cellulose produced in stationary and agitated culture, *Cellulose* 11 (2004) 403–411.
- [31] G. Guhados, W. Wan, J.L. Hutter, Measurement of the elastic modulus of single bacterial cellulose fibers using atomic force microscopy, *Langmuir* 21 (2005) 6642–6646, <https://doi.org/10.1021/la0504311>.
- [32] A. Basu, K. Heitz, M. Strømme, K. Welch, N. Ferraz, Ion-crosslinked wood-derived nanocellulose hydrogels with tunable antibacterial properties: candidate materials for advanced wound care applications, *Carbohydr Polym* 181 (2017) 345–350, <https://doi.org/10.1016/j.carbpol.2017.10.085>.
- [33] N. Lavoine, I. Desloges, A. Dufresne, J. Bras, Microfibrillated cellulose – its barrier properties and applications in cellulosic materials: a review, *Carbohydr Polym* 90 (2012) 735–764, <https://doi.org/10.1016/j.carbpol.2012.05.026>.
- [34] A. Sannino, C. Demitri, M. Madaghiele, Biodegradable cellulose-based hydrogels: design and applications, *Materials* 2 (2009) 353–373, <https://doi.org/10.3390/ma2020353>.
- [35] H. Dong, J.F. Snyder, K.S. Williams, J.W. Andzelm, Cation-induced hydrogels of cellulose nanofibrils with tunable moduli, *Biomacromolecules* 14 (2013) 3338–3345, <https://doi.org/10.1021/bm400993f>.
- [36] J.C. Courtenay, M.A. Johns, F. Galembeck, C. Deneke, E.M. Lanzoni, C.A. Costa, J.L. Scott Ram, I. Sharma, J.C. Courtenay, Á.M.A. Johns, Á.J.L. Scott, Á.R.I. Sharma, M.A. Johns, Á.R.I. Sharma, F.C. Galembeck, Á. Deneke, Á.E.M. Lanzoni, Á.C.A. Costa, F. Galembeck, J.L. Scott, Surface modified cellulose scaffolds for tissue engineering, *Cellulose* 24 (2017) 253–267, <https://doi.org/10.1007/s10570-016-1111-y>.

- [37] L. Fu, J. Zhang, G. Yang, Present status and applications of bacterial cellulose-based materials for skin tissue repair, *Carbohydr Polym* 92 (2013) 1432–1442, <https://doi.org/10.1016/j.carbpol.2012.10.071>.
- [38] P. Muangman, S. Opananon, S. Suwanchot, O. Thangthed, Efficiency of microbial cellulose dressing in partial-thickness burn wounds, *J Am Col Certif Wound Spec* 3 (2011) 16–19, <https://doi.org/10.1016/j.jcws.2011.04.001>.
- [39] E. Yun, X. Loh, N. Mohamad, M.B. Fauzi, M.H. Ng, S.F. Ng, M. Cairul, I.M. Amin, Development of a bacterial cellulose-based hydrogel cell carrier containing keratinocytes and fibroblasts for full-thickness wound healing, *Sci Rep* (2018), <https://doi.org/10.1038/s41598-018-21174-7>.
- [40] F. Ahmadi, Z. Oveisi, S.M. Samani, Z. Amoozgar, Chitosan based hydrogels: characteristics and pharmaceutical applications, *Res Pharm Sci* 10 (2015) 1–16.
- [41] Y. Ren, H. Xie, X. Liu, J. Bao, W. Yu, X. Ma, Comparative investigation of the binding characteristics of poly-L-lysine and chitosan on alginate hydrogel, *Int J Biol Macromol* 84 (2016) 135–141, <https://doi.org/10.1016/j.ijbiomac.2015.12.008>.
- [42] W. Gao, J.C. Lai, S.W. Leung, Functional enhancement of chitosan and nanoparticles in cell culture, tissue engineering, and pharmaceutical applications, *Front Physiol* 3 (2012) 321, <https://doi.org/10.3389/fphys.2012.00321>.
- [43] K. Lee, W. Ha, W. Park, Blood compatibility and biodegradability of partially N-acetylated chitosan derivatives, *Biomaterials* 16 (1995) 1211–1216.
- [44] C.M. E.M. Varoni, S. Vijayakumar, E. Canciani, A. Cochis, L. De Nardo, G. Lodi, L. Rimondini, Chitosan-based trilayer scaffold for multitissue periodontal regeneration, *J Dent Res* 97 (2018) 303–311, <https://doi.org/10.1177/0022034517736255>.
- [45] T. Kean, M. Thanou, Biodegradation, biodistribution and toxicity of chitosan, *Adv Drug Deliv Rev* 62 (2010) 3–11, <https://doi.org/10.1016/j.addr.2009.09.004>.
- [46] A. Hasanovic, M. Zehl, G. Reznicek, C. Valenta, Chitosan-tripolyphosphate nanoparticles as a possible skin drug delivery system for aciclovir with enhanced stability, *J Pharm Pharmacol* 61 (2009) 1609–1616.
- [47] J. Berger, M. Reist, A. Chenite, O. Felt-Baeyens, J.M. Mayer, R. Gurny, Pseudo-thermosetting chitosan hydrogels for biomedical application, *Int J Pharm* 288 (2005) 17–25, <https://doi.org/10.1016/j.ijpharm.2004.07.036>.
- [48] A. Montembault, C. Viton, A. Domard, Rheometric study of the gelation of chitosan in aqueous solution without cross-linking agent, *Biomacromolecules* 6 (2005) 653–662, <https://doi.org/10.1021/bm049593m>.
- [49] T.A. Rickett, Z. Amoozgar, C.A. Tucheck, J. Park, Y. Yeo, R. Shi, Rapidly photo-cross-linkable chitosan hydrogel for peripheral neurosurgeries, *Biomacromolecules* 12 (2011) 57–65, <https://doi.org/10.1021/bm101004r>.
- [50] Y. Hayashi, S. Yamada, K.Y. Guchi, Z. Koyama, T. Ikeda, Chitosan and fish collagen as biomaterials for regenerative medicine, *Mar Med Foods* 65 (2012) 107–120, <https://doi.org/10.1016/B978-0-12-416003-3.00006-8>.
- [51] N. Charernsriwilaiwat, P. Opanasopit, T. Rojanarata, T. Ngawhirunpat, Lysozyme-loaded, electrospun chitosan-based nanofiber mats for wound healing, *Int J Pharm* 427 (2012) 379–384, <https://doi.org/10.1016/j.ijpharm.2012.02.010>.
- [52] T.H. Dai, M. Tanaka, Y.Y. Huang, M.R. Hamblin, Chitosan preparations for wounds and burns: antimicrobial and wound-healing effects, *Expert Rev Anti Infect Ther* 9 (2011) 857–879, <https://doi.org/10.1586/eri.11.59>.
- [53] H. Liu, Y. Du, X. Wang, L. Sun, Chitosan kills bacteria through cell membrane damage, *Int J Food Microbiol* (2004), <https://doi.org/10.1016/j.ijfoodmicro.2004.01.022>.

- [54] M.H. Periyah, A.S. Halim, A.R. Hussein, A.Z. Mat Saad, A.H. Abdul Rashid, K. Noorsal, In vitro capacity of different grades of chitosan derivatives to induce platelet adhesion and aggregation, *Int J Biol Macromol* 52 (2013) 244–249, <https://doi.org/10.1016/j.ijbiomac.2012.10.001>.
- [55] B.L. Bennett, Bleeding control using hemostatic dressings: lessons learned, *Wilderness Environ Med* 28 (2017) 39–49, <https://doi.org/10.1016/j.wem.2016.12.005>.
- [56] M. Rodriguez-Vazquez, B. Vega-Ruiz, R. Ramos-Zuniga, D.A. Saldana-Koppel, L.F. Quinones-Olvera, Chitosan and its potential use as a scaffold for tissue engineering in regenerative medicine, *BioMed Res Int* 2015 (2015) 821279, <https://doi.org/10.1155/2015/821279>.
- [57] C. Chatelet, O. Damour, A. Domard, C. Chatelet, O. Damour, A. Domard, Influence of the degree of acetylation on some biological properties of chitosan films, *Biomaterials* 22 (2001) 261–268.
- [58] A.B.M. Hilmi, A.S. Halim, A. Hassan, C.K. Lim, K. Noorsal, I. Zainol, In vitro characterization of a chitosan skin regenerating template as a scaffold for cells cultivation, *SpringerPlus* 2 (2013) 1–9, <https://doi.org/10.1186/2193-1801-2-79>.
- [59] C. Chatelet, O. Damour, A. Domard, Influence of the degree of acetylation on some biological properties of chitosan films, *Biomaterials* 22 (2001) 261–268.
- [60] K.S. Kang, G.T. Veeder, P.J. Mirrasoul, T. Kaneko, I.W. Cottrell, Agar-like polysaccharide produced by a pseudomonas species: production and basic properties, *Appl Environ Microbiol* 43 (1982) 1086–1091.
- [61] T. Osmalek, A. Froelich, S. Tasarek, Application of gellan gum in pharmacy and medicine, *Int J Pharm* 466 (2014) 328–340, <https://doi.org/10.1016/j.ijpharm.2014.03.038>.
- [62] B.N. Singh, L.D. Trombetta, K.H. Kim, Pharmaceutical development and technology biodegradation behavior of gellan gum in simulated colonic media biodegradation behavior of gellan gum in simulated colonic media, *Pharm Dev Technol* 94 (2005) 399–407, <https://doi.org/10.1081/PDT-200035793>, <https://doi.org/10.1081/PDT-200035793>.
- [63] S. Suri, R. Banerjee, In vitro evaluation of in situ gels as short term vitreous substitutes, *J Biomed Mater Res* 79 (2006) 650–664, <https://doi.org/10.1002/jbm.a.30917>.
- [64] H. Lee, S. Fisher, M.S. Kallos, C.J. Hunter, Optimizing gelling parameters of gellan gum for fibrocartilage tissue engineering, *J Biomed Mater Res B Appl Biomater* 98 B (2011) 238–245, <https://doi.org/10.1002/jbm.b.31845>.
- [65] C.J. Ferris, K.J. Gilmore, G.G. Wallace, M. in het Panhuis, Modified gellan gum hydrogels for tissue engineering applications, *Soft Matter* 9 (14) (2013) 3705–3711, <https://doi.org/10.1039/b000000x>.
- [66] J.T. Oliveira, L.S. Gardel, T. Rada, L. Martins, M.E. Gomes, R.L. Reis, Injectable gellan gum hydrogels with autologous cells for the treatment of rabbit articular cartilage defects, *J Orthop Res* 28 (2010) 1193–1199, <https://doi.org/10.1002/jor.21114>.
- [67] S.R. Moxon, A.M. Smith, Controlling the rheology of gellan gum hydrogels in cell culture conditions, *Int J Biol Macromol* 84 (2016) 79–86, <https://doi.org/10.1016/j.ijbiomac.2015.12.007>.
- [68] M.W. Lee, H.F. Tsai, S.M. Wen, C.H. Huang, Photocrosslinkable gellan gum film as an anti-adhesion barrier, *Carbohydr Polym* 90 (2012) 1132–1138, <https://doi.org/10.1016/j.carbpol.2012.06.064>.
- [69] R. Mehvar, Dextran for targeted and sustained delivery of therapeutic and imaging agents, *J Contr Release* 69 (2000) 1–25.
- [70] S.P. Massia, J. Stark, Immobilized RGD peptides on surface-grafted dextran promote biospecific cell attachment, *J Biomed Mater Res* 56 (2001) 390–399.

- [71] G. Sun, Y.I. Shen, C.C. Ho, S. Kusuma, S. Gerecht, Functional groups affect physical and biological properties of dextran-based hydrogels, *J Biomed Mater Res* 93 (2010) 1080–1090, <https://doi.org/10.1002/jbm.a.32604>.
- [72] S. Moller, J. Weisser, S. Bischoff, M. Schnabelrauch, Dextran and hyaluronan methacrylate based hydrogels as matrices for soft tissue reconstruction, *Biomol Eng* 24 (2007) 496–504, <https://doi.org/10.1016/j.bioeng.2007.08.014>.
- [73] G. Sun, X. Zhang, Y.I. Shen, R. Sebastian, L.E. Dickinson, K. Fox-Talbot, M. Reinblatt, C. Steenbergen, J.W. Harmon, S. Gerecht, Dextran hydrogel scaffolds enhance angiogenic responses and promote complete skin regeneration during burn wound healing, *Proc Natl Acad Sci U S A* 108 (2011) 20976–20981, <https://doi.org/10.1073/pnas.1115973108>.
- [74] Y.-I. Shen, H.-H. Greco, S. A. Papa, J. Burke, S.W. Volk, S. Gerecht, Acellular hydrogel for regenerative burn wound healing: translation from a porcine model HHS Public Access, *J Invest Dermatol* 135 (2015) 2519–2529, <https://doi.org/10.1038/jid.2015.182>.
- [75] K.M. Park, M.R. Blatchley, S. Gerecht, The design of dextran-based hypoxia-inducible hydrogels via in situ oxygen-consuming reaction, *Macromol Rapid Commun* 35 (2014) 1968–1975, <https://doi.org/10.1002/marc.201400369>.
- [76] M. Voigt, M. Schauer, D.J. Schaefer, C. Andree, R. Horch, G.B. Stark, Cultured epidermal keratinocytes on a microspherical transport system are feasible to reconstitute the epidermis in full-thickness wounds, *Tissue Eng* 5 (1999) 563–572, <https://doi.org/10.1089/ten.1999.5.563>.
- [77] G.D. Prestwich, D.M. Marecak, J.F. Marecek, K.P. Vercruyse, M.R. Ziebell, Controlled chemical modification of hyaluronic acid: synthesis, applications, and biodegradation of hyalazide derivatives, *J Contr Release* 53 (1998) 93–103.
- [78] T. Brown, U. Laurent, Fraser, Turnover of hyaluronan in synovial joints: elimination of labelled hyaluronan from the knee joint of the rabbit, *Exp Physiol* 76 (1991) 125–134, <https://doi.org/10.1113/expphysiol.1991.sp003474>.
- [79] C.E. Schanté, G. Zuber, C. Herlin, T.F. Vandamme, Chemical modifications of hyaluronic acid for the synthesis of derivatives for a broad range of biomedical applications, *Carbohydr Polym* 85 (2011) 469–489, <https://doi.org/10.1016/j.carbpol.2011.03.019>.
- [80] I.P. Monteiro, D. Gabriel, B.P. Timko, M. Hashimoto, S. Karajanagi, R. Tong, A.P. Marques, R.L. Reis, D.S. Kohane, A two-component pre-seeded dermal-epidermal scaffold, *Acta Biomater* 10 (2014) 4928–4938, <https://doi.org/10.1016/j.actbio.2014.08.029>.
- [81] R. Bennett, M. Taher, Restylane persists for 23 months found during Mohs Micrographic Surgery - a source of confusion with hyaluronic acid surrounding basal cell carcinoma, *Dermatol Surg* (2005) 1366–1369.
- [82] S. Bowman, M.E. Awad, M.W. Hamrick, M. Hunter, S. Fulzele, Recent advances in hyaluronic acid based therapy for osteoarthritis, *Clin Transl Med* 7 (2018) 6, <https://doi.org/10.1186/s40169-017-0180-3>.
- [83] K.T. Dicker, L.A. Gurski, S. Pradhan-Bhatt, R.L. Witt, M.C. Farach-Carson, X. Jia, Hyaluronan: a simple polysaccharide with diverse biological functions, *Acta Biomater* 10 (2014) 1558–1570, <https://doi.org/10.1016/j.actbio.2013.12.019>.
- [84] C.-H. Law, J.-M. Li, H.-C. Chou, Y.-H. Chen, H.-L. Chan, Hyaluronic acid-dependent protection in H9C2 cardiomyocytes: a cell model of heart ischemia–reperfusion injury and treatment, *Toxicology* 303 (2013) 54–71, <https://doi.org/10.1016/j.tox.2012.11.006>.
- [85] C. Wu, H. Chou, J. Li, Y. Chen, J. Chen, Y. Chen, H. Chan, Hyaluronic acid-dependent protection against alkali-burned human corneal cells, (2013) 388–396. doi:10.1002/elps.201200342.

- [86] A. D'agostino, A. Stellavato, L. Corsuto, P. Diana, R. Filosa, A. La Gatta, M. De Rosa, C. Schiraldi, Is molecular size a discriminating factor in hyaluronan interaction with human cells? *Carbohydr Polym* 157 (2017) 21–30, <https://doi.org/10.1016/j.carbpol.2016.07.125>.
- [87] S. Misra, V.C. Hascall, R.R. Markwald, S. Ghatak, Interactions between hyaluronan and its receptors (CD44, RHAMM) regulate the activities of inflammation and cancer, *Front Immunol* 6 (2015) 201, <https://doi.org/10.3389/fimmu.2015.00201>.
- [88] S.R. King, W.L. Hickerson, K.G. Proctor, Beneficial actions of exogenous hyaluronic acid on wound healing, *Surgery* 109 (1991) 76–84. <http://www.ncbi.nlm.nih.gov/pubmed/1984639>.
- [89] H.-M. Wang, Y.-T. Chou, Z.-H. Wen, Z.-R. Wang, C.-H. Chen, M.-L. Ho, J.M. Brandner, Novel biodegradable porous scaffold applied to skin regeneration, (2013). doi: 10.1371/journal.pone.0056330.
- [90] M.T. Cerqueira, L.P. da Silva, T.C. Santos, R.P. Pirraco, V.M. Correlo, A.P. Marques, R.L. Reis, Human skin cell fractions fail to self-organize within a gellan gum/hyaluronic acid matrix but positively influence early wound healing, *Tissue Eng* 20 (2014) 1369–1378, <https://doi.org/10.1089/ten.tea.2013.0460>.
- [91] M. Kuroyanagi, A. Yamamoto, N. Shimizu, A. Toi, T. Inomata, A. Takeda, Y. Kuroyanagi, Development of anti-adhesive spongy sheet composed of hyaluronic acid and collagen containing epidermal growth factor, *J Biomater Sci Polym Ed* 25 (2014) 1253–1265.
- [92] Z. Wu, L. Fan, B. Xu, Y. Lin, P. Zhang, X. Wei, Use of decellularized scaffolds combined with hyaluronic acid and basic fibroblast growth factor for skin tissue engineering, *Tissue Eng* 21 (2015) 390–402, <https://doi.org/10.1089/ten.tea.2013.0260>.
- [93] Y.-K. Lin, Y. Matsumoto, Y. Kuroyanagi, S. Kagawa, A bilayer hyaluronic acid wound dressing to promote wound healing in diabetic ulcer, *J Bioact Compat Polym* 24 (2009), <https://doi.org/10.1177/0883911509341161>.
- [94] R. Simman, W. Mari, S. Younes, Use of Hyaluronic Acid – Based Biological Bilaminar Matrix in Wound Bed Preparation : A Case Series, 2018, pp. 3–5.
- [95] A. Faga, G. Nicoletti, F. Brenta, S. Scevola, G. Abatangelo, P. Brun, Hyaluronic acid three-dimensional scaffold for surgical revision of retracting scars: a human experimental study, *Int Wound J* 10 (2013) 329–335, <https://doi.org/10.1111/j.1742-481X.2012.00981.x>.
- [96] G. Gravante, D. Delogu, N. Giordan, G. Morano, A. Montone, G. Esposito, The use of hyalomatrix PA in the treatment of deep partial-thickness burns, *J Burn Care Res* 28 (2007) 269–274, <https://doi.org/10.1097/BCR.0B013E318031A236>.
- [97] S.K. Han, S.Y. Kim, R.J. Choi, S.H. Jeong, W.K. Kim, Comparison of tissue-engineered and artificial dermis grafts after removal of basal cell carcinoma on face - a pilot study, *Dermatol Surg* 40 (2014) 460–467, <https://doi.org/10.1111/dsu.12446>.
- [98] S.J. Delatte, J. Evans, A. Hebra, W. Adamson, H.B. Othersen, E.P. Tagge, Effectiveness of beta-glucan collagen for treatment of partial-thickness burns in children, *J Pediatr Surg* 36 (2001) 113–118, <https://doi.org/10.1053/jpsu.2001.20024>.
- [99] H. Ismail, M. Irani, Z. Ahmad, Starch-based hydrogels: present status and applications, *Int J Polym Mater Polym Biomater* 62 (2013) 411–420, <https://doi.org/10.1080/00914037.2012.719141>.
- [100] J. Ngoenkam, A. Faikrua, S. Yasothornsrikul, J. Viyoch, Potential of an injectable chitosan/starch/beta-glycerol phosphate hydrogel for sustaining normal chondrocyte function, *Int J Pharm* 391 (2010) 115–124, <https://doi.org/10.1016/j.ijpharm.2010.02.028>.
- [101] M. Biophysics, *Cell Physiology Sourcebook*, n.d.

- [102] S. Van Vlierberghe, P. Dubruel, E. Schacht, Biopolymer-based hydrogels as scaffolds for tissue engineering applications: a review, *Biomacromolecules* 12 (2011) 1387–1408, <https://doi.org/10.1021/bm200083n>.
- [103] M. Garcia-Fuentes, A.J. Meinel, M. Hilbe, L. Meinel, H.P. Merkle, Silk fibroin/hyaluronan scaffolds for human mesenchymal stem cell culture in tissue engineering, *Biomaterials* 30 (2009) 5068–5076, <https://doi.org/10.1016/j.biomaterials.2009.06.008>.
- [104] U.J. Kim, J. Park, C. Li, H.J. Jin, R. Valluzzi, D.L. Kaplan, Structure and properties of silk hydrogels, *Biomacromolecules* 5 (2004) 786–792, <https://doi.org/10.1021/bm0345460>.
- [105] S. Kapoor, S.C. Kundu, Silk protein-based hydrogels: promising advanced materials for biomedical applications, *Acta Biomater* 31 (2016) 17–32, <https://doi.org/10.1016/j.actbio.2015.11.034>.
- [106] R. Ghassemifar, S. Redmond, Zainuddin, T. V Chirila, Advancing towards a tissue-engineered tympanic membrane: silk fibroin as a substratum for growing human eardrum keratinocytes, *J Biomater Appl* 24 (2010) 591–606, <https://doi.org/10.1177/0885328209104289>.
- [107] B. Kundu, S.C. Kundu, Silk sericin/polyacrylamide in situ forming hydrogels for dermal reconstruction, *Biomaterials* 33 (2012) 7456–7467, <https://doi.org/10.1016/j.biomaterials.2012.06.091>.
- [108] H. Teramoto, T. Kameda, Y. Tamada, Preparation of gel film from *Bombyx mori* silk sericin and its characterization as a wound dressing, *Biosci Biotechnol Biochem* 72 (2008) 3189–3196, <https://doi.org/10.1271/bbb.80375>.
- [109] Z. Wang, Y. Zhang, J. Zhang, L. Huang, J. Liu, Y. Li, G. Zhang, S.C. Kundu, L. Wang, Exploring natural silk protein sericin for regenerative medicine: an injectable, photoluminescent, cell-adhesive 3D hydrogel, *Sci Rep* 4 (2014) 7064, <https://doi.org/10.1038/srep07064>.
- [110] K. Tsubouchi, Y. Igarashi, Y. Takasu, H. Yamada, Sericin enhances attachment of cultured human skin fibroblasts, *Biosci Biotechnol Biochem* 69 (2005) 403–405, <https://doi.org/10.1271/bbb.69.403>.
- [111] D.A. Hickman, C.L. Pawlowski, U.D.S. Sekhon, J. Marks, A. Sen Gupta, Biomaterials and advanced technologies for hemostatic management of bleeding, *Adv Mater* 30 (2018) 1700859, <https://doi.org/10.1002/adma.201700859>.
- [112] P.J.M. Bouten, M. Zonjee, J. Bender, S.T.K. Yauw, H. Van Goor, J.C.M. Van Hest, R. Hoogenboom, The chemistry of tissue adhesive materials, *Prog Polym Sci* 39 (2014) 1375–1405, <https://doi.org/10.1016/j.progpolymsci.2014.02.001>.
- [113] K. Foster, D. Greenhalgh, R.L. Gamelli, D. Mazingo, N. Gibran, M. Neumeister, S.Z. Abrams, E. Hantak, L. Grubbs, B. Ploder, N. Schofield, L.H. Riina, Efficacy and safety of a fibrin sealant for adherence of autologous skin grafts to burn wounds: results of a phase 3 clinical study, *J Burn Care Res* 29 (2008) 293–303, <https://doi.org/10.1097/BCR.0b013e31816673f8>.
- [114] L.J. Currie, J.R. Sharpe, R. Martin, The use of fibrin glue in skin grafts and tissue-engineered skin replacements: a review, *Plast Reconstr Surg* 108 (2001) 1713–1726. <http://www.ncbi.nlm.nih.gov/pubmed/11711954>.
- [115] CRYOSEAL® FS SYSTEM, 2007. <https://www.fda.gov/downloads/Biologics/BloodVaccines/BloodProducts/ApprovedProducts/PremarketApprovalsPMAs/UCM093321.pdf>.
- [116] K.T. Yamamoto, L.M. DeJoseph, Efficacy and safety of artiss fibrin tissue sealant use in rhytidectomy: a review of 120 cases, *Surg J* 3 (2017) 69–74, <https://doi.org/10.1055/s-0037-1599237>.

- [117] C.M. Bhamidipati, J.S. Coselli, S.A. LeMaire, BioGlue in 2011: what is its role in cardiac surgery? *J Extra Corpor Technol* 44 (2012) P6–P12.
- [118] H.K. Chenault, S.K. Bhatia, W.G. Dimaio, G.L. Vincent, W. Camacho, A. Behrens, Sealing and healing of clear corneal incisions with an improved dextran aldehyde-PEG amine tissue adhesive, *Curr Eye Res* 36 (2011) 997–1004, <https://doi.org/10.3109/02713683.2011.606590>.
- [119] D. Miki, K. Dastgheib, T. Kim, A. Pfister-Serres, K.A. Smeds, M. Inoue, D.L. Hatchell, M.W. Grinstaff, A photopolymerized sealant for corneal lacerations, *Cornea* 21 (2002) 393–399, <https://doi.org/10.1097/00003226-200205000-00012>.
- [120] J.M.G. Reyes, S. Herretes, A. Pirouzmanesh, D.A. Wang, J.H. Elisseeff, A. Jun, P.J. McDonnell, R.S. Chuck, A. Behrens, A modified chondroitin sulfate aldehyde adhesive for sealing corneal incisions, *Investig Ophthalmol Vis Sci* 46 (2005) 1247–1250, <https://doi.org/10.1167/iovs.04-1192>.
- [121] D. Eyrich, F. Brandl, B. Appel, H. Wiese, G. Maier, M. Wenzel, R. Staudenmaier, A. Goepferich, T. Blunk, Long-term stable fibrin gels for cartilage engineering, *Biomaterials* 28 (2007) 55–65, <https://doi.org/10.1016/j.biomaterials.2006.08.027>.
- [122] Y. Li, H. Meng, Y. Liu, B.P. Lee, Fibrin gel as an injectable biodegradable scaffold and cell carrier for tissue engineering, *Sci World J* (2015), <https://doi.org/10.1155/2015/685690>.
- [123] O. Gsib, J.-L. Duval, M. Goczkowski, M. Deneufchatel, O. Fichet, V. Larreta-Garde, S. Bencherif, C. Egles, Evaluation of fibrin-based interpenetrating polymer networks as potential biomaterials for tissue engineering, *Nanomaterials* 7 (2017) 436, <https://doi.org/10.3390/nano7120436>.
- [124] F. Lee, M. Kurisawa, Formation and stability of interpenetrating polymer network hydrogels consisting of fibrin and hyaluronic acid for tissue engineering, *Acta Biomater* 9 (2013) 5143–5152, <https://doi.org/10.1016/j.actbio.2012.08.036>.
- [125] C.-M. Han, L.-P. Zhang, J.-Z. Sun, H.-F. Shi, J. Zhou, C.-Y. Gao, Application of collagen-chitosan/fibrin glue asymmetric scaffolds in skin tissue engineering, *J Zhejiang Univ - Sci B* 11 (2010) 524–530, <https://doi.org/10.1631/jzus.B0900400>.
- [126] S. Cox, M. Cole, B. Tawil, Behavior of human dermal fibroblasts in three-dimensional fibrin clots: dependence on fibrinogen and thrombin concentration, *Tissue Eng* 10 (2004) 942–954, <https://doi.org/10.1089/1076327041348392>.
- [127] J. Kopp, M.G. Jeschke, A.D. Bach, U. Kneser, R.E. Horch, Applied tissue engineering in the closure of severe burns and chronic wounds using cultured human autologous keratinocytes in a natural fibrin matrix, *Cell Tissue Bank* 5 (2004) 89–96, <https://doi.org/10.1023/B:CATB.0000034082.29214.3d>.
- [128] P. Langa, A. Wardowska, J. Zieliński, J. Podolak-Popinigis, P. Sass, P. Sosnowski, K. Kondej, A. Renkielska, P. Sachadyn, P. Trzonkowski, M. Piłula, Transcriptional profile of in vitro expanded human epidermal progenitor cells for the treatment of non-healing wounds, *J Dermatol Sci* 89 (2017) 272–281, <https://doi.org/10.1016/j.jdermsci.2017.12.003>.
- [129] V. Falanga, S. Iwamoto, M. Chartier, T. Yufit, J. Butmarc, N. Kouttab, G. Colvin, P. Carson, Autologous bone marrow-derived cultured mesenchymal stem cells delivered in a fibrin spray accelerate healing in murine and human cutaneous wounds, *J Invest Dermatol* 127 (2007) S49.
- [130] V. Carriel, I. Garzón, J.M. Jiménez, A.C.X. Oliveira, S. Arias-Santiago, A. Campos, M.C. Sánchez-Quevedo, M. Alaminos, Epithelial and stromal developmental patterns in a novel substitute of the human skin generated with fibrin-agarose biomaterials, *Cells Tissues Organs* 196 (2012) 1–12, <https://doi.org/10.1159/000330682>.

- [131] A. Meana, J. Iglesias, M. Del Rio, F. Larcher, B. Madrigal, M.F. Fresno, C. Martin, F. San Roman, F. Tevar, Large surface of cultured human epithelium obtained on a dermal matrix based on live fibroblast-containing fibrin gels, *Burns* 24 (1998) 621–630.
- [132] R. Mittermayr, P. Slezak, N. Haffner, D. Smolen, J. Hartinger, A. Hofmann, J. Schense, D. Spazierer, J. Gampfer, A. Goppelt, H. Redl, Controlled release of fibrin matrix-conjugated platelet derived growth factor improves ischemic tissue regeneration by functional angiogenesis, *Acta Biomater* 29 (2016) 11–20, <https://doi.org/10.1016/j.actbio.2015.10.028>.
- [133] A. Gugerell, W. Pasteriner, S. Nurnberger, J. Kober, A. Meinl, S. Pfeifer, J. Hartinger, S. Wolbank, A. Goppelt, H. Redl, R. Mittermayr, Thrombin as important factor for cutaneous wound healing: comparison of fibrin biomatrices in vitro and in a rat excisional wound healing model, *Wound Repair Regen* 22 (2014) 740–748, <https://doi.org/10.1111/wrr.12234>.
- [134] V.R. Sherman, W. Yang, M.A. Meyers, The materials science of collagen, *J Mech Behav Biomed Mater* 52 (2015) 22–50, <https://doi.org/10.1016/j.jmbbm.2015.05.023>.
- [135] S. Chattopadhyay, R.T. Raines, Collagen-based biomaterials for wound healing, *Biopolymers* 101 (2014) 821–833, <https://doi.org/10.1002/bip.22486>.
- [136] N. Dagalakis, J. Flink, P. Stasikelis, J.F. Burke, I.V. Yannas, Design of an artificial skin. Part III. Control of pore structure, *J Biomed Mater Res* 14 (1980) 511–528, <https://doi.org/10.1002/jbm.820140417>.
- [137] J.F. Burke, I.V. Yannas, W.C. Quinby Jr., C.C. Bondoc, W.K. Jung, Successful use of a physiologically acceptable artificial skin in the treatment of extensive burn injury, *Ann Surg* 194 (1981) 413–428.
- [138] N.E. O'connor, J.B. Mulliken, S. Banks-Schlegel, O. Kehinde, H. Green, grafting of burns with cultured epithelium prepared from autologous epidermal cells, *Clin Gastroenterol Br J Surg* 7 (1978) 555–569.
- [139] J.G. Rheinwald, H. Green, Serial cultivation of strains of human epidermal keratinocytes: the formation of keratinizing colonies from single cells, *Cell* 6 (1975) 331–343, [https://doi.org/10.1016/S0092-8674\(75\)80001-8](https://doi.org/10.1016/S0092-8674(75)80001-8).
- [140] H. Green, O. Kehinde, J. Thomas, Growth of cultured human epidermal cells into multiple epithelia suitable for grafting, *Cell Biol* 76 (1979) 5665–5668.
- [141] J.F. Hansbrough, S.T. Boyce, M.L. Cooper, T.J. Foreman, Burn wound closure with cultured autologous keratinocytes and fibroblasts attached to a collagen-glycosaminoglycan substrate, *Jama* 262 (1989) 2125–2130.
- [142] T.D. Sargeant, A.P. Desai, S. Banerjee, A. Agawu, J.B. Stopek, An in situ forming collagen-PEG hydrogel for tissue regeneration, *Acta Biomater* 8 (2012) 124–132, <https://doi.org/10.1016/j.actbio.2011.07.028>.
- [143] C.J. Doillon, Porous collagen sponge wound dressings: in vivo and in vitro studies, *J Biomater Appl* 2 (1988) 562–578. <http://www.ncbi.nlm.nih.gov/pubmed/3058927>.
- [144] K.R. Chalimidi, Y. Kumar, U. Anand Kini, Efficacy of collagen particles in chronic non healing ulcers, *J Clin Diagn Res* (2015), <https://doi.org/10.7860/JCDR/2015/11782.6001>.
- [145] D.L.N. Snyder, B.A. Sullivan, M. Karen, S.M. Schoelles, N. Sullivan, K.M. Schoelles, Skin Substitutes for Treating Chronic Wounds, Agency for Healthcare Research and Quality (US), 2012. <http://www.ncbi.nlm.nih.gov/pubmed/25356454>.
- [146] S. Suzuki, K. Matsuda, N. Isshiki, Y. Tamada, K. Yoshioka, Y. Ikada, Clinical evaluation of a new bilayer “artificial skin” composed of collagen sponge and silicone layer, *Br J Plast Surg* 43 (1990) 47–54.
- [147] M.J.A. van Luyn, P.B. van Wachem, L.H.H.O. Damink, P.J. Dijkstra, J. Feijen, P. Nieuwenhuis, Secondary cytotoxicity of cross-linked dermal sheep collagens during

- repeated exposure to human fibroblasts, *Biomaterials* 13 (1992) 1017–1024, [https://doi.org/10.1016/0142-9612\(92\)90153-F](https://doi.org/10.1016/0142-9612(92)90153-F).
- [148] M. Kremer, E. Lang, A.C. Berger, Evaluation of dermal-epidermal skin equivalents ('composite-skin') of human keratinocytes in a collagen-glycosaminoglycan matrix (Integra artificial skin), *Br J Plast Surg* 53 (2000) 459–465, <https://doi.org/10.1054/bjps.2000.3368>.
- [149] P.A. Golinski, N. Zoller, S. Kippenberger, H. Menke, J. Bereiter-Hahn, A. Bernd, [Development of an engraftable skin equivalent based on matriderm with human keratinocytes and fibroblasts], *Handchir Mikrochir Plast Chir* 41 (2009) 327–332, <https://doi.org/10.1055/s-0029-1234132>.
- [150] V.C. van der Veen, M.B.A. van der Wal, M.C.E. van Leeuwen, M.M.W. Ulrich, E. Middelkoop, Biological background of dermal substitutes, *Burns* 36 (2010) 305–321, <https://doi.org/10.1016/j.burns.2009.07.012>.
- [151] R.S. Kirsner, The use of Apligraf in acute wounds, *J Dermatol* 25 (1998) 805–811.
- [152] C. Pham, J. Greenwood, H. Cleland, P. Woodruff, G. Maddern, Bioengineered skin substitutes for the management of burns: a systematic review, *Burns* 33 (2007) 946–957, <https://doi.org/10.1016/j.burns.2007.03.020>.
- [153] R.J. Kumar, R.M. Kimble, R. Boots, S.P. Pegg, Treatment of partial-thickness burns: a prospective, randomized trial using Transcyte, *ANZ J Surg* 74 (2004) 622–626, <https://doi.org/10.1111/j.1445-1433.2004.03106.x>.
- [154] K. Vig, A. Chaudhari, S. Tripathi, S. Dixit, R. Sahu, S. Pillai, V.A. Dennis, S.R. Singh, Advances in skin regeneration using tissue engineering, *Int J Mol Sci* (2017), <https://doi.org/10.3390/ijms18040789>.
- [155] S. Natesan, D.O. Zamora, N.L. Wrice, D.G. Baer, R.J. Christy, Bilayer hydrogel with autologous stem cells derived from debrided human burn skin for improved skin regeneration, *J Burn Care Res* 34 (2013) 18–30, <https://doi.org/10.1097/BCR.0b013e3182642c0e>.
- [156] A. Skardal, D. Mack, E. Kapetanovic, A. Atala, J.D. Jackson, J. Yoo, S. Soker, Bioprinted amniotic fluid-derived stem cells accelerate healing of large skin wounds, stem cells transl, *Med* 1 (2012) 792–802, <https://doi.org/10.5966/sctm.2012-0088>.
- [157] Y.-B.B. Lee, S. Polio, W. Lee, G. Dai, L. Menon, R.S. Carroll, S.-S.S. Yoo, Bio-printing of collagen and VEGF-releasing fibrin gel scaffolds for neural stem cell culture, *Exp Neurol* 223 (2010) 645–652, <https://doi.org/10.1016/j.expneurol.2010.02.014>.
- [158] D.S.A. Hickman, C.L. Pawlowski, U.D.S. Sekhon, J. Marks, A. Sen Gupta, Biomaterials and advanced technologies for hemostatic management of bleeding, *Adv Mater* 30 (2018) 1–40, <https://doi.org/10.1002/adma.201700859>.
- [159] A. Sood, M.S. Granick, N.L. Tomaselli, Wound dressings and comparative effectiveness data, *Adv Wound Care* 3 (2014) 511–529, <https://doi.org/10.1089/wound.2012.0401>.
- [160] A. Jones, D. Vaughan, Hydrogel dressings in the management of a variety of wound types: a review, *J Orthop Nurs* 9 (2005).
- [161] [www.smith-nephew.com](http://www.smith-nephew.com), (n.d.). <http://www.smith-nephew.com/professional/products/advanced-wound-management/intrasite-gel/> (accessed June 2, 2018).
- [162] Purilon gel, (n.d.). [www.coloplast.co.uk/purilon-gel-en-gb.aspx](http://www.coloplast.co.uk/purilon-gel-en-gb.aspx) (accessed June 11, 2018).
- [163] E. Jude, S. Sally, Debridement of diabetic foot ulcers, *Edwards Jud Stapley Sally Debridement Diabet Foot Ulcers Cochrane Database Syst Rev* 1 (2010), <https://doi.org/10.1002/14651858.CD003556.Pub2>. John Wiley Sons, Ltd Chichester, UK.
- [164] Granugel, (n.d.). <https://www.convatec.co.uk/products/pc-wound-granugel/granugel-gel#> (accessed June 11, 2018).

- [165] B.G. Kozen, S.J. Kircher, J. Henao, F.S. Godinez, A.S. Johnson, An alternative hemostatic dressing: comparison of CELOX, HemCon, and QuikClot, *Acad Emerg Med* 15 (2008) 74–81, <https://doi.org/10.1111/j.1553-2712.2007.00009.x>.
- [166] J.F. Kragh Jr., J.K. Aden, J. Steinbaugh MSG, M. Bullard, M.A. Dubick, Gauze vs XSTAT in wound packing for hemorrhage control, *Am J Emerg Med* 33 (2015) 974–976, <https://doi.org/10.1016/j.ajem.2015.03.048>.
- [167] Woun'Dres Collagen Hydrogel, (n.d.). [https://www.coloplast.us/woundres-collagen-hydrogel-1-en-us.aspx#section=product-variants\\_4](https://www.coloplast.us/woundres-collagen-hydrogel-1-en-us.aspx#section=product-variants_4).
- [168] J. Schneider, T. Biedermann, D. Widmer, I. Montano, M. Meuli, E. Reichmann, C. Schiestl, Matriderm® versus integra®: a comparative experimental study, *Burns* 35 (2009) 51–57, <https://doi.org/10.1016/j.burns.2008.07.018>.
- [169] A. Batorsky, J. Liao, A.W. Lund, G.E. Plopper, J.P. Stegemann, Encapsulation of adult human mesenchymal stem cells within collagen-agarose microenvironments, *Biotechnol Bioeng* 92 (2005) 492–500, <https://doi.org/10.1002/bit.20614>.
- [170] M.N. Nicholas, M.G. Jeschke, S. Amini-Nik, Cellularized bilayer pullulan-gelatin hydrogel for skin regeneration, *Tissue Eng* 22 (2016) 754–764, <https://doi.org/10.1089/ten.tea.2015.0536>.
- [171] R. Nathoo, N. Howe, G. Cohen, Skin substitutes: an overview of the key players in wound management, *J Clin Aesthet Dermatol* 7 (2014) 44–48. [https://www.ncbi.nlm.nih.gov/pmc/articles/PMC4217293/pdf/jcad\\_7\\_10\\_44.pdf](https://www.ncbi.nlm.nih.gov/pmc/articles/PMC4217293/pdf/jcad_7_10_44.pdf).
- [172] D.M. Supp, S.T. Boyce, Engineered skin substitutes: practices and potentials, *Clin Dermatol* 23 (2005) 403–412, <https://doi.org/10.1016/j.clindermatol.2004.07.023>.
- [173] A.D. Metcalfe, M.W.J. Ferguson, Tissue engineering of replacement skin: the crossroads of biomaterials, wound healing, embryonic development, stem cells and regeneration, *J R Soc Interface* 4 (2007) 413–417, <https://doi.org/10.1098/rsif.2006.0179>.
- [174] S.T. Boyce, A.L. Lalley, Tissue engineering of skin and regenerative medicine for wound care, *Burn Trauma* 6 (2018) 4, <https://doi.org/10.1186/s41038-017-0103-y>.
- [175] M.N. Nicholas, M.G. Jeschke, S. Amini-Nik, Methodologies in creating skin substitutes, *Cell Mol Life Sci* 73 (2016) 3453–3472, <https://doi.org/10.1007/s00018-016-2252-8>.
- [176] L.K. Branski, D.N. Herndon, C. Pereira, R.P. Mlcak, M.M. Celis, J.O. Lee, A.P. Sanford, W.B. Norbury, X.J. Zhang, M.G. Jeschke, Longitudinal assessment of Integra in primary burn management: a randomized pediatric clinical trial, *Crit Care Med* 35 (2007) 2615–2623, <https://doi.org/10.1097/01.CCM.0000285991.36698.E2>.
- [177] K. Hori, A. Osada, T. Isago, H. Sakurai, Comparison of contraction among three dermal substitutes: morphological differences in scaffolds, *Burns* 43 (2017) 846–851, <https://doi.org/10.1016/j.burns.2016.10.017>.
- [178] K. Kawai, S. Suzuki, Y. Tabata, Y. Ikada, Y. Nishimura, Accelerated tissue regeneration through incorporation of basic fibroblast growth factor-impregnated gelatin microspheres into artificial dermis, *Biomaterials* 21 (2000) 489–499.
- [179] A. Carolina, C. Wosgrau, T. Da, S. Jeremias, F. Leonardi, M.J. Pereima, G. Di Giunta, A. Gonçalves Trentin, Comparative experimental study of wound healing in mice: pelnac versus integra, (2015). doi:10.1371/journal.pone.0120322.
- [180] C.D. HINMAN, H. MAIBACH, Effect of air exposure and occlusion on experimental human skin wounds, *Nature* 200 (1963) 377–378, <https://doi.org/10.1038/200377a0>.
- [181] J.P.E. Junker, R.A. Kamel, E.J. Caterson, E. Eriksson, Clinical impact upon wound healing and inflammation in moist, wet, and dry environments, *Adv Wound Care* 2 (2013) 348–356, <https://doi.org/10.1089/wound.2012.0412>.

- [182] N. Scuderi, T. Anniboletti, B. Carlesimo, M.G. Onesti, Clinical application of autologous three-cellular cultured skin substitutes based on esterified hyaluronic acid scaffold: our experience, *In Vivo* 23 (2009) 991–1003.
- [183] M.A. Meruane, M. Rojas, K. Marcelain, The use of adipose tissue-derived stem cells within a dermal substitute improves skin regeneration by increasing neoangiogenesis and collagen synthesis, *Plast Reconstr Surg* 130 (2012) 53–63, <https://doi.org/10.1097/PRS.0b013e3182547e04>.
- [184] K.L. Gardien, E. Middelkoop, M.M. Ulrich, Progress towards cell-based burn wound treatments, *Regen Med* 9 (2014) 201–218, <https://doi.org/10.2217/rme.13.97>.
- [185] B. Dash, Z. Xu, L. Lin, A. Koo, S. Ndon, F. Berthiaume, A. Dardik, H. Hsia, Stem cells and engineered scaffolds for regenerative wound healing, *Bioengineering* 5 (2018) 23, <https://doi.org/10.3390/bioengineering5010023>.
- [186] R.I. Freshney, *Culture of Animal Cells - A Manual of Basic Technique and Specialized Applications*, 2010, <https://doi.org/10.1002/9780471747598>.
- [187] E.N. Lamme, H.J.C. De Vries, H. Van Veen, G. Gabbiani, W. Westerhof, E. Middelkoop, Extracellular matrix characterization during healing of full-thickness wounds treated with a collagen/elastin dermal substitute shows improved skin regeneration in pigs, *J Histochem Cytochem* (1996), <https://doi.org/10.1177/44.11.8918906>.
- [188] A. Robinet, Elastin-derived peptides enhance angiogenesis by promoting endothelial cell migration and tubulogenesis through upregulation of MT1-MMP, *J Cell Sci* 118 (2005) 343–356, <https://doi.org/10.1242/jcs.01613>.
- [189] A. Danin, G. Georgesco, A. Le Touze, A. Penaud, R. Quignon, G. Zakine, Assessment of burned hands reconstructed with Integra W by ultrasonography and elastometry, *Burns* 38 (2012) 998–1004, <https://doi.org/10.1016/j.burns.2012.02.017>.
- [190] S. Böttcher-Haberzeth, T. Biedermann, C. Schiestl, F. Hartmann-Fritsch, J. Schneider, E. Reichmann, M. Meuli, Matriderm® 1 mm versus Integra® Single Layer 1.3 mm for one-step closure of full thickness skin defects: a comparative experimental study in rats, *Pediatr Surg Int* 28 (2012) 171–177, <https://doi.org/10.1007/s00383-011-2990-5>.
- [191] N.S. Moiemien, K.C. Lee, D. Herndon (Eds.), *The Role of Alternative Wound Substitutes in Major Burn Wounds and Burn Scar Resurfacing*, fifth ed., Elsevier Inc., 2018 <https://doi.org/10.1016/B978-1-4377-2786-9.00017-5>.
- [192] I. Jones, L. Currie, R. Martin, A guide to biological skin substitutes, *Br J Plast Surg* 55 (2002) 185–193, <https://doi.org/10.1054/bjps.2002.3800>.
- [193] C.S. Hankin, J. Knispel, M. Lopes, A. Bronstone, E. Maus, Clinical and cost efficacy of advanced wound care matrices for venous ulcers, *JMCP J Manag Care Pharm* 18 (2012). [www.Amcp.Org](http://www.Amcp.Org). <https://www.jmcp.org/doi/pdf/10.18553/jmcp.2012.18.5.375>.
- [194] J. Bradford, R.U. Desai, L. Ristovska, A. Kate, G. Cummings, H.G. Birnbaum, M. Skornicki, D.J. Margolis, N.B. Parsons, B. Rice, Economic outcomes among Medicare patients receiving bioengineered cellular technologies for treatment of diabetic foot ulcers, *J Med Econ J Med Econ* 18 (2015), <https://doi.org/10.3111/13696998.2015.1031793>.
- [195] M.J. Carter, C.E. Fife, D. Walker, B. Thomson, Estimating the applicability of wound care randomized controlled trials to general wound-care populations by estimating the percentage of individuals excluded from a typical wound-care population in such trials, *Adv Skin Wound Care* 22 (2009) 316–324, <https://doi.org/10.1097/01.ASW.0000305486.06358.e0>.
- [196] S.T. Boyce, D.J. Christianson, J.F. Hansbrough, Structure of a collagen-GAG dermal skin substitute optimized for cultured human epidermal keratinocytes, *J Biomed Mater Res* 22 (1988) 939–957, <https://doi.org/10.1002/jbm.820221008>.

- [197] D. Heimbach, A. Luterman, J. Burke, A. Cram, D. Herndon, J. Hunt, T.M. Jordan, W. Mcmanus, L. Solem, G. Warden, B. Zawacki, D.M. Heimbach, Artificial dermis for major burns a multi-center randomized clinical trial, in: *Present. 108th Annu. Meet. Am. Surg. Assoc. San Fr. California, May., 1988*.
- [198] D.M. Heimbach, G.D. Warden, A. Luterman, M.H. Jordan, N. Ozobia, C.M. Ryan, D.W. Voigt, W.L. Hickerson, J.R. Saffle, F.A. DeClement, R.L. Sheridan, A.R. Dimick, Multicenter postapproval clinical trial of Integra® Dermal Regeneration Template for burn treatment, *J Burn Care Rehabil* 24 (2003) 42–48, <https://doi.org/10.1097/00004630-200301000-00009>.
- [199] D. Won Lee, M. Chul Lee, H. Roh, W. Jai Lee, Multilayered implantation using acellular dermal matrix into nude mice, *J Mater Sci Mater Med* 25 (2014) 2669–2676, <https://doi.org/10.1007/s10856-014-5281-6>.
- [200] H. Rysseel, G. Germann, O. Kloeters, E. Gazyakan, C.A. Radu, Dermal substitution with Matriderm® in burns on the dorsum of the hand, *Burns* 36 (2010) 1248–1253, <https://doi.org/10.1016/j.burns.2010.05.003>.
- [201] D.J. Wainwright, Use of an acellular allograft dermal matrix (AlloDerm) in the management of full-thickness burns, *Burns* 21 (1995).
- [202] S.B. Glasberg, D. Light, AlloDerm and strattice in breast reconstruction: a comparison and techniques for optimizing outcomes, *Plast Reconstr Surg* 129 (2012) 1223–1233, <https://doi.org/10.1097/PRS.0b013e31824ec429>.
- [203] S. Becker, M. Saint-Cyr, C. Wong, P. Dauwe, P. Nagarkar, J.F. Thornton, Y. Peng, AlloDerm versus dermamatrix in immediate expander-based breast reconstruction: a preliminary comparison of complication profiles and material compliance, *Plast Reconstr Surg* 123 (2009) 1–6, <https://doi.org/10.1097/PRS.0b013e3181904bff>.
- [204] U. Mirastschijski, C. Kerzel, R. Schnabel, S. Strauss, K.H. Breuing, Complete horizontal skin cell resurfacing and delayed vertical cell infiltration into porcine reconstructive tissue matrix compared to bovine collagen matrix and human dermis, *Plast Reconstr Surg* 132 (2013) 861–869, <https://doi.org/10.1097/PRS.0b013e31829fe461>.
- [205] M. Romanelli, V. Dini, M. Bertone, Randomized comparison of OASIS wound matrix versus moist wound dressing in the treatment of difficult-to-heal wounds of mixed arterial/venous etiology, *Adv Skin Wound Care* 23 (2010) 34–38, <https://doi.org/10.1097/01.ASW.0000363485.17224.26>.
- [206] I. Lebbi, F.W.R.C. Vandekerckhove, J. Bouquet, D. Jolinière, A.R. Günthert, L. Knabben, G. Kanagalingam, S. Imboden, Acellular Dermal Matrix (Permacol®) for heterologous immediate Breast reconstruction after skin-sparing Mastectomy in Patients with Breast cancer: a single-institution experience and a review of the literature, 3 (2017). doi: 10.3389/fmed.2016.00072.
- [207] A. Pirayesh, H. Hoeksema, C. Richters, J. Verbelen, S. Monstrey, Glyaderm® dermal substitute: clinical application and long-term results in 55 patients, *Burns* 41 (2015) 132–144, <https://doi.org/10.1016/j.burns.2014.05.013>.
- [208] A.M. Reyzelman, I.B. DPM, Human acellular dermal wound matrix for treatment of DFU: literature review and analysis, *J Wound Care* 24 (2015) 128–134, <https://doi.org/10.12968/jowc.2015.24.3.128>.
- [209] S. Cazzell, D. Vayser, H. Pham, J. Walters, A. Reyzelman, B. Samsell, K. Dorsch, M. Moore, A randomized clinical trial of a human acellular dermal matrix demonstrated superior healing rates for chronic diabetic foot ulcers over conventional care and an active acellular dermal matrix comparator, *Wound Repair Regen* 25 (2017) 483–497, <https://doi.org/10.1111/wrr.12551>.

- [210] S.A. Brigido, The use of an acellular dermal regenerative tissue matrix in the treatment of lower extremity wounds: a prospective 16-week pilot study, *Int Wound J* 3 (2006) 181–187, <https://doi.org/10.1111/j.1742-481X.2006.00209.x>.
- [211] P. Waymack, R.G. Duff, M. Sabolinski, T. Apligraf, The effect of a tissue engineered bilayered living skin analog, over meshed split-thickness autografts on the healing of excised burn wounds, *Burns* 26 (2000) 609–619.
- [212] K.G. Donohue, P. Carson, M. Iriondo, L. Zhou, L. Saap, K. Gibson, V. Falanga, Safety and efficacy of a bilayered skin construct in full-thickness surgical wounds, *J Dermatol* 32 (2005) 626–631, <https://doi.org/10.1111/j.1346-8138.2005.tb00811.x>.
- [213] J.M. Centanni, J.A. Straseski, A. Wicks, J.A. Hank, C.A. Rasmussen, M.A. Lokuta, M.J. Schurr, K.N. Foster, L.D. Faucher, D.M. Caruso, A.R. Comer, B. Lynn Allen-Hoffmann, StrataGraft skin substitute is well-tolerated and is not acutely immunogenic in patients with traumatic wounds: results from a prospective, randomized, controlled dose escalation trial 253 (2011) 672–683, <https://doi.org/10.1097/SLA.0b013e318210f3bd>.
- [214] M.J. Schurr, K.N. Foster, J.M. Centanni, A.R. Comer, A. Wicks, A.L. Gibson, C.L. Thomas-Virnig, S.J. Schlosser, L.D. Faucher, M.A. Lokuta, B.L. Allen-Hoffmann, Phase I/II clinical evaluation of StrataGraft: a consistent, pathogen-free human skin substitute, *J Trauma* 66 (2009) 866–873, <https://doi.org/10.1097/TA.0b013e31819849d6>, discussion 873–4.
- [215] S. Gibbs, H.M. Van Den Hoogenband, G. Kirtschig, C.D. Richters, S.W. Spiekstra, M. Breetveld, R.J. Scheper, E.M. De Boer, Autologous full-thickness skin substitute for healing chronic wounds, *Br J Dermatol* 155 (2006) 267–274, <https://doi.org/10.1111/j.1365-2133.2006.07266.x>.
- [216] J. Still, P. Glat, P. Silverstein, J. Griswold, D. Mozingo, The use of a collagen sponge/living cell composite material to treat donor sites in burn patients, *Burns* 29 (2003) 837–841, [https://doi.org/10.1016/S0305-4179\(03\)00164-5](https://doi.org/10.1016/S0305-4179(03)00164-5).
- [217] M. Eisenberg, D. Llewelyn, Surgical management of hands in children with recessive dystrophic epidermolysis bullosa: use of allogeneic composite cultured skin grafts, *Br J Plast Surg Br Assoc Plast Surg* 51 (1998) 608–613.
- [218] C. Oostendorp, P.J.E. Uijtdewilligen, E.M. Versteeg, T.G. Hafmans, E.H. Van Den Bogaard, P.K.J.D. De Jonge, A. Pirayesh, J.W. Von Den Hoff, E. Reichmann, W.F. Daamen, T.H. Van Kuppevelt, Visualisation of newly synthesised collagen in vitro and in vivo, *Nat Publ Gr* (2015), <https://doi.org/10.1038/srep18780>.
- [219] S.T. Boyce, P.S. Simpson, M.T. Rieman, P.M. Warner, K.P. Yakuboff, J.K. Bailey, J.K. Nelson, L.A. Fowler, R.J. Kagan, Randomized, paired-site comparison of autologous engineered skin substitutes and split-thickness skin graft for closure of extensive, full-thickness burns, *J Burn Care Res* 38 (2017) 61–70, <https://doi.org/10.1097/BCR.0000000000000401>.
- [220] L. Uccioli, A clinical investigation on the characteristics and outcomes of treating chronic lower extremity wounds using the TissueTech autograft system, *Low Extrem Wounds* 2 (3) (2003) 140–151, <https://doi.org/10.1177/1534734603258480>.